Synthesis, Characterization and Catalytic Activity of Half sandwich Ruthenium(II) Complexes Based on N/N, N/O and O/O Donor Ligands

Ph.D. Thesis

By

AMBIKESH DHAR DWIVEDI

DISCIPLINE OF CHEMISTRY

INDIAN INSTITUTE OF TECHNOLOGY INDORE

APRIL 2018

Synthesis, Characterization and Catalytic Activity of Half sandwich Ruthenium(II) Complexes Based on N/N, N/O and O/O Donor Ligands

A THESIS

*Submitted in partial fulfillment of the
requirements for the award of the degree*

of

DOCTOR OF PHILOSOPHY

By

AMBIKESH DHAR DWIVEDI

(Roll No. 1301231001)

DISCIPLINE OF CHEMISTRY

INDIAN INSTITUTE OF TECHNOLOGY INDORE

APRIL 2018

INDIAN INSTITUTE OF TECHNOLOGY INDORE

CANDIDATE'S DECLARATION

I hereby certify that the work which is being presented in the thesis entitled **Synthesis, Characterization and Catalytic Activity of Half sandwich Ruthenium(II) Complexes Based on N/N, N/O and O/O Donor Ligands** in the partial fulfillment of the requirements for the award of the degree of **DOCTOR OF PHILOSOPHY** and submitted in the **DISCIPLINE OF CHEMISTRY, Indian Institute of Technology Indore**, is an authentic record of my own work carried out during the time period from JANUARY 2014 to APRIL 2018 under the supervision of **Dr. SANJAY KUMAR SINGH**, Associate Professor, Discipline of Chemistry, Indian Institute of Technology Indore.

The matter presented in this thesis has not been submitted by me for the award of any other degree of this or any other institute.

Signature of the student with date
(AMBIKESH DHAR DWIVEDI)

This is to certify that the above statement made by the candidate is correct to the best of my knowledge.

Signature of Thesis Supervisor with date
(Dr. SANJAY KUMAR SINGH)

AMBIKESH DHAR DWIVEDI has successfully given his Ph.D. Oral Examination held on………………..

Signature of Chairperson (OEB)
Date:

Signature of External Examiner
Date:

Signature(s) of Thesis Supervisor(s)
Date:

Signature of PSPC Member #1
Date:

Signature of PSPC Member #2
Date:

Signature of Convener, DPGC
Date:

Signature of Head of Discipline
Date:

ACKNOWLEDGMENTS

Words are short to express my deep sense of gratitude, but at the end of my thesis, it is my great pleasure to thank them all who contributed in many ways to the success of this study and made it an unforgettable experience for me. Thank you!!

Ambikesh

✺ ✺ ✺ ✺

This Thesis is Dedicated

To

My Beloved Parents, Brothers

&

Respected Teachers

✺ ✺ ✺ ✺

Ambikesh D. Dwivedi

SYNOPSIS

This thesis comprises of six chapters, which deals with the synthesis and characterization of various half-sandwich ruthenium(II) complexes and their application in various catalytic reactions. These complexes are revealing its flexible chemistry, supply as excellent precursors and find important applications in many catalytic organic transformations. The first chapter describes the literature survey about the previously reported transition metal based homogeneous catalysts, and motivation to design new nitrogen and oxygen donor ligands based metal complexes for important catalytic reactions. Subsequent chapters describes the detailed study about the synthesis, characterization and catalytic activity of newly synthesized half-sandwich ruthenium(II) complexes based on nitrogen and oxygen donor ligands and systematic investigation on the structure-activity relationship and mechanistic aspects of the studied catalytic reactions. The newly synthesized complexes have been successfully employed for several catalytic reactions such as ring opening, ring hydrogenation and C-H bond activation reactions under ambient reaction conditions. In the last chapter, conclusion and future scope of this research work is briefly discussed.

The main objectives of my research work are as following,

- To synthesize highly efficient catalytic system based on substituted ethylenediamine donor arene-ruthenium(II) complexes for the ruthenium and formic acid based tandem catalytic transformation of bioderived furans to levulinic acid and diketones in aqueous aerobic conditions.
- To study the role of ethylenediamine ligated half-sandwich arene-ruthenium(II) complexes as precursor for *in situ* generation of active Ru/C catalyst for the catalytic ring hydrogenation of arenes in water.
- To design and develop the troponate/aminotroponate arene-ruthenium(II) complexes and study their ligand-tuned mechanistic pathway for direct C-H Bond arylation with aryl chlorides in water.
- To synthesize and characterize cyclopentadienyl-ruthenium(II)-pyridylamine complexes and their application in catalytic transformation of bio-derived furans to levulinic acid and diketones in water.

Chapter 1. Introduction and background: Design and synthesis of homogeneous catalyst based on transition metal complexes

Design, synthesis and characterization of transition metal complexes and their use as active homogeneous catalysts for various organic reactions have received extensive attention in the field of organometallics and catalysis. Most important things about homogeneous catalysts is the easy of studying mechanistic pathway of catalytic reactions and hence on easy fine tuning of catalytic activity and understand structure-activity relationship. Among various metal catalysts explored so far, ruthenium metal gained preference over other metals for homogeneous catalysis, because of its variable oxidation states, its rich coordination properties and ability to accommodate a wide range of ligands in different coordination geometries. Thus, ruthenium based complexes compose a flexible class of active catalysts for synthetic organic chemistry and various other applications. More importantly, cautious selection of metal and ligands plays a very important role to design and synthesize homogeneous catalyst with tuned properties. In this context, we synthesize and characterization of various N/N, N/O and O/O donor ligand based arene-ruthenium and cyclopentadienyl-ruthenium half sandwich complexes has been undertaken to explore the catalytic activity of these complexes in field of biomass transformation, selective ring hydrogenation and C-H bond activation reactions in aqueous aerobic condition. Moreover, this thesis also comprises a detailed mechanistic investigation to understand the catalytic reactions pathway and their structure-activity relationship in the studied complexes.

Chapter 2. Ruthenium and formic acid based tandem catalytic transformation of bioderived furans to levulinic acid and diketones in water

This chapter comprises the synthesis and characterization of arene-ruthenium(II) complexes (**[Ru]-1** – **[Ru]-8**) based on simple and readily available ethylenediamine (or its derivatives) ligands. The studied complexes exhibited high activity for catalytic ring opening of furans and its derivatives under environmentally benign conditions in water.
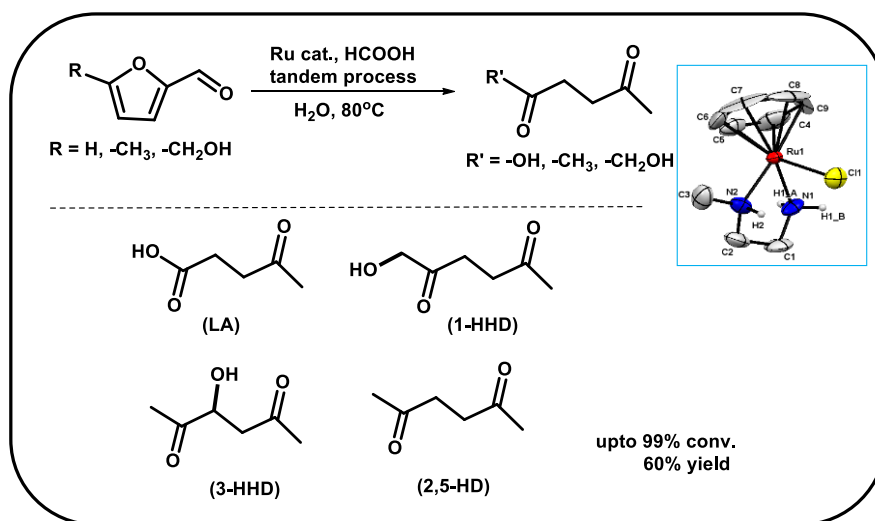
Figure 1. *Catalytic conversion of furans to LA and diketones in the presence of ethylenediamine based arene-Ru(II) complex in water.*

Synthesis of arene-Ru(II) complexes based on simple and easily available ethylenediamine ligand were carried out and characterized by ESI-MS, NMR, CHN elemental analysis and also structure for some of the complexes were authenticated by single crystal XRD analysis. These synthesized complexes exhibited high efficiency for the catalytic activity, stability and water solubility. Remarkably, these complexes exhibited high efficients for catalytic ring opening of bioderived furans to open ring products such as value added ketoacid (LA) and diketones (1-HHD, 3-HHD, and 2,5-HD) in the presence of formic acid at 80 °C in water and open atmosphere. Mechanistic investigation showed the profound effect of an N-H bond present in the arene-ruthenium complexes on the catalytic transformation of furans to ketoacid (LA) and diketones (1-HHD, 3-HHD, and 2,5-HD). ^{1}H NMR experiments with variable formic acid concentration evidenced a tandem mode of catalytic conversion of furfural to LA via the formation of the hydrogenated intermediate, furfuryl alcohol.

Chapter 3. Catalytic ring hydrogenation of arenes in water over in situ generated ruthenium nanoparticles immobilized on carbon

This chapter comprises the selective catalytic ring hydrogenation of various (hetero)arene, over the *in situ* generated Ru/C from an organometallic precursor ($[(\eta^6$-$C_6H_6)Ru(en)Cl]PF_6$) in the presence of formic acid. The cooperative effect of the arene-ruthenium(II) catalyst and ethylenediamine ligand activate formic acid to H_2 which resulted in the *in situ* generation of active ruthenium nanoparticles and H_2 gas to achieved facile tandem catalytic hydrogenation of a wide range of arenes and heteroarenes in water at 150 °C. Further, the reaction temperature has a determining role in the generation of Ru/C nanoparticles, by enhancing the rate of reduction of the precursor ethylenediamine ligand based arene-ruthenium(II) complex to ruthenium nanoparticles (Ru(0)). Consequently, the *in situ* generated ruthenium Ru/C nanoparticle was characterized with the help of TEM, SEM and Powder XRD observations. The Hg(0) poisoning experiments also suggested the heterogeneous nature of the catalyst. Further, using the *in situ* generated Ru/C catalyst, a wide range of aromatic and heteroaromatic compounds which analogous to lignin-derived fragments were also effectively hydrogenated to corresponding alicyclic products and thus the present catalytic system may also be used in the field of biomass transformation reactions.
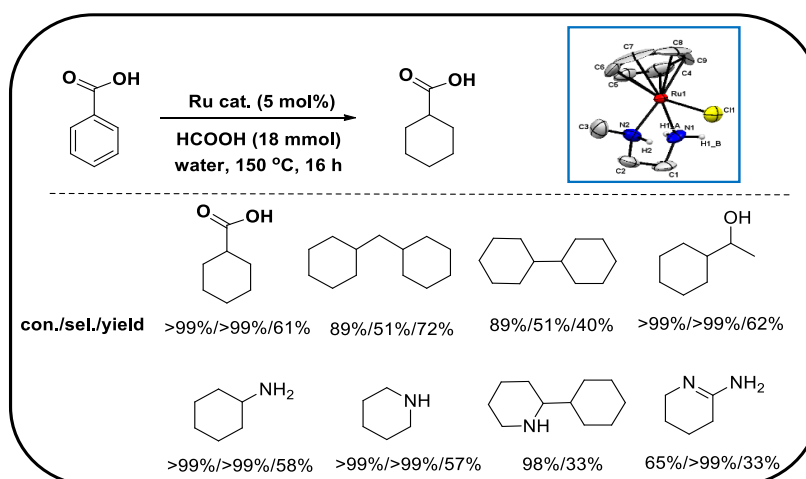
Figure 2. *Catalytic ring hydrogenation of (hetero)arene over in situ generated ruthenium nanoparticles in water.*

Chapter 4. Troponate-/Aminotroponate Ruthenium-Arene complexes: Synthesis, characterization and ligand tuned mechanistic pathway for direct C-H bond arylation with arylchlorides in water

This chapter contains the design, synthesis and characterization of a series of highly water soluble half sandwich arene-ruthenium(II) complexes **[Ru]-9 – [Ru]-16** of general formula $[(\eta^6\text{-arene})\text{Ru(troponate-/aminotroponate)Cl}]^+$ (arene = C_6H_6 and $C_{10}H_{14}$) ligated with bidentate (O,O and O,N) troponate-/aminotroponate ligands. Molecular structure of the complexes **[Ru]-13** and **[Ru]-15** were also authenticated by single-crystal X-ray diffraction. These newly synthesized (η^6-arene)-ruthenium(II) complexes based on troponate-/aminotroponate ligands are highly efficient for C-H bond arylation reaction of 2-arylpyridine in water. Our finding demonstrated that the structure-activity relationship plays a major role to achieve efficient selectivity in C-H activation of arylpyridine by these complexes. Moreover, the selectivity of mono- and diarylation of aryl pyridine is significantly affected by the steric bulkiness of the carboxylate additives.
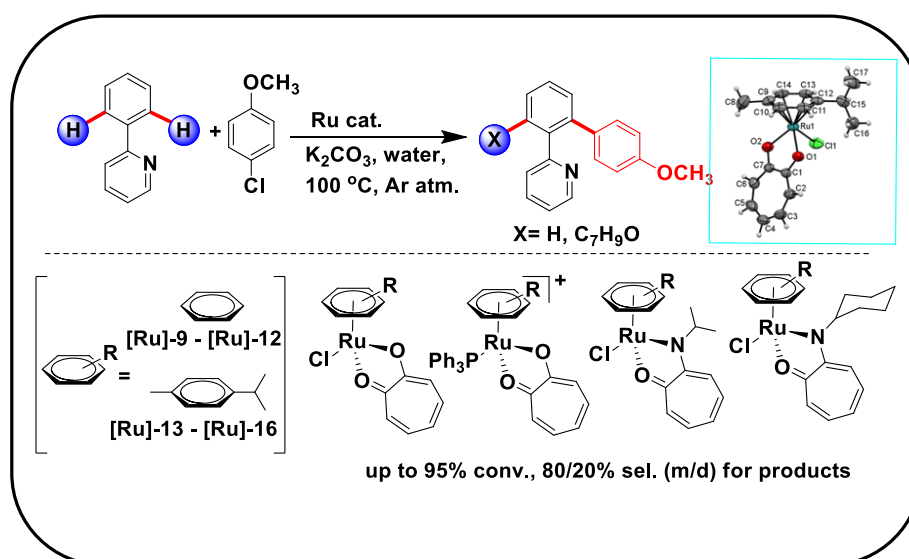
Figure 3. *C-H bond arylation of 2-phenylpyrdine catalysed by troponate/aminotroponate based arene-ruthenium(II) complexes.*

Mechanistic investigations performed by using mass spectral studies demonstrated the presence of several important cyclometallated intermediates species. Hence a possible catalytic pathway has been proposed as the initial formation of cycloruthenated species directed by deprotonation of 2-phenylpyridine

assisted by mild base (carbonate) and the relative strength of the troponate-/aminotroponate ligand and η^6-arene. This motivates the formation of cyclometallated species with arene-ruthenium(II) and 2-phenylpyridine ($[(\eta^6\text{-}$arene$)$Ru$(\kappa^2\text{-}CN\text{-}$phenylpyridine$)$(OH$_2$)$]^+$) by removal of troponate/aminotroponate ligands while another cyclometallated species formed by decoordination of η^6-arene ring and retaining troponate-/aminotroponate ligand is 2-phenylpyridine-Ru-troponate/aminotroponate ($[(\kappa^2\text{-}$troponate/aminotroponate$)$Ru$(\kappa^2\text{-}CN\text{-}$phenylpyridine$)$(OH$_2$)$_2]$). DFT calculations also support the experimental evidences for the formation of these intermediate species. Subsequently, with the oxidative addition of arylchloride over these C-H activated cyclometallated intermediate and then the reductive elimination led to the formation of C-H arylated product.

Chapter 5. Cyclopentadienyl-Ru(II)-pyridylamine complexes: Synthesis, X-ray structure and application in catalytic transformation of bio-derived furans to levulinic acid and diketones in water

This chapter comprises design and synthesis of a series of highly stable and efficient half-sandwich cyclopentadienyl-Ru(II) complexes **[Ru]-17** – **[Ru]-23** bearing pyridylamine/pyridylimine ligands. Molecular structures of all the complexes were authenticated by single crystal X-ray diffraction.
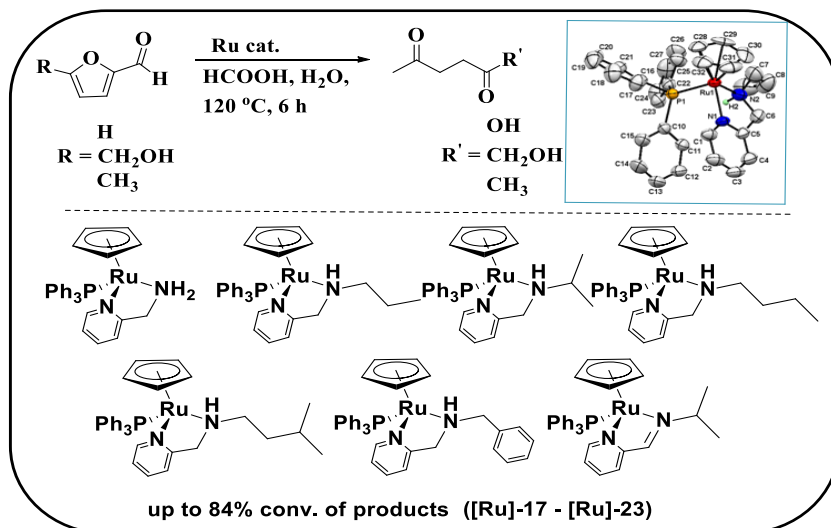
Figure 4. *Catalytic ring opening of furfural and its derivatives to LA and diketones in an aqueous medium over η^5-Cp-Ru-pyridylamine complexes.*

These synthesized complexes were employed for the catalytic ring opening of furans (furfural, 5-HMF and 5-MF) to levulinic acid and various diketones (3-hydroxyhexane-2,5-dione (3-HHD), 1-hydroxyhexane-2,5-dione (1-HHD) and hexane-2,5-dione (HD)) in the presence of formic acid and water at 120 °C. Our experimental finding demonstrated the significant role of the N-substitution (electronic and steric effect), where the complex **[Ru]-18** (η^5-Cp-Ru-*N*-propylpyridylamine complex) exhibited higher catalytic activity (TON of 16.8 and TTN 58.4) than other η^5-Cp-Ru-pyridylamine and η^5-Cp-Ru-pyridylimine complexes. Moreover, the flexible pyridylimine ligands may also show a remarkable κ^2-κ^1-κ^2 convertible behavior and hence facilitated the efficient transfer hydrogenation reaction by creating a new vacant site. Thus the observed high catalytic activity of synthesized complexes attributed to the combined effect of bulkiness, flexibility, and basicity of the pyridylamine ligands.

Chapter 6. Conclusions and future scope of work

6.1. Conclusions: A series of arene/Cp-Ru(II) complexes containing substituted ethylenediamine, troponate/aminotroponate, and pyridylamine/imine ligands have been synthesized and molecular structure of most of these complexes were confirmed by single crystal X-ray diffraction. Ethylenediamine based arene-Ru(II) complexes and pyridylamine/imine ligands based Cp-Ru(II) complexes were found to be active for the tandem catalytic transformations of bioderived furans, such as furfural, 5-hydroxymethylfurfural (5-HMF), and 5-methylfurfural (5-MF), to levulinic acid (LA) and diketones, 1-hydroxyhexane-2,5-dione (1-HHD), 3-hydroxyhexane-2,5-dione (3-HHD), and hexane-2,5-dione (2,5-HD). Moreover, ethylenediamine based arene-Ru(II) complexes were also employed as precursor for the *in situ* synthesis of Ru nanoparticles immoblized on carbon (Ru/C) and hence catalyzed the ring hydrogenation of homo/heteroarene in the presence of formic acid and these studies revealed the crucial role of −NH group to facilitate transfer hydrogenation. Moreover, the flexible hemilabile nature of pyridylamine ligands also advantageously contributed in the observed high catalytic activity of η^5-Cp-Ru(II) complexes. Machanistic investigations inferred the formation of furfuryl alcohol an important reaction intermediate via transfer hydrogenation

which further undergoes an acid catalyzed hydrilytic ring opening to LA, hence demonstrate the role of the ruthenium catalyst and the formic acid in reaction.

Troponate/Aminotroponate based arene-Ru(II) complexes catalyzed efficient C-H bond arylation of arylpyridine in water, where the selectivity toward mono- vs diarylation of arylpyridines was found to be directed by the steric bulkiness of the carboxylate additives. Mechanistic studies performed using mass-spectral studies revealed the formation of several key cyclometalated intermediates species and therefore provided strong evidence that cloruthenation step was driven by carbonate-assisted deprotonation of 2-phenylpyridine. Moreover, formation of cyclometalated 2-phenylpyridine Ru-arene species, $[(\eta^6$-arene)Ru(κ^2-C,Nphenylpyridine)(OH$_2$)]$^+$ and cyclometalated 2-phenylpyridine Ru-troponate/aminotroponate species $[(\kappa^2$-troponate/aminotroponate)Ru(κ^2-C,N-phenylpyridine)(OH$_2$)$_2$] was depended on the relative strength of the η^6-arene and the troponate/aminotroponate ligand by decoordination of troponate/aminotroponate ligands. DFT studied also well complemented over the experimental findings and support the formation of such species for these complexes. Moreover, synthesized complexes were found to be highly air stable even at higher temperature ~120 °C, and most of them are highly water soluble, which help them to easy recovery and reuse for successive catalytic cycles and thus these complexes may be find application for catalytic reaction in aqueous and open atmospheric conditions even at higher temperature.

6.2. Future scope: Synthesis and characterization of homogeneous catalysts based on readily available nitrogen based ligands may provide an opportunity to develop air stable and highly water soluble catalysts to perform catalytic reactions under environmental benign reaction conditions. Modification of ligands either by the formation of pyridylamine/imine or substitution of simple ligand to bulky and strong coordinated ligands may lead to the synthesis of highly active catalysts for various catalytic reactions such as transfer hydrogenation, oxidations, H$_2$ generation and C-H bond activation reaction. Further, detailed mechanistic study under controlled catalytic reaction conditions, identification, and characterization of essential organometallic and organic intermediates species, may also help to establish the structure-activity relationship and enhance the understanding of the

catalytic reaction pathway further and stabilize the structure-activity relationship. A well designed highly active catalyst will essentially find application in industries for the production of fine chemicals and fuel to cater the global demand of the society.

Publications included in the thesis:

1. **Dwivedi A. D.**, Gupta K., Tyagi D., Rai R. K., Mobin S. M., Singh S. K.* (**2015**) Ruthenium-formic acid tandem catalytic transformation of bioderived furans to levulinic acid and diketones in water, *ChemCatChem*, 7, 4050-4058 (DOI: 10.1002/cctc.201501021). (**IF 4.803**)

2. **Dwivedi A. D.**, Binnani C.; Tyagi D., Rawat, K., Li, P.-Z., Zhao, Y., Mobin, S. M., Pathak B., Singh S. K.* (**2016**), Troponate-/Aminotroponate ruthenium-arene complexes: Synthesis, structure and ligand tuned mechanistic pathway for direct C-H bond arylation with arylchlorides in water, *Inorg. Chem.*, 55, 6739-6749 (DOI: 10.1021/acs.inorgchem.6b01028). (**IF 4.857**)

3. **Dwivedi A. D.**, Rai R. K., Gupta K., Singh S. K.* (**2017**), Catalytic hydrogenation of arenes in water over in-situ generated ruthenium nanoparticles immobilized on carbon, *ChemCatChem*, 9,1930-1938 (DOI: 10.1002/cctc.201700056). (**IF 4.803**)

4. **Dwivedi A. D.**, Sahu V. K., Mobin S. M., Singh S. K.* (**2018**), Cyclopentadienyl-Ru(II)-pyridylamine complexes: Synthesis, X-ray structure, and application in catalytic transformation of bio-derived furans to levulinic acid and diketones in water, *Inorg. Chem.*, 57, 4777-4787 (DOI: 10.1021/acs.inorgchem.8b00536). (**IF 4.857**)

Publications not included in the thesis

5. Tyagi D., Rai R. K., **Dwivedi A. D.**, Mobin S. M., Singh S. K.* (**2015**), Phosphine-free ruthenium-arene complex for low temperature one-pot catalytic conversion of aldehydes to primary amides in water, *Inorg. Chem. Front.*, 2, 116-124 (DOI: 10.1039/C4QI00115J). (**IF 4.036**)

6.   Gupta, K., Tyagi D., **Dwivedi A. D.**, Mobin S. M., Singh S. K.* (**2015**), Catalytic transformation of bio-derived furans to valuable ketoacid and diketones by water-soluble ruthenium catalysts, *Green Chem.*, 2015, 17, 4618-4627 (DOI: 10.1039/C5GC01376C). **(IF 9.125)**

7.   Tyagi D., Binnani C., Rai R. K., **Dwivedi A. D.**, Gupta K., Li P.-Z., Zhao Y., Singh S. K.* (**2016**), Ruthenium catalyzed oxidative homocoupling of arylboronic acids in water: Ligand tuned reactivity and mechanistic study, *Inorg. Chem.*, 55, 6332-6343 (DOI: 10.1021/acs.inorgchem.6b01115). **(IF 4.857)**

8.   Gupta K., Rai R. K., **Dwivedi A.D.**, Singh S. K.* (**2017**), Catalytic aerial oxidation of biomass-derived furans to furan carboxylic acids in water over bimetallic Ni-Pd alloy nanoparticles, *ChemCatChem*, 9,2760 -2767 (DOI: 10.1002/cctc.201600942). (**IF 4.803**)

Conferences and Workshop

International

1.   Poster presentation at 17th Biennial International sympossium in *Modern Trends in Inorganic Chemistry* (MTIC-XVII) organized by CSIR-NCL Pune, IISER Pune and SP University in Pune, Maharastra, (December 2017); **Dwivedi A. D.**, Awasthi M. K., Singh S. K.*, Ruthenium-Catalyzed Ring Hydrogenation of (Hetero)arenes in Water.

National

1.   Poster presentation in *16thCRSI National Symposium in Chemistry* at Indian Institute of Technology (IIT) Bombay (**February 2014**); **Dwivedi A. D.**, Tyagi D., Rai R. K., Singh, S. K.*, A Greener Approach to Ruthenium Catalyzed Synthesis of Amides from Aldehydes.

2.   Poster presentation in *Frontiers of Organometallic Chemistry* (FOMC-2016) organized by IIT-Indore in Thiruvananthapuram, Kerala, (**December 2016**); **Dwivedi A. D.**, Binnani C., Singh S. K.*, Synthesis and

Characterization of Ruthenium-Arene complexes containing O,O, and O,N donor ligands for C-H bond arylation in water.

3. Attended *17thCRSI National Symposium in Chemistry* at National Chemical Laboratory (NCL), Pune (**February 2015**); **Dwivedi A. D.**, Tyagi D., Gupta K. G., Singh, S. K.*, Catalytic conversion of bio-derived components to bio-fuel components.

TABLE OF CONTENTS

its derivatives

LIST OF FIGURES

mmol) at 150 ºC.

Chapter 4. Troponate-/Aminotroponate Ruthenium-Arene complexes: Synthesis, characterization and ligand tuned mechanistic pathway for direct C-H bond arylation with arylchlorides in water

LIST OF SCHEMES

Chapter 4. Troponate-/Aminotroponate Ruthenium-Arene complexes: Synthesis, characterization and ligand tuned mechanistic pathway for direct C-H bond arylation with arylchlorides in water

Chapter 5. Cyclopentadienyl-Ru(II)-pyridylamine complexes: Synthesis, X-ray structure and application in catalytic transformation of bio-derived furans to levulinic acid and diketones in water

LIST OF TABLES

Chapter 5. Cyclopentadienyl-Ru(II)-pyridylamine complexes: Synthesis, X-ray structure and application in catalytic transformation of bio-derived furans to levulinic acid and diketones in water

NOMENCLATURE

α	Alpha
β	Beta
γ	Gamma
Å	Angstrom
λ	Wavelength
μ	Micro
σ	Sigma
π	Pi
η	Eta
δ	Delta
J	Coupling constant
Hz	Hertz
MHz	Mega hertz
K	Kelvin
D	Density
V	Volume
mmol	Milli Molar
cm	Centimeter
°	Degree
°C	Degree centigrade
μL	Microliter
a. u.	Arbitrary Unit
min	Minute
mL	Milliliter
Mm	Millimeter
M	Molar
ν	frequency

ACRONYMS

Arene-Ru(II)	Arene ruthenium (II) complexes
Cp-Ru(II)	Cyclopentadienyl-ruthenium(II) complexes
[Ru]-A1	[(η^6-C$_6$H$_6$)RuCl$_2$}$_2$]
[Ru]-A2	[(η^6-C$_{10}$H$_{14}$)RuCl$_2$}$_2$]
[Ru]-1	[(η^6-C$_6$H$_6$)Ru(ethylenediamine)Cl]PF$_6$
[Ru]-2	[(η^6-C$_6$H$_6$)Ru(N-methylethylenediamine)Cl]PF$_6$
[Ru]-3	[(η^6-C$_6$H$_6$)Ru(N,N-dimethylethylenediamine)Cl]PF$_6$
[Ru]-4	[(η^6-C$_6$H$_6$)Ru(N,N,N'-trimethylethylenediamine)Cl]PF$_6$
[Ru]-5	[(η^6-C$_{10}$H$_{14}$)Ru(ethylenediamine)Cl]PF$_6$
[Ru]-6	[(η^6-C$_{10}$H$_{14}$)Ru(N-methylethylenediamine)Cl]PF$_6$
[Ru]-7	[(η^6-C$_{10}$H$_{14}$)Ru(N,N-dimethylethylenediamine)Cl]PF$_6$
[Ru]-8	[(η^6-C$_{10}$H$_{14}$)Ru(N,N,N'-trimethylethylenediamine)Cl]PF$_6$
[Ru]-9	[(η^6-C$_6$H$_6$)Ru(troponate)Cl]
[Ru]-10	[(η^6-C$_6$H$_6$)Ru(troponate)PPh$_3$]Cl
[Ru]-11	[(η^6-C$_6$H$_6$)Ru(2-(isopropylamino)cyclohepta-2,4,6-trienone)Cl]
[Ru]-12	[(η^6-C$_6$H$_6$)Ru(2-(cyclohexylamino)cyclohepta-2,4,6-trienone)Cl]
[Ru]-13	[(η^6-C$_{10}$H$_{14}$)Ru(troponate)Cl]
[Ru]-14	[(η^6-C$_{10}$H$_{14}$)Ru(troponate)PPh$_3$]Cl
[Ru]-15	[(η^6-C$_{10}$H$_{14}$)Ru(2-(isopropylamino)cyclohepta-2,4,6-trienone)Cl]
[Ru]-16	[(η^6-C$_{10}$H$_{14}$)Ru(2-(cyclohexylamino)cyclohepta-2,4,6-trienone)Cl]
[Ru]-A3	[(η^5-C$_5$H$_5$)Ru(PPh$_3$)$_2$Cl]
[Ru]-17	[(η^5-C$_5$H$_5$)RuPPh$_3$(2-(aminomethyl)pyridine]PF$_6$
[Ru]-18	[(η^5-C$_5$H$_5$)RuPPh$_3$(N-(pyridin-2-ylmethyl)propan-1-amine]PF$_6$
[Ru]-19	[(η^5-C$_5$H$_5$)RuPPh$_3$(N-(pyridin-2-ylmethyl)propan-2-amine]PF$_6$

[Ru]-20	[(η^5-C$_5$H$_5$)RuPPh$_3$(N-(pyridin-2-ylmethyl)butan-1-amine]PF$_6$
[Ru]-21	[(η^5-C$_5$H$_5$)RuPPh$_3$(3-methyl-N-(pyridin-2-ylmethyl)butan-1-amine]PF$_6$
[Ru]-22	[(η^5-C$_5$H$_5$)RuPPh$_3$(N-benzyl-1-(pyridin-2-yl)methanamine]PF$_6$
[Ru]-23	[(η^5-C$_5$H$_5$)RuPPh$_3$(N-(pyridin-2-ylmethylene)propan-2-amine]PF$_6$
NMR	Nuclear Magnetic Resonance
HMBC	Heteronuclear Multiple Bond Correlation
UV-vis	UV-visible Spectroscopy
ESI-MS	Electrospray Ionization- Mass Spectrometry
HRMS	High Resolution Mass Spectroscopy
GC-MS	Gas Chromatography-Mass Spectrometry
TGA	Thermogravimetric Analysis
FTIR	Fourier Transform Infrared
TLC	Thin Layer Chromatography
SCXRD	Single Crystal X-ray Diffraction
PXRD	Powder X-ray Diffraction
SEM	Scanning Electron Microscope
TEM	Transmission Electron Microscope
EDX	Energy Dispersive X-ray spectroscopy
GOF	Goodness of fit
CDCl$_3$	Chloroform-d
D$_2$O	Deuterium oxide
DMSO-d_6	Dimethylsulphoxide-d_6
pH	The negative logarithm of hydronium-ion concentration ($-\log_{10}$ [H$_3$O$^+$])
Ar	Argon
O$_2$	Oxygen
H$_2$	Dihydrogen
N$_2$	Nitrogen
o	Ortho
m	Meta

p	Para
py	Pyridine
Im	Imine
en	Ethylenediamine
Me$_1$en	N-methylethylenediamine
(Me)$_2$en	N,N-dimethylethylenediamine
(Me)$_3$en	N,N,N-trimethylethylenediamine
TMEDA	Tetramethylethylenediamine
Mes	Mesityl
NHC	N-heterocyclic carbene
PCy$_3$	Tricyclohexylphosphine
PPh$_3$	Triphenylphosphine
s	Singlet
d	Doublet
t	Triplet
q	Quartet
m	Multiplet
ppm	Parts per million
r.t.	Room temperature
temp.	Temperature
equiv.	Equivalent
TMS	Trimethylsilyl
TON	Turnover number
TTN	Total tunover number
TOF	Turnover frequency
abs	Absorption
br	Broad
calc.	Calculated
cat.	Catalyst
cm^3	Cubic centimeter
cy	Cyclohexane
Et	Ethyl
Me	Methyl

^{i}Pr	*iso*-propyl
Ph	Phenyl
g	Gram
mg	Miligram
h	Hour
EtOH	Ethanol
DMF	Dimethylformamide
MeOH	Methanol
DCE	Dichloroethane
AcOH	Acetic acid
CH$_3$CN	Acetonitrile
Et$_3$N	Triethylamine
atm	Atmospheres (pressure)

Chapter 1

Introduction and background: Design and synthesis of homogeneous catalysts based on transition metal complexes

1.1. Half sandwich transition metal complexes: History and Background

Ruthenium is d-block metal rarely found on earth and it belongs to the platinum group of metals. It is obtained from the wastes of refining and it is mostly used in the catalytic processes because it shows an extended range of oxidation state (0 to +8).[1] Important feature of ruthenium coordinated complexes include their capability to stabilized reactive intermediate species like metal hydride, metal-carbene and oxo-metal their and good electron transfer property. Nowadays ruthenium complexes are used as redox reagents in chemical reaction due to their high redox property.[2] Progress of ruthenium chemistry are due to their high applicability and have huge possibility for future scope. A large number of the reactions are catalyzed by ruthenium complexes due to their specific properties like high electron transfer, lower redox potential, higher Lewis acidity and higher stability.[3] More attention towards ruthenium complexes have been directed due to their high stability and ability to get easily converted in a controlled synthetic procedure.

A summary about synthesis of mono and binuclear ruthenium complexes with the different type of monodentate and bidentate ligands are explored. Catalytic activity of these complexes in various type of chemical reactions like hydrogenation, C-C coupling,[4] C-H activation,[5] dehydrogenation,[6] transfer hydrogenation,[7] and discussion of their reaction mechanism and selectivity are important features of coordination chemistry.[3] Ruthenium based organometallic complexes are mostly stable in lower oxidation states when connected with ligands like cyclopentadienyls, arenes, allyls, carbonyl, cyano and nitrile groups.[8] Because of this, the chemistry of conjugated polyhepto hydrocarbon coordinated ruthenium complexes are studied in the different area of research mainly in catalysis. Mostly mononuclear or binuclear ruthenium and osmium arene complexes are present in either zero or +2 oxidation state. 'Half-sandwich' complexes form by reaction of mononuclear ruthenium(II) with arene/cyclopentadienyl ligands. It is also called *'piano-stool'* complex because of it resemble like *piano-stool*. Half-sandwich complexes shows a pseudo-octahedral geometry, as shown in Figure 1.1.[9] The three coordination sites are occupied by

polyhepto hydrocarbon (η^6-arene or η^5-Cp) ring. It is placed at the roof of the *piano-stool* and the other three coordination sites are occupied with mono or bidentate ligands which resembles like legs of *piano-stool*. Half sandwich complexes are organometallic in nature and contain a metal bound unidentate, bidentate and tridentate ligands in one side and cyclic polyhapto ligand on another side of the metal center. Half sandwich ruthenium organometallic complexes resemble geometry like *piano stool* which is containing cyclic conjugated hydrocarbon as a roof of the table, and three other ligands show as legs of a stool. In this half sandwich *piano stool* complexes the metal center is surrounded by either three monodentate ligands or one mono and one bidentate other than the one conjugated cyclic polyhapto hydrocarbon ligands.[9,10]Among all the half sandwich complexes, ruthenium based arene/cyclopentadienyl half sandwich complexes are more explored. This is because of its high stability, easily synthesized and its multiple applications in diverse field of catalytic reactions. Chemical and biological activities of half-sandwich complexes are highly influenced by the nature of chelating ligands, leaving groups and conjugated cyclic polyhapto hydrocarbons.[9,11] The three coordination sites can be occupied by other ligands (monodentate/bidentate), while the cyclic polyhapto ligand are tightly bonded to metal center and protects it against oxidation from Ru(II) to Ru(III).[12]
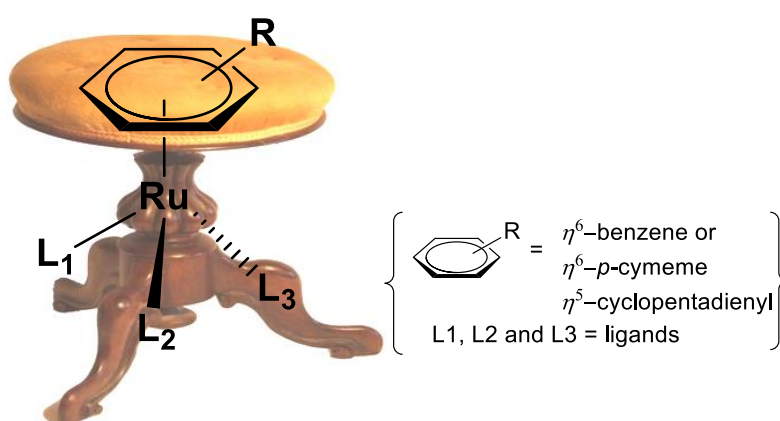
Figure 1.1. *Piano stool structure of half sandwich arene-Ru(II) complex.*

Arene-ruthenium half-sandwich complexes are prepared by using arene-ruthenium dimer as a precursor and a variety of mono (N, O, P) and bidentate (N/N, N/O, O/O, N/P etc.) ligands.[9,13,14] The η^6-arene-Ru(II) and η^5-Cp-Ru(II) moiety acts as a spectator ligand, and it stabilize the 'Ruthenium' in +2 oxidation state by preventing over oxidation of metal center (Figure 1.1). [9,13]

The important feature of polyhapto hydrocarbon (arene/cyclopentadienyl ring) ligands is its ability to enhance the catalytic activity by a suitable substitution on arene ring. Arene systems are hydrophilic in nature shown good water solubility. These characteristic features control the activity and selectivity of complexes for various catalytic applications. Arene ligand prefer ruthenium as a metal for formation of various half sandwich complexes because of its potential application like, mild reaction conditions, high yield, variable oxidation states, and high solubility in aqueous medium. One of the most common example of arene-Ru(II) complexes, with a chelating bidentate ethylene diamine (en) ligand $[(\eta^6\text{-}C_6H_6)Ru(en)Cl]^+$, have shown amazing results in the field of pharmaceutical, biological and catalysis. In half sandwich arene-ruthenium(II) complexes selection of ligand (mono or bidentate) and leaving group also play significant role to control the activity and selectivity of the catalytic reaction. The structural characterization of the half sandwich arene-Ru(II) complexes is authenticated by single crystal X-ray diffraction, NMR (^1H, ^{13}C, ^{15}N, ^{31}P etc.), mass spectrometry, infrared spectroscopy, and elemental analyses. Synthesis of dicationic, monocationic or neutral arene-Ru(II) complexes depends on the type of ligand used either monodentate or bidentate (homo/hetero) (Scheme 1.1).[9a]
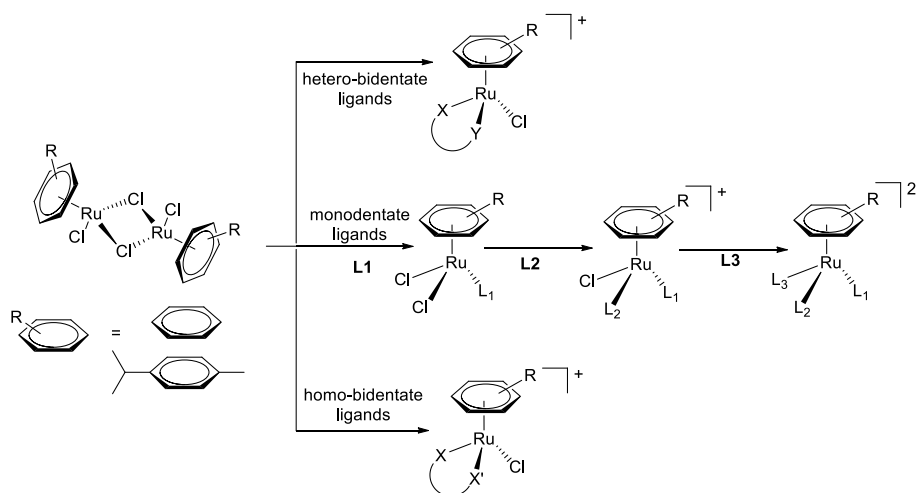
Scheme 1.1. *Synthesis of arene-Ru(II) complexes based on various ligands. Reproduced from ref. 9a with permission from Royal Society of Chemistry.*

1.2. Half sandwich transition metal complexes: Application in catalysis

The term catalysis was first used by Berzelius in 1836 to recognize a new species which can enhance the rate of chemical reaction. The catalysts are the substances which speed up the rate of the reaction by reducing activation energy. It enhances the rate of reaction when added in the reaction, without being consumed or produced in the catalytic system. Catalyst left unchanged after the reaction which is reused in next step.[15] Therefore the importance of catalysis gives immensely in the chemical industry beginning with the twentieth century.

Nowadays more than 95% of chemicals are produced via a process that contains at least one catalytic step. Having a significant contribution toward preparing cost-effective and environmentally benign which can fulfill the criteria of the green chemistry principle introduced by Anastas and Warner in 1998.[16] Catalyst has become the substance that is the gives shortcut to the lengthy reactions. In this same context half sandwich transition metal complexes have been used as a catalyst for various important organic transformation reactions.

Half sandwich transition metal complexes are one of the most important classes of organometallic catalysts which are usually used as homogeneous catalysts. They are synthesized by using an organometallic metal precursor with suitable ligands system. Catalytic activity of the homogeneous catalysts based on half sandwich transition metal complexes depends on metal ligand bond strength, metal coordination number and its ability to show variable oxidation state. Substitutions in ligands present inside the coordination sphere of transition metal complexes also play an important role in its catalytic activity. Also, the catalytic activity and product selectivity controlled by the interaction of metal complexes with substrate and reagent (solvent) molecules. It provides a range of catalytic system for various organic transformation reactions. Various steps of the homogeneous catalysts to complete their catalytic cycle and form desired products like, coordination and dissociation of ligand from metal center followed by oxidative addition and reductive elimination of central metal atom and finally insertion and elimination of substrate and product respectively from metal center.

1.3. Complexes based on nitrogen and oxygen donor ligands

Most of the research in the last few years is based on the synthesis of complexes containing nitrogen, oxygen and phosphorous donor ligands because of its reactivity, structural properties, and catalytic activity. Phosphorous is a soft base while nitrogen

and oxygen is hard base. When organometallic complexes coordinated by a bidentate ligand, contains both soft and hard ligands they show hemilabile behavior, which is useful for the catalytic reaction. Nitrogen having σ-donor ability can stabilize metal in higher oxidation state while phosphorous (π-acceptor ability), stabilized to metal in the low oxidation state. Hence phosphorous induces the metal center more susceptible towards oxidative addition reactions. Hard donor ligand (N, O) is easily decoordinated from the metal center and therefore provide the vacant site for binding of reactant moiety during catalytic reactions.[17]

1.3.1. Importance of amine based ligands

- Amine-based ligands are very simple, cheap and extremely abundant in nature, and show tremendous activities. Amine-based ligands are very easy to dissociate or re-associate to transition metal during the catalytic reaction. They help to enhance catalytic activity and provide as a free coordination site for incoming reactant moiety.

- Electronic and steric factors for amine based ligands with different electron withdrawing and electron donating group substitutions on amine nitrogen and also bulkier or smaller group may influence the activity and tune the selectivity considerably for catalytic reactions.

- Nature of amine (aromatic or aliphatic) also paid greater influence towards the activity and selectivity of synthesized transition metal complexes.

1.3.2. Advantages of tropolone/aminotropolone based ligands

- Tropolone and aminotropolone based bidentate (O/O, O/N donor) complexes form strong five-membered strained chelating ring with the central metal due to its unique features likes keto-enol tautomerism.

- Negative charge predominantly accumulated on nitrogen atoms of aminotropolone ligand and tropolone having hydroxy group (enolic) analogous to β-diketone favors the higher catalytic activity toward various organic reactions like C-H bond activation.

- Tropolone or aminotropolones significantly contribute to the stability of these complexes because of its large seven member planar homoaromatic rings.

1.3.3. Importance of pyridylamine/pyridylimine based ligands

- Synthesis and characterization of bidentate pyridylamine and pyridylimine based ligands are easy to prepare by simple condensation of aldehydes and corresponding amines.

- For stabilization of ruthenium complexes in lower oxidation states bidentate N/N' donor ligands are effective in comparison to O,O donor ligands.

- Pyridylamine/pyridylimine ligands may also act as hemilabile ligand due to the reversible coordination behavior of pyridylamine/pyridylimine ligands (κ^1 (pyridyl only) – κ^2 (both pyridyl and amino/imino)) with (η^5-C$_5$H$_5$)-Ru(II) center.

- Activity of pyridylamine/pyridylimine ligands changes by the increasing or decreasing of the bulkiness through substitution of electron rich or electron deficient group which stabilize or destabilize the activities of active reaction intermediates.

1.4. Example of some important half sandwich ruthenium complexes in catalysis

1.4.1. Shvo's catalyst

Precursors of Shvo's catalyst [{2,3,4,5-Ph$_4$((η^5-C$_4$CO)}$_2$H]Ru$_2$(CO)$_4$(μ-H), (**1**) discovered by Shvo in 1984.[18] Shvo's catalyst is the well-known η^5-Cp-Ru(II) based catalyst. It is used in transfer hydrogenation and it demonstrates that metal and ligands play an important role in the control of conversion and selectivity. Precursor of Shvo's catalyst has been mainly used for the hydrogenation of a variety of ketones and aldehydes. It is used for transfer hydrogenation of ketones by using formic acid, alcohols, and sodium formate, as reducing agents. The conversion of levulinic acid (LA) to γ-valerolactone (GVL) was achieved selectively by using formic acid in the presence of [{2,3,4,5-Ph$_4$((η^5-C$_4$CO)}$_2$H]Ru$_2$(CO)$_4$(μ-H).[18d] In precursor of Shvo's catalyst each ruthenium is coordinated by one functionalized cyclopentadienyl, two carbonyl ligands and one hydride ligand bridged by two ruthenium atoms and also one another proton connected by two oxygen of the cyclopentadienyl ligands. This feature of Shvo's catalyst provides high stability to catalyst in air and moisture even at a higher temperature. In the mechanistic study, transfer hydrogenation is reversible dissociation of Shvo's catalyst precursors to active mononuclear species, [{1-OH,2,3,4,5-Ph$_4$(η^5-C$_5$}Ru(CO)$_2$H] (**2**) and [{2,3,4,5-Ph$_4$(η^4-C$_4$C=O}Ru(CO)$_2$] (**3**) in which later one are 16e$^-$ species. Shvo's catalyst is the first report of a bifunctional

metal-ligand catalyst. Transfer hydrogenations of ketones are concerted hydride transfer, one from the metal to the carbonyl carbon and other one from proton of the hydroxycyclopentadienyl to the oxygen of carbonyl group (Scheme 1.2).
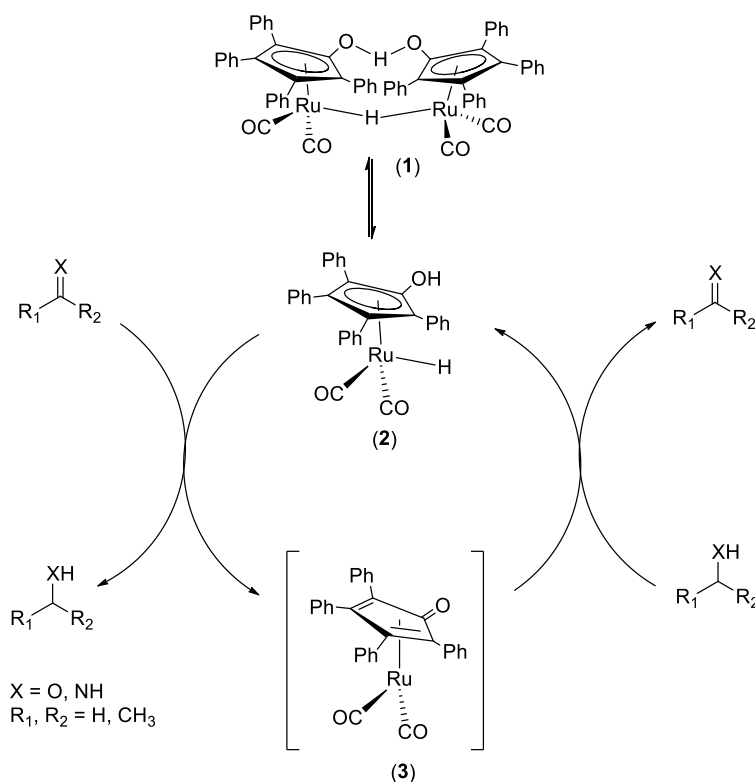
Scheme 1.2. *Activation of Shvo's catalyst into monomers and their mechanism of hydrogenation and dehydrogenation. Reproduced from ref. 18c with permission from American Chemical Society.*

1.5. Catalytic reactions based on Nitrogen and oxygen donor half sandwich arene-Ru(II) complexes

1.5.1. Noyori catalyst

An important half sandwich arene-ruthenium(II) complexes based on N/N donor ligands is known as Noyori catalysts. It is novel, highly active and efficient catalyst for enantioselective hydrogenation of ketones. Noyori develops a chiral ruthenium catalyst known as Noyori asymmetric hydrogenation catalyst and it is used for enantioselective hydrogenation of aldehydes, imines and ketones. Two catalysts diphosphane/diamine-Ru and BINAP/diamine-Ru (Figure 1.2), first one is used for the asymmetric hydrogenation of simple ketones and the other one is used for functionalized ketones. These catalysts are widely applicable in industrial processes. The product obtained from hydrogenations by Noyori catalysts are used for the

production of numerous drugs like carbapenem (antibiotic) levofloxacin (antibacterial) and antipsychotic agent.[19]
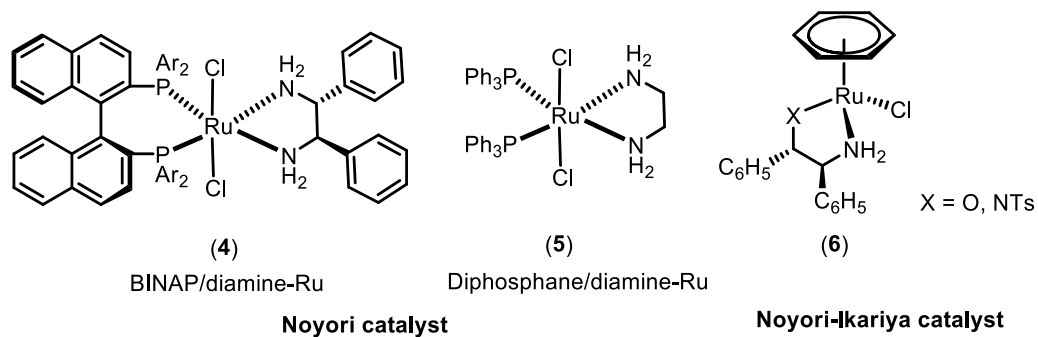
Figure 1.2. *Noyori and Noyori-Ikariya catalysts. Reproduced from ref. 19(a) with permission from Royal Society of Chemistry.*
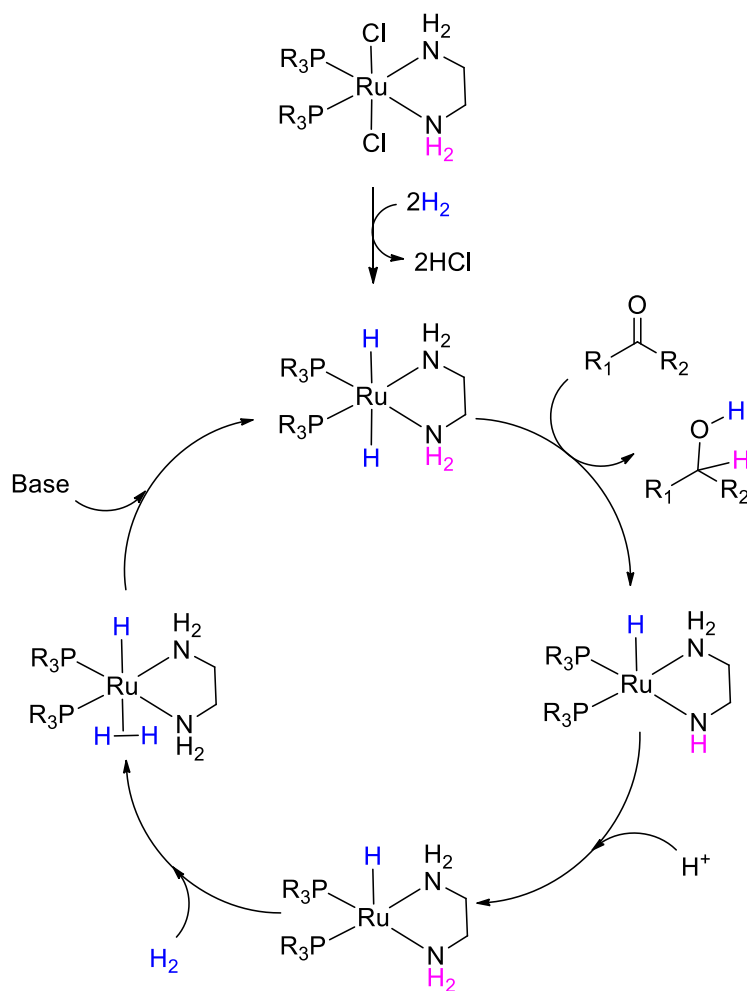
Scheme 1.3. *Mechanistic pathway for asymmetric hydrogenation of simple ketone Noyori catalysts.*

The Diphosphane/diamine-Ru dihalide catalyst can hydrolyzed only simple cyclic ketones with the help of a base. In mechanistic pathway the activation of (diphosphane)$_2$(diamine)$_2$ruthenium complex by the addition of the H$_2$ gas. After that step transfer of hydrogen from amine group of activated catalyst and metal-hydride to ketone through a transition state.[20] After this reformation of the ruthenium dihydride species with the help of base by reaction of hydrogen and ruthenium complex (Scheme 1.3) occurs.
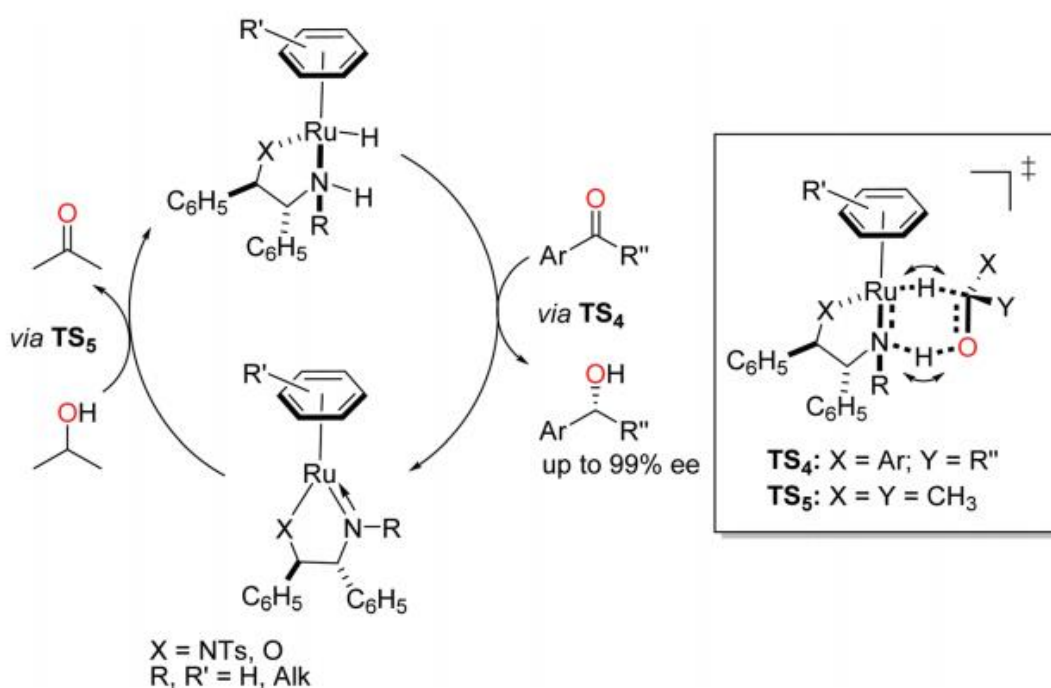
Scheme 1.4. *Catalytic cycle for the transfer hydrogenation of aromatic ketones by an active form of the Noyori-Ikariya catalyst. Adapted from ref. 19(a) with permission from Royal Society of Chemistry.*

Noyori catalysts are one of the most strong and efficient catalysts for the synthesis of chiral (optically active) alcohol. This is the most efficient process of hydrogenation explored in the 1990s. Noyori and Noyori-Ikariya discovered a novel and efficient catalyst for enantioselective hydrogenation and transfer hydrogenation of aromatic ketones, *trans*-[RuCl$_2$\{(S)-binap\}\{(S,S)-dpen\}] (**4**) and (S)-[(η^6-arene)RuCl\{(R,R)-XCH(Ph)CH(Ph)NH$_2$\}] [X = NTs, O] (**6**) as shown in Scheme 1.4, respectively. Noyori-Ikariya *et al.* explored the catalytic cycle of transfer hydrogenation of aromatic ketone in the presence of iPrOH/base catalyzed (S)-[(η^6-arene)RuCl\{(R,R)-XCH(Ph)CH(Ph)NH$_2$\}] [X = NTs, O]. Formation of metal-

hydride bond via transition state occures in which first transfer of hydrogen from isopropanol to ruthenium metal and in the next step reduction of ketone to alcohol by transfer of proton (hydride species) happens. After this one from metal and another from −NH in concerted manner (Scheme 1.4).

Recently Gordon *et al*. explored the effect of N-H groups and alkylations on Noyori based catalyst on the rate of hydride transfer for transfer hydrogenation of ketones. They observed that analogue of Noyori catalyst (**7**) with *N,N* donor bidentate ligand hydrogenate acetophenone acts effectively within 5 min at room temperature and gives 100% yield. The rate of hydride transfer gradually decreases by alkylation on −N-H group but it was observed that the catalytic activity of this catalyst become zero when all hydrogen of nitrogen atoms are substituted by methyl groups (Scheme 1.5). To conclude the role of −N-H ligand has been given toward the formation of metal hydride (Ru-H) species, which help for concerted hydride transfer via outer sphere mechanism in the transfer hydrogenation reaction.[21]
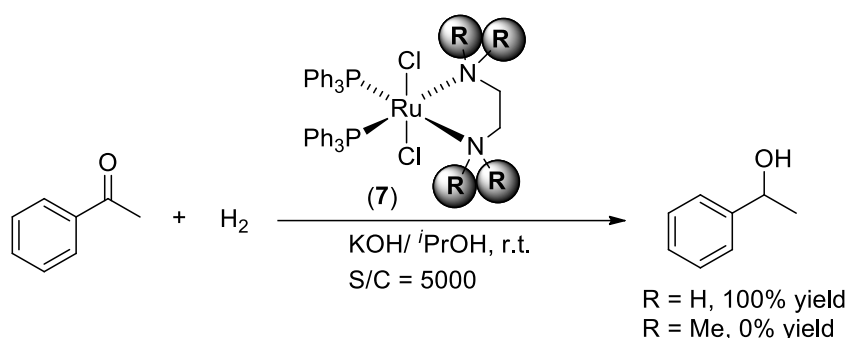
Scheme 1.5. *Hydrogenation ketone catalyzed by Noyori catalysts. Reproduced from ref. 21(a) with permission from American Chemical Society.*

1.5.2. Half sandwich arene-Ru(II) catalyzed dehydrogenation of formic acid

Recently various groups observed that formic acid is a good chemical source for hydrogen storage and carrier. Due to its favorable properties allowing it to stored, handled and transported easily with safety. In this context, Guan *et al.* explored the mechanistic study of dehydrogenation of formic acid catalyzed by half sandwich arene-Ru(II) complexes based on N,N' diimine ligand. They proposed two types of reaction pathway for intermediate hydride transfer species in the catalytic reaction.[22] Different intermediate species from the aqueous solution of complex was observed under mass spectrometry (Scheme 1.6). They found that dissociation of

chloride from **8** to form **9** in the aqueous solution followed by deprotonation of **9** to form **10**. In the presence of excess HCOO$^-$ in the solution, species **10** undergo deprotonation to form neutral species **11**. But it is not observed in mass spectrum because of strong equilibrium between **10** and **11**. Here equilibrium between **10** and **11** are highly pH sensitive and hence the role of species **10** is maximum in the catalytic reactions.
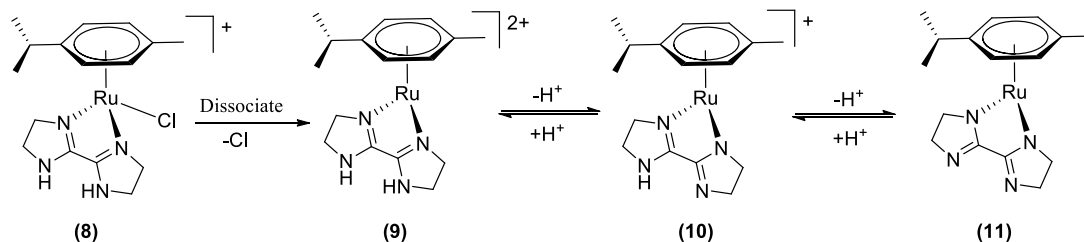
Scheme 1.6. *Different intermediates of arene-ruthenium(II)-N,N-diimine complex. Reproduced from ref. 22 with permission from American Chemical Society.*

1.5.3. Arene-Ru(II) catalyzed ring hydrogenation of benzene

Ring hydrogenation is comparatively difficult to catalyze by transition metal. Mostly ring hydrogenation is catalyzed by heterogeneously with various types of noble metal nanoparticles catalysts.[23,24] Selective hydrogenation of aromatic ring is one of the most important and useful catalytic reactions. It provides a convenient way to synthesize a variety of cyclic hydrocarbons which is industrially applicable in the field of feedstock of important chemicals, pharmaceuticals and materials.[25] Selective hydrogenation of aromatic ring over the different functional group is always difficult because of aromaticity. It requires higher energy to reduce ring double bond in comparison to a functional group like ketone, carboxylic, nitro, etc. Consequently, the development of an efficient methodology for the conversion of renewable lignocellulosic biomass to important value-added fine chemicals attracts recent attention. Particularly, selective hydrogenation of lignin-derived aromatic compounds have been gain more attention because it gives various industrially important alicyclic products.[23] Due to low reactivity of cyclohexane its functionalization is very challenging task. Nowadays synthesis and functionalization of cyclohexane and its derivative are obtained by selective hydrogenation of precursor aromatic compounds. They have gained attention from the scientific researchers including industrial and pharmaceuticals. Particularly synthesis of

cyclohexanecarboxylic acid by selective hydrogenation of benzoic acid has been given attention because cyclohexanecarboxylic acid is an important organic intermediate for the synthesis of some drugs like ansatrienin and praziquantel.[26] Remarkable work of Finke *et al.* established that catalytic reactions performed at higher temperature and pressure (110 °C and 60 atm H_2) by using ruthenium based precursor complexes as a catalyst. They suggested that here active catalytic species are *in situ* generated Ru(0) nanoparticles, for the hydrogenation of benzene to cyclohexane (Scheme 1.7).[27] Some analogous classical example suggested by them are that under optimize reaction condition, *in situ* generation of active catalytic species of metal nanoparticles from homogeneous metal complexes give high catalytic activity towards ring hydrogenation of benzene.[28]
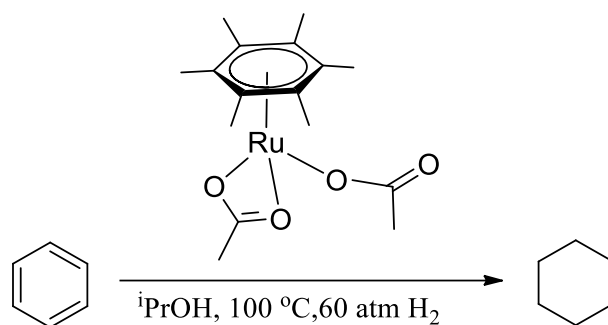
Scheme 1.7. *Benzene ring hydrogenation is catalyzed by the precatalys Ru(II)(η^6-C_6Me_6)(OAc)$_2$. Reproduced from ref. 25b with permission from American Chemical Society.*

1.5.4. C-H Bond activation and functionalization catalyzed by arene-Ru(II) complexes

Direct activation and functionalization of inert C-H bonds by using homogeneous catalysts have gained interest for several decades.[29b] Recently, ruthenium(II) complex based catalysts are extensively used because ruthenium complexes are non-expensive, easy to prepare and stable in air and water. It gives high efficiency for coupling reactions from sp^2 C-H bonds activation through alkenylation or arylation with (hetero)aryl halides.[29] Selectivity for monoarylation and diarylation is challenging when two unprotected *ortho* C-H hydrogen is present. In functional arenes, diarylation of *ortho* C-H bonds is perform with ruthenium(II) complex as catalysts, in that case, possibility for the formation of 5-membered ruthenacycle

intermediate is very high. In C-H bond activation reactions, Ru(II) complexes are most suitable under cyclometalation step (the important step for C-H bond activation) via cleavage of C-H bond than insertion of ruthenium metal in between C-H bond.[29a] A variety of organometallic ruthenium(II) complexes have been used for the C-H bond activation reaction. Ackermann *et al*. reported the C-H bond activation of (hetero)arenes are catalyzed by ligand-free ruthenium catalyst $(RuCl_3.xH_2O)$.[30] However, arene-Ru(II) dimer complexes, $(\{(\eta^6\text{-arene})RuCl_2\}_2)$ also shows enormous catalytic activity for C-H activation reactions.[5]

Dixneuf *et al*. reported arene sp^2 C-H bond arylation reaction catalyzed by ruthenium(II) species, in water at 120 °C is a beneficial influence of KOPiv or KOAc for conversion. The ratio of monoarylated and diarylated product is useful.[46] They prepared several half-sandwich arene-Ru(II) complexes which employed for aromatic C_{sp}^2-H bond activation or functionalization via C-C bond formation (cross-coupling). In the first step deprotonation of *ortho* C-H bond in the presence of a mild base (carbonate) followed by formation of cyclometallated intermediate is the key step in the catalytic pathway of C-H bond activation. Jutand *et al*. explored the kinetic studies of the C-H bond arylation of 2-phenylpyridine catalyzed by $Ru(OAc)_2(\eta^6\text{-}C_{10}H_{14})$ (Scheme 1.8). They conclude that the co-product, HOAc works as autocatalytic for monoarylation of 2-phenylpyridine and this reaction is suppressed in the presence of K_2CO_3 because of it quenches the HOAc co-product form in reaction.
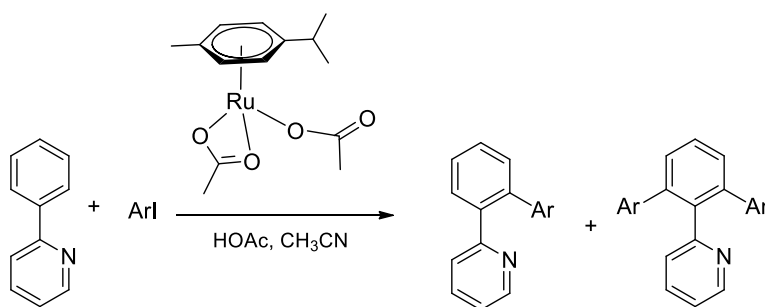
Scheme 1.8. *Arylation of 2-phenylpyridine with aryl halide through C-H bond activation catalyzed by Ru(II) complexes.*

Mechanistic studies show that the interaction of *ortho* carbon of 2-phenylpyridine with Ru(II) center is followed by intermolecular deprotonation with the help of decoordinated carboxylate species. In Scheme 1.9 two Ru[II] key intermediate species A and B[+], species A is formed by intermolecular deprotonation

of 2-phenylpyridine by AcO⁻ ion present in the solution and species B⁺ formed by substitution of AcO⁻ by solvent which is active for oxidative addition of aryl halide. Hence carboxylic acid play important role via accelerating the rate of acetate dissociation from $Ru(OAc)_2(C_{10}H_{14})$ thus enhancing the formation of species B⁺ from species A (Scheme 1.9).
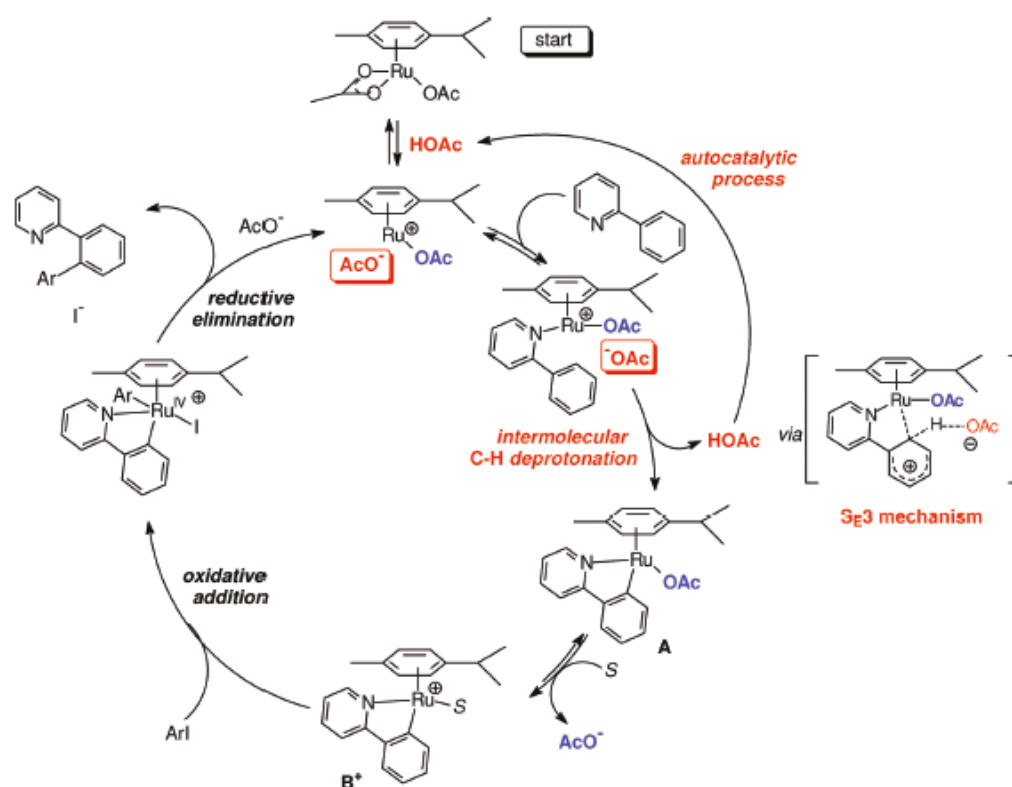
Scheme 1.9. *Autocatalysis for C-H bond activation of 2-phenylpyridine catalyzed by arene-Ru(II) complexes. Adapted from ref. 29h with permission from American Chemical Society.*

1.5.5. Half sandwich arene-Ru(II) catalyzed transfer hydrogenation of ketones

Along with the Rh(I) and Ir(III) based complexes, (η^6-arene)-ruthenium(II) based half sandwich complexes have also gained great attention towards transfer hydrogenation of ketones because of their ability to form metal-hydrides, a key intermediate species for transfer hydrogenation of ketones.[31] Most of the ligands explored for such arene-Ru(II) half sandwich complexes catalyzed transfer hydrogenation reactions are those containing N, O, S, C and P donor atoms.
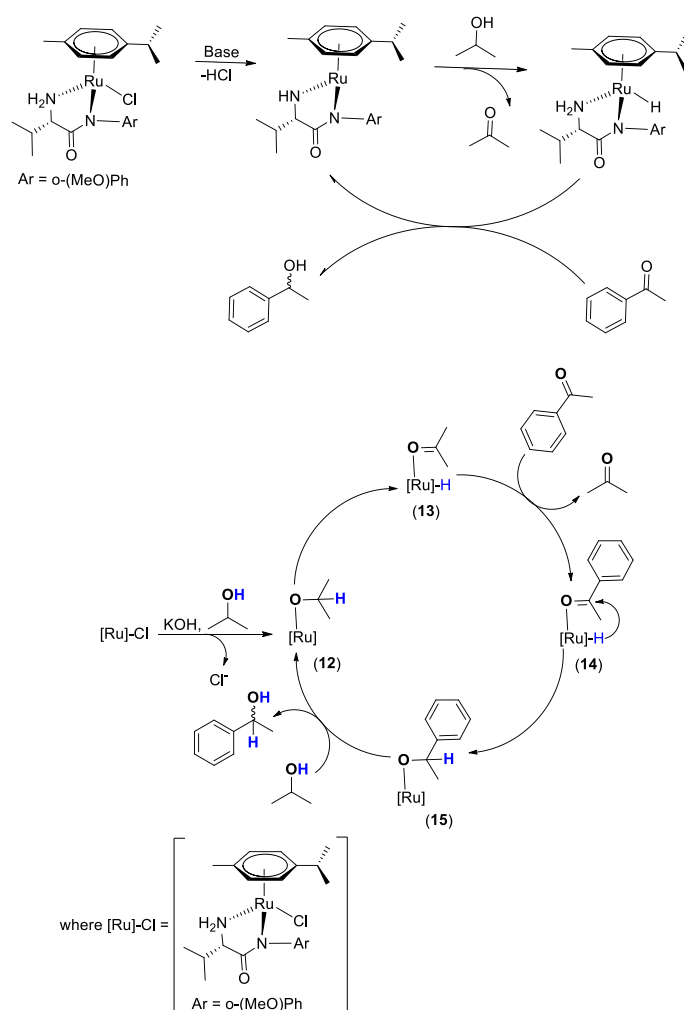
Scheme 1.10. *Catalytic transfer hydrogenation of acetophenone over half sandwich arene-Ru(II) complexes. Reproduced from ref. 31a.*

Rogolino *et al.* reported that arene-Ru(II) complexes containing nitrogen based amino-amide ligands have been effectively applied for the asymmetric transfer hydrogenation of ketones in the presence of KOH and isopropanol. These synthesized complexes were found to have application in a wide range of ketone to corresponding alcohol. In the mechanistic investigation of catalytic transfer hydrogenation reaction start with the formation of Ru-iso-propoxide complex (**12**), subsequent β-elimination gives active Ru-H species (**13**) is followed by coordination of substrate with ruthenium metal center (**14**). In the next step, the transfer of hydride from metal center to carbonyl group of substrate to form corresponding alcohol (Scheme 1.10). Activity and selectivity of these complexes is easily tuned by substitutions on amine and carbon of amino-amide group of ligands.

1.5.6. Aldehyde-water shift reaction catalyzed by arene-Ru(II) complexes

Carboxylic acid is a one of the important classes of fundamental organic group because of its wide applications in the field of organic chemistry. They used as a precursor for synthesis of various organic functional groups like ester, amide etc. They also explore in synthesis of polyester (plastics) as one monomer units.

Recently Goldberg *et al.* reported efficient and selective aldehyde-water shift reaction catalyzed by using half sandwich (η^6-C$_{10}$H$_{14}$)-Ru(II) precatalysts, where water used as an oxidant to convert aldehydes in to carboxylic acids. This type of reaction is also known as "aldehyde-water shift" (AWS) reaction (Scheme 1.11).[32] Herein, they report a homogeneous catalyst which give both higher conversion and selectivity for AWS reaction. This is explored by a series of (η^6-C$_{10}$H$_{14}$)-Ru(II) complexes (**16**, **17**, **18** and **19**) and shows its role to control the conversion and selectivity of product. However, the previously reported results suggest some of the mononuclear catalyst for AWS reactions to gives either low conversion high selectivity or high conversion low selectivity. Previously reported catalyst [(η^6-C$_{10}$H$_{14}$)Ru-(bpy)OH$_2$][OTf]$_2$, for AWS reaction gives higher selectivity (95%) but the conversion of reactant observed is very low (4%) even after a long time and at 105 °C. Interestingly, theoretical calculation suggests a reaction pathway containing metal-hydride as key intermediate for proposed reaction. Most importantly, basicity of metal-hydride bond decides the reactions are aldehyde water shift or disproportionation. For that they explored a series of (η^6-C$_{10}$H$_{14}$)-Ru(II) diamine complexes (Ru(TsDPEN), Ru(PDA), Ru(TsPDA) and Ru(TMEDA)) for AWS reaction. AWS reaction catalyzed by Ru(TsDPEN) and Ru(PDA) are always homogeneous in nature during catalytic reaction and give good conversion/selectivity while in the case of Ru(TsPDA) conversion was drastically decreases due insolubility of complexes in reaction mexure. AWS reaction also given by precursor complex ([(η^6-C$_{10}$H$_{14}$)RuCl$_2$]$_2$) and give a similar type of result (72% cov./86% sel.) but after a reaction formation of a dark heterogeneous substance. Ru(TMEDA) also gives a simillar type of results. It indicates that TMEDA decoordinate during catalytic reaction. They conclude that the most active catalyst for AWS reaction are Ru(PDA) because strong basicity of the metal-hydride.
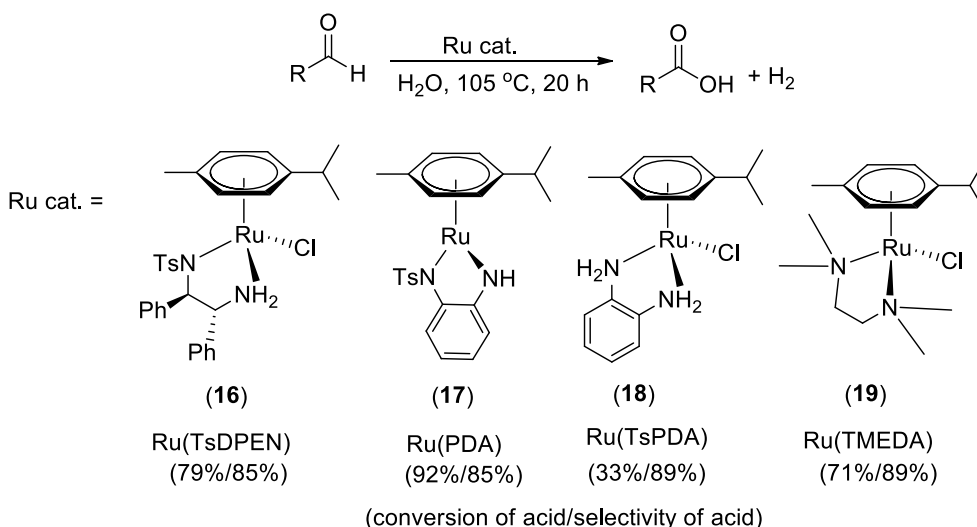
Scheme 1.11. *Aldehyde-water shift (AWS) reaction catalyzed by Arene-Ru(II) complexes. Reproduced from ref. 32 with permission from American Chemical Society.*

1.5.7. Arene-Ru(II) catalyzed conversion of aldehyde to amide

Amide is one of the most important functional group in the field of polymers, natural products and pharmaceuticals. Aldehydes are very important and promising starting materials for synthesis of amide. This is because of its non-toxic nature and easy availability. Moreover, reaction pathway is follows by well known Beckmann-type rearrangement in which transition metal complexes have been catalyzed by one-pot coupling reaction of aldehydes and hydroxylamine for synthesis of primary amides (Scheme 1.12). Herein, the first step *in situ* generation of aldoxime intermediate via Beckmann rearrangement after that dehydration of nitrile and followed by $-C\equiv N$ bond hydration to form corresponding amide. Most importantly very few report for half sandwich arene-ruthenium(II) catalyzed conversion of aldehyde to amide via aldoxime intermediate in aqueous aerobic condition. Cadierno *et al.* reports a half sandwich arene-ruthenium(II) complex $[(\eta^6\text{-}C_6Me_6)RuCl_2\{P(NMe_2)_3\}]$ which gives high yields of amides, from aldehyde through aldoxime rearrangement in aqueous condition but its requirement is higher reaction temperature(100 °C) and inert atmosphere. However, Singh *et al.* explored a catalytic activity of half sandwich arene-ruthenium(II) complexes based on nitrogen donor ligands $[(\eta^6\text{-}\text{arene})RuCl_2(C_6H_5NH_2)]$ (η^6-arene $=$ C_6H_6, $C_{10}H_{14}$) for synthesis of amide from aldehyde via aldoxime intermediate in aqueous aerobic condition in higher selectivity and yield (Scheme 1.12).[33]
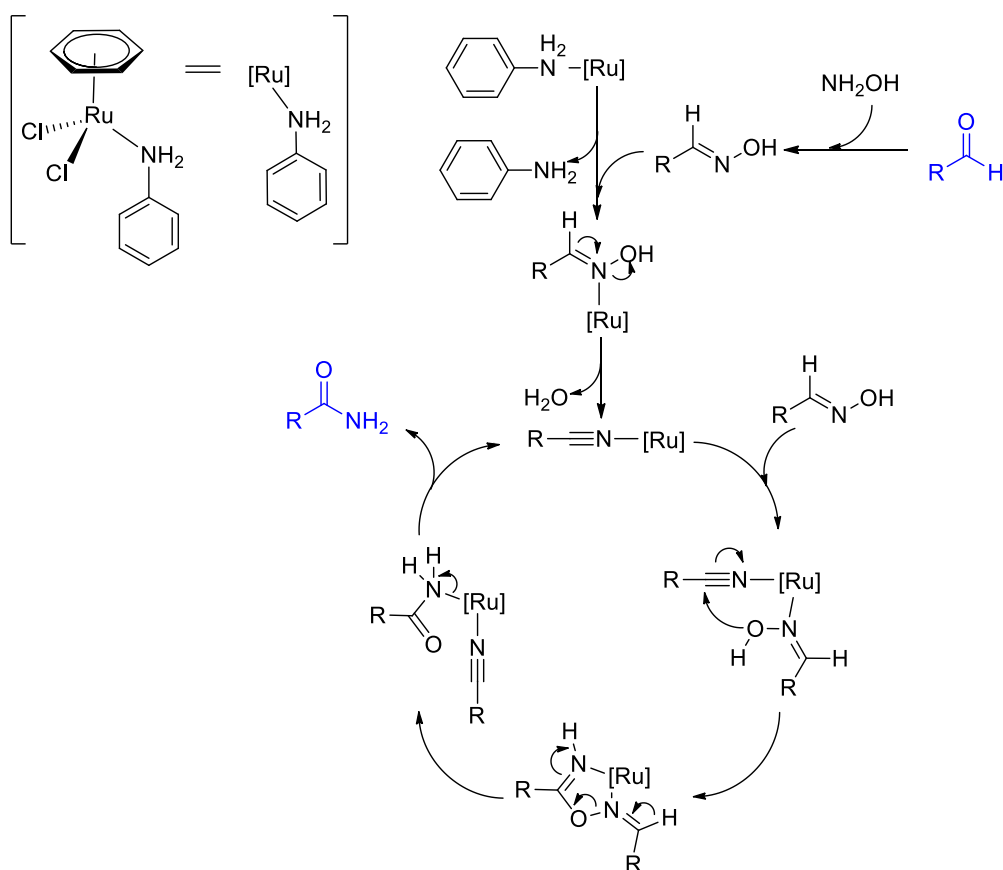
Scheme 1.12. *Half sandwich arene-ruthenium(II) complexes catalyzed the conversion of aldehyde to amide via aldoxime intermediate. Reproduces from ref. 33b with permission from Royal Society of Chemistry.*

1.5.8. Arene-Ru(II) catalyzed dehydrogenation of primary amines to form nitriles

Production of hydrogen is an important and promising area of research because of its use as a substituted energy source. Generation of hydrogen is well explored but main aim is to generation in large extent. For use of hydrogen as alternate energy source, require an efficient system for hydrogen storage and transportation. Recently Mata *et al.* develop a N-heterocyclic carbene (NHC) based catalytic system ($[(\eta^6\text{-}C_{10}H_{14})\text{-}Ru(NHC)Cl_2]$) for potential application of the amine/nitrile pair in the liquid organic hydrogen carrier (LOHC). Here $[(\eta^6\text{-}C_{10}H_{14})\text{-}Ru(NHC)Cl_2]$ is active and efficient catalyst for conversion of primary amine to nitrile with generation of two mole of hydrogen gas (Scheme 1.13). [34]
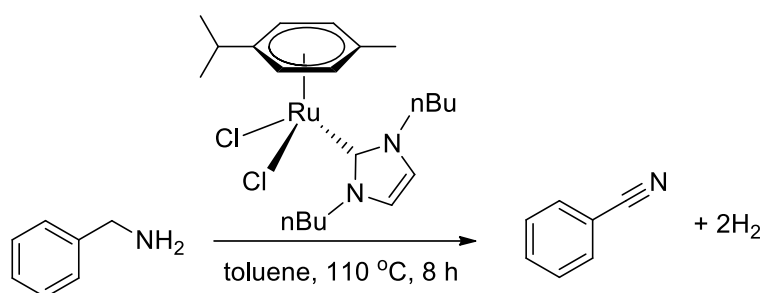
Scheme 1.13. *Catalytic dehydrogenation of benzyl amine to benzonitrile.*
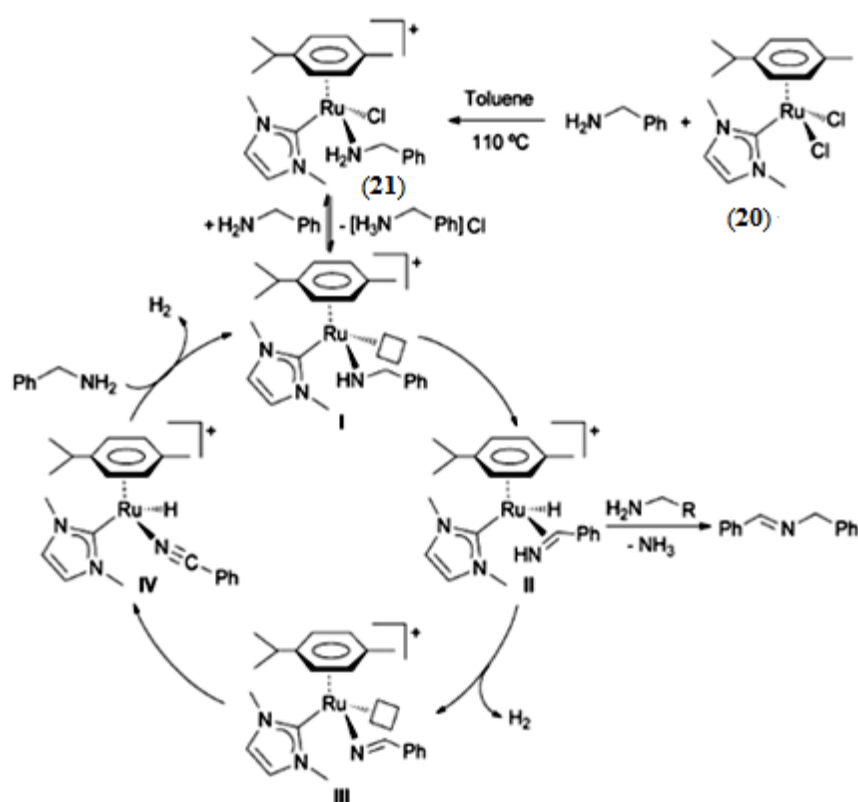
Scheme 1.14. *Proposed reaction pathway for the dehydrogenation of primary amines catalyzed by [(η^6-$C_{10}H_{14}$)Ru(NHC)Cl$_2$] complexes. Adapted from ref. 34 with permission from Willey Online Library.*

In mechanistic investigation activation of catalyst is temperature dependent, in first step catalyst activated by substitution of chloride by amine in catalyst ([(η^6-$C_{10}H_{14}$)-Ru(NHC)Cl$_2$]) (**20**) to form **21**. Complex **21** is equilibrium with complex **I** promoted by second molecule of amine. Species **II** (ruthenium hydride-imine) formed by β elimination of complex **I**. Formation of imine byproduct by the attack of

second molecule of amine on species **II**. An important step of these catalytic cycles is the release of two hydrogen molecule. They proposed that the releases of two hydrogen molecules, one from ruthenium hydride species (**II**) and one from coordinated imine ligands of species **IV** and most probably it release as dihydrogen species. (Scheme 1.14.)

1.6. Catalytic reactions based on half sandwich cyclopentadienyl-ruthenium(II) complexes

Cyclopentadienyl group is one of the important and most ubiquitous ligands in the field of organometallic chemistry. Development of cyclopentadienyl-Ru(II) (η^5-C_5H_5-Ru(II)) complexes has paid remarkable interest.[9] Cyclopentadienyl containing ruthenium complexes have been the interesting topic for many research groups in past five decades because of its potential application as a starting material. A wide range of catalytic reactions of the cyclopentadienyl ruthenium complexes like hydrogen transfer, hydrosilylation, asymmetric synthesis, small molecule activation, ring closing metathesis biological application, etc is reported due to its stability, chemical reactivity and structural properties.[9b] One of the most important (η^5-C_5H_5)-Ru(II) based catalyst for transfer hydrogenation is Shvo's catalyst, which established the participation of metal and the ligand to control the reactivity and selectivity.[18]

Synthesis and characterization of cyclopentadienyle based half sandwich complexes with various monodentate and bidentate (homo/hetero) ligands also show a broad area of research. It also has great potential to be used for a homogeneous catalysis in various transformation reactions. Cyclopentadienyl-Ru(II) complexes shows higher stability toward acid and water even at higher temperature and pressure in comparison to the arene-ruthenium(II) based half sandwich complexes because of bonding between ruthenium metal center and anionic cyclopentadienyl ligand. Bonding between metal center and anionic cyclopentadienyl ligand is stronger than the bonding between metal center and neutral η^6-arene ligand. Synthesis of dicationic, monocationic or neutral cyclopentadienyl-ruthenium(II) complexes is depends on the type of ligand used bidentate (homo or hetero) or monodentate (Scheme 1.15).
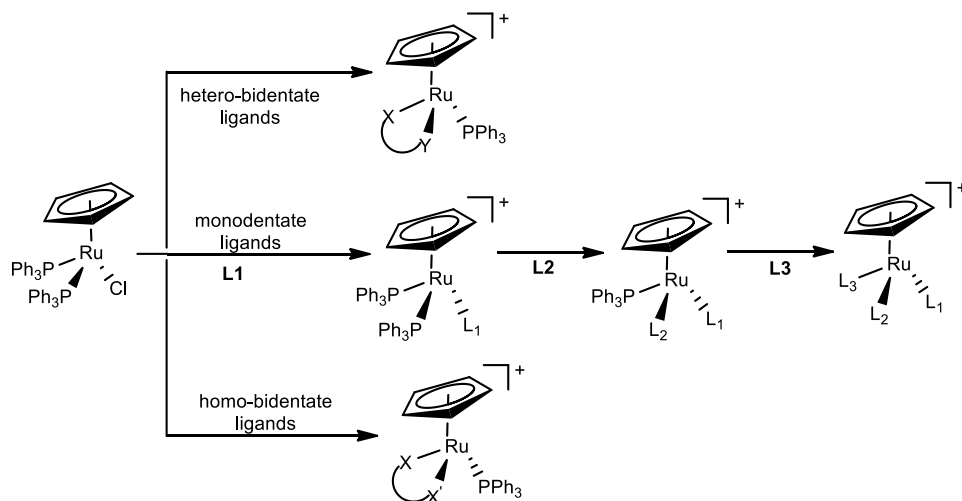
Scheme 1.15. *Synthesis of (η^5-C$_5$H$_5$)-Ru(II) complexes based on various mono/bidentate ligands.*

1.6.1. Cyclopentadienyl-Ru(II) catalyzed transfer hydrogenations reaction

Recently Nikonov *et al*. proposed a mechanistic pathway for transfer hydrogenation reaction catalyzed by half sandwich cyclopentadienyl-Ru(II) complexes in the presence of ammonium formate. The pre-catalysts **22** were first converts into **23** and **24**. After that formation of hypothetical 16e$^-$ κ^1-formate complex Cp(^{i}Pr$_3$P)Ru(κ^1-O$_2$CH) (**25**) by heating followed by the elimination of CO$_2$ via the β-hydrogen shift to give the metal hydride species (**26**). The species **26** coordinates with the substrate to form an intermediate species Cp(^{i}Pr$_3$P)RuH(η^2-O=CMePh) (**27**). Species **27** gives the corresponding alcohol as a product after the migration of hydride from metal center to substrate and metathesis with ammonium formate. Finally regenerates the catalyst (**25**) for next catalytic cycle (Scheme 1.16). Nikonov *et al*. conclude that the complex **23** and **24** are active catalyst for transfer hydrogenation reaction. [35]
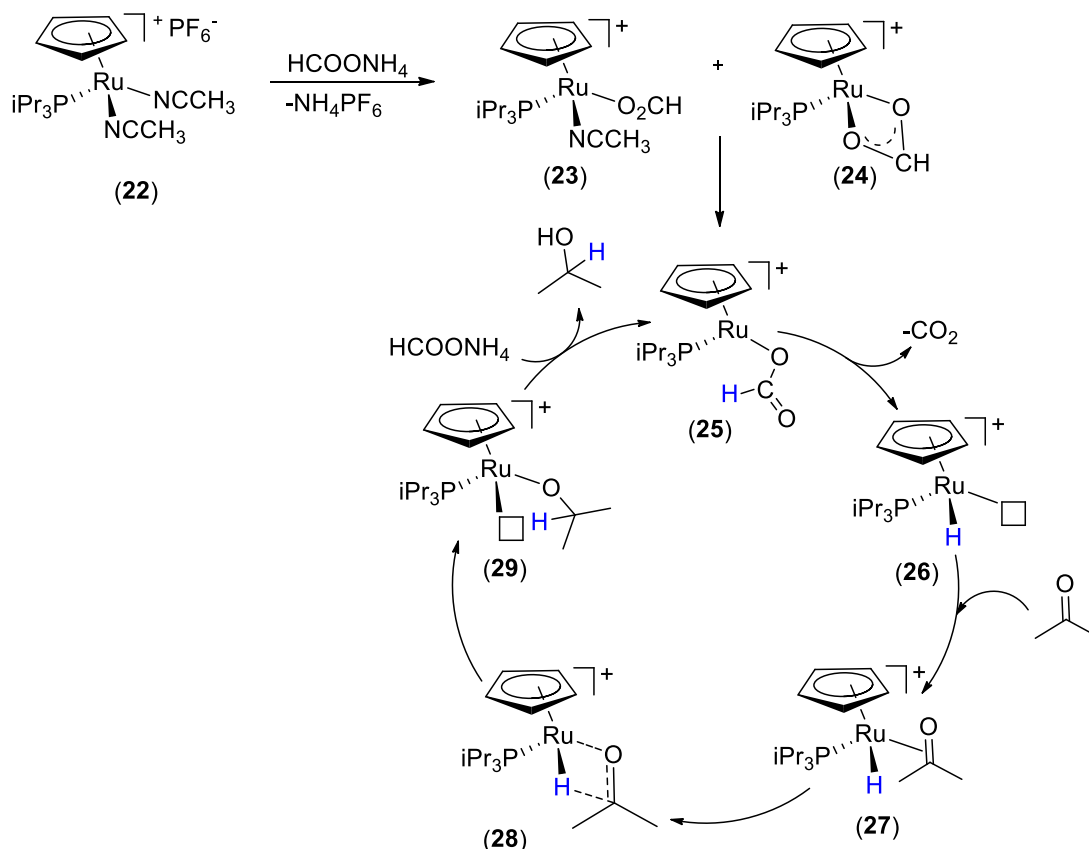
Scheme 1.16. *Proposed mechanism of cyclopentadienyl-Ru(II) catalyzed transfer hydrogenation. Reproduced from ref. 35a with permission from Willey Online Library.*

1.6.2. C-H bond activation catalyzed by half sandwich (η^5-C₅H₅)-Ru(II) complexes

A new synthetic route of selective incretion of a new functional group via C-H bond activation (new C-C bond formation) has been found to be an efficient methodology for various organic syntheses including researcher and industries. It is most important and applicable for synthesis of target-oriented organic compounds.

Sames *et al.* explored selective C-H bond functionalization over a cyclopentadienyl-Ru(II) complexes.[36] They selected 2-phenylimidazole as core moiety for selective arylation via C-H functionalization. C-4 arylation of 2-phenylimidazole was achieved by using iodoarenes as the aryl donors. It is catalyzed by Pd/PPh₃ (palladium catalyst) and magnesium oxide as the base. Switching of arylation from C-4 to C-2' position was achieved by using a ruthenium complex as a catalyst [(η^5-C₅H₅)-Ru(Ph₃P)₂Cl] and Cs₂CO₃ as a base. They found that [(η^5-C₅H₅)-Ru(Ph₃P)₂Cl] is a most efficient catalytic for selective C-2' arylation of 2-

phenylimidazole in a good yield of monoarylated products (84%), the scope of [(η^5-C$_5$H$_5$)-Ru(Ph$_3$P)$_2$Cl] catalyzed C-2' arylation was explored by the substitution on aryl halide. Yield depends on nature of substituent (electron-withdrawing and electron-donating) presents on arylhalide (Scheme 1.17).
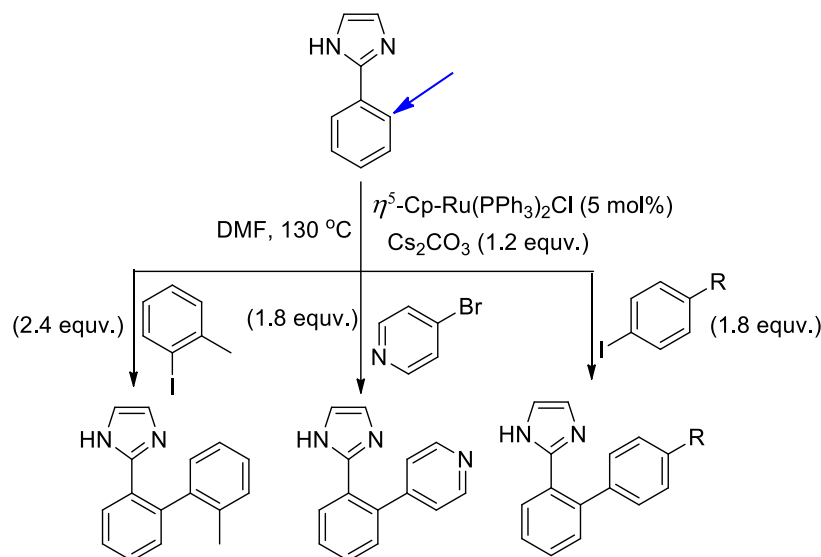
Scheme 1.17. *Selective 2'-Arylation of 2-Phenylimidazole catalyzed by (η^5-C$_5$H$_5$)-Ru(II) complexes.*

1.6.3. Half-Sandwich cyclopentadienyl-ruthenium(II) catalyzed C-C Coupling reactions between alkenes and diazo compounds

In past few decades, researchers have given more attention towards C-C coupling reaction due to their wide application in synthesis of various heteroarene, natural products and pharmaceuticals. In this context, Rigo *et al.* demonstrates the catalytic application of [(η^5-C$_5$H$_5$)Ru(PPh$_3$)$_2$Cl] (**30**) for cyclopropanation reaction of styrene and other alkenes in the presence of ethyl diazoacetate (EDA) with high cis selectivity. Half-sandwich ruthenium complexes have been proved as an promising candidate for catalytic cyclopropanation of styrene with ethyl diazoacetate in the absence of solvent molecule (Scheme 1.18).[37]Catalytic activity of [(η^5-C$_5$H$_5$)Ru(PPh$_3$)$_2$Cl] kind of ruthenium complexes depends on relative strength for phosphine dissociation. Further, the attack of EDA on 16e⁻ species (**31**) to form the ruthenium carbene complex (**32**) is followed by nucleophilic attack of styrene on carbene complex. Rigo and co-workers conclude that catalytic pathway for cis selectivity has gone through carbene intermediate [(η^5-C$_5$H$_5$)Ru(=CHCO$_2$-Et)(PR$_3$)Cl] .

23
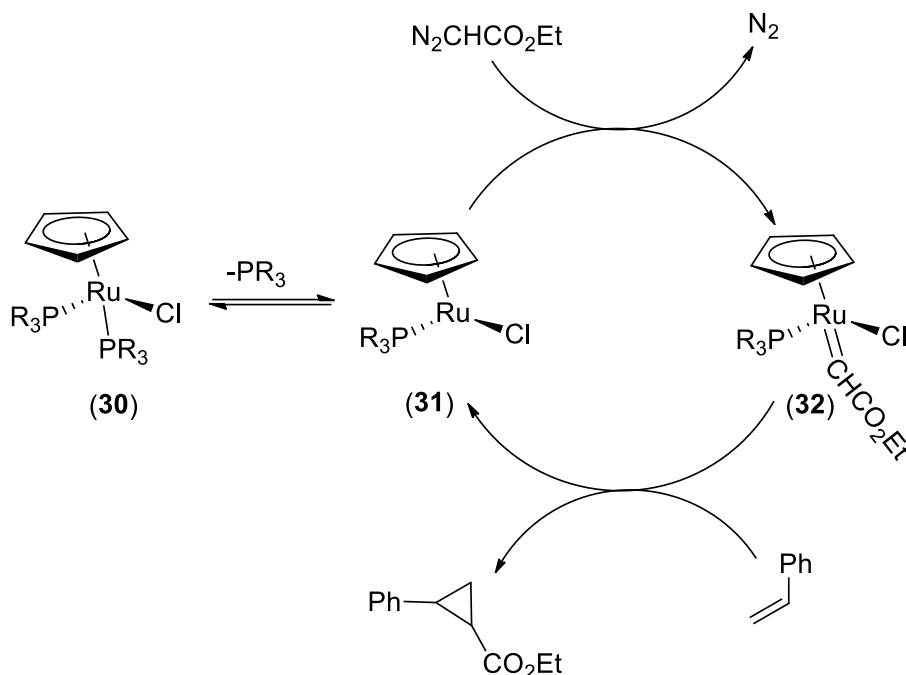
Scheme 1.18. *Half-Sandwich cyclopentadienyl-ruthenium(II) catalyzed cyclopropanation of styrene with ethyl diazoacetate. Reproduced from ref. 37.*

1.6.4. Cp* Iridium(III) half-sandwich complexes catalyzed hydrolytic ring opening of 5-HMF to diketones

5-Hydroxymethylfurfural (5-HMF) is a flexible platform feedstock, which comes after selective dehydration of fructose and from isomerization/dehydration of glucose. It is one of the 5-HMF and regarded as one of the potential building blocks for production of value added chemicals and fuels. It is a starting material for various important chemicals such as levulinic acid (LA), 1-hydroxyhexane-2,5-dione (1-HHD), 2,5-bis(hydroxymethyl)furan, alcohols, 2,5-dimethylfuran and so on, which obtained after hydrogenation and/or hydrolysis of 5-HMF. These synthesized chemicals have been further used as precursor for various industrial applications like, fuel additives, polymers, preparation of dyes, and pharmaceutical applications. Mostly, diketones and its derivatives are used to synthesis of a wide range of valuable chemicals like, amines, pyrrolidine, alcohols, and cycloketones.

Recently, Zhang *et al*. reported the catalytic ring opening of 5-HMF to bioketone, which catalyzed by Cp*-Iridium(III) halh sandwich complexes.[38] It is a new methodology for synthesis of ketones via one-step catalytic reaction of

bioderived 5-hydroxymethylfurfural and its derivatives. Bipyridine based Cp*-Iridium(III) complexes exhibit higher catalytic activity for hydrogenation/hydrolytic ring opening of 5-HMF and derivatives to diketones. The mechanistic investigation of catalytic reaction gives the first carbonyl group to get reduced to hydroxyl group. This assist and enhance the hydrolytic ring opening, followed by hydrogenation of α,β-unsaturated carbonyl species to give final product (Scheme 1.19).
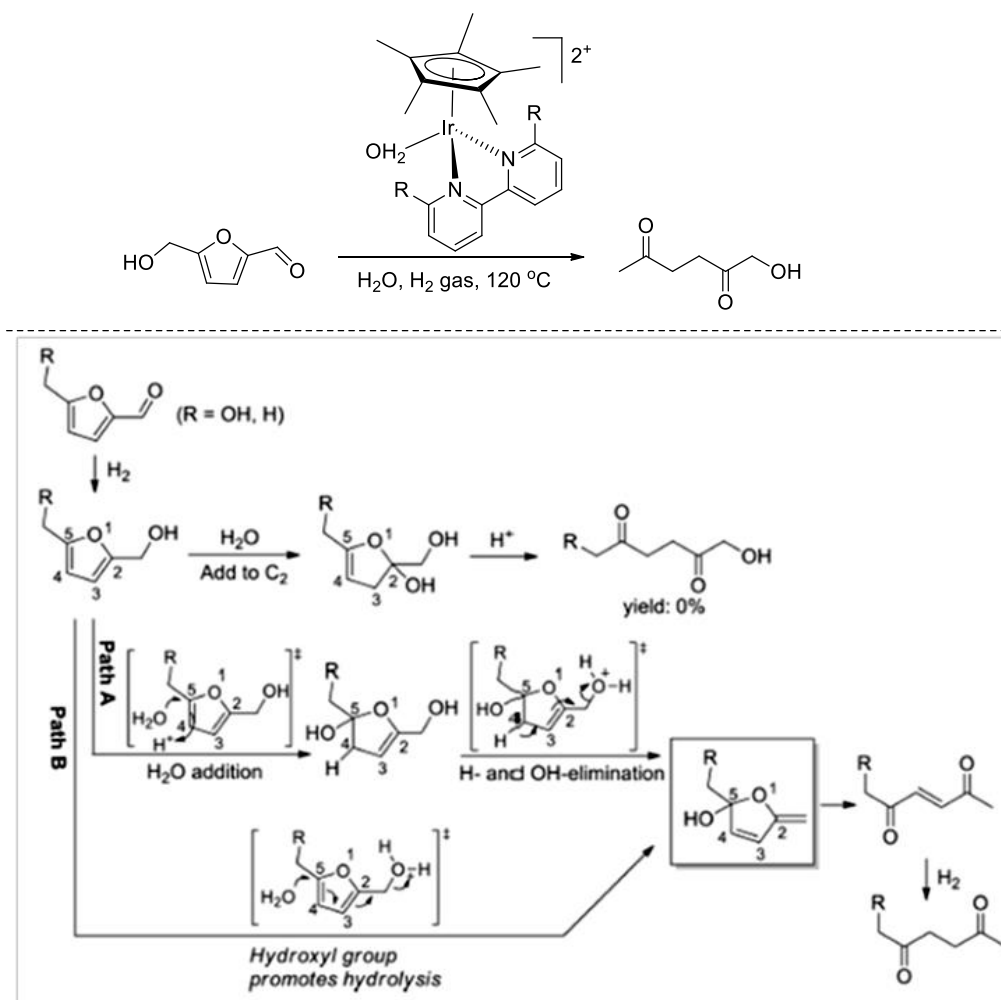
Scheme 1.19. *Catalytic ring opening 5-HMF to bio-diketones. Adapted from ref. 38 with permission from American Chemical Society*

1.7. Mechanistic aspects of the catalytic reactions

One of the most important characteristics of homogeneous catalysts is their easy study and understanding of catalytic reaction mechanism, which provides the exact

information about catalytic reaction pathway. It is a powerful tool to interpret the reaction pathway for particular catalytic reaction. It helps to find limitations of a particular type of reaction and also help to overcome for those limitations. Mechanistic investigations provide better understanding of the catalytic pathway to overcome the limitations like the efficiency of the catalyst, thus increasing the catalytic activity and selectivity of the reaction. In literature, various reports shows that the studies focus on reaction pathway with the help of various instrumental techniques.[39] To understand the exact reaction pathway, various experimental techniques, NMR[29h] (^{1}H, ^{13}C, ^{31}P etc.), GC-MS[38a] and mass[40] spectrometric analysis are the most widely used for characterization of *in situ* generated catalytically active intermediates species. FT-IR and UV spectroscopic studies also found the interactions between catalyst and substrate by showing difference in absorption band of metal coordinated species in comparison to starting substrate. One of the most important tools to trap and isolate the intermediate species is crystallization by slow evaporation of solvent, rapid cooling, diffusion of different solvents, layering of immiscible solvents etc. This species further characterized by single crystal X-ray diffraction studies. Isotopic labeling technique is also one of the important tools to provide extensive information about the product formation and catalytic pathway by the exchange of isotope.[38b] DFT study as a modern technique for mechanistic investigation, also gives fate of different active intermediate species. It also gives information about the stability of different intermediate species by different calculations related to energy for intermediate species. To study the rate of reaction and effect of reaction conditions on the rate of chemical reaction performed a kinetic study for catalytic reaction. Kinetic study[41] gives information about the rate determining step and transition state of reaction.

1.8. Objectives of my thesis

The designing, synthesis and characterization of highly efficient half sandwich transition-metal complexes and its catalytic activity in the area of homogeneous catalysis for synthesis of highly demanded and valuable organic compounds which have industrial importance. To fulfill the fundamental requirement of industries, half sandwich ruthenium complexes are found to be most suitable contestant among other transition metals complexes by virtue of their versatile activity and unique

functionalities. Thus, inspired by the versatile activities of ruthenium based metal complexes, this thesis is targeted to achieve following goals.

- To synthesized a highly efficient, environmentally benign, and robust catalytic system based on substituted ethylenediamine donor arene-ruthenium(II) complexes, for the ruthenium and formic acid based tandem catalytic transformation of bioderived furans to levulinic acid and diketones in aqueous aerobic conditions.

- To study the catalytic activity of ethylenediamine ligand based half-sandwich arene-ruthenium(II) complexes, for the ring hydrogenation of arenes in water over *in situ* generated ruthenium nanoparticles immobilized on carbon.

- To design and develop the troponate/aminotroponate based half sandwich arene- ruthenium(II) complexes and study their ligand-tuned mechanistic pathway for direct C-H bond arylation with aryl chlorides in water.

- To design and synthesized a series of cyclopentadienyl-ruthenium(II)-pyridylamine complexes and their application in catalytic transformation of bio-derived furans to levulinic acid and diketones in water.

1.9. Strategy adopted during the study

- Design and development of metal complex with suitable ligand
- Characterization of synthesized complexes by various instrumental techniques (NMR, MS, Single crystal-XRD, FT-IR, UV-Vis spectroscopy, elemental analyses, Thermogravimetrical analysis)
- Optimization of reaction condition:
- Effect of reaction temperature and time
- Effect of solvent
- Catalysts screening and loading
- Effect of reaction atmosphere
- Effect of additives
- Scope of the reaction:
    a. Study a variety of substrate
- Isolation and purification of products:
    a. Isolation and purification by column chromatography

27

- Applicability of products/catalyst:
  a. Extensive literature study for the plausible application of synthesized products in various field like industries, pharmaceuticals etc.
  b. Applicability of synthesized complexes for the gram scale synthesis for industrially important reactions.
- Mechanistic study by:
  a. Isolation and crystallization of key intermediates species characterization by Mass, NMR and single-crystal X-ray diffraction studies
  b. To understand the reaction pathway with the help of UV-Vis, GC-MS and FT-IR spectroscopic analysis
  c. DFT study for different intermediate species

1.10. Organization of thesis

In *chapter 1*, significant literature reports for history and background of half sandwich transition metal complexes, their synthesis and catalytic applications in various organic transformation reactions with mechanistic investigations have been presented.

In *chapter 2*, design, synthesis and characterization of ethylenediamine based half-sandwich ruthenium complexes and study of ruthenium, formic acid based tandem catalytic transformation of bioderived furans to levulinic acid and diketones in water.

In *chapter 3*, study the catalytic ring hydrogenation of arenes in water over *in situ* generated ruthenium nanoparticles immobilized on carbon.

In *chapter 4*, troponate-/aminotroponate ruthenium-arene complexes: synthesis, structure and ligand tuned mechanistic pathway for direct C-H bond arylation with arylchlorides in water.

In *chapter 5*, cyclopentadienyl-Ru(II)-pyridylamine/pyridylimine complexes for the transformation of furans to its ring open products.

In *chapter 6*, conclusion and future scope of the present thesis work has been described with the findings and limitations.

1.11. References

1. Greenwood N. N., Earnshaw A. (1997), ˈ*Chemistry of the elements*ˈ, Second ed., Elsevier, Oxford (ISBN: 9780080501093).

2. Qu P., Thompson D. W., Meyer G. L. (2000), Temperature-dependent electron injection from Ru(II) polypyridyl compounds with low lying ligand field states to titanium dioxide, *Langmuir*, 16, 4662-4671 (DOI: 10.1021/la0001528).

3. Naota T., Takaya H., Murahashi S.-I. (1998), Ruthenium-Catalyzed Reactions for Organic Synthesis, *Chem. Rev.*, 98, 2599-2660 (DOI: 10.1021/cr9403695).

4. Guo X., Deng G., Lia C.-J. (2009), Ruthenium-Catalyzed Oxidative Homo-Coupling of 2-Arylpyridines, *Adv. Synth. Catal.*, 351, 2071-2074 (DOI: 10.1002/adsc.200900375).

5. Arockiam P. B., Fischmeister C., Bruneau C., Dixneuf P. H. (2013), Ruthenium(II)-catalyzed selective monoarylation in water and sequential functionalisations of C–H bonds, *Green Chem.*, 15, 67-71 (DOI: 10.1039/c2gc36222h).

6. Nielsen M., Alberico E., Baumann W., Drexler H.-J., Junge H., Gladiali S., Beller M. (2013), Low-temperature aqueous-phase methanol dehydrogenation to hydrogen and carbon dioxide, *Nature*, 495, 85-89 (DOI:10.1038/nature11891).

7. Pandiarajan D., Ramesh R. (2013), Ruthenium(II) half-sandwich complexes containing thioamides: Synthesis, structures and catalytic transfer hydrogenation of ketones, *J. Organomet. Chem.,* 723, 26-35 (DOI: 10.1016/j.jorganchem.2012.10.003).

8. Elschenbroich C. (2006), ”*Organometallics*” Wiley-VCH: Weinheim, (ISBN 978-3-527-29390-2).

9. (a) Kumar P., Gupta R. K., Pandey D. S. (2014), Half-sandwich arene ruthenium complexes: synthetic strategies and relevance in catalysis, *Chem. Soc. Rev.*, 43, 707-733 (DOI: 10.1039/c3cs60189g); (b) Kumar P., Singh A. K., Sharma S., Pandey D. S. (2009), Structures, preparation and catalytic activity of ruthenium cyclopentadienyl complexes based on pyridyl-phosphine

ligand. *J. Organomet. Chem.*, 694, 3643-3652 (DOI: 10.1016/j.jorganchem.2009.07.011); (c) Ganter C. (2003), Chiral organometallic half-sandwich complexes with defined metal configuration. *Chem. Soc. Rev.*, 32, 130-138 (DOI: 10.1039/b205996g).

10. (a) Ferrer Flegeau E., Bruneau C., Dixneuf P. H., Jutand A. (2011), Autocatalysis for C–H Bond Activation by Ruthenium(II) Complexes in Catalytic Arylation of Functional Arenes, *J. Am. Chem. Soc.*, 133, 10161-10170 (DOI: dx.doi.org/10.1021/ja201462n); (b) Smith G. S., Therrien B. (2011), Targeted and multifunctional arene ruthenium chemotherapeutics, *Dalton Trans.*, 40, 10793-10800 (DOI: 10.1039/c1dt11007a).

11. Habtemariam A., Melchart M., Ferna`ndez R., Parsons S., Oswald I. D. H., Parkin A., Fabbiani F. P. A., Davidson J. E., Dawson A., Aird R. E., Jodrell D. I., Sadler P. J. (2006), Structure-Activity Relationships for Cytotoxic Ruthenium(II) Arene Complexes Containing N,N-, N,O-, and O,O-Chelating Ligands, *J. Med. Chem.*, 49, 6858-6868 (DOI: 10.1021/jm060596m).

12. Ikariya T., Blacker A. J. (2007), Asymmetric Transfer Hydrogenation of Ketones with Bifunctional Transition Metal-Based Molecular Catalysts, *Acc. Chem. Res.*, 40, 1300-1308 (DOI: 10.1021/ar700134q).

13. (a) Fujii A., Hashiguchi S., Uematsu N., Ikariya T., Noyori R. (1996), Ruthenium(II)-Catalyzed Asymmetric Transfer Hydrogenation of Ketones Using a Formic Acid-Triethylamine Mixture, *J. Am. Chem. Soc.*, 118, 2521-2522 (DOI: 10.1021/ja954126l); (b) Dwivedi A. D., Gupta K., Tyagi D., Rai R. K., Mobin S. M., Singh S. K. (2015), Ruthenium and Formic Acid Based Tandem Catalytic Transformation of Bioderived Furans to Levulinic Acid and Diketones in Water, *ChemCatChem*, 7, 4050-4058 (DOI: 10.1002/cctc.201501021); (c) Gupta K., Tyagi D., Dwivedi A. D., Mobin S. M., Singh S. K. (2015), Catalytic transformation of bio-derived furans to valuable ketoacids and diketones by water-soluble ruthenium catalysts, *Green Chem.*, 17, 4618-4627 (DOI: 10.1039/C5GC01376C).

14. (a) Higgins S. J., Nichols R. J., Martin S., Cea P., van der Zant H. S. J., Richter M. M., Low P. J. (2011), Looking Ahead: Challenges and Opportunities in Organometallic Chemistry, *Organometallics*, 30, 7-12 (DOI: 10.1021/om100919r); (b) Drozdzak R., Allaert B., Ledoux N., Dragutan I., Dragutan V., Verpoort F. (2005), Ruthenium complexes bearing bidentate

Schiff base ligands as efficient catalysts for organic and polymer syntheses, *Coord. Chem. Rev.*, 249, 3055-3074 (DOI: 10.1016/j.ccr.2005.05.003).

15.	Farnetti E., Di Monte R., Kašpar J. (2009), Inorganic and Bio-Inorganic Chemistry -Volume 2, Encyclopedia of life support system, University of Trieste, Trieste, Italy (ISBN: 978-1-84826-664-3).

16.	(a) Rouh A. M. (2004), Chiral Chemistry, *Chem. Eng. News Arch.*, 82, 47-62 (DOI: 10.1021/cen-v082n024.p047); (b) Birch, A. J., Williamson, D. H. (2011), Homogeneous Hydrogenation Catalysts in Organic Synthesis, *Organic Reactions*, 24, 1-186 (DOI: 10.1002/0471264180.or024.01); (c) Thayer A N. N. M. (2007), Cover Story, *Chem. Eng. News Arch.*, 85, 11-19 (DOI: 10.1021/cen-v085n032.p011).

17.	(a) Kumar P., Yadav M., Singh A. K., Pandey D. S. (2010), Synthetic, Spectral, Structural, and Catalytic Aspects of Some *Piano-Stool* Complexes Containing 2-(2-Diphenylphosphanylethyl)pyridine, *Eur. J. Inorg. Chem.*, 704-715 (DOI: 10.1002/ejic.200901004); (b) Espinet P., Soulantica K. (1999), Phosphine-pyridyl and related ligands in synthesis and catalysis, *Coord. Chem. Rev.*, 193-195, 499 (DOI: 10.1016/S0010-8545(99)00140-X).

18.	(a) Blum Y., Shvo Y. (1984), Catalytically Reactive Ruthenium Intermediates in the Homogeneous Oxidation of Alcohols to Esters, *Isr. J. Chem.*, 24, 144-148 (DOI: 10.1002/ijch.198400024); (b) Shvo Y., Czarkie D., Rahamim Y., Chodosh D. F. (1986), A New Group of Ruthenium Complexes: Structure and Catalysis, *J. Am. Chem. Soc.*, 108, 7400-7402 (DOI: 10.1021/ja00283a041); (c) Conley B. L., Pennington-Boggio M. K., Boz E., Williams T. J. (2010), Discovery, Applications, and Catalytic Mechanisms of Shvo's Catalyst, *Chem. Rev.*, 110, 2294-2312 (DOI: 10.1021/cr9003133); (d) Fábos V., Mika L. T., Horváth I. T. (2014), Selective Conversion of Levulinic and Formic Acids to γ-Valerolactone with the Shvo Catalyst, *Organometallics*, *33*, 181-187 (DOI: 10.1021/om400938h); (e) He D., Horvath I. T. (2017), Application of silica-supported Shvo's catalysts for transfer hydrogenation of levulinic acid with formic acid, *J. Organomet. Chem.*, 847, 263-269 (DOI: dx.doi.org/10.1016/j.jorganchem.2017.05.039).

19.	(a) Noyori R., Ohkuma T. (2001), Asymmetric Catalysis by Architectural and Functional Molecular Engineering: Practical Chemo- and Stereoselective Hydrogenation of Ketones, *Angew. Chem., Int. Ed.*, 40, 40-73 (DOI:

10.1002/1521-3773); (b) Dub P. A., Gordon J. C. (2016), The mechanism of enantioselective ketone reduction with Noyori and Noyori-Ikariya bifunctional catalysts, *Dalt. Trans.*, 45, 6756-6781 (DOI: 10.1039/C6DT00476H); (c) Noyori R. (1993), *Asymmetric Catalysis in Organic Synthesis*, John Wiley & Sons: New York, 56-82 (ISBN: 978-0-471-57267-1); (d) Ohkuma T., Ooka H., Yamakawa M., Ikariya T., Noyori R. (1996), Stereoselective Hydrogenation of Simple Ketones Catalyzed by Ruthenium(II) Complexes, *J. Org. Chem.*, 61, 4872-4873 (DOI: 10.1021/jo960997h).

20. Ohkuma T., Ooka H., Ikariya T., Noyori R. (1995), Preferential hydrogenation of aldehydes and ketones, *J. Am. Chem. Soc.*, 117, 10417 (DOI: 10.1021/ja00146a041).

21. (a) Dub P. A., Scott B. L., Gordon J. C. (2017), Why Does Alkylation of the N-H Functionality within M/NH Bifunctional Noyori-Type Catalysts Lead to Turnover?, *J. Am. Chem. Soc.*, 139, 1245-1260 (DOI: 10.1021/jacs.6b11666); (b) Noyori R., Hashiguchi S. (1997), Asymmetric Transfer Hydrogenation Catalyzed by Chiral Ruthenium Complexes, *Acc. Chem. Res.*, 30, 97-102 (DOI: 10.1021/ar9502341); (c) Noyori R., Ohkuma T. (2001), Asymmetric Catalysis by Architectural and Functional Molecular Engineering: Practical Chemo- and Stereoselective Hydrogenation of Ketones, *Angew. Chem., Int. Ed.*, 40, 40-73 (DOI: 10.1002/1521-3773); (d) Haack K.-J., Hashiguchi S., Fujii A., Ikariya T., Noyori R. (1997), The Catalyst Precursor, Catalyst, and Intermediate in the RuII-Promoted Asymmetric Hydrogen Transfer between Alcohols and Ketones, *Angew. Chem., Int. Ed.*, 36, 285-288 (DOI: 10.1002/anie.199702851); (e) Alonso D. A., Brandt P., Nordin S. J. M., Andersson P. G. (1999), Ru(arene)(amino alcohol)-Catalyzed Transfer Hydrogenation of Ketones: Mechanism and Origin of Enantioselectivity, *J. Am. Chem. Soc.*, 121, 9580-9588 (DOI: 10.1021/ja9906610); (f) Yamakawa M., Ito H., Noyori R. (2000), The Metal−Ligand Bifunctional Catalysis: A Theoretical Study on the Ruthenium(II)-Catalyzed Hydrogen Transfer between Alcohols and Carbonyl Compounds, *J. Am. Chem. Soc.*, 122, 1466-78 (DOI: 10.1021/ja991638h).

22. Guan C., Zhang D.-D., Pan Y., Iguchi M., Ajitha M. J., Hu J., Li H., Yao C., Huang M.-H., Min S., Zheng J., Himeda Y., Kawanami H., Huang K.-W. (2017), Dehydrogenation of Formic Acid Catalyzed by a Ruthenium

Complex with an N,N′-Diimine Ligand, *Inorg. Chem.*, 56, 438-445 (DOI: 10.1021/acs.inorgchem.6b02334).

23. (a) Gilkey M. J., Xu B. (2016), Heterogeneous Catalytic Transfer Hydrogenation as an Effective Pathway in Biomass Upgrading, *ACS Catal.*, 6, 1420-1436 (DOI: 10.1021/acscatal.5b02171); (b) Cui X., Surkus A. -E., Junge K., Topf C., Radnik J., Kreyenschulte C., Beller M. (2016), Highly selective hydrogenation of arenes using nanostructured ruthenium catalysts modified with a carbon–nitrogen matrix, *Nat. Commun.*, (DOI: 10.1038/ncomms11326); (c) Zhang J., Teo J., Chen X., Asakura H., Tanaka T., Teramura K., Yan N. (2014), A Series of NiM (M = Ru, Rh, and Pd) Bimetallic Catalysts for Effective Lignin Hydrogenolysis in Water, *ACS Catal.*, 4, 1574-1583 (DOI.org/10.1021/cs401199f).

24. (a) Bi H., Tan X., Dou R., Pei Y., Qiao M., Sun B., Zong B. (2016), Ru–B nanoparticles on metal–organic frameworks as excellent catalysts for hydrogenation of benzene to cyclohexane under mild reaction conditions, *Green Chem.*, 18, 2216-2221 (DOI: 10.1039/c5gc02683k); (b) Yoon B., Pan H.-B., Wai C. M. (2009), Relative Catalytic Activities of Carbon Nanotube-Supported Metallic Nanoparticles for Room-Temperature Hydrogenation of Benzene, *J. Phys. Chem. C*, 113, 1520-1525 (DOI: 10.1021/jp809366w); (c) Morioka Y., Matsuoka A., Binder K., Knappett B. R., Wheatley A. E. H., Naka H. (2016), Selective hydrogenation of arenes to cyclohexanes in water catalyzed by chitinsupported ruthenium nanoparticles, *Catal. Sci. Technol.*, 6, 5801-5805 (DOI: 10.1039/c6cy00899b); (d) Nowicki A., Le Boulaire V., Roucoux A. (2007), Nanoheterogeneous Catalytic Hydrogenation of Arenes: Evaluation of the Surfactant-Stabilized Aqueous Ruthenium(0) Colloidal Suspension, *Adv. Synth. Catal.*, 349, 2326-2330 (DOI: 10.1002/adsc.200700208); (e) Prechtl M. H. G., Scariot M., Scholten J. D., Machado G., Teixeira, S. R., Dupont J.(2008), Nanoscale Ru(0) Particles: Arene Hydrogenation Catalysts in Imidazolium Ionic Liquids, *Inorg. Chem.*, 47, 8995-9001 (DOI: 10.1021/ic801014f).

25. (a) Wei Y., Rao B., Cong X., Zeng X. (2015), Highly Selective Hydrogenation of Aromatic Ketones and Phenols Enabled by Cyclic (Amino)(alkyl)carbene Rhodium Complexes, *J. Am. Chem. Soc.*, 137, 9250-9253 (DOI: 10.1021/jacs.5b05868); (b) Thomas J. M., Johnson B. F. G., Raja R., Sankar

G., Midgley P. A. (2003), High-Performance Nanocatalysts for Single-Step Hydrogenations, *Acc. Chem. Res*., 36, 20-30 (DOI: 10.1021/ar990017q); (c) Gual A., Godard C., Castillón S., Claver C. (2010), Soluble transition-metal nanoparticles-catalysed hydrogenation of arenes, *Dalton Trans.*, 39, 11499-11512 (DOI: 10.1039/c0dt00584c); (d) Qi S. -C., Wei X. -Y., Zong Z. -M., Wang Y. -K. (2013), Application of supported metallic catalysts in catalytic hydrogenation of arenes, *RSC Adv*., 3, 14219-14232 (DOI: 10.1039/c3ra40848e); (e) Zhong J., Chen J., Chen L. (2014), Selective hydrogenation of phenol and related derivatives, *Catal. Sci. Technol*., 4, 3555-3569 (DOI: 10.1039/c4cy00583j).

26.   Moore B. S., Poralla K., Floss H. G. (1993), Biosynthesis of the cyclohexanecarboxylic acid starter unit of .omega.-cyclohexyl fatty acids in Alicyclobacillus acidocaldarius, *J. Am. Chem. Soc.*, 115, 5267-5274 (DOI: 10.1021/ja00065a043).

27.   (a) Hagen C. M., Vieille-Petit L., Laurenczy G., Suss-Fink G., Finke R. G. (2005) Supramolecular Triruthenium Cluster-Based Benzene Hydrogenation Catalysis: Fact or Fiction?, *Organometallics*, 24, 1819-1831 (DOI: 10.1021/om048976y); (b) Widegren J. A., Bennett M. A., Finke R. G. (2003), Is It Homogeneous or Heterogeneous Catalysis? Identification of Bulk Ruthenium Metal as the True Catalyst in Benzene Hydrogenations Starting with the Monometallic Precursor, Ru(II)(η^6-C$_6$Me$_6$)(OAc)$_2$, Plus Kinetic Characterization of the Heterogeneous Nucleation, Then Autocatalytic Surface-Growth Mechanism of Metal Film Formation, *J. Am. Chem. Soc.*, 125, 10301-10310 (DOI: 10.1021/ja021436c); (c) Hagen C. M., Widegren J. A., Maitlis P. M., Finke R. G. (2005), Is It Homogeneous or Heterogeneous Catalysis? Compelling Evidence for Both Types of Catalysts Derived from [Rh(η^5-C$_5$Me$_5$)Cl$_2$]$_2$ as a Function of Temperature and Hydrogen Pressure, *J. Am. Chem. Soc.*, 127, 4423-4432 (DOI: 10.1021/ja044154g).

28.   Crabtree R. H. (2012), Resolving Heterogeneity Problems and Impurity Artifacts in Operationally Homogeneous Transition Metal Catalysts, *Chem. Rev.*, 112, 1536-1554 (DOI: 10.1021/cr2002905).

29.   (a) Singh K. S., Dixneuf P. H. (2013), Direct C-H bond Arylation in Water Promoted by (O,O)- and (O,N)-Chelate Ruthenium(II) Catalysts, *ChemCatChem*, 5, 1313-1316 (DOI: 10.1002/cctc.201300031); (b) Arockiam

P. B., Bruneau C., Dixneuf P. H. (2012), Ruthenium(II)-Catalyzed C–H Bond Activation and Functionalization, *Chem. Rev.*, 112, 5879-5918 (DOI: 10.1021/cr300153j); (c) Giunta D., Hölscher M., Lehmann C W., Mynott R., Wirtz C., Leitner W. (2003), Room Temperature Activation of Aromatic C-H Bonds by Non-Classical Ruthenium Hydride Complexes Containing Carbene Ligands, *Adv. Synt. Catal.*, 345, 1139-1145 (DOI: 10.1002/adsc.200303091); (d) Flender C., Adams A. M., Roizen J. L., McNeill E., Du Bois J., Zare R. N. (2014), Speciation and decomposition pathways of ruthenium catalysts used for selective C-H hydroxylation, *Chem. Sci.*, 5, 3309-3314 (DOI: 10.1039/C4SC01050G); (e) Kozhushkov S. I., Ackermann L. (2013), Ruthenium-catalyzed direct oxidative alkenylation of arenes through twofold C-H bond functionalization, *Chem. Sci.*, 4, 886-896 (DOI: 10.1039/C2SC21524A); (f) Schröder D. (2012), Applications of Electrospray Ionization Mass Spectrometry in Mechanistic Studies and Catalysis Research, *Acc. Chem. Res.*, 45, 1521-1532 (DOI: 10.1021/ar3000426); (g) Arockiam P. B., Bruneau C., Dixneuf P. H. (2012), Ruthenium(II)-Catalyzed C–H Bond Activation and Functionalization, *Chem. Rev.*, 112, 5879-5918 (DOI: 10.1021/cr300153j); (h) Ferrer-Flegeau, E.; Bruneau, C.; Dixneuf, P. H.; Jutand, A. (2011), Autocatalysis for C–H Bond Activation by Ruthenium(II) Complexes in Catalytic Arylation of Functional Arenes, *J. Am. Chem. Soc.*, 133, 10161-10170 (DOI: 10.1021/ja201462n).

30.   (a) Ackermann L., Althammer A., Born R. (2007), [RuCl$_3$(H$_2$O)$_n$]-Catalyzed Direct Arylations with Bromides as Electrophiles, *Synlett*, 2007, 2833-2836 (DOI: 10.1055/s-2007-990838); (b) Ackermann L., Althammer A., Born R. (2008), [RuCl$_3$(H$_2$O)$_n$]-catalyzed direct arylations, *Tetrahedron*, 64, 6115-6124 (DOI: j.tet.2008.01.050); (c) Oi S., Fukita S., Hirata N., Watanuki N., Miyano S., Inoue Y. (2001), Ruthenium Complex-Catalyzed Direct Ortho Arylation and Alkenylation of 2-Arylpyridines with Organic Halides, *Org. Lett.*, 3, 2579-2581 (DOI: 10.1021/ol016257z).

31.   (a) Pelagatti P., Carcelli M., Calbiani F., Cassi C., Elviri L., Pelizzi C., Rizzotti U., Rogolino D. (2005), Transfer Hydrogenation of Acetophenone Catalyzed by Half-Sandwich Ruthenium(II) Complexes Containing Amino Amide Ligands. Detection of the Catalytic Intermediates by Electrospray Ionization Mass Spectrometry, *Organometallics*, 24, 5836-5844 (DOI:

10.1021/om050519); (b) Mohan, N., Ramesh R. (2016), Transfer hydrogenation of ketones catalyzed by half-sandwich (η^6-*p*-cymene) ruthenium(II) complexes incorporating benzoylhydrazone ligands, *Appl. Organometal. Chem.*, 1-9 (DOI: 10.1002/aoc.3648); (c) Yamakawa M., Ito H., Noyori R. (2000), The Metal-Ligand Bifunctional Catalysis: A Theoretical Study on the Ruthenium(II)-Catalyzed Hydrogen Transfer between Alcohols and Carbonyl Compounds, *J. Am. Chem. Soc.*, 122, 1466-1478 (DOI: 10.1021/ja991638h); (d) Gichumbi J. M., Friedrich H. B., Omondi B. (2016), Application of arene ruthenium(II) complexes with pyridine-2-carboxaldimine ligands in the transfer hydrogenation of ketones, *J. Mol. Catal.*, 416, 29-38 (DOI: 10.1016/j.molcata.2016.02.012).

32. Brewster T. P., Goldberg J. M., Tran J. C., Heinekey D. M., Goldberg K. I. (2016), High Catalytic Efficiency Combined with High Selectivity for the Aldehyde-Water Shift Reaction using (para-cymene)Ruthenium Precatalysts, *ACS Catal.*, 6, 6302-6305 (DOI: 10.1021/acscatal.6b02130).

33. (a) R. Garcı́a-Álvarez, Dı́az-Álvarez A. E., Crochet P., Cadierno V. (2013), Ruthenium-catalyzed one-pot synthesis of primary amides from aldehydes in water, *RSC Advances*, 3, 5889-5894 (DOI: 10.1039/c3ra23195j); (b) Tyagi D., Rai R. K., Dwivedi A. D., Mobin S. M., Singh S. K. (2015), Phosphine-free ruthenium-arene complex for low temperature one-pot catalytic conversion of aldehydes to primary amides in water, *Inorg. Chem. Front.*, 2, 116-124 (DOI: 10.1039/c4qi00115j).

34. Ventura-Espinosa D., Marza-Beltran A., Mata J. A. (2016), Catalytic Hydrogen Production by Ruthenium Complexes from the Conversion of Primary Amines to Nitriles: Potential Application as a Liquid Organic Hydrogen Carrier, *Chem. Eur., J.* 22, 17758-17766 (DOI: 10.1002/chem.201603423).

35. (a) Mai V. H., Lee S.-H., Nikonov G. I. (2017), Transfer Hydrogenation of Unsaturated Substrates by Half-sandwich Ruthenium Catalysts using Ammonium Formate as Reducing Reagent, *Chemistry Select*, 2, 7751-7757 (DOI: 10.1002/slct.201701423); (b) Lee S.-H., Gutsulyak D. V., Nikonov G. I. (2013), Chemo- and Regioselective Catalytic Reduction of N-Heterocycles by Silane, *Organometallics*, 32, 4457-4464 (DOI: 10.1021/om400269q); (c) Lee S.-H., Nikonov G. I. (2015), Transfer Hydrogenation of Ketones,

Nitriles, and Esters Catalyzed by a Half-Sandwich Complex of Ruthenium, *ChemCatChem*, 7, 107-113 (DOI: 10.1002/cctc.201402780).

36. Sezen B., Sames D. (2003), Diversity Synthesis via C-H Bond Functionalization: Concept-Guided Development of New C-Arylation Methods for Imidazoles, *J. Am. Chem. Soc.*, 125, 10580-10585 (DOI: 10.1021/ja036157j).

37. (a) Baratta W., Herrmann W. A., Kratzer R. M., Rigo P. (2000), Half-Sandwich Ruthenium(II) Catalysts for C-C Coupling Reactions between Alkenes and Diazo Compounds, *Organometallics*, 19, 3664-3669 (DOI: 10.1021/om0003537); (b) Baratta W., Zotto A. D., Rigo P. (1999), Half-Sandwich Ruthenium(II) Complexes as Catalysts for Stereoselective Carbene-Carbene Coupling Reactions, *Organometallics*, 18, 5091-5096 (DOI: 10.1021/om990582x); (c) Becker E., Stingl V., Mereiter K., Kirchner K. (2006), Formation of a Half-Sandwich Triscarbene Ruthenium Complex: Oxidative Coupling of 2,7-Nonadiyne Mediated by [RuCp(IPr^i)(CH$_3$CN)$_2$]$^+$ (IPri) 1,3-bis(2,6-diisopropylphenyl)imidazol-2-ylidene), *Organometallics*, 25, 4166-4169 (DOI: 10.1021/om060345b).

38. (a) Xu Z., Yan P., Xu W., Liu X., Xia Z., Chung B., Jia S., Zhang Z. C. (2015), Hydrogenation/Hydrolytic Ring Opening of 5-HMF by Cp*-Iridium(III) Half-Sandwich Complexes for Bioketones Synthesis, *ACS Catal.*, 5, 788-792 (DOI: 10.1021/cs501874v); (b) Xu Z., Yan P., Li H., Liu K., Liu X., Jia S., Zhang Z. C. (2016), Active Cp*Iridium(III) Complex with ortho-Hydroxyl Group Functionalized Bipyridine Ligand Containing an Electron-Donating Group for the Production of Diketone from 5-HMF, *ACS Catal.*, 6, 3784-3788 (DOI: 10.1021/acscatal.6b00826).

39. Jia W-G., Zhang H., Zhang T., Xie D., Ling S., Sheng E-H. (2016), Half-Sandwich Ruthenium Complexes with Schiff-Base Ligands: Syntheses, Characterization, and Catalytic Activities for the Reduction of Nitroarenes, *Organometallics*, 35, 503-512 (DOI: 10.1021/acs.organomet.5b00933).

40. (a) Tyagi, D.; Binnani, C.; Rai, R. K.; Dwivedi, A. D.; Gupta, K.; Li, P.-Z.; Zhao, Y.; Singh, S. K. (2016), Ruthenium-Catalyzed Oxidative Homocoupling of Arylboronic Acids in Water: Ligand Tuned Reactivity and Mechanistic Study, *Inorg. Chem.*, 55, 6332-6343 (DOI: 10.1021/acs.inorgchem.6b01115); (b) Dwivedi, A. D.; Binnani, C.; Tyagi, D.; Rawat, K. S.; Li, P.-Z.; Zhao, Y.;

Mobin, S. M.; Pathak, B.; Singh, S. K. (2016), Troponate/Aminotroponate Ruthenium-Arene Complexes: Synthesis, Structure, and Ligand-Tuned Mechanistic Pathway for Direct C−H Bond Arylation with Aryl Chlorides in Water, *Inorg. Chem.*, 55, 6739-6749 (DOI: 10.1021/acs.inorgchem.6b01028).

41. Blackmond, D. G. (2015), Kinetic Profiling of Catalytic Organic Reactions as a Mechanistic Tool, *J. Am. Chem. Soc.*, 137, 10852-10866 (DOI: 10.1021/jacs.5b05841).

Chapter 2

Ruthenium and formic acid based tandem catalytic transformation of bioderived furans to levulinic acid and diketones in water

2.1. Introduction

Development of new methodologies for biomass transformation is gaining extensive attention. As biomass, a viable resource of carbon and extensively dispersed in nature, has shown its potential for the production of carbon-based energy sources and several valuable platform chemicals, it can probably replace or provide an alternative to the currently used fossil fuel and fine chemicals.[1] Since direct usage of biomass is not sustainable to date, the transformation of carbohydrates (monosaccharide or disaccharide)[2-4] or bioderived furans (such as 5-hydroxymethylfurfural (5-HMF) or furfural)[5] to fuel components or chemicals has been extensively studied in recent years, as these are regarded as key components of biomass. In particular, the furans (5-HMF or furfural) has received considerable attention for its transformation to several valuable chemicals and biofuel, possibly due to the inherent structural patterns available in these furans.[5-7] Several chemical processes such as hydrogenation and/or hydrolysis reaction directed transformation of furans to important chemicals such as levulinic acid (LA), succinic acid, diketones, furfuryl alcohol, 2,5-dimethyl furan, 2,5-bis(hydroxymethyl)furan, pentane-2,5-diol and others,[5,6] whereas furan carboxylic acids can be obtained by selective oxidation of formyl groups of furfural and its derivatives.[7] Complete hydrogenation and hydrolytic ring opening of furans and its aldol adduct with extended carbon chain, obtained by aldol condensation of furfural or its derivatives with acetone, may produce C5-C9 alkanes for direct application as a fuel.[8] Moreover, one of the diketone product, 3-hydroxyhexane-2,5-dione (3-HHD), also known as Henze's ketol, obtained during the catalytic transformation of 5-MF, is known for its significant biologicaly activity and was also identified in plant extract.[9] Ketoacids and diketones obtained from the catalytic transformation of furans has been extensively used as platform chemicals for the production of several important fine chemicals (e.g. esters, alcohols, lactones, amines and cycloketones) or biofuel

components as blenders for gasoline.[10] Particularly, ketoacid (LA) has been identified by US-DOE as one of the important target chemicals in their biomass program.[11] Some of the key features such as the presence of carbonyl group, carboxylic group and α-H present in LA, resulted in its usage as an important key starting material in several important reactions for the industrial applications (Scheme 2.1).[12] Some of the very important end products obtained from LA are calcium levulinate (a new supplement for calcium), 5-aminolevulinic acid (photodynamic therapy (PDT) of tumor like human meningioma, and a biodegradable herbicide), γ-valerolactone (GVL) and 2-methyltetrahydrofuran (as fuel blender), and so on.
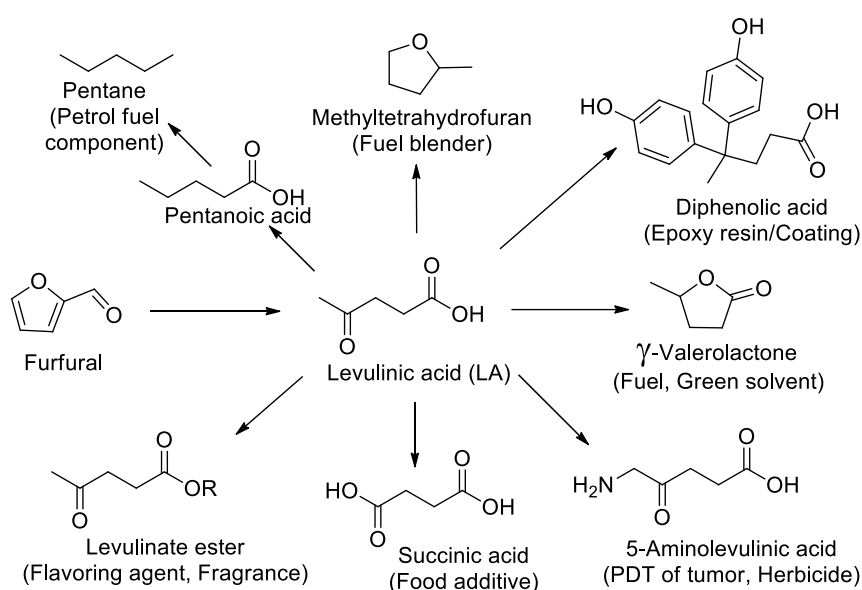
Scheme 2.1. *Selected applications of levulinic acid.*

Several new and diverse catalytic processes for selective transformation of furan derivatives into open ring components are being explored, particularly, using heterogeneous catalysts.[5-7,13-15] For instance, Au nanoparticles were reported for direct conversion of 5-HMF to corresponding diketones by hydrogenation/hydrolytic ring opening in the presence of H_3PO_4.[14] In the same direction, Pd/C catalyst is also reported for similar transformations of 5-HMF/furfural to diketones and ketoacids by using CO_2/H_2O (120 °C) or Amberlyst 70 (170 °C).[15] However, homogenous catalysts for this class of reactions are seldom reported. Zhang *et al.* reported Cp*-iridium complexes catalyzed conversion of furans to ketones, under 20 bar of H_2 gas at 110 °C, where reaction proceeded with catalytic hydrogenation of 5-HMF followed by ring opening reaction facilitated by *in situ* generated acid.[16]

Recently, we also explored the catalytic efficacy of 8-aminoquinoline coordinated arene-ruthenium(II) catalyst for the transformation of furans to LA and diketones.[17]

Arene-Ru(II) complexes, such as ethylenediamine based ruthenium complexes or Shvo's catalyst, represent a well established class of active catalysts for efficient hydrogenation of carbonyl groups in ketones, aldehydes, esters, C-N double bond in imines, or C-C double bonds in styrene or furfuryl alcohol.[18] The excellent synergistic cooperation of metal to ligand in these complexes, such as the availability of N-H bonds to facilitate transfer hydrogenation reactions, accounts the high catalytic performances of complexes for hydrogenation reactions by using H_2 or other alternative H-donor e.g. formic acid.[18,19] These insights encouraged us to employ the arene-Ru(II) complexes containing simple ethylenediamine based ligands for the highly efficient transformation of bioderived furans to open ring components. Moreover, using formic acid not only satisfies the requirement of an H-donor but also also provides plenty of H^+ ions. However, it is worth mentioning here that using excess of acid may lead to humin formation from furan derivatives.[20] Furthermore, the high aqueous solubility and stability displayed by most of the arene-Ru(II) complexes may offer easy recovery and reuse of the catalyst. Although, literature reports highlight the competence of several ruthenium complexes for hydrogenation of furfural and 5-hydroxymethylfurfural (5-HMF) to corresponding alcohols (furfuryl alcohol and 2,5-bis(hydroxymethyl)furan),[21] but employing arene-Ru(II) complexes with formic acid for tandem catalytic transformation of furans is rarely explored.[17] Therefore, to enrich and enhance the understanding about the ruthenium catalyst based catalytic transformation of furans, development of new highly active and water-soluble catalytic systems are highly required.

In our continuous efforts in this direction, we report here the use of highly water soluble arene-Ru(II) complexes containing simple ethylenediamine based ligands for the tandem catalytic transformation of bioderived furans to open ring components (ketoacids and diketones), in water under moderate reaction conditions. A structure-activity relationship in terms of N-H bond availability was also explored. An important reaction intermediate, furfuryl alcohol, was identified by ^{1}H NMR which provided more insights on the mechanism of the catalytic transformation of furfural to LA, and also the role of ruthenium catalyst and the formic acid. Moreover, the biomass feedstock of furans, fructose, was also catalytically transformed to diketones with limited conversion. Herein, we also reported the X-ray structural

characterization of the representative arene-Ru(II) complexes employed for the catalytic reactions.

2.2. Results and Discussion

2.2.1. Syntheses and characterization of arene-Ru(II) catalysts.

Cationic monometallic arene-Ru(II) complexes ([Ru]-1 – [Ru]-8) containing ethylenediamine ligand or its derivatives (Scheme 2.2) were synthesized by treating the dichloro bridged arene-Ru(II) dimer with an appropriate bidentate ethylenediamine based ligand in methanol at room temperature.[22] Identities of the synthesized complexes were established by NMR, elemental analysis and ESI mass, and the results were corroborated well with the proposed formula of the complexes as $[(\eta^6\text{-arene})RuCl(\kappa^2\text{-L})]^+$ (where η^6-arene = C_6H_6 and $C_{10}H_{14}$, and L = $H_2NCH_2CH_2NH_2$ (en), $H_2NCH_2CH_2NH(CH_3)$ (Me$_1$en), $H_2NCH_2CH_2N(CH_3)_2$ (Me$_2$en) and $(CH_3)HNCH_2CH_2N(CH_3)_2$ (Me$_3$en).
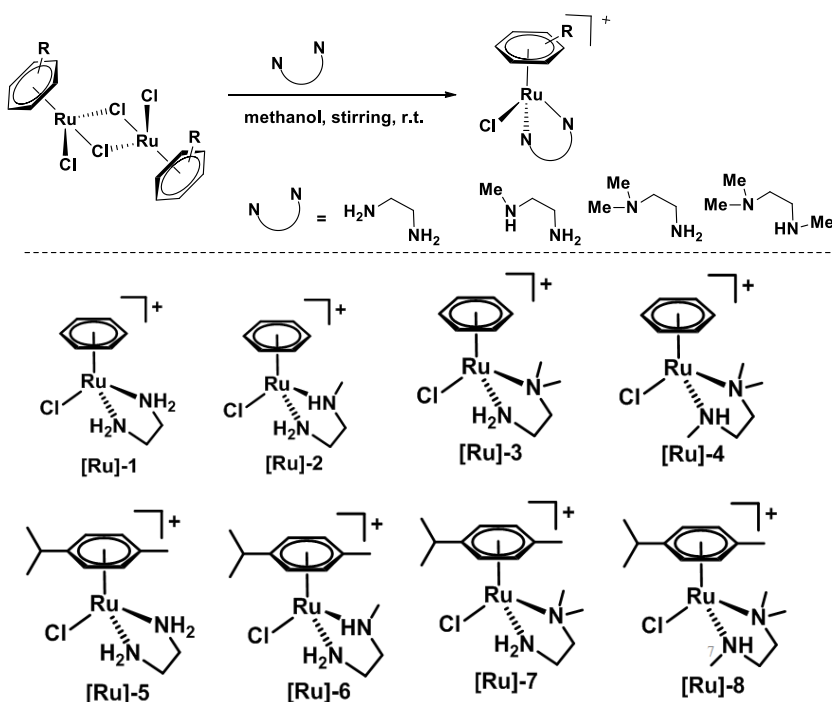
Scheme 2.2. Schematic representation of arene-Ru(II) catalysts [Ru]-1 – [Ru]-8.

Suitable crystals of arene-Ru(II) complexes ([Ru]-2, [Ru]-6, [Ru]-7 and [Ru]-8), grown by slow evaporation of the solution of the respective complexes in methanol/dichloromethane mixture, were subjected to single-crystal X-ray diffraction analysis to confirm the structure as $[(\eta^6\text{-}C_6H_6)RuCl(Me_1en)]PF_6$ ([Ru]-2), $[(\eta^6\text{-}C_{10}H_{14})RuCl(Me_1en)]PF_6$ ([Ru]-6), $[(\eta^6\text{-}C_{10}H_{14})RuCl(Me_2en)]PF_6$ ([Ru]-7) and

$[(\eta^6\text{-}C_{10}H_{14})RuCl(Me_3en)]PF_6$ (**[Ru]-8**), respectively (Figure 2.1-2.4 and Tables 2.1-2.2).

Figure 2.1. *Single crystal X-ray structure of complex **[Ru]-2** with 35% probability of thermal ellipsoids. Anionic counterpart (PF6) and hydrogen atoms (except at nitrogen) are omitted for the sake of clarity. Selected bond length (Å): $Ru1\text{-}C_{avg}$ = 2.141, $Ru1\text{-}C_{ct}$ = 1.658, Ru1-Cl1 = 2.406(3), Ru1-N1 = 2.113(8), Ru1-N2 = 2.153(8), N1-C1 = 1.444(17), N2-C2 = 1.439(16), bond angles (º): N1-Ru1-N2 = 79.8(4), N1-Ru1-Cl1 = 84.2(3), N2-Ru1-Cl1 = 83.6(3) and torsion angle (º): N1-C1-C2-N2 = -45.3(2).*

Figure 2.2. *Single crystal X-ray structure of complex **[Ru]-6** with 35% probability of thermal ellipsoids. Anionic counterpart (PF6) and hydrogen atoms (except at nitrogen) are omitted for the sake of clarity. Selected bond length (Å): $Ru1\text{-}C_{avg}$ = 2.186, $Ru1\text{-}C_{ct}$ = 1.664, Ru1-Cl1 = 2.406(3), Ru1-N1 = 2.178(9), Ru1-N2 = 2.126(10), N1-C1 = 1.395(17), N2-C2 = 1.469(2), bond angles (º): N1-Ru1-N2 = 78.3(4), N1-Ru1-Cl1 = 85.4(3), N2-Ru1-Cl1 = 88.0(3) and torsion angle (º): N1-C1-C2-N2 = -56.0(1).*
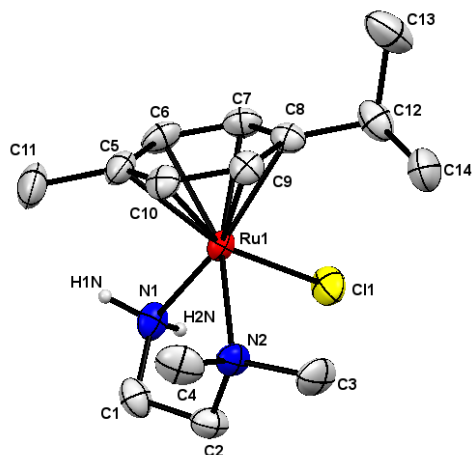
Figure 2.3. *Single crystal X-ray structure of complex **[Ru]-7** with 35% probability of thermal ellipsoids. Anionic counterpart (PF6) and hydrogen atoms (except at nitrogen) are omitted for the sake of clarity. Selected bond length (Å): $Ru1\text{-}C_{avg} = 2.187$, $Ru1\text{-}C_{ct} = 1.673$, $Ru1\text{-}Cl1 = 2.401(9)$, $Ru1\text{-}N1 = 2.132(3)$, $Ru1\text{-}N2 = 2.198(3)$, $N1\text{-}C1 = 1.465(5)$, $N2\text{-}C2 = 1.491(5)$, bond angles (º): $N1\text{-}Ru1\text{-}N2 = 79.18(11)$, $N1\text{-}Ru1\text{-}Cl1 = 83.88(9)$, $N2\text{-}Ru1\text{-}Cl1 = 88.10(9)$ and torsion angle (º): $N1\text{-}C1\text{-}C2\text{-}N2 = 56.4(4)$.*
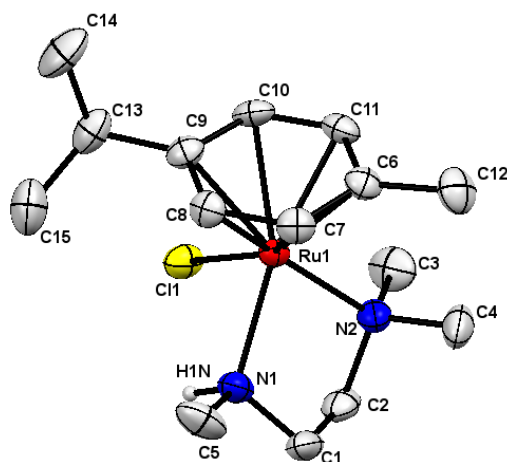
Figure 2.4. *Single crystal X-ray structure of complex **[Ru]-8** with 35% probability of thermal ellipsoids. Anionic counterpart (PF6) and hydrogen atoms (except at nitrogen) are omitted for the sake of clarity. Selected bond length (Å): $Ru1\text{-}C_{avg} = 2.204$, $Ru1\text{-}C_{ct} = 1.694$, $Ru1\text{-}Cl1 = 2.423(8)$, $Ru1\text{-}N1 = 2.154(3)$, $Ru1\text{-}N2 = 2.197(3)$, $N1\text{-}C1 = 1.489(5)$, $N2\text{-}C2 = 1.496(4)$, bond angles (º): $N1\text{-}Ru1\text{-}N2 = 79.81(12)$, $N1\text{-}Ru1\text{-}Cl1 = 82.41(8)$, $N2\text{-}Ru1\text{-}Cl1 = 85.59(8)$ and torsion angle (º): $N1\text{-}C1\text{-}C2\text{-}N2 = 56.9(4)$.*

Table 2.1. *Crystal data and structure refinement details for complexes [Ru]-2, [Ru]-6, [Ru]-7 and [Ru]-8*

	[Ru]-2	[Ru]-6	[Ru]-7	[Ru]-8
empirical formula	$C_9H_{16}ClF_6N_2P$ Ru	$C_{13}H_{19}ClF_6N_2P$ Ru	$C_{14}H_{26}ClF_6N_2P$ Ru	$C_{15}H_{28}ClF_6N_2P$ Ru
fw	433.73	484.79	503.86	517.88
T (K)	150(2)	150(2)	150(2)	150(2)
λ (Å)	1.5418	0.71073	1.5418	1.5418
cryst system	Monoclinic	Triclinic	Monoclinic	Monoclinic
space group	P 21/n	P -1	P 21/n	P 21/c
cryst size, mm	0.26 x 0.21 x 0.18	0.23 x 0.19 x 0.14	0.23 x 0.18 x 0.14	0.33 x 0.28 x 0.23
a, Å	8.851(3)	8.6884(3)	12.6627(2)	8.6754(2)
b, Å	15.444(6)	10.3152(6)	14.3424(2)	23.4767(3)
c, Å	11.304(6)	12.0165(5)	11.3038(2)	11.0493(2)
α, deg	90	107.066(4)	90	90
β, deg	103.97(5)	95.581(3)	107.307(2)	110.119(2)
γ, deg	90	107.616(4)	90	90
V, Å^3	1499.5(12)	960.57(8)	1959.98(5)	2113.09(7)
Z	4	2	4	4
ρ_{calcd}, g cm^{-3}	1.921	1.676	1.708	1.628
μ, mm^{-1}	11.677	1.091	9.027	8.390
F(000)	856	482	1016	1048
θ range, deg	4.94 – 71.90	3.12 – 26.39	5.13 – 71.31	3.77 – 71.44
completeness to θ_{max}	97.4 %	99.8 %	98.2 %	98.8 %
no. of data collected/unique data	7881 / 2861 [R(int) = 0.0687]	7533/ 3930 [R(int) = 0.0362]	11585 / 3752 [R(int) = 0.0250]	13705 / 4063 [R(int) = 0.0229]
params/restraints	183/0	222/0	231/0	241/0
goodness of fit on F^2	1.035	1.198	1.027	1.082

	[Ru]-2	[Ru]-6	[Ru]-7	[Ru]-8
final R	R1 = 0.0828	R1 = 0.0956	R1 = 0.0389	R1 = 0.0357
indices [$I >$	wR2 = 0.2158	wR2 = 0.2684	wR2 = 0.1053	wR2 = 0.0932
$2\sigma(I)$]				
R indices (all	R1 = 0.0893	R1 = 0.1152	R1 = 0.0407	R1 = 0.0366
data)	wR2 = 0.2249	wR2 = 0.2934	wR2 = 0.1076	wR2 = 0.0939

Table 2.2. *Selected bond lengths and bond angles for complexes* **[Ru]-2**, **[Ru]-6**, **[Ru]-7** *and* **[Ru]-8**

	[Ru]-2	[Ru]-6	[Ru]-7	[Ru]-8
Bond lengths (Å)				
Ru1-N1	2.113(8)	2.178(9)	2.132(3)	2.154(3)
Ru1-N2	2.153(8)	2.126(10)	2.198(3)	2.197(3)
Ru1-C_t	1.658	1.664	1.673	1.694
Ru1-$C_{avg.}$	2.141	2.186	2.187	2.204
Ru1-Cl1	2.406(3)	2.406(3)	2.401(9)	2.423(8)
N1-C1	1.444(17)	1.395(17)	1.465(5)	1.489(5)
N2-C2	1.439(16)	1.469(2)	1.491(5)	1.496(4)
C1-C2	1.53(2)	1.63(2)	1.489(5)	1.487(6)
N2-C3	1.431(15)	1.42(2)	1.493(5)	1.478(5)
N2-C4			1.488(5)	1.485(5)
N1-C5				1.464(5)
Bond angles (°)				
N1-Ru1-N2	79.8(4)	78.3(4)	79.18(11)	79.81(12)
N1-Ru1-Cl1	84.2(3)	85.4(3)	83.88(9)	82.41(8)
N2-Ru1-Cl1	83.6(3)	88.0(3)	88.10(9)	85.59(8)
C_t-Ru1-N1	128.23	127.49	130.86	132.56
C_t-Ru1-N2	133.34	132.80	132.86	133.87
C_t-Ru1-Cl1	129.46	127.74	125.59	124.55

All the complexes display analogous molecular structures with the characteristic *piano-stool* geometry of arene-Ru(II) complexes, with the η^6-coordinated arene ring as the top and the two nitrogen atoms of the respective ethylenediamine based ligand and one chloride ligand as three legs. The complexes

[Ru]-2, **[Ru]-7** and **[Ru]-8** crystallize in monoclinic *P* 21 space group, whereas the complex **[Ru]-6** in triclinic *P*-1 space group. The arene ring (η^6-C$_6$H$_6$ or η^6-C$_{10}$H$_{14}$) appears almost planar for all the complexes, where the centroid of the arene ring is displaced by 1.65-1.69 Å from the Ru(II) center. The Ru–nitrogen and Ru–chloride bonds distances are within the range of 2.11–2.19 Å and 2.40–2.42 Å, respectively, which is close to those reported previously for related arene-Ru(II) complexes.[22,23] Moreover, the Cl–Ru–N and N–Ru–N bond angles range are 82.4°–88.1° and 78.3°–79.8°, respectively, and those between the legs and the centroid of the η^6-arene ring (C$_{Ct}$) is 124.5°–133.8°, the observed values are comparable to those reported for other analogous complexes.[22,23]

2.2.2. Catalytic transformation of furan and its derivatives. Catalytic efficacy of the water soluble catalysts **[Ru]-1 − [Ru]-8** was explored for the aqueous-phase tandem transformation of furan derivatives into LA and diketones. Readily available furan derivative, furfural (**1a**), was selected as model substrate for the catalytic reaction. In the first set of experiments the influence of the additive (formic acid), temperature, structural parameters such as η^6-coordinated arene and the N-H bonds in ethylenediamine based ligands, on the catalytic transformation of furfural to LA was investigated.
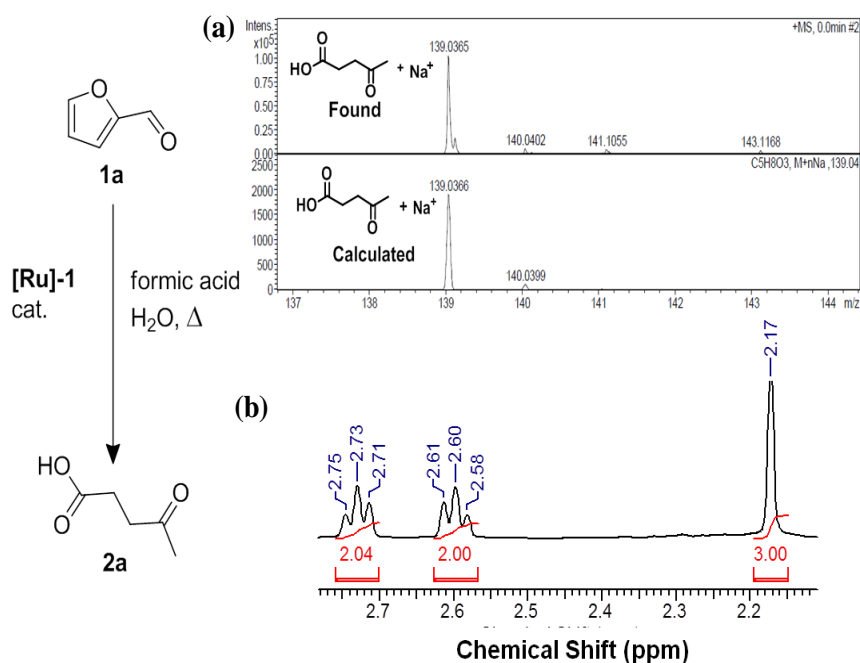
Figure 2.5. *Catalytic transformation of furfural to LA in the presence of **[Ru]-1** catalyst and formic acid in water, and the identification of LA by (a) HRMS and (b) ^{1}H NMR.*

Initial results inferred that complete conversion of furfural (**1a**) to LA (**2a**) with > 99% selectivity was achieved with the 5 mol% **[Ru]-1** catalyst in the presence of 12 equivalents of formic acid after 24 h at 80 °C. Analysis of the product by ^{1}H (2.73 (t, -CH_2, C2), 2.60 (t, -CH_2, C3) and 2.17 (s, -CH_3, C5) ppm), ^{13}C NMR and HRMS further confirmed the formation of product LA (m/z found 139.0365 [C$_5$H$_8$O$_3$ + Na$^+$] and m/z calculated 139.0366 [C$_5$H$_8$O$_3$ + Na$^+$]) (Figure 2.5). These results, indeed, inferred the decisive role of the **[Ru]-1** catalyst, with a positive cooperation from formic acid, for the tandem catalytic transformation of furfural with high selectivity to LA.
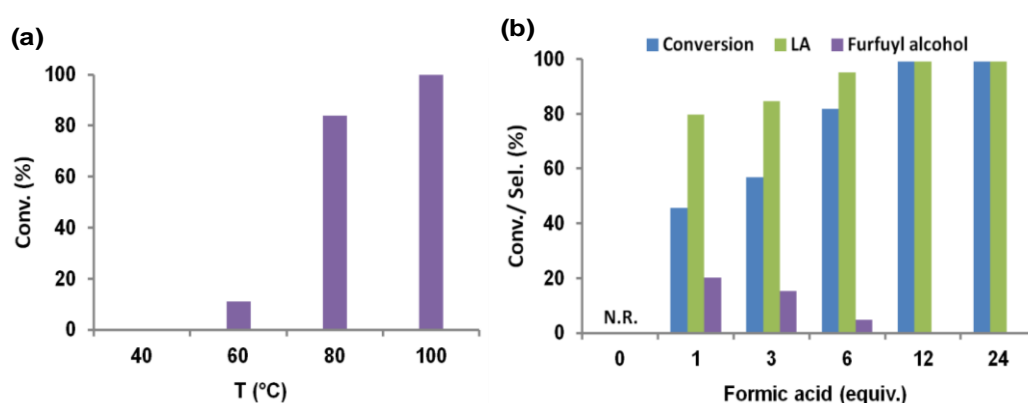
Figure 2.6. *Effect of (a) reaction temperature, and (b) formic acid concentration on the catalytic transformation of furfural to LA in the presence of **[Ru]-1** catalyst in water. Reaction conditions: (a) furfural (1.0 mmol), catalyst (5 mol%), formic acid (12 equiv.) and water (10 mL) at different temperature for 8 h. (b) furfural (1.0 mmol), catalyst (5 mol%), formic acid (as specified) and water (10 mL) at 100 °C for 8 h.*

Further, the reaction completion time was fine tuned by optimising the reaction temperature (Figure 2.6a). Decreasing the reaction temperature to 60 °C resulted in a significant loss of the catalytic activity, and at 40 °C catalytic reaction was even stopped. However, reaction performed at 100 °C displayed complete conversion of furfural to LA in shorter reaction time of 8 h. To further optimize the formic acid amount, reactions were performed with a formic acid amount ranging from 0 to 24 equivalents (results are presented in Figure 2.6b). A complete conversion of furfural with >99% selectivity for LA was achieved in the presence of ≥12 equivalents of formic acid whereas decreasing the formic acid amount below 12 equivalents resulted a decrement in conversion of furfural as well as the selectivity

for LA was also compromised. Interestingly, for the catalytic reaction with lower formic acid amount, the hydrogenated intermediate, furfuryl alcohol, was also observed along with the LA. Moreover, it is worth mentioning that, no conversion of furfural was observed for the catalytic reaction performed in the absence of formic acid (Figure 2.6b). Interestingly, when furfural was treated with formic acid, in the absence of the catalyst, only humin formation was observed (Figure 2.7).[20]
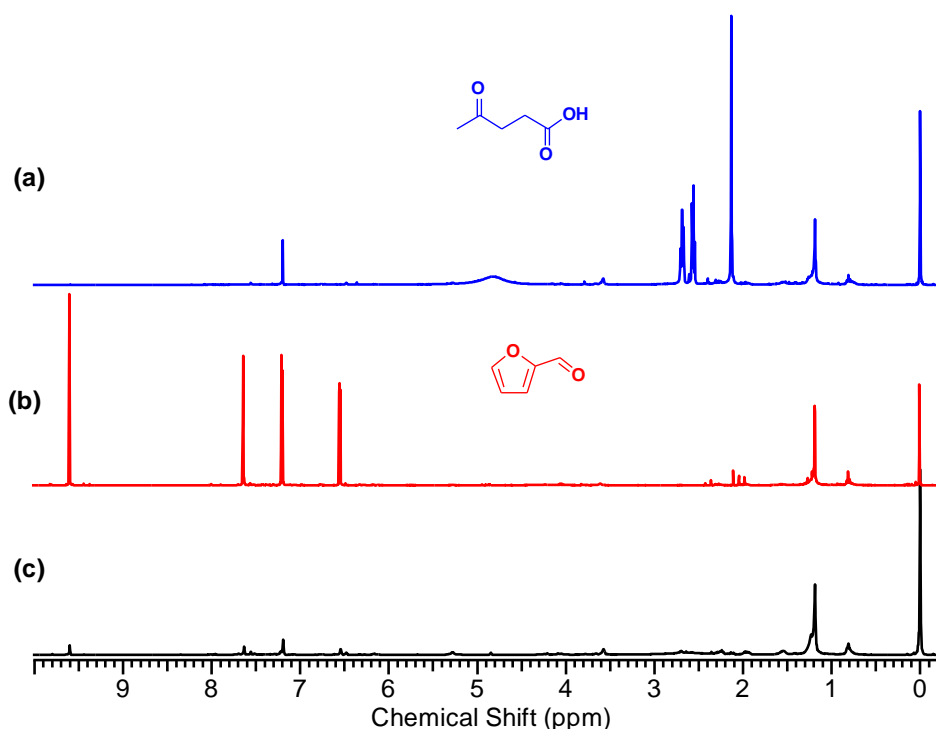
Figure 2.7. *^{1}H NMR spectra of reaction mixture obtained after the reaction of furfural in the presence of (a) 5 mol% **[Ru]-1** and HCOOH (12 equiv.), (b) 5 mol% **[Ru]-1** but without HCOOH and (c) without catalyst but with HCOOH (12 equiv.), at 100 °C in water for 12 h.*

Furthermore, replacement of formic acid with short chain or bulky acids such as acetic acid, propionic acid or *iso*-butyric acid also was also resulted with no conversion of furfural (Table 2.3). As the formation of metal–hydride bond, a crucial step of transfer hydrogenation reaction, is only possible in the presence of formic acid, other acids could not contribute to metal catalysed transfer hydrogenation for the transformation of furfural to furfuryl alcohol, and therefore resulted in no reaction. Further to support the dual role of formic acid during the catalytic reaction, experiment was performed for the transformation of furfural in the presence of **[Ru]-**

1 catalyst, by replacing formic acid with hydrogen gas under optimized reaction conditions. In contrary to high activity achieved in the presence of formic acid, replacing formic acid with hydrogen gas resulted in no conversion of furfural. These observations strongly support the significant role of formic acid for the tandem catalytic transformation of furfural to levulinic acid via furfuryl alcohol, where the crucial step transfer hydrogenation step can takes place only in the presence of formic acid but not with other organic acids or hydrogen gas under our optimized reaction conditions.

Table 2.3. Influence of additives on the catalytic transformation of furfural to LA in the presence of [Ru]-1. Reaction Conditions: furfural (1.0 mmol), acid (12 equiv.), catalyst (5 mol%), and water (10 mL)

Entry	Additive	T (ºC) / t (h)	Conv. (%)
1	formic acid	100/8	>99
2	formic acid	80/8	84
3	formic acid	60/8	11
4	formic acid	40/8	0
5	acetic acid	100/8	n.r.
6	propionic acid	100/8	n.r.
7	iso-butyric acid	100/8	n.r.
8	hydrogen gas	100/8	n.r.

Having the optimised reaction conditions, the influence of other analogous arene-Ru(II) catalyst, **[Ru]-2 − [Ru]-8** containing either varying ethylenediamine derivatives or η^6-arene ligands, on the catalytic transformation of furfural to LA was investigated. As depicted from Figure 2.8, among the various ethylenediamine ligands used, the ruthenium catalysts **[Ru]-1** and **[Ru]-5,** having unsubstituted ethylenediamine, outperformed. The catalytic activity was in the order of **[Ru]-1** > **[Ru]-2 > [Ru]-3 > [Ru]-4**, which clearly depicted the significant role of N-H bond in the enhanced catalytic activity of **[Ru]-1** catalyst. Moreover, a close analogue of the highly active **[Ru]-1** catalyst containing N-tosylated ethylenediamine (Ts-en) ligand in place of ethylenediamine was found to be only slightly less active than **[Ru]-1** catalyst. Though, the Ru-*p*-cymene catalyst (**[Ru]-5**) was found to be slightly less

active than its close analogue, Ru-benzene catalyst (**[Ru]-1**), an analogous trend in the catalytic activity was also observed with the change in the N-H entities for the catalysts **[Ru]-6 − [Ru]-8** (Figure 2.8).
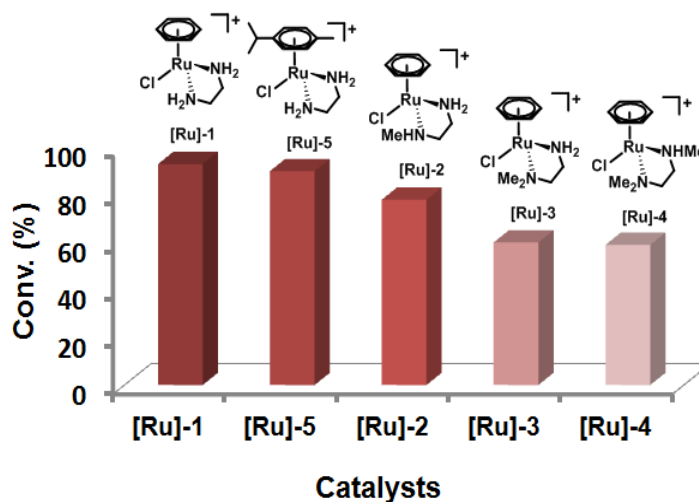
Figure 2.8. *Catalytic transformation of furfural to LA by arene-Ru(II) complexes in water. Reaction conditions: furfural (1.0 mmol), catalyst (5 mol%), formic acid (12 equiv.) and water (10 mL) at 100 °C for 8 h.*

These observations inferred a significant structure–activity relationship that drives the catalytic activity of the studied arene-Ru(II) complexes. The role of N-H bonds present in the ruthenium complexes during the transfer hydrogenation process is well established.[24] As the mechanistic study of the catalytic transformation of furfural inferred an initial transfer hydrogenation of furfural to furfuryl alcohol, which subsequently undergoes formic acid assisted hydrolytic ring opening to levulinic acid. We strongly believe that, in our case also N-H bonds play a significant role to control the catalytic activity of the studied ruthenium complexes, particularly for the initial transformation of furfural to furfuryl alcohol, and therefore **[Ru]-1**, with high availability of N-H bonds, showed the highest catalytic activity. Moreover, the higher activity of the benzene complex over *p*-cymene complex was presumably due to the combined steric and electronic effect of the arene ligands.[24] Thus, all the further optimization and exploration of the catalytic transformation reactions of furan derivatives was done using the highly active ruthenium catalyst **[Ru]-1**.

To further investigate the progress of the catalytic reaction and to identify any possible intermediate component (possibly the hydrogenated products), UV-visible and ^{1}H NMR spectra were collected as a function of time for the catalytic

transformation of furfural to LA in the presence of **[Ru]-1** catalyst, in water at 100 °C (results are shown in Figure 2.9 and 2.10). With increasing reaction time, a gradual decrease was observed in the intensity of the absorption band at 276 nm in UV-visible spectrum, corresponding to furfural (Figure 2.9). Although the band due to LA was not distinguishable, the observed UV-visible pattern indicated that furfural was being used up during the course of the reaction. The kinetic plot (Figure 2.9, inset) of the catalytic reaction, based on the absorbance values at 276 nm for the initial 8 h, showed a linear correlation between $\ln(C_t/C_0)$ and reaction time which inferred that the reaction follows pseudo-first-order kinetics ($k = 5.67 \times 10^{-5}$ s^{-1}). A series of reactions for the catalytic transformation of furfural was further carried out using a fixed initial concentration (1.2 mol/L) of formic acid while varying the concentration of furfural (0.05 mol/L to 0.15 mol/L). Initial rates indicated that the catalytic reaction follows first-order kinetics with furfural concentration (Figure 2.10). Moreover, kinetic study performed using a fixed concentration of furfural (0.10 mol/L) with varying formic acid concentration (0.6 mol/L to 2.4 mol/L) inferred that, in contrary to the trends observed with furfural concentration, the reaction rate was not sensitive to the concentration of formic acid (Table 2.4).
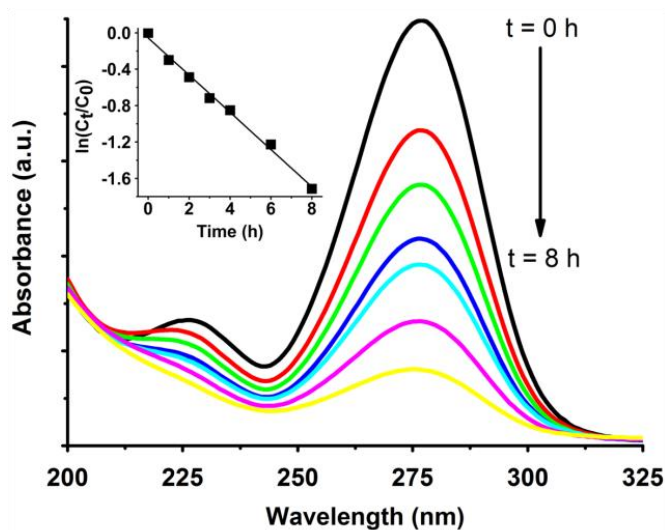
Figure 2.9. *UV-visible (inset: kinetic profile for the initial 8 h at 276 nm) spectra as a function of time for the catalytic transformation of furfural to LA in water. Reactions were performed using 5 mol% arene-Ru(II) catalyst **[Ru]-1** in the presence of formic acid (12 equiv.) at 100 °C.*

Table 2.4. *Kinetic study by UV-Vis spectrophotometry for the catalytic transformation of furfural to LA in the presence of **[Ru]-1** catalyst (5 mol%) with varying amount of furfural and formic acid at 100 °C in water (10 mL)*

Experiment No.	Rate of the reaction mol/L.s	Furfural mol/L (mmol)	Formic acid mol/L (equiv.)
1	0.63×10^{-4}	0.15 (1.5)	1.2 (12)
2	0.35×10^{-4}	0.10 (1.0)	1.2 (12)
3	0.28×10^{-4}	0.05 (0.5)	1.2 (12)
4	0.42×10^{-4}	0.10 (1.0)	2.4 (24)
5	0.39×10^{-4}	0.10 (1.0)	0.6 (6)
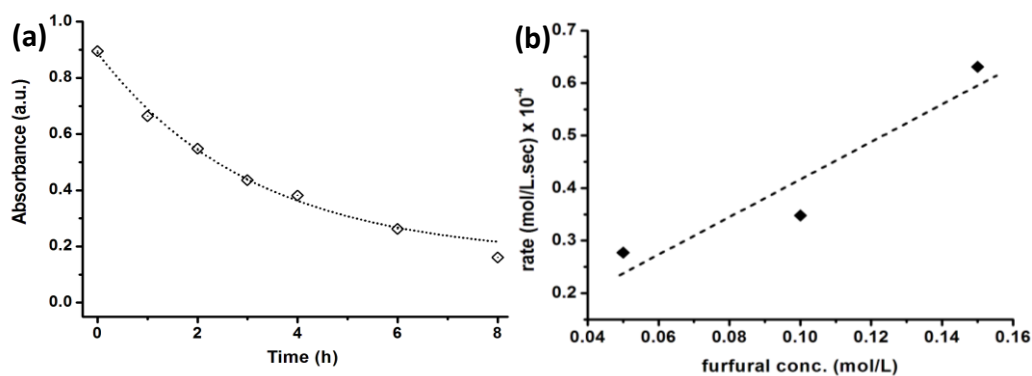
Figure 2.10. *(a) UV-Vis spectrum of the reaction progress for the catalytic transformation of furfural (1.0 mmol, 0.1 mol/L) in the presence of **[Ru]-1** catalyst (5 mol%) with formic acid (12 equivalents, 1.2 mol/L) at 100 °C. (b) Initial rate vs furfural concentration for catalytic reactions carried out with varying initial furfural concentrations.*

Time scaled ^{1}H NMR spectra was performed to monitor the progress of the **[Ru]-1** catalyzed transformation of furfural over a period of 12 h, and observed that the intensity of resonance due to LA at 2.73 (t, -CH_2, C2), 2.60 (t, -CH_2, C3) and 2.17 (s, -CH_3, C5) ppm increases with the progress of the catalytic reaction (Figure 2.11a). The reaction profile with respect to time, shown in Figure 2.11b), depicted that in the initial hours of the catalytic reaction, there is the formation of the hydrogenated intermediate, furfuryl alcohol, however this intermediate soon disappeared with the progress of the catalytic reaction and LA appeared as the only major product. These results are in accordance with previous reports, where the

reaction performed employing the furfuryl alcohol, instead of furfural, its facile transformation to LA was comfortably achieved even in the absence of the catalyst.[17]
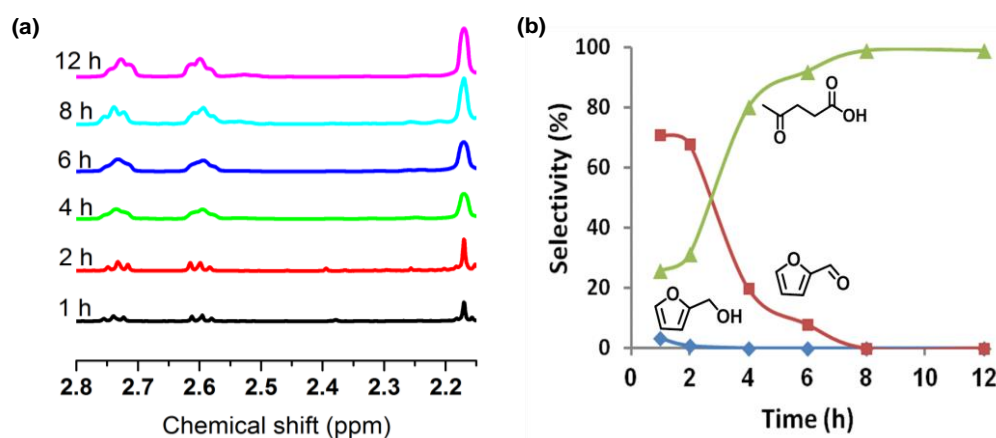
Figure 2.11. *(a) Time scaled ^1H NMR spectra and (b) corresponding reaction profile for the catalytic transformation of furfural to LA in water using 5 mol% **[Ru]-1** catalyst in the presence of formic acid (12 equiv.) at 100 °C.*

The assumption that the intermediate, furfuryl alcohol, presumably undergoes facile ring opening in the presence of formic acid, was further supported by the appearance of furfuryl alcohol in the reactions performed with less amount (<12 equivalents) of formic acid. However, furfuryl alcohol soon disappeared with the increase in the formic acid amount in the catalytic reaction.
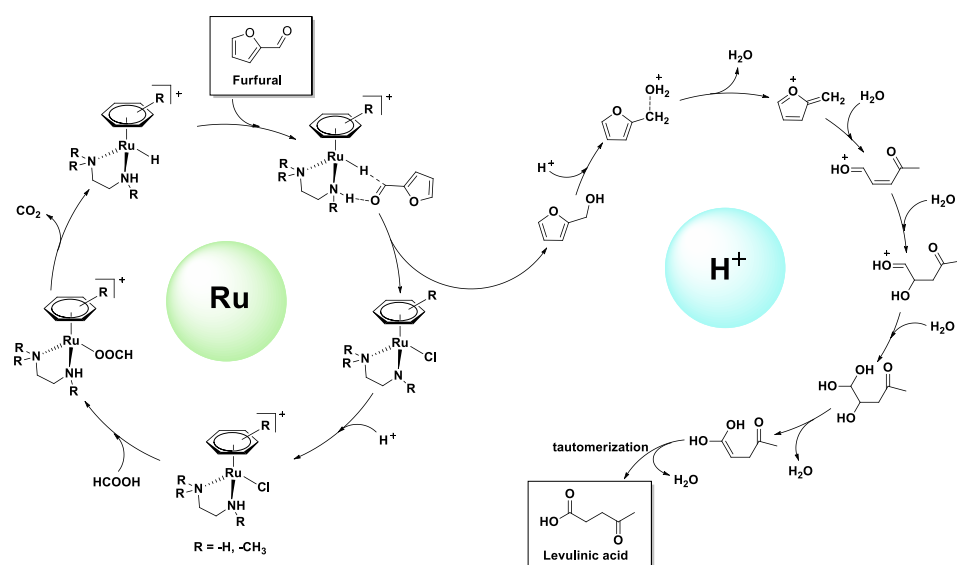
Scheme 2.3. *Plausible reaction pathway for the tandem catalytic transformation of furfural to LA.*

54

These important observations and isolation of the intermediate, furfuryl alcohol, inferred that presumably the **[Ru]-1** catalyst initially catalyzed the hydrogenation of furfural to corresponding furfuryl alcohol by transfer hydrogenation using formic acid as H-source, later furfuryl alcohol instantly undergoes ring opening to LA by an acid promoted hydrolysis to achieve the tandem catalytic transformation of furfural to levulinic acid, as exemplified in Scheme 2.3.[16,17]
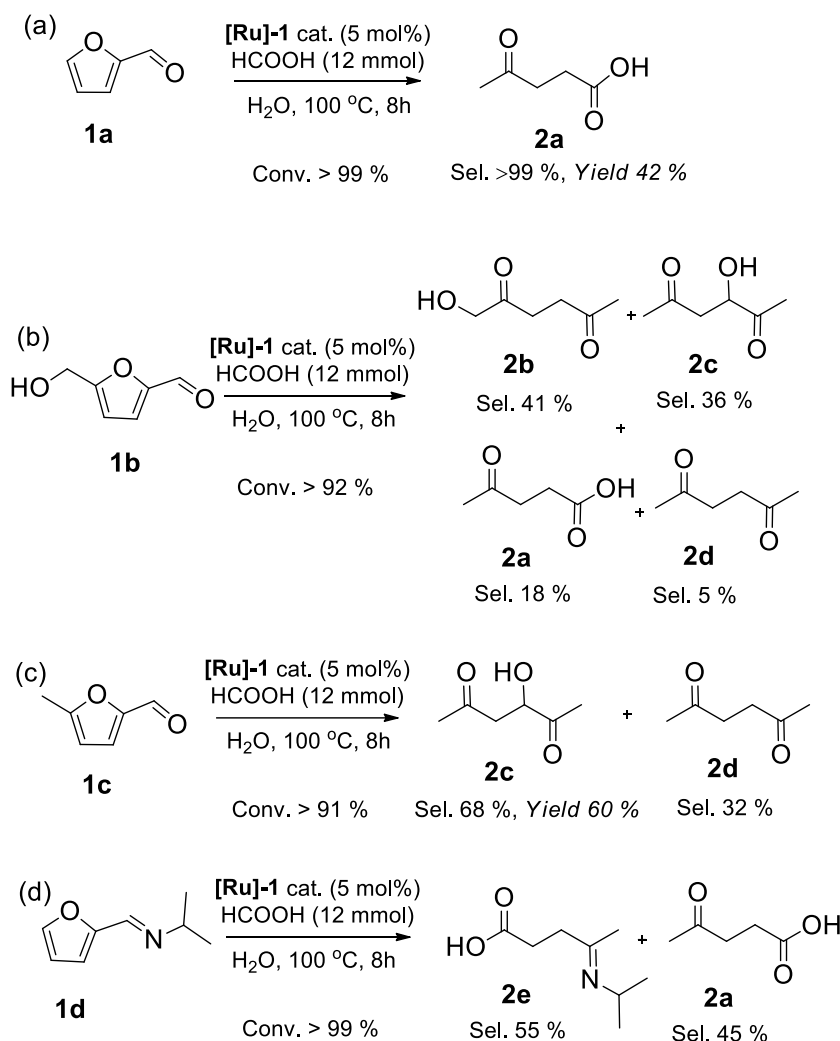
Scheme 2.4. *Catalytic transformation of furan by [Ru]-1 catalyst in water.*

To further investigate the generality of the **[Ru]-1** catalyst, catalytic transformation of other furan derivatives having different substituents at 2 and 5 positions, such as 5-HMF (**1b**), 5-MF (**1c**) and N-(furan-2-ylmethylene)propan-2-amine (**1d**), were investigated under the optimized reaction conditions (5 mol%

[Ru]-1, 12 equiv. formic acid, 100 °C, 8 h) (Scheme 2.4). Complete conversion of furfural with > 99% selectivity to LA (isolated yield 42%) was achieved in 8 h (Scheme 2.4(a)). Under identical reaction conditions, 92% conversion of 5-HMF was achieved, where 1-HHD (**2b**), 3-HHD (**2c**), LA (**2a**) and 2,5-HD (**2d**) were observed as products with relative selectivities of 41%, 36%, 18% and 5%, respectively (Scheme 2.4(b)). Conversion of 5-HMF to 1-HHD was also in accordance with previous reports, were it was reported as one of the major product using the catalytic systems based on Pd/C, Cp*Ir-complexes, or arene-Ru(II) catalysts.[15,16,17] Reaction with 5-MF (**2c**) yielded 60 % of 3-HHD (**2c**), where the relative selectivity for 3-HHD and 2,5-HD were 68% and 32%, respectively (Scheme 2.4(c)). Moreover, reaction was also performed with N-(furan-2-ylmethylene)propan-2-amine (**1d**), obtained by the condensation of furfural with isopropylamine. Interestingly, the reaction products obtained were LA and isopropylamine condensed LA (N-isopropylimino)pentanoic acid, (**2e**) in approximately 1:1 molar ratio. The formation of the product **2e** inferred that presumably imine bond in the substrate **1d** hydrolyzed during the catalytic reaction and later on condensed with the ketonic group of the LA to yield **2e**.

2.2.3. Catalyst stability, recovery and recycling. The thermal stability of the ruthenium catalysts, **[Ru]-1** was studied by performing ^{1}H NMR experiments and thermal gravimetric analysis (TGA) measurements. The decomposition of the catalyst was monitored at certain interval of time (0 ~ 72 h) by ^{1}H NMR spectroscopy, where no traces of decomposition were observed (Figure 2.12). Moreover, the TGA graphs clearly indicated that **[Ru]-1** catalyst is stable up to 200 °C (Figure 2.13).
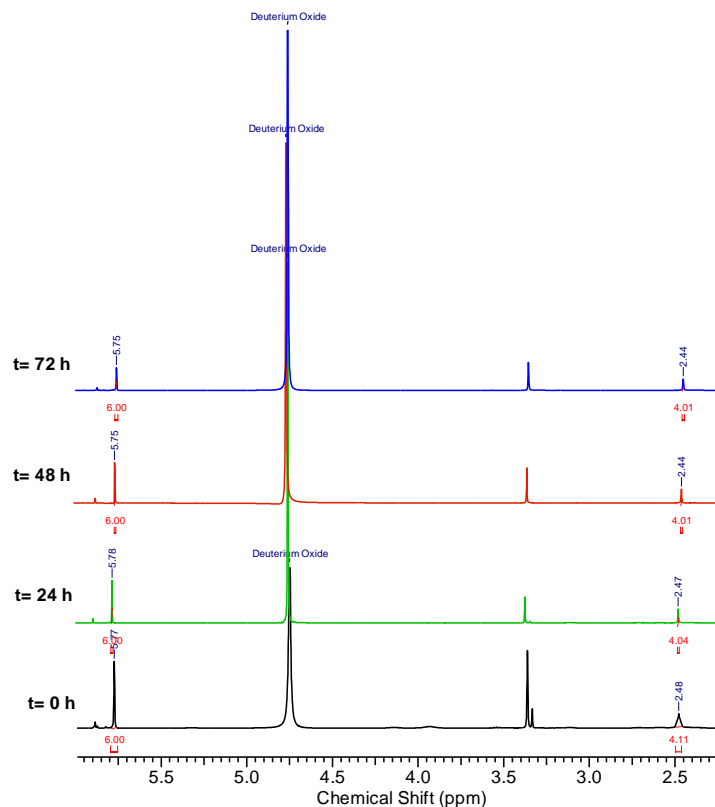
Figure 2.12. *^{1}H NMR spectra for the thermal stability of **[Ru]-1** catalyst at 100 °C in D$_2$O.*
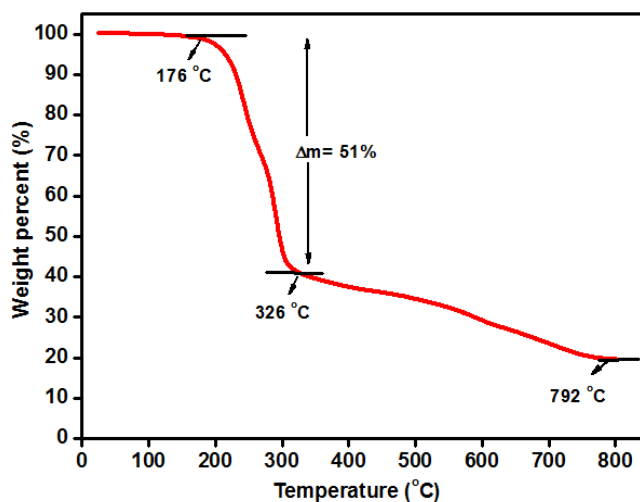
Figure 2.13. *Thermal gravimetric analysis (TGA) graph of **[Ru]-1** catalyst.*

Further, the mercury poisoning experiment showed no significant change in the catalytic activity of **[Ru]-1** catalyst in the presence of an excess of Hg(0), which strongly supported the homogenous nature of the catalyst. Although the homogeneous nature of the catalyst provides several advantages, the easy recovery of catalysts for homogeneous catalytic reactions remains an inherent limitation.

57

However, we are indeed fortunate that the high aqueous solubility of the **[Ru]-1** catalyst gave us an opportunity for easy recovery the catalyst and its reuse for further catalytic cycles for the transformation of furfural to LA. After each catalytic run, reaction mixture was extracted using a suitable organic solvent, while the catalyst, which remains in the aqueous phase, was straight away used for the next catalytic run by adding the additional specified amount of the furfural and formic acid. The **[Ru]-1** catalyst was recycled for at least five consecutive catalytic cycles, without significant loss in the catalytic activity (Figure 2.14).
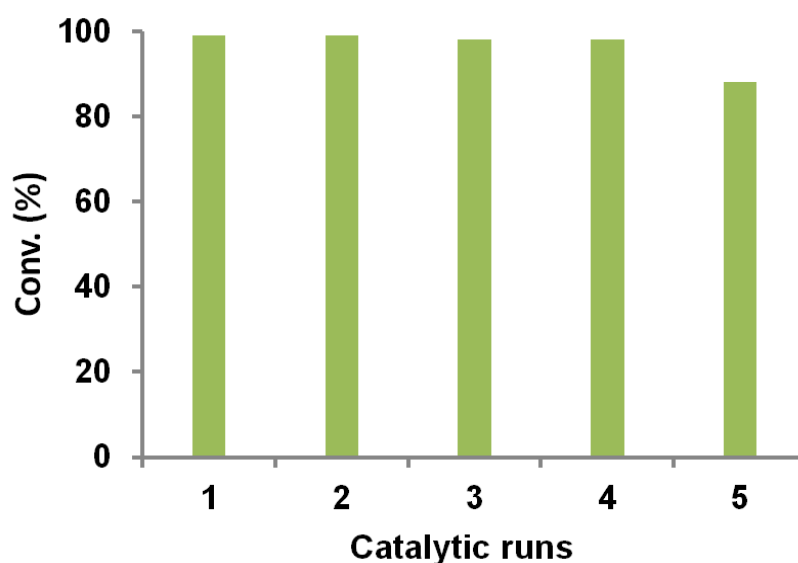
Figure 2.14. *Recyclability of **[Ru]-1** catalyst for the catalytic transformation of furfural to LA in the presence of formic acid (12 equiv.) in water at 100 °C.*

These results further demonstrated the high stability of the **[Ru]-1** catalyst in water. Moreover, the scanning electron microscopic (SEM) images (Figure 2.15) of the fresh catalyst and the catalyst recovered after the catalytic reaction for the **[Ru]-1** catalyst showed no remarkable morphological changes in the catalyst during the reaction. These observations were further authenticated by the appearance of peaks corresponding to protons and carbon atoms of the ethylenediamine and arene ligands in the NMR spectra of the **[Ru]-1** catalyst recovered after the catalytic reactions (Figure 2.16), which is in consistence with the those of the fresh **[Ru]-1** catalyst. Moreover, the above analyses ensure that there is no significant deformation in the catalyst structure, which is consistent with the observed high catalytic recyclability,

up to five consecutive catalytic runs, for catalyst for the studied catalytic transformation.
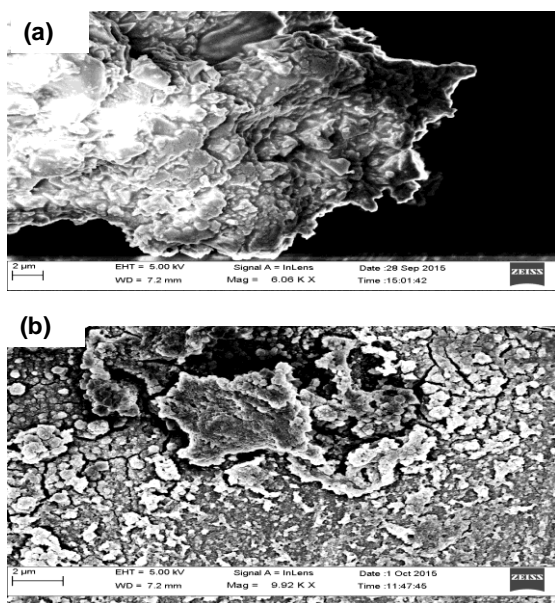
Figure 2.15. Scanning electron microscopic (SEM) images of [Ru]-1 catalyst (a) fresh and (b) recovered after the catalytic reaction.
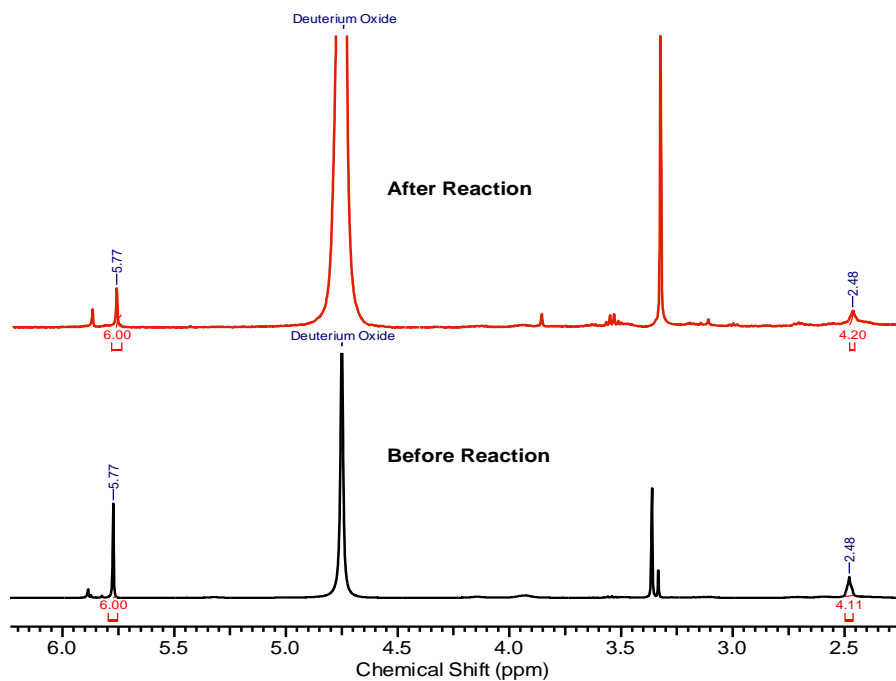
Figure 2.16. ^{1}H NMR spectra of [Ru]-1 catalyst recovered after the catalytic reaction.

2.2.4. Catalytic transformation of fructose to LA and diketones. The obtained results were further explored for the catalytic transformation of fructose to LA and diketones in the presence of 5 mol% **[Ru]-1** catalyst (Scheme 2.5).
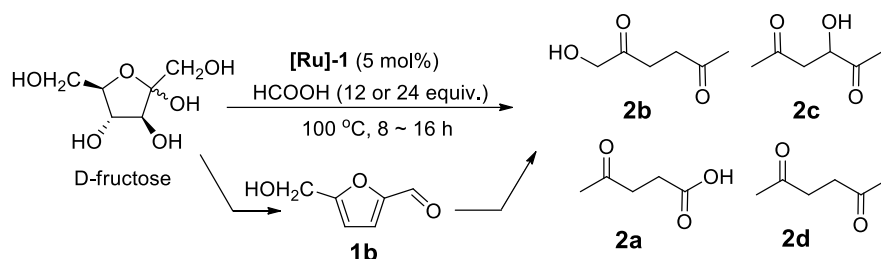
Scheme 2.5. *Catalytic transformation of fructose to LA and diketones*

After heating fructose at 100 °C for 8 h in presence of 12 equiv. of formic acid, conversion of fructose to 1-HHD and LA were obtained as major product with 27% and 51% selectivity respectively, along with 5-HMF (5%), diketone (4%) and 3-HHD (13%) as minor products. The reaction products obtained from fructose transformation were found to be analogous to the products obatined with 5-HMF, suggesting that presumably the reaction proceeds through the initial formation of 5-HMF.[3] Moreover, with the increase in the reaction time to 16 h or double the formic acid amount (24 equiv.), selectivity towards 1-HHD also increased and 87% selectivity was observed with the reaction performed at 100 °C for 16 h in the presence of 12 equivalents of formic acid. Unfortunately, attempts to use glucose in place to fructose failed, possibly because **[Ru]-1** catalyst cannot catalyze the isomerisation of glucose to fructose. Despite low fructose transformation observed for the catalytic reaction, it is worth noting that the direct catalytic transformation of fructose to open-ring components such as LA and diketones can also be acheived with ruthenium based homogenous catalysts.

Acquainted facts show that most of the studies on the transformation of furans are performed in auto-clave using mineral acids or H$_2$ gas with high pressure and temperature.[15-16, 25-28] Among these, there are many reports on the catalytic transformation of 5-HMF to ketoacids and diketones particularly using heterogeneous catalysts, whereas studies with homogenous catalyst are very few.[14,15b,16,17,25-30] Li *et al.* employed Amberlyst 70 for furfural transformation in rwater as well as methanol and observed that furfural converted to polymer in both

reactions medium.[15a] Even over Pd/Al$_2$O$_3$ with Amberlyst 70 using 70 bar H$_2$ at 165 °C in methanol only 23.1% and 2.4% yields of methyl-levulinate and levulinic acid were achieved, while Pd/Al$_2$O$_3$ was found to be inactive.[26] Riisager *et al.* explored Ru(OH)$_x$/Al$_2$O$_3$ catalyst for the aerobic oxidation of 5-HMF at 140 °C, where LA was observed as a side product along with the oxygenated products like 2,5-furandicarboxylic acid and so on.[30] Also, LA was observed as a by-product during the catalytic hydrogenation of furfural and 5-HMF over Pd-Ir/SiO$_2$ catalyst.[27] In the transformation of furans mostly catalysts are active at higher temperature [Pd/C (120 °C), Au/Nb$_2$O$_5$ (140 °C), Pd/Al$_2$O$_3$ (140 °C), Ni-Al$_2$O$_3$ (180 °C)].[14,15b,28,29] Catalytic transformation with homogeneous catalysts showed narrow product distribution and more selectivity towards open ring products, for instance Cp*-Ir catalyst and arene-Ru(II) catalyst.[16,17] Moreover, ruthenium based homogeneous catalysts were found to be highly active and recyclable even in aqueous medium.[17] In the present study, catalyst based arene-Ru complexes containing ethylene diamine ligand were also found to be highly active and stable even at 100 °C in water and open atmospheric conditions, and can be recycled up to five consecutive catalytic cycles without any significant loss in the catalytic activity. Moreover, the studied arene-Ru catalyst has shown potential to convert fructose to LA and diketones (1-HHD, 3-HHD, 2,5-HD) in water under moderate reaction conditions.

2.3. Conclusions

Highly active water soluble homogenous catalysts based on arene-ruthenium(II) complexes containing simple and easily available ethylenediamine (or its derivatives) ligands, were successfully employed for the catalytic transformation of bioderived furans into open ring value added ketoacid (LA) and diketones (1-HHD, 3-HHD and 2,5-HD) in the presence of formic acid. Depending upon the furan used, formic acid concentration, reaction temperature and the catalyst, catalytic conversion, selectivity and the product distribution can be fine tuned. A significant effect of N-H bonds present in the ruthenium catalyst on catalytic transformation reaction was also observed, where the highly active catalyst has the higher number of N-H bonds. Moreover, direct catalytic transformation of fructose to 1-HHD and LA was also achieved with limited conversion. Mechanistic studies involving ^{1}H NMR and experiments with variable formic acid concentration revealed a tandem mode of catalytic transformation of furfural to LA via the hydrogenated intermediate, furfuryl

alcohol. Furthermore, high aqueous solubility and stability of the ruthenium catalyst offers its easy recovery and reusability for at least 5 consecutive catalytic runs without any significant loss of the catalytic activity. Through our study, we demonstrated a significant cooperation between the ruthenium catalyst and formic acid to achieve high catalytic turnover for the transformation of furans. We believe that this work will encourage extensive research on the design and development of simple yet active catalysts for this or several other important catalytic transformations for application in fine chemical industries and bio-fuel based energy sector.

2.4. Experimental

2.4.1. Materials and instrumentations. All reactions were performed without inert gas protection, using chemicals of high purity purchased from Aldrich and Alfa Aesar. Dichloro bridged arene-Ru(II) precursors [{(η^6-C_6H_6)RuCl$_2$}$_2$] and [{(η^6-$C_{10}H_{14}$)RuCl$_2$}$_2$] were synthesized according to the literature procedures.[31] The catalytic reactions were monitored using a thin layer chromatography (TLC). ^{1}H NMR (400 MHz), ^{13}C NMR (100 MHz) and ^{31}P NMR (161.97 MHz) spectra were recorded at 298 K using CDCl$_3$, D$_2$O or DMSO-d_6 as the solvent on a Bruker Avance 400 spectrometer. Tetramethylsilane (TMS) was used as an external standard and the chemical shifts in ppm are reported relative to the center of the singlet at 7.26 ppm for CDCl$_3$, 4.75 for D$_2$O and 2.49 ppm for DMSO-d_6 in ^{1}H NMR and to the center of the triplet at 77.0 ppm for CDCl$_3$ and 39.50 ppm for DMSO-d_6 in ^{13}C NMR. Suitable single crystal of the arene-Ru(II) complexes **[Ru]-2**, **[Ru]-6**, **[Ru]-7** and **[Ru]-8** was subjected to single crystal X-ray structural studies using Agilent Technologies Supernova CCD system. ESI (positive and negative mode) and high-resolution mass spectra (HRMS) were recorded on a micro TF-Q II mass spectrometer. UV–visible spectra were performed on Varian Cary 100 Bio UV-visible spectrophotometer and Shimadzu UV-1700 PharmaSpec UV-VIS Spectrophotometer using a 10 mm quartz cuvette. To study kinetics of catalytic reactions by UV-visible spectrophotometry, a small portion of the reaction mixture (100 μL), taken at different time intervals, was added to 3 mL of distilled water and spectra were obtained. To calculate rate constant of the catalytic reaction, the ratio of C$_t$ and C$_0$, where C$_t$ is the concentration at time 't' and C$_0$ is the initial concentration, was measured using the relative intensity ratio of the respective absorbance A$_t$/A$_0$ at 276 nm. GC-MS analysis was performed on

Perkin Elmers GC gas chromatograph Clarus 680 coupled with a Perkin Elmers mass spectrometer Clarus SQ8T in the EI (Electron Impact) mode using a capillary column ELITE 5 (30 m × 0.25 mm). Thermal gravimetric analyses (TGA) were performed on the Mettler Toledo thermal analysis system. Scanning electron microscopy (SEM) images and elemental mapping data were collected on Carl Zeiss supra 55 (operating voltage 15 kV), using amorphous carbon-coated 400 mesh copper grids for depositing sample.

2.4.2. Single crystal X-ray diffraction Studies. Single-crystal X-ray structural studies of the arene-Ru(II) complexes **[Ru]-2**, **[Ru]-6**, **[Ru]-7** and **[Ru]-8** were performed on a CCD Agilent Technologies (Oxford Diffraction) SUPER NOVA diffractometer. Data were collected at 150(2) K using graphite-monochromated Cu Kα radiation ($\lambda\alpha$ = 1.5418 Å) for **[Ru]-2**, **[Ru]-7** and **[Ru]-8**, whereas Mo Kα radiation ($\lambda\alpha$ = 0.71073 Å) for **[Ru]-6**. The strategy for the data collection was evaluated using the CrysAlisPro CCD software. The data were collected using the standard 'phi-omega' scans techniques, and were scaled and reduced using CrysAlisPro RED software. The structures were solved by direct methods using SHELXS-97, and refined using full matrix least-squares with SHELXL-97, refining on F2.[32] The positions of all the atoms were obtained by direct methods. All non-hydrogen atoms were refined anisotropically. The remaining hydrogen atoms were placed in geometrically constrained positions, and refined with isotropic temperature factors, generally 1.2Ueq of their parent atoms. The crystal and refinement data are summarized in Table 2.1. Selected bond lengths and bond angles are summarized in Tables 2.2. CCDC deposition numbers are 1054457, 1054458, 1055781, and 1055782, respectively for the complexes **[Ru]-2**, **[Ru]-6**, **[Ru]-7** and **[Ru]-8**. This data can be obtained free of charge via www.ccdc.cam.ac.uk (or from the Cambridge Crystallographic Data Center, 12 union Road, Cambridge CB21 EZ, UK; Fax: (+44) 1223-336-033; or deposit@ccdc.cam.ac.uk).

2.4.3. General procedure for the synthesis of complexes

Synthesis of ruthenium catalysts ([Ru]-1 − [Ru]-8). Arene-Ru(II) complexes **[Ru]-1 − [Ru]-8** were synthesized using a literature reported method with some modifications.[22] Methanol solution (25 mL) of the dichloro bridged arene-Ru(II) dimer (0.2 mmol) and a suitable ethylenediamine or N-substituted ethylenediamine (0.4 mmol) was stirred at room temperature for 3 h, filtered and NH_4PF_6 was added

to the filtrate. Total volume of the solution was slowly reduced to 10 mL on a rotary evaporator and after cooling overnight at 4 °C, the microcrystalline product was obtained, which was collected by filtration, washed with ether and recrystallized from methanol-DCM/ether.

(a) Preparation of complex [(η^6-C$_6$H$_6$)RuCl(en)]PF$_6$ ([Ru]-1)
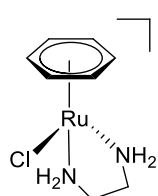
The **[Ru]-1** was synthesized using [(η^6-C$_6$H$_6$)RuCl$_2$]$_2$ (0.100 g, 0.2 mmol), as ruthenium precursor and the ligand, ethylenediamine (en) (27.4 μl, 0.41mmol). Yield: 85% (0.143 g). ^{1}H NMR (400 MHz, DMSO-d_6): δ (ppm) = 6.69 (b, 2H), 5.69 (s, 6H), 4.09 (b, 2H), 2.31-2.21 (m, 4H).^{13}C NMR (100 MHz, DMSO-d_6): δ (ppm) = 82.74, 44.31, 36.51. ^{31}P NMR (161.97 MHz, DMSO-d_6): δ (ppm) = -144 (sep, PF$_6$). MS (ESI) m/z calculated for [(η^6-C$_6$H$_6$)RuCl(en)]$^+$: 274.9 [M+], found 274.9 [M+]. Anal. Calcd: C, 22.89; H, 3.36; N, 6.67. Found: C, 22.91; H, 3.31; N, 6.65. IR on KBr (v cm^{-1}): 831 (PF$_6$ stretching), 557 (PF$_6$ bending).

(b) Preparation of complex [(η^6-C$_6$H$_6$)RuCl(Me$_1$en)]PF$_6$ ([Ru]-2)
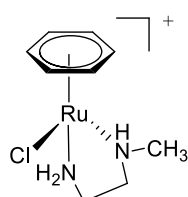
The **[Ru]-2** was synthesized using [(η^6-C$_6$H$_6$)RuCl$_2$]$_2$ (0.100 g, 0.2 mmol), as ruthenium precursor and the ligand, N-methylethylenediamine (Me$_1$en) (35.7 μl, 0.41 mmol). Yield: 88% (0.152 g). ^{1}H NMR (400 MHz, DMSO-d_6): δ (ppm) = 6.69 (b, 2H), 5.73 (s, 6H), 3.03 (d, J = 4.0 Hz, 3H), 2.47-2.44 (m, 2H), 2.10-2.07 (m, 2H). ^{13}C NMR (100 MHz, DMSO-d_6): δ (ppm) = 83.06, 56.84, 45.63, 41.57. ^{31}P NMR (161.97 MHz, DMSO-d_6): δ (ppm) = -144 (sep, PF$_6$). MS (ESI) m/z calculated for [(η^6-C$_6$H$_6$)RuCl(Me$_1$en)]$^+$: 289.0 [M+], found 288.9 [M+]. Anal. Calcd: C, 24.92; H, 3.72; N, 6.46. Found: C, 24.91; H, 3.66; N, 6.50. IR on KBr (v cm^{-1}): 834 (PF$_6$ stretching), 559 (PF$_6$ bending).

(c) Preparation of complex [(η^6-C$_6$H$_6$)RuCl(Me$_2$en)]PF$_6$ ([Ru]-3)
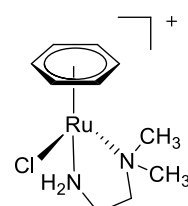
The **[Ru]-3** was synthesized using [(η^6-C$_6$H$_6$)RuCl$_2$]$_2$ (0.100 g, 0.2 mmol), as ruthenium precursor and the ligand, N,N-dimethylethylenediamine (Me$_2$en) (44.7 μl, 0.41 mmol). Yield: 88% (0.159 g). ^{1}H NMR (400 MHz, DMSO-d_6): δ (ppm) = 6.93 (b, 2H), 5.80 (s, 6H), 3.11 (s, 3H) 2.90 (s, 3H), 2.64-2.61 (m, 2H), 2.37-2.29 (m, 2H). ^{13}C NMR (100 MHz, DMSO-d_6): δ (ppm) =83.73, 61.85, 55.99, 54.04, 42.11. ^{31}P NMR

(161.97 MHz, DMSO-d_6): δ (ppm) = -144 (sep, PF$_6$). MS (ESI) m/z calculated for [(η^6-C$_6$H$_6$)RuCl(Me$_2$en)]$^+$: 303.0 [M+], found 303.0 [M+]. Anal. Calcd: C, 26.82; H, 4.05; N, 6.26. Found: C, 26.61; H, 4.08; N, 6.20. IR on KBr (v cm^{-1}): 838 (PF$_6$ stretching), 557 (PF$_6$ bending).

(d) Preparation of complex [(η^6-C$_6$H$_6$)RuCl(Me$_3$en)]PF$_6$ ([Ru]-4)
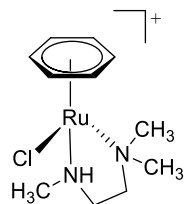
The **[Ru]-4** was synthesized using [(η^6-C$_6$H$_6$)RuCl$_2$]$_2$ (0.100 g, 0.2 mmol), as ruthenium precursor and the ligand, N,N,N'-trimethylethylenediamine (Me$_3$en) (53.3 μl, 0.41 mmol). Yield: 86% (0.160 g). ^{1}H NMR (400 MHz, DMSO-d_6): δ (ppm) = 5.84 (s, 6H), 4.53 (b, 1H), 3.21 (s, 3H), 3.09 (d, J = 4.0 Hz, 3H), 2.88 (s, 3H), 2.62-2.58 (m, 2H), 2.30-2.23 (m, 2H). ^{13}C NMR (100 MHz, DMSO-d_6): δ (ppm) = 84.04, 61.05, 56.16, 54.34, 53.34, 45.87. ^{31}P NMR (161.97 MHz, DMSO-d_6): δ (ppm) = -144 (sep, PF$_6$). MS (ESI) m/z calculated for [(η^6-C$_6$H$_6$)RuCl(Me$_3$en)]$^+$: 317.0 [M+], found 317.0 [M+]. Anal. Calcd: C, 28.61; H, 4.37; N, 6.07. Found: C, 28.69; H, 4.32; N, 6.01. IR on KBr (v cm^{-1}): 835 (PF$_6$ stretching), 558 (PF$_6$ bending).

(e) Preparation of complex [(η^6-C$_{10}$H$_{14}$)RuCl(en)]PF$_6$ ([Ru]-5)
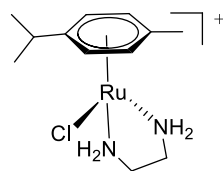
The **[Ru]-5** was synthesized using [(η^6-C$_{10}$H$_{14}$)RuCl$_2$]$_2$ (0.123 g, 0.2 mmol), as ruthenium precursor and the ligand, ethylenediamine (en) (27.4 μl, 0.41 mmol). Yield: 84% (0.131 g). ^{1}H NMR (400 MHz, DMSO-d_6): δ (ppm) = 6.14 (b, 2H), 5.58 (d, J = 5.5 Hz, 2H), 5.42 (d, J = 5.5 Hz, 2H), 4.16 (b, 2H), 2.85-2.78 (m, 1H), 2.35-2.27 (m, 2H), 2.22-2.14 (m, 2H), 2.30 (s, 3H), 1.19 (d, J = 8.0 Hz, 6H). ^{13}C NMR (100 MHz, DMSO-d_6): δ (ppm) = 103.83, 96.20, 81.76, 80.31, 44.15, 36.72, 30.12, 22.32, 17.53. ^{31}P NMR (161.97 MHz, DMSO-d_6): δ (ppm) = -144 (sep, PF$_6$). MS (ESI) m/z calculated for [(η^6-C$_{10}$H$_{14}$)RuCl(en)]$^+$: 331.0 [M+], found 331.0 [M+]. Anal. Calcd: C, 30.29; H, 4.66; N, 5.89. Found: C, 30.31; H, 4.56; N, 5.80. IR on KBr (v cm^{-1}): 835 (PF$_6$ stretching), 559 (PF$_6$ bending).

(f) Preparation of complex [(η^6-C$_{10}$H$_{14}$)RuCl(Me$_1$en)]PF$_6$ ([Ru]-6)
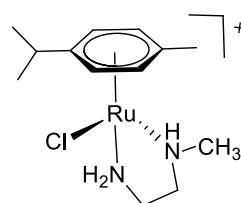
The **[Ru]-6** was synthesized using [(η^6-C$_{10}$H$_{14}$)RuCl$_2$]$_2$ (0.123 g, 0.2 mmol), as ruthenium precursor and the ligand, N-methylethylenediamine (Me$_1$en) (35.7 μl, 0.41 mmol). Yield: 82% (0.132 g). ^{1}H NMR (400 MHz, DMSO-d_6): δ (ppm) =

6.70 (d, J = 6.0 Hz, 1H), 6.37 (d, J = 6.0 Hz, 1H), 5.66 (d, J = 6.0 Hz, 1H), 5.53 (d, J = 6.0 Hz, 1H), 3.72 (b, 1H), 2.83-2.79 (m, 1H), 2.68 (s, 3H), 2.29-2.26 (m, 2H), 2.14 (s, 3H), 2.08-1.86 (m, 2H), 1.19 (b, 6H). ^{13}C NMR (100 MHz, DMSO-d_6): δ (ppm) = 106.03, 94.78, 81.87, 81.45, 80.32, 52.09, 45.12, 42.12, 30.17, 22.72, 21.19, 17.02. ^{31}P NMR (161.97 MHz, DMSO-d_6): δ (ppm) = -144 (sep, PF$_6$). MS (ESI) m/z calculated $[(\eta^6\text{-C}_{10}\text{H}_{14})\text{RuCl}(\kappa^2\text{-N,N-H}_2\text{NCH}_2\text{CH}_2\text{NH(CH}_3))]^+$: 345.0 [M+], found 345.0 [M+]. Anal. Calcd: C, 31.88; H, 4.94; N, 5.72. Found: C, 31.87; H, 4.98; N, 5.71. IR on KBr (v cm^{-1}): 838 (PF$_6$ stretching), 559 (PF$_6$ bending).

(g) Preparation of complex [(η^6-C$_{10}$H$_{14}$)RuCl(Me$_2$en)]PF$_6$ ([Ru]-7)
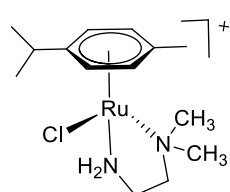
The **[Ru]-7** was synthesized using $[(\eta^6\text{-C}_{10}\text{H}_{14})\text{RuCl}_2]_2$ (0.123 g, 0.2 mmol), as ruthenium precursor and the ligand, N,N-dimethylethylenediamine (Me$_2$en) (44.7 µl, 0.41 mmol). Yield: 84% (0.138g). ^{1}H NMR (400 MHz, DMSO-d_6): δ (ppm) = 6.19 (b, 2H), 5.84 (d, J = 6.0 Hz, 1H), 5.72 (d, J = 6.0 Hz, 1H), 5.48 (d, J = 6.0 Hz, 1H), 5.36 (d, J = 6.0 Hz, 1H), 3.06 (s, 3H), 2.91-2.88 (m, 1H) 2.83 (s, 3H), 2.65-2.55 (m, 2H), 2.35-2.29 (m, 2H), 2.20 (s, 3H), 1.22 (b, 6H). ^{13}C NMR (100 MHz, DMSO-d_6): δ (ppm) = 106.25, 94.28, 85.32, 81.60, 81.05, 79.25, 61.64, 56.15, 53.56, 42.30, 30.27, 22.72, 20.97, 17.19. ^{31}P NMR (161.97 MHz, DMSO-d_6): δ (ppm) = -144 (sep, PF$_6$). MS (ESI) m/z calculated $[(\eta^6\text{-C}_{10}\text{H}_{14})\text{RuCl(Me}_2\text{en)}]^+$: 359.0 [M+], found 359.0 [M+]. Anal. Calcd: C, 33.37; H, 5.20; N, 5.56. Found: C, 33.34; H, 5.24; N, 5.58. IR on KBr (v cm^{-1}): 838 (PF$_6$ stretching), 557 (PF$_6$ bending).

(h) Preparation of complex [(η^6-C$_{10}$H$_{14}$)RuCl(Me$_3$en)]PF$_6$ ([Ru]-8)
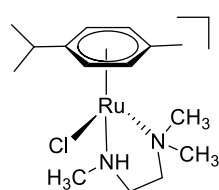
The **[Ru]-8** was synthesized using $[(\eta^6\text{-C}_{10}\text{H}_{14})\text{RuCl}_2]_2$ (0.123 g, 0.2 mmol), as ruthenium precursor and the ligand, N,N,N'-trimethylethylenediamine (Me$_3$en) (53.3 µl, 0.41 mmol). Yield: 85% (0.144 g). ^{1}H NMR (400 MHz, DMSO-d_6): δ (ppm) = 5.85 (d, J = 6.0 Hz, 1H), 5.79 (d, J = 6.0 Hz, 1H), 5.72 (d, J = 6.0 Hz, 1H), 5.47 (d, J = 6.2 Hz, 1H), 4.54 (b, 1H), 3.16 (s, 3H), 3.00 (d, J = 8.0 Hz, 3H), 2.85 (s, 3H), 2.90-2.86 (m, 1H), 2.60-2.57 (m, 2H), 2.35-2.28 (m, 2H), 2.17 (s, 3H), 1.22(d, J = 8.0 Hz, 6H). ^{13}C NMR (100 MHz, DMSO-d_6): δ (ppm) = 107.99, 94.69, 85.68, 84.88, 78.37, 78.02, 60.85, 56.12, 54.37, 53.36, 45.13, 30.50, 22.36, 21.11, 17.84. ^{31}P NMR (161.97 MHz, DMSO-d_6): δ (ppm) = -144 (sep, PF$_6$). MS (ESI) m/z calculated $[(\eta^6\text{-}$

$C_{10}H_{14})RuCl(Me_3en)]^+$: 373.0 [M+], found 373.0 [M+]. Anal. Calcd: C, 34.79; H, 5.45; N, 5.41. Found: C, 34.83; H, 5.39; N, 5.36. IR on KBr (v cm^{-1}): 838 (PF$_6$ stretching), 557 (PF$_6$ bending).

2.4.4. Catalytic reaction for the conversion of furans/fructose to LA/diketones.

To an aqueous suspension (10 mL) of arene-Ru(II) catalyst (5 mol%), furan/fructose (1.0 mmol) and formic acid (as specified) were added and the reaction mixture was stirred for a specified time, at 100 °C in an oil bath. After the catalytic reaction, the reaction mixture was extracted with ethylacetate (4 x 10 mL), the organic extract was washed with the brine solution (5 mL) and dried over Na$_2$SO$_4$. The solvent was removed in *vacuo*. The obtained products were separated by column chromatography on silica gel with hexane/ethylacetate as eluents. The product 3-hydroxyhexane-2,5-dione (3-HHD) obtained from the catalytic transformation of 5-methylfurfural (5-MF) was separated and purified by column chromatography on silica gel with 10% ethylacetate-hexane mixture (400 mL). Then, the product was isolated by removing the solvent in *vacuo*. The product levulinic acid (LA) was obtained by adding saturated sodium bicarbonate solution in the organic extract (reduced volume to *ca.* 5 mL) till effervescence ceases. Then the mixture was washed with ethylacetate (4 x 10 mL). The combined water portion was neutralized by dil. hydrochloric acid, and the product was extracted by ethylacetate (4 x 10 mL). LA was isolated by removing the solvent in vacuum. During the extraction, separation and purification process the organic and aqueous portion was continuously monitored by thin layer chromatography (TLC) under UV chamber or by staining with iodine. The reaction products were identified by ^{1}H NMR, ^{13}C NMR, HRMS, and GCMS. Conversions and selectivity were determined by ^{1}H NMR. Isolated yields were determined from the products obtained from the purification process as described above.

2.4.5. Products from the catalytic transformation of furan and its derivatives

Levulinic acid (LA): ^{1}H NMR (400 MHz, CDCl$_3$): δ (ppm) = 2.73 (t, J = 6.2 Hz, 2H), 2.60 (t, J = 6.2 Hz, 2H), 2.17 (s, 3H). ^{13}C NMR (100 MHz, CDCl$_3$): δ (ppm) = 206.64, 177.55, 37.69, 29.83, 27.61. HRMS (ESI) m/z: calculated 139.04 [C$_5$H$_8$O$_3$ + Na$^+$], found 139.036 [C$_5$H$_8$O$_3$ + Na$^+$].
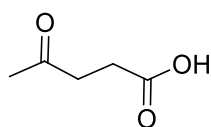
3-Hydroxyhexane-2,5-dione (3-HHD): ^{1}H NMR (400 MHz, CDCl$_3$): δ (ppm) = 4.34 (dd, J_1 = 6.5 Hz, J_2 = 3.7 Hz, 1H), 3.74 (b, 1H), 2.96 (dd, J_1 = 17.0 Hz, J_2 = 4.0Hz, 1H), 2.83 (dd, J_1 = 17.3 Hz, J_2 = 6.5 Hz, 1H), 2.25 (s, 3H), 2.21 (s, 3H).
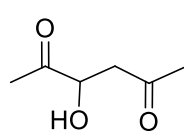
1-Hydroxyhexane-2,5-dione (1-HHD): ^{1}H NMR (400 MHz, CDCl$_3$): δ (ppm) = 4.31 (s, 2H), 2.82 (t, J = 6.5 Hz, 2H), 2.61 (t, J = 6.2 Hz, 2H), 2.18 (s, 3H).
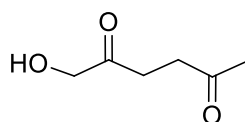
Hexane-2,5-dione (2,5-HD): ^{1}H NMR (400 MHz, CDCl$_3$): δ (ppm) = 2.60 (s, 4H), 2.08 (s, 6H), ^{13}C NMR (100 MHz, CDCl$_3$): δ (ppm) = 206.41, 35.93, 28.91. HRMS (ESI) m/z: calculated 137.06 [C$_6$H$_{10}$O$_2$ + Na$^+$], found 137.100 [C$_6$H$_{10}$O$_2$ + Na$^+$].
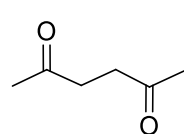
4-(Isopropylimino)pentanoic acid (4-IPA): ^{1}H NMR (400 MHz, CDCl$_3$): δ (ppm) = 4.04- 3.94 (m, 1H), 2.77 (t, J = 6.5 Hz, 2H), 2.36 (t, J = 6.5 Hz, 2H), 2.16 (s, 3H), 1.11 (d, J = 8.0 Hz, 6H).
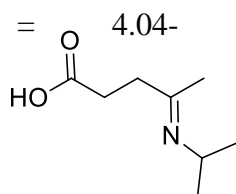
Note: The contents of this work have been reproduced with the permission from The Wiley online library (*ChemCatChem* 2015, *7*, 4050-4058 (DOI: 10.1002/cctc.201501021) and License Number 4234580022391.

2.5. References

1.   (a) Klass D. L., (2014), *Biomass for Renewable Energy, Fuels, and Chemicals*; Academic Press: san Diego, 1998; (b) Sheldon R. A. (2016), Green and sustainable manufacture of chemicals from biomass: state of the art, *Green Chem.*, 16, 950-963 (DOI: 10.1039/c3gc41935e); (c) Climent M. J., Corma A., Iborra S. (2014), Conversion of biomass platform molecules into fuel additives and liquid hydrocarbon fuels, *Green Chem.*, 16, 516-547 (DOI: 10.1039/c3gc41492b); (d) Hu L., Zhao G., Hao W., Tang X., Sun Y., Lin L., Liu S. (2012), Catalytic conversion of biomass-derived carbohydrates into fuels and chemicals via furanic aldehydes, *RSC Adv.*, 2, 11184-11206 (DOI: 10.1039/c2ra21811a); (e) de Vyver S.V., Geboers J., Jacobs P.A., Sels

B.F. (2011), Recent Advances in the Catalytic Conversion of Cellulose. *ChemCatChem*, 3, 82-94 (DOI: 10.1002/cctc.201000302); (f) Corma A., Iborra S., Velty A. (2007), Chemical Routes for the Transformation of Biomass into Chemicals. *Chem. Rev.*, 107, 2411-2502 (DOI: 10.1021/cr050989d); (g) Petrus L., Noordermeer M.A. (2006), Biomass to biofuels, a chemical perspective, *Green Chem.*, 8, 861-867 (DOI: 10.1039/b605036k); (h) Huber G.W., Chheda J.N., Barrett C.J., Dumesic J.A. (2005), Production of Liquid Alkanes by Aqueous-Phase Processing of Biomass-Derived Carbohydrates, *Science*, 308, 1446-1450 (DOI: 10.1126/science.1111166).

2. (a) Ruppert A. M., Weinberg K., Palkovits R. (2012), Hydrogenolysis Goes Bio: From Carbohydrates and Sugar Alcohols to Platform Chemicals, *Angew. Chem., Int. Ed.*, 51, 2564-2601 (DOI: 10.1002/anie.201105125); (b) Xing R., Subrahmanyam A. V., Olcay H., Qi W., van Walsum G. P., Pendse H., Huber G. W. (2010), Production of jet and diesel fuel range alkanes from waste hemicellulose-derived aqueous solutions, *Green Chem.*, 12, 1933-1946 (DOI: 10.1039/C0GC00263A).

3. (a) Tajvidi K., Hausoul P. J. C., Palkovits R. (2014), Hydrogenolysis of Cellulose over Cu-Based Catalysts-Analysis of the Reaction Network *ChemSusChem*, 7, 1311-1317 (DOI: 10.1002/cssc.201300978); (b) Yepez A., Garcia A., Climent M. S., Romero A. A., Luque R. (2014), Catalytic conversion of starch into valuable furan derivatives using supported metal nanoparticles on mesoporous aluminosilicate materials, *Catal. Sci. Technol.*, 4, 428-434 (DOI: 10.1039/c3cy00762f); (c) Alamillo R., Crisci A. J., Gallo J. M. R., Scott S. L., Dumesic J. A. (2013), A Tailored Microenvironment for Catalytic Biomass Conversion in Inorganic-Organic Nanoreactors, *Angew. Chem., Int. Ed..*, 52, 10349-10351(DOI: 10.1002/anie.201304693); (d) Yepez A., Pineda A., Garcia A., Romero A. A., Luque R. (2013), Chemical transformations of glucose to value added products using Cu-based catalytic systems, *Phys. Chem. Chem. Phys.*, 15, 12165-12172 (DOI: 10.1039/c3cp50707f); (e) Kimura H., Nakahara M., Matubayasi N. (2013), Solvent Effect on Pathways and Mechanisms for D-Fructose Conversion to 5-Hydroxymethyl-2-furaldehyde: In Situ 13C NMR Study, *J. Phys. Chem. A*, 117, 2102-2113 (DOI: 10.1021/jp312002h); (f) Zhang J., Weitz E. (2012), An

in Situ NMR Study of the Mechanism for the Catalytic Conversion of Fructose to 5-Hydroxymethylfurfural and then to Levulinic Acid Using [13]C Labeled D-Fructose, *ACS Catal.*, 2, 1211-1218 (DOI: 10.1021/cs300045r); (g) Thananatthanachon T., Rauchfuss T. B. (2010), Efficient Route to Hydroxymethylfurans from Sugars via Transfer Hydrogenation, *ChemSusChem*, 3, 1139-1141 (DOI: 10.1002/cssc.201000209).

4. (a) Yi X., Delidovich I., Sun Z., Wang S., Wang X., Palkovits R. (2015), A heteropoly acid ionic crystal containing Cr as an active catalyst for dehydration of monosaccharides to produce 5-HMF in water, *Catal. Sci. Technol.*, 5, 2496-2502 (DOI: 10.1039/c4cy01555j); (b) Ramli N. A. S., Amin N. A. S. (2015), A new functionalized ionic liquid for efficient glucose conversion to5-hydroxymethyl furfural and levulinic acid, *J. Mol. Catal. A: Chem.*, 407, 113-121 (DOI: 10.1016/j.molcata.2015.06.030); (c) Huang H., Denard C. A., Alamillo R., Crisci A. J., Miao Y., Dumesic J. A., Scott S. L., Zhao H. (2014), Tandem Catalytic Conversion of Glucose to 5-Hydroxymethylfurfural with an Immobilized Enzyme and a Solid Acid, *ACS Catal.*, 4, 2165-2168 (DOI: 10.1021/cs500591f); (d) Wu L., Song J., Zhang B., Zhou B., Zhou H., Fan H., Yang Y., Han B. (2014), Very efficient conversion of glucose to 5-hydroxymethylfurfural in DBU-based ionic liquids with benzenesulfonate anion, *Green Chem.*, 16, 3935-3941 (DOI: 10.1039/c4gc00311j); (e) Song J., Fan H., Ma J., Han B. (2013), Conversion of glucose and cellulose into value-added products in water and ionic liquid, *Green Chem.*, 15, 2619-2635 (DOI: 10.1039/c3gc41141a); (f) Richter F. H., Pupovac K., Palkovits R., Schüth F. (2013), Set of Acidic Resin Catalysts To Correlate Structure and Reactivity in Fructose Conversion to 5-Hydroxymethylfurfural, *ACS Catal.*, 3, 123-127 (DOI: 10.1021/cs3007439); (g) Crisci A. J., Tucker M. H., Lee M.-Y., Jang S. G., Dumesic J. A., Scott S. L. (2011), Acid-Functionalized SBA-15-Type Silica Catalysts for Carbohydrate Dehydration, *ACS Catal.*, 1, 719-728 (DOI: 10.1021/cs2001237); (h) Hu S., Zhang Z., Song J., Zhou Y., Han B. (2009), Efficient conversion of glucose into 5-hydroxymethylfurfural catalyzed by a common Lewis acid SnCl4 in an ionic liquid, *Green Chem.*, 11, 1746-1749 (DOI: 10.1039/b914601f).

5.	(a) van Putten R. J., van der Waal J. C., de Jong E., Rasrendra C. B., Heeres H. J., de Vries J. G. (2013), Hydroxymethylfurfural, A Versatile Platform Chemical Made from Renewable Resources, *Chem. Rev.*, 113, 1499-1597 (DOI: 10.1021/cr300182k); (b) Nakagawa Y., Tamura M., Tomishige K. (2013), Catalytic Reduction of Biomass-Derived Furanic Compounds with Hydrogen, *ACS Catal.*, 3, 2655-2668 (DOI: 10.1021/cs400616p); (c) Serrano-Ruiz J. C., Luque R., Sepulveda-Escribano A. (2011), Transformations of biomass-derived platform molecules: from high added-value chemicals to fuels via aqueous-phase processing, *Chem. Soc. Rev.*, 40, 5266-5281 (DOI: 10.1039/c1cs15131b).

6.	(a) Liu S., Amada Y., Tamura M., Nakagawa Y., Tomishige K. (2014), One-pot selective conversion of furfural into 1,5-pentanediol over a Pd-added Ir–ReOx/SiO2 bifunctional catalyst, *Green Chem.*, 16, 617-626 (DOI: 10.1039/c3gc41335g); (b) Yang Y., Du Z., Huang Y., Lu F., Wang F., Gao J., Xu J. (2013), Conversion of furfural into cyclopentanone over Ni-Cu bimetallic catalysts, *Green Chem.*, 15, 1932-1940 (DOI: 10.1039/c3gc37133f); (c) Chen J., Lu F., Zhang J., Yu W., Wang F., Gao J., Xu J. (2013), Immobilized Ru Clusters in Nanosized Mesoporous Zirconium Silica for the Aqueous Hydrogenation of Furan Derivatives at Room Temperature, *ChemCatChem*, 5, 2822-2826 (DOI: 10.1002/cctc.201300316); (d) Nakagawa Y., Nakazawa H., Watanabe H., Tomishige K. (2012), Total Hydrogenation of Furfural over a Silica-Supported Nickel Catalyst Prepared by the Reduction of a Nickel Nitrate Precursor, *ChemCatChem*, 4, 1791-1797 (DOI: 10.1002/cctc.201200218); (e) Xu W., Wang H., Liu X., Ren J., Wang Y., Lu G. (2011), Direct catalytic conversion of furfural to 1,5-pentanediol by hydrogenolysis of the furan ring under mild conditions over Pt/Co2AlO4 Catalyst, *Chem. Commun.*, 47, 3924-3926 (DOI: 10.1039/c0cc05775d).

7.	(a) Artz J., Mallmann S., Palkovits R. (2015), Selective Aerobic Oxidation of HMF to 2,5-Diformylfuran on Covalent Triazine Frameworks-Supported Ru Catalysts, *ChemSusChem*, 8, 672-679 (DOI: 10.1002/cssc.201403078); (b) Gallo J. M. R., Alonso D. M., Mellmer M. A., Dumesic J. A. (2013), Production and upgrading of 5-hydroxymethylfurfural using heterogeneous catalysts and biomass-derived solvents, *Green Chem.*, 15, 85-90 (DOI: 10.1039/c2gc36536g); (c) Grasset F. L., Katryniok B., Paul S., Nardello-

Rataj V., Pera-Titus M., Clacens J.-M., Campo F. D., Dumeignil F. (2013), Selective oxidation of 5-hydroxymethylfurfural to 2,5- diformylfuran over intercalated vanadium phosphate oxides, *RSC Adv.*, 3, 9942-9948 (DOI: 10.1039/c3ra41890a); (d) Pasini T., Piccinini M., Blosi M., Bonelli R., Albonetti S., Dimitratos N., Lopez-Sanchez J. A., Sankar M., He Q., Kiely C. J., Hutchings G. J., Cavani F. (2011), Selective oxidation of 5-hydroxymethyl-2-furfural using supported gold-copper nanoparticles, *Green Chem.*, 13, 2091-2099 (DOI: 10.1039/c1gc15355b); (e) Davis S. E., Houk L. R., Tamargo E. C., Datye A. K., Davis R. J. (2011), Oxidation of 5-hydroxymethylfurfural over supported Pt, Pd and Au catalysts, *Catal. Today*, 160, 55-60 (DOI: 10.1016/j.cattod.2010.06.004).

8. (a) Xia Q.-N., Cuan Q., Liu X.-H., Gong X.-Q., Lu G.-Z., Wang Y.-Q. (2014), Pd/NbOPO$_4$ Multifunctional Catalyst for the Direct Production of Liquid Alkanes from Aldol Adducts of Furans, *Angew. Chem., Int. Ed.*, 53, 9755-9760 (DOI: 10.1002/anie.201403440); (b) Li M., Xu X., Gong Y., Wei Z., Hou Z., Li H., Wang Y. (2014), Ultrafinely dispersed Pd nanoparticles on a CN@MgO hybrid as a bifunctional catalyst for upgrading bioderived compounds, *Green Chem.*, 16, 4371-4377 (DOI: 10.1039/c4gc00850b); (c) Li G., Li N., Li S., Wang A., Cong Y., Wang X., Zhang T. (2013), Synthesis of renewable diesel with hydroxyacetone and 2-methyl-furan, *Chem. Commun.*, 49, 5727-5729 (DOI: 10.1039/c3cc42296h); (d) Sutton A. D., Waldie F. D., Wu R., Schlaf M., Silks III L. A. P., Gordon J. C. (2013), The hydrodeoxygenation of bioderived furans into alkanes, *Nature Chem.*, 5, 428-432 (DOI: 10.1038/NCHEM.1609); (e) Sitthisa S., Resasco D. E. (2011), Hydrodeoxygenation of Furfural Over Supported Metal Catalysts: A Comparative Study of Cu, Pd and Ni, *Catal. Lett.*, 141, 784-791 (DOI 10.1007/s10562-011-0581-7); (f) Xinghua Z., Tiejun W., Longlong M., Chuangzhi W. (2010), Aqueous-phase catalytic process for production of pentane from furfural over nickel-based catalysts, *Fuel*, 89, 2697-2702 (doi: 10.1016/j.fuel.2010.05.043).

9. Alberg D. G., Poulsen T. B., Bertelsen S., Christensen K. L., Birkler R. D., Johannsen M., Jørgensen K. A. (2009), Organocatalysis with endogenous compounds: Towards novel non-enzymatic reactions, *Bioorg. Med. Chem. Lett.*, 19, 3888-3891 (DOI:10.1016/j.bmcl.2009.03.128).

10. Zhang J., Wu S. B., Li B., Zhang H. D. (2012), Advances in the Catalytic Production of Valuable Levulinic Acid Derivatives, *ChemCatChem*, 4, 1230-1237 (DOI: 10.1002/cctc.201200113).

11. Bozell J. J., Petersen G. R. (2010), Technology development for the production of biobased products from biorefinery carbohydrates-the US Department of Energy's "Top 10" revisited, *Green Chem.*, 12, 539-554 (DOI: 10.1039/b922014c).

12. (a) Song J., Wu L., Zhou B., Zhou H., Fan H., Yang Y., Meng Q., Han B. (2015), A new porous Zr-containing catalyst with a phenate group: an efficient catalyst for the catalytic transfer hydrogenation of ethyl levulinate to γ-valerolactone, *Green Chem.*, 17, 1626-1632 (DOI: 10.1039/c4gc02104e); (b) Phanopoulos A., White A. J. P., Long N. J., Miller P. W. (2015), Catalytic Transformation of Levulinic Acid to 2-Methyltetrahydrofuran Using Ruthenium-N-Triphos Complexes, *ACS Catal.*, 5, 2500-2512 (DOI: 10.1021/cs502025t); (c) Tang X., Zeng X., Li Z., Li W., Jiang Y., Hu L., Liu S., Sun Y., Lin L. (2015), In Situ Generated Catalyst System to Convert Biomass-Derived Levulinic Acid to γ -Valerolactone, *ChemCatChem*, 7, 1372-1379 (DOI: 10.1002/cctc.201500115); (d) Tan J., Cui J., Deng T., Cui X., Ding G., Zhu Y., Li Y. (2015), Water-Promoted Hydrogenation of Levulinic Acid to γ-Valerolactone on Supported Ruthenium Catalyst, *ChemCatChem*, 7, 508-512 (DOI: 10.1002/cctc.201402834); (e) Tang X., Li Z., Zeng X., Jiang Y., Liu S., Lei T., Sun Y., Lin L. (2015), In Situ Catalytic Hydrogenation of Biomass-Derived Methyl Levulinate to γ-Valerolactone in Methanol, *ChemSusChem*, 8, 1601-1607 (DOI: 10.1002/cssc.201403392); (f) Podolean I., Kuncser V., Gheorghe N., Macovei D., Parvulescu V. I., Coman S. M. (2013), Ru-based magnetic nanoparticles (MNP) for succinic acid synthesis from levulinic acid, *Green Chem.*, 15, 3077-3082 (DOI: 10.1039/c3gc41120f); (g) Wright W. R. H., Palkovits R. (2012), Development of Heterogeneous Catalysts for the Conversion of Levulinic Acid to γ -Valerolactone, *ChemSusChem*, 5, 1657-1667 (DOI: 10.1002/cssc.201200111); (h) Berkovitch G., Doron D., Nudelman A., Malik Z., Rephaeli A. (2008), Novel Multifunctional Acyloxyalkyl Ester Prodrugs of 5-Aminolevulinic Acid Display Improved Anticancer Activity Independent and Dependent on Photoactivation, *J. Med. Chem.*, 51, 7356-7369 (DOI:

10.1021/jm8008794); (i) Vallinayagam R., Schmitt F., Barge J., Wagnieres G., Wenger V., Neier R., Juillerat-Jeanneret L. (2008), Glycoside Esters of 5-Aminolevulinic Acid for Photodynamic Therapy of Cancer, *Bioconjugate Chem.*, 19, 821-839 (DOI: 10.1021/bc700324r).

13.   Sankar M., Dimitratos N., Miedziak P. J., Wells P. P., Kiely C. J., Hutchings G. J. (2012), Designing bimetallic catalysts for a green and sustainable future, *Chem. Soc. Rev.*, 41, 8099-8139 (DOI: 10.1039/c2cs35296f).

14.   Ohyama J., Kanao R., Esaki A., Satsuma A. (2014), Conversion of 5-hydroxymethylfurfural to a cyclopentanone derivative by ring rearrangement over supported Au nanoparticles, *Chem. Commun.*, 50, 5633-5636 (DOI: 10.1039/c3cc49591d).

15.   (a) Hu X., Westerhof R. J. M., Wu L., Dong D., Li C.-Z. (2015), Upgrading biomass-derived furans via acid-catalysis/hydrogenation: the remarkable difference between water and methanol as the solvent, *Green Chem.*, 17, 219-224 (DOI: 10.1039/c4gc01826e); (b) Liu F., Audemar M., Vigier K. D. O., Clacens J.-M., Campo F. D., Jerome F. (2014), Palladium/Carbon Dioxide Cooperative Catalysis for the Production of Diketone Derivatives from Carbohydrates, *ChemSusChem*, 7, 2089-2095 (DOI: 10.1002/cssc.201402221).

16.   Xu Z., Yan P., Xu W., Liu X., Xia Z., Chung B., Jia S., Zhang Z. C. (2015), Hydrogenation/Hydrolytic Ring Opening of 5-HMF by Cp*-Iridium(III) Half-Sandwich Complexes for Bioketones Synthesis, *ACS Catal.*, 5, 788-792 (DOI: 10.1021/cs501874v).

17.   Gupta K., Tyagi D., Dwivedi A. D., Mobin S. M., Singh S. K. (2015), Catalytic transformation of bio-derived furans to valuable ketoacids and diketones by water-soluble ruthenium catalysts, *Green Chem.*, 17, 4618-4627 (DOI: 10.1039/c5gc01376c).

18.   (a) Kumar P., Gupta R. K., Pandey D. S. (2014), Half-sandwich arene ruthenium complexes: synthetic strategies and relevance in catalysis, *Chem. Soc. Rev.*, 43, 707-733 (DOI: 10.1039/c3cs60189g); (b) Warner M. C., Casey C. P., Bäckvall J.-E. (2011), *Top. Organomet. Chem.*, 37, 85-125; (c) Conley B. L., Pennington-Boggio M. K., Boz E., Willims T. J. (2010), Discovery, Applications, and Catalytic Mechanisms of Shvo's Catalyst, *Chem. Rev.*, 110, 2294-2312 (DOI: 10.1021/cr9003133); (d) Karvembu R., Prabhakaran R.,

Natarajan K. (2005), Shvo's diruthenium complex: a robust catalyst, *Coord. Chem. Rev.*, 249, 911-918 (DOI: 10.1016/j.ccr.2004.09.025).

19. Gong L. H., Cai Y.-Y., Li X.-H., Zhang Y.-N., Su J., Chen J.-S. (2014), Room-temperature transfer hydrogenation and fast separation of unsaturated compounds over heterogeneous catalysts in an aqueous solution of formic acid, *Green Chem.*, 16, 3746-3751 (DOI: 10.1039/c4gc00981a).

20. (a) Wang F.-F., Shi A.-W., Qin X.-X., Liu C.-L., Dong W.-S. (2011), Dehydration of fructose to 5-hydroxymethylfurfural by rare earth metal trifluoromethanesulfonates in organic solvents, *Carbohydr. Res.*, 346, 982-985 (DOI: 10.1016/j.carres.2011.03.009); (b) Hu X., Westerhof R. J. M., Dong D., Wu L., Li C.-Z. (2014), Acid-Catalyzed Conversion of Xylose in 20 Solvents: Insight into Interactions of the Solvents with Xylose, Furfural, and the Acid Catalyst, *ACS Sust. Chem. Eng.*, *2*, 2562-2575 (dx.doi.org/10.1021/sc5004659).

21. (a) Pasini T., Solinas G., Zanotti V., Albonetti S., Cavani F., Vaccari A., Mazzanti A., Ranieri S., Mazzoni R. (2014), Substrate and product role in the Shvo's catalyzed selective hydrogenation of the platform bio-based chemical 5-hydroxymethylfurfural, *Dalton Trans.*, *43*, 10224-10234 (DOI: 10.1039/c4dt00304g); (b) Busetto L., Fabbri D., Mazzoni R., Salmi M., Torri C., Zanotti V. (2011), Application of the Shvo catalyst in homogeneous hydrogenation of bio-oil obtained from pyrolysis of white poplar: New mild upgrading conditions, *Fuel*, *90*, 1197-1207 (DOI: 10.1016/j.fuel.2010.10.036).

22. Morris R. E., Aird R. E., Murdoch P. d. S., Chen H. M., Cummings J., Hughes N. D., Parsons S., Parkin A., Boyd G., Jodrell D. I., Sadler P. J. (2001), Inhibition of Cancer Cell Growth by Ruthenium(II) Arene Complexes, *J. Med. Chem.*, *44*, 3616-3621 (DOI: 10.1021/jm010051m).

23. (a) Tyagi D., Rai R. K., Dwivedi A. D., Mobin S. M., Singh S. K. (2015), Phosphine-free ruthenium-arene complex for low temperature one-pot catalytic conversion of aldehydes to primary amides in water, *Inorg. Chem. Front.*, *2*, 116-124 (DOI: 10.1039/c4qi00115j); (b) Singh S. K., Trivedi M., Chandra M., Sahay A. N., Pandey D. S. (2004), Luminescent Piano-Stool Complexes Incorporating 1-(4-Cyanophenyl)imidazole: Synthesis, Spectral,

and Structural Studies, *Inorg. Chem.*, *43*, 8600-8608 (DOI: 10.1021/ic049256m).

24. Fujii A., Hashiguchi S., Uematsu N., Ikariya T., Noyori R. (1996), Ruthenium(II)-Catalyzed Asymmetric Transfer Hydrogenation of Ketones Using a Formic Acid-Triethylamine Mixture, *J. Am. Chem. Soc.*, *118*, 2521-2522 (DOI: 10.1021/ja954126l).

25. Girisuta B., Janssen L. P. B. M., Heeres H. J. (2006), A kinetic study on the decomposition of 5-hydroxymethylfurfural into levulinic acid, *Green Chem.*, *8*, 701-709 (DOI: 10.1039/b518176c).

26. Hu X., Song Y., Wu L., Gholizadeh M., Li C. -Z. (2013), One-Pot Synthesis of Levulinic Acid/Ester from C5 Carbohydrates in a Methanol Medium, *ACS Sustainable Chem. Eng.*, *1*, 1593-1599 (DOI: 10.1021/sc400229w).

27. Nakagawa Y., Takada K., Tamura M., Tomishige K. (2014), Total Hydrogenation of Furfural and 5-Hydroxymethylfurfural over Supported Pd–Ir Alloy Catalyst, *ACS Catal.*, 4, 2718-2726 (DOI: 10.1021/cs500620b).

29. Tuteja J., Choudhary H., Nishimura S., Ebitani K. (2014), Direct Synthesis of 1,6-Hexanediol from HMF over a Heterogeneous Pd/ZrP Catalyst using Formic Acid as Hydrogen Source, *ChemSusChem*, 7, 96-100 (DOI: 10.1002/cssc.201300832).

28. Kong X., Zheng R., Zhu Y., Ding G., Zhu Y., Li Y.-W. (2015), Rational design of Ni-based catalysts derived from hydrotalcite for selective hydrogenation of 5-hydroxymethylfurfural, *Green Chem.*, 17, 2504-2514 (DOI: 10.1039/c5gc00062a).

30. Gorbanev Y. Y., Kegnæs S., Riisager A. (2011), ORIGINAL PAPER Effect of Support in Heterogeneous Ruthenium Catalysts Used for the Selective Aerobic Oxidation of HMF in Water, *Top Catal.*, 54, 1318-1324 (DOI 10.1007/s11244-011-9754-2).

31. (a) Bennett M. A., Huang T., Matheson T. W., Smith A. K. (1982), (η6-Hexamethylbenzene)Ruthenium Complexes, *Inorg. Synth.*, 21, 74-78 (DOI: 10.1002/9780470132524.ch16); (b) Zelonka R. A., Baird M. C. (1972), Benzene Complexes of Ruthenium(I1), *Can. J. Chem.*, 50, 3063-3072 (DOI: 10.1139/v72-486).

32. Sheldrick G. M. (2008), Program for Crystal Structure Solution and Refinement, University of Goettingen, Goettingen, Germany, *Acta Crystallogr., Sect. A,*, 64, 112-122 (DOI: 10.1107/S0108767307043930).

Chapter 3

Catalytic hydrogenation of arenes in water over *in situ* generated ruthenium nanoparticles immobilized on carbon

3.1. Introduction

Aromatic and heteroaromatic ring hydrogenation in one of the most important industrially applicable methodology because it provide a convenient way to synthesize a wide range of cyclic hydrocarbons.[1-4] Till now, fossil raw materials remains the main source of origin for the aromatic compounds. Therefore, the development of efficient processes for the conversion of renewable lignocellulosic biomass to value-added fine chemicals attracts considerable recent attention.[5] In this regard, selective hydrogenation of liginin-derived aromatic compounds to corresponding alicyclic products is of particular importance.[6-7] Since, functionalization of cyclohexane is challenging due to the low reactivity of cyclohexane, synthesis of cyclohexane and its derivative by hydrogenation of aromatic precursors attracted extensive scientific and industrial attention.[6,8-16] For instance, chemoselective hydrogenation of benzoic acid to cyclohexanecarboxylic acid has gained great attention, as the hydrogenated product cyclohexanecarboxylic acid is an important organic intermediate in pharmaceuticals for the synthesis of drugs like praziquantel and ansatrienin.[17] However, selective hydrogenation of aromatic ring is challenging particularly in the presence of several reducible functional group, because of it is an energy consuming reaction due to the resonance energy of aromatic ring and also the aromatic ring hydrogenation is least preferred in the presence of other reducible functional groups.

Hydrogenation of benzoic acid and its derivative were reported earlier using stoichiometric amount of Na-K alloys.[18] However, being environmentally friendly and efficient (recyclable catalyst) catalytic hydrogenation process has gained advantages over stoichiometric hydrogenation reaction. Therefore, several efficient catalysts based on monometallic Pd, Pt, Rh, Ru, and several alloys were explored for aromatic ring hydrogenation of benzoic acid and its derivatives.[19-31] However most of the catalytic reactions were performed usually under high pressure of H_2, which may have several safety concerns. Among these catalysts, ruthenium catalyzed catalysts are attractive, because of its low cost and almost comparable activity than

those of highly active Pd catalyst.[6,8,10,12,15,19,24-27,31] Interestingly, most of the active catalysts are those which are supported on carbonaceous materials.[6,9,19-21,24,25,27,28,30,31] Notably, recent findings inferred that stabilizers, such as surfactants or ligands, significantly control the catalytic properties of metal nanoparticles.[15,26,30,31] Recently, Beller *et al.* reported highly selective hydrogenation of arenes over ruthenium nanoparticle catalysts modified with a carbon-nitrogen matrix.[6] More recently, Li *et al.* also reported ruthenium nanoparticles immobilized on mesoporous carbon as highly active catalyst for the hydrogenation of benzoic acid to cyclohexanecarboxylic acid.[27] Hence, several synthetic procedures for the synthesis of Ru/C nanoparticles have been explored, but in most of the cases high temperature (up to 450 $^{\circ}$C), high pressure (up to 60 bar) of H_2 gas, and externally added carbon supports were used to synthesise Ru/C nanoparticles.[32-36]

On the other hand designing effective organometallic catalyst for the hydrogenation of (hetero)arenes has also received significant attention in recent years. Zeng *et al.* have recently reported selective hydrogenation of aromatic ring of ketone and phenols using cyclic(amino)alkyl carbene rhodium complexes using H_2 (5 bar) gas.[37] Notably, ruthenium arene complexes based on nitrogen donor ligands, such as ethylenediamine derived ligands has also been identified as a well established class of transfer hydrogenation catalysts,[38-42] and therefore we anticipated that these complexes could be a good candidate to achieve arene ring hydrogenation under a precisely tuned reaction condition. Reaction of the precursor, ruthenium-arene dimer, with ethylenediamine (en) in a suitable solvent led to the straightforward synthesis of cationic [(η^6-arene)Ru(en)Cl]$^+$ complex.[43-44] We have recently explored such complexes for a tandem catalytic transformation of furan to ketoacid and diketones with an aid of formic acid as H-source.[44] Recently, Fan *et al.* have also explored analogues complexes for enantioselective hydrogenation of naphthalene derivatives in the presence of H_2 gas.[45-46] Notably, the above and plenty of several other transfer hydrogenation/hydrogenation reactions catalyzed by (arene)Ru-en based complex are targeted mostly towards C=O or C=N bonds.[38-42,44-46] *However*, at elevated temperature (60-100°C) using high pressure H_2 gas (10-60 bar), hydrogenation of C=C bond (aromatic and others) were also successfully attempted using ruthenium complexes.[47-50]

Striking work of Finke *et al.* established that at higher temperature (110 °C and 60 atm H_2) catalytic reaction performed using ruthenium metal complexes, instead of ruthenium complex, traces of Ru(0) nanoparticles, generated *in situ*, are the active catalytic species for the hydrogenation of benzene.[50-52] These and other analogous classical findings suggested that under tuned condition deliberate *in situ* generation of active metal nanoparticles from metal complexes may resulted in high catalytic activity.[53] Therefore, we report herein a facile hydrogenation of a wide range of arenes and heteroarenes by *in situ* generated active ruthenium nanoparticles immobilized on carbon and H_2 gas from an organometallic precursor, $[(\eta^6\text{-}C_6H_6)Ru(en)Cl]^+$, and formic acid, respectively via a tandem catalytic process in water. We also investigated the effect of ligands to achieve high catalytic activity for ruthenium catalyst. Using this methodology, several substrates analogous to lignin-derived fragments were also successfully hydrogenated to corresponding alicyclic products.

3.2. Results and discussion

At the outset of our experiments, hydrogenation of arenes was performed using benzoic acid as a model substrate (Scheme 1). A teflon coated autoclave containing $[(\eta^6\text{-}C_6H_6)Ru(en)Cl]PF_6$ (5 mol %) dissolved in 10 mL water was added to benzoic acid and formic acid. The sealed autoclave was heated at a constant temperature of 150 °C for 16 h. Results inferred a complete conversion of benzoic acid (**1**) to cyclohexanecarboxylic acid (**1a**) with >99% selectivity.

Complete disappearance of aromatic peaks in ^1H and ^{13}C NMR and the formation of new peak corresponding to aliphatic C-H, further confirmed the formation of cyclohexanecarboxylic acid (**1a**). HRMS analysis is also in good agreement with that of cyclohexanecarboxylic acid (m/z for cyclohexanecarboxylic acid + Na^+ 151.0730 (calcd.) and 151.0734 (found)). Interestingly, when reaction was conducted using $RuCl_3.xH_2O$, instead of $[(\eta^6\text{-}C_6H_6)Ru(en)Cl]PF_6$, reaction could not proceed (Scheme 3.1, and Table 3.1). Moreover, reaction performed with a phosphine containing (arene)Ru complex, $[(\eta^6\text{-}C_6H_6)RuPPh_3Cl_2]$, or in the presence of (arene)Ru dimer $[\{(\eta^6\text{-}C_6H_6)RuCl\}_2]$, also resulted in no conversion of benzoic acid (Scheme 3.1 and Table 3.1). These results inferred that it is not just the Ru metal but also the overall structural ingredients of the $[(\eta^6\text{-}C_6H_6)Ru(en)Cl]PF_6$ which play

a crucial role in the observed high catalytic activity towards benzoic acid (**1**) to cyclohexanecarboxylic acid (**1b**) conversion.
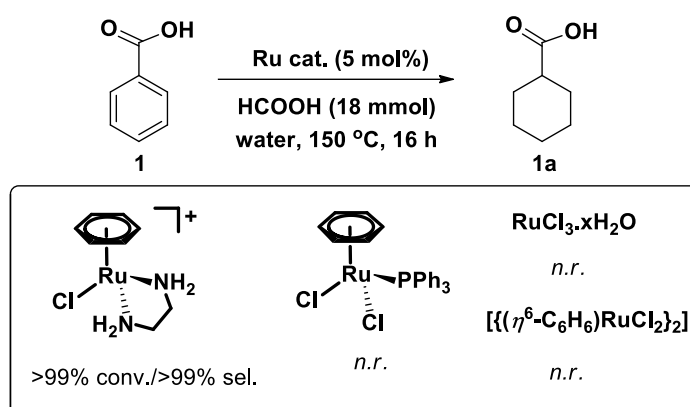
Scheme 3.1. *Catalytic hydrogenation of benzoic acid to cyclohexanecarboxylic acid using several ruthenium precursors in water*

Table 3.1. *Effect of different catalyst on the catalytic ring hydrogenation of benzoic acid[a]*

S. No.	Catalyst	Conversion (%)	Selectivity (%)
1	$[(\eta^6\text{-}C_6H_6)RuCl(en)]PF_6$	>99	>99
2	$RuCl_3.xH_2O$	0	0
3	$[(\eta^6\text{-}C_6H_6)RuCl_2PPh_3]$	0	0
4	$[(\eta^6\text{-}C_6H_6)RuCl_2]_2$	0	0
5[54]	Ru nanoparticle prepared by $RuCl_3.xH_2O$ +NaBH$_4$+PVP	0	0
6[55]	Ru nanoparticle prepared by ($RuCl_3.xH_2O$ +EG)	0	0
7[55]	Ru nanoparticle prepared by (Ru(acac)$_3$+TEG)	0	0

[a]Reaction conditions: Benzoic acid (1.0 mmol), HCOOH (18 equiv.), ruthenium catalyst (5 mol%), H_2O (10 mL), 150 °C, 16 h.

Notably, in transfer hydrogenation catalysts, ligands having N-H bonds play determining role particularly to help in the activation of H-source.[38-42] It is evident from the literature that among the ruthenium based catalysts explored for HCOOH to H_2 conversion or hydrogenation using HCOOH, the most active catalysts are one those having nitrogen based ligand.[44,56,57] Presence of nitrogen was found to be advantageous in these complexes, because of its crucial involvement in providing

protic (–NH) hydrogen and subsequently in the facile release of H_2 gas by stabilising various intermediate by H-bond. For instance in a very recent report, Huang *et al.* demonstrated H_2 production from HCOOH catalysed by a Ru complex having diamine based nitrogen ligands.[56] Moreover, result showed that reaction pathway following the participation of –NH is more favourable. Moreover, we have also investigated several Ru complexes with ligands having –NH bonds, and observed that these catalysts demonstrated high catalytic active for hydrogenation reaction using HCOOH as H-source.[44,57] Therefore, presence of nitrogen ligands in the studied ruthenium complex $[(\eta^6\text{-}C_6H_6)Ru(en)Cl]^+$ is crucial to achieve high catalytic activity.

To gather further evidence to support the crucial role of formic acid as H-source in the hydrogenation of benzoic acid, catalytic reaction was performed by replacing formic acid with other organic acids such as acetic acid, propionic acid and isobutyric acid (Figure 3.1a). Contrary to the high conversion of benzoic acid to cyclohexanecarboxylic acid achieved in the presence of formic acid, reaction with other organic acid resulted in no conversion of benzoic acid. Furthermore, decreasing the formic acid contents (<18 equiv.), resulted in the decrease in the conversion of benzoic acid. Notably, in the absence of formic acid reaction could not proceed (Figure 3.1b, and Table 3.2). These observations attributed to a strong structure-activity relationship of the $[(\eta^6\text{-}C_6H_6)Ru(en)Cl]^+$ having N-H bonds and the crucial role of formic acid as a H-source.[44,57]
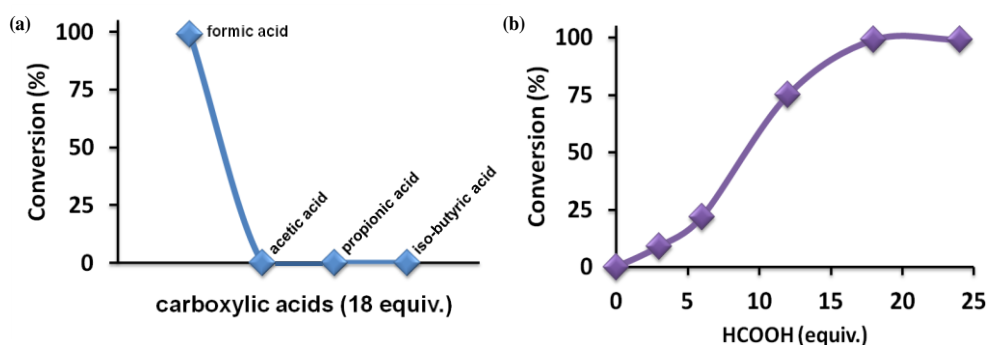
Figure 3.1. *Ruthenium catalyzed hydrogenation of benzoic acid to cyclohexanecarboxylic acid with (a) several organic acids (18 equiv.), and (b) varying amount of formic acid (0–24 equiv). Reaction conditions: (a) benzoic acid (1.0 mmol), catalyst (5 mol%), carboxylic acid and water (10 mL) at 150 °C for 16 h.*

Table 3.2. *Effect of formic acid concentration on the catalytic ring hydrogenation of benzoic acid*[a]

S. No.	HCOOH (mmol)	Conversion (%)	Selectivity (%)
1	0	0	0
2	3	9	>99
2	6	22	>99
3	12	75	>99
4	18	>99	>99
5	24	>99	>99

[a]Reaction conditions: Benzoic acid (1.0 mmol), H_2O (10 mL), ruthenium catalyst precursor (5 mol%), 150 °C, 16 h.

To investigate if $[(\eta^6\text{-}C_6H_6)Ru(en)Cl]^+$ can also catalyze the decomposition of HCOOH to H_2, experiment was performed $[(\eta^6\text{-}C_6H_6)Ru(en)Cl]PF_6$ and HCOOH (S/C = 20) in water at 150 °C (in the absence of the substrate). Results inferred that indeed the $[(\eta^6\text{-}C_6H_6)Ru(en)Cl]^+$ is catalytically active for the decomposition of HCOOH to H_2, and complete conversion of HCOOH to H_2 and CO_2 was achieved in 4 h (TOF = 5.0 h^{-1}) (Figure 3.2). Moreover, catalytic hydrogenation of benzoic acid at lower reaction temperature of 120 °C or 100 °C, resulted in the very poor conversion or ended with no reaction at all. However, at 170 °C, complete conversion of benzoic acid to cyclohexanecarboxylic acid was achieved in lesser reaction time (10 h) (Figures 3.3 and Tables 3.3).
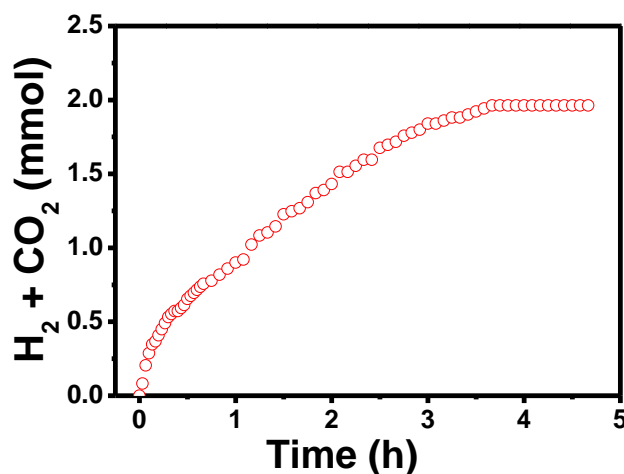
Figure 3.2. *Decomposition of formic acid (1.0 mmol) to H_2 and CO_2 using ruthenium catalyst ([(η^6-C_6H_6)Ru(en)Cl]PF$_6$) (0.05 mmol) at 150 °C.*
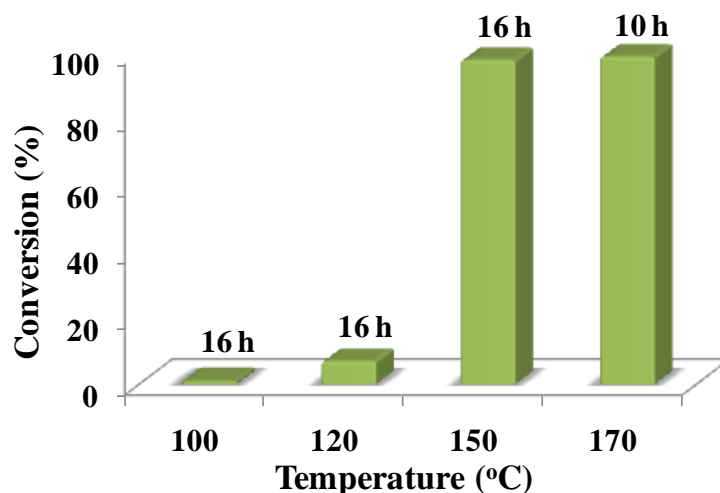
Figure 3.3. *Effect of formic acid concentration on the catalytic ring hydrogenation of benzoic acid to cyclohexanecarboxylic acid in the presence of ruthenium catalyst in water. Reaction conditions: benzoic acid (1.0 mmol), ruthenium catalyst precursor (5 mol%), formic acid (18 equiv.) and water (10 mL) at different temperature for 16 h.*

Table 3.3. *Effect of reaction temperature on the catalytic ring hydrogenation of benzoic acid[a]*

S. No.	Temperature (°C)	Time (h)	Conversion (%)	Selectivity (%)
1	100	16	0	>99
2	120	16	7	>99
3	150	16	98	>99
4	170	10	>99	>99

[a]Reaction conditions: Benzoic acid (1.0 mmol), HCOOH (18 equiv.), ruthenium catalyst precursor (5 mol%), H_2O (10 mL), 16 h.

Notably, during the catalytic reaction, initial dark brown colour of the reaction mixture turned to black turbid suspension. The resulting black particles were separated by centrifugation and were analysed further (Figure 3.4, and Figure 3.5). Powder X-ray diffraction pattern (XRD) showed the formation of hexagonal closed pack (*hcp*) Ru nanoparticles with a prominent (2Θ) peak at 44° indexed to (101) lattice planes of Ru (JCPDS 06-0663).[24] Moreover, presence of a broad peek centred at a 2Θ value of 25 °C, suggesting formation of a carbon supported Ru nanoparticle (Ru/C).[24,27]
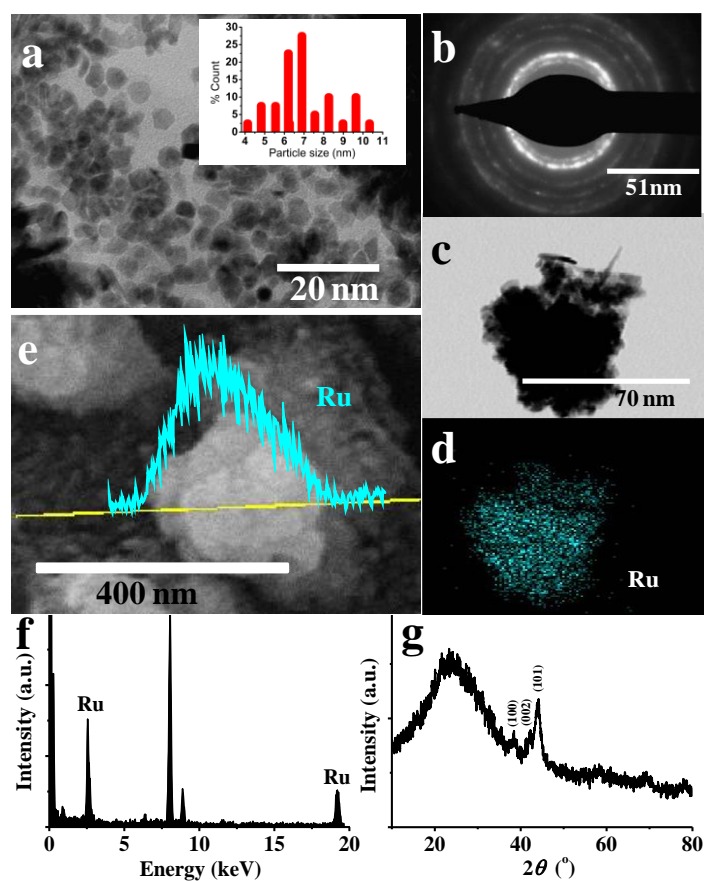
Figure 3.4. *Characterization of ruthenium nanoparticle catalyst. (a) TEM with histogram (inset). (b) SAED. (c-d) Elemental mapping of corresponding TEM image. (e) SEM-EDX line scan and (f) EDX mapping. (g) Powder XRD pattern.*
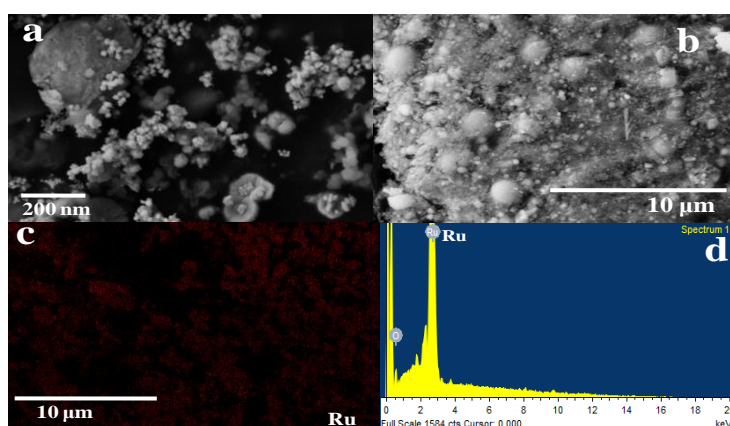
Figure 3.5. *SEM images and corresponding EDX mapping of ruthenium nanoparticle generated in situ from the catalyst precursor $[(\eta^6\text{-}C_6H_6)Ru(en)Cl]PF_6$*

86

The TEM image of Ru/C nanoparticles showed the presence of *ca* 7 nm sized, nearly spherical nanoparticles (Figure 3.4a) consistent with XRD, selective area electron diffraction (SAED) pattern also revealed the presence of (101) lattice plane of *hcp* Ru nanoparticles. Energy-dispersive X-ray spectroscopy (EDX) (Figure 3.4) and elemental mapping (Figure 3.5) further support the presence of well dispersed Ru nanoparticles. In agreement with the above analyses, ICP-IES analysis also confirmed the presence of Ru metal. Moreover, the supernatant obtained after catalytic reaction was also analysed by ^{1}H NMR and mass spectral analysis (Figure 3.6). Results revealed that the characteristic peaks of organometallic-Ru complex $[(\eta^6\text{-}C_6H_6)Ru(en)Cl]PF_6$ were completely vanished in ^{1}H NMR, and also the molecular ion peak of the $[(\eta^6\text{-}C_6H_6)Ru(en)Cl]^+$ at m/z 275.2 was absent in the supernatant. The above observations suggested the complete conversion of organometallic-Ru complex to Ru/C nanoparticles.
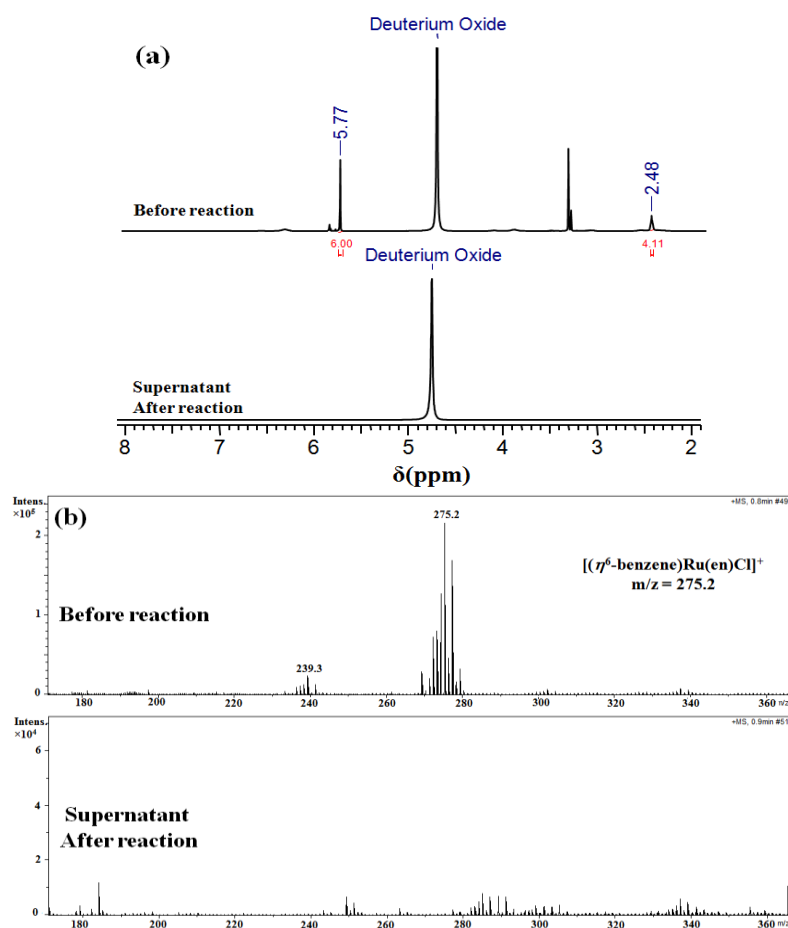
Figure 3.6*. (a) ^{1}H NMR and (b) mass spectra of supernatant obtained after the reaction of $[(\eta^6\text{-}C_6H_6)Ru(en)Cl]PF_6$ and HCOOH, under optimized reaction condition.*

To further establish the nature of the active catalyst, hydrogenation experiments were performed by using pre-synthesised Ru/C nanoparticles, obtained from the organometallic precursor ([(η^6-C$_6$H$_6$)Ru(en)Cl]PF$_6$), in the presence of external H$_2$ gas and HCOOH, respectively. The pre-synthesised Ru/C nanoparticles exhibited good catalytic activity toward the hydrogenation reaction in the presence of external hydrogen gas, but could not catalyze the hydrogenation reaction in the presence of HCOOH. Worthy to mention that, the [(η^6-C$_6$H$_6$)Ru(en)Cl]PF$_6$ was not able to catalyze arene hydrogenation in the presence of H$_2$ gas. However, the organometallic complex catalyses the facile transformation of HCOOH to H$_2$ gas[44,56,57] under the optimized reaction conditions which subsequently generate the Ru/C as a active catalysts for the hydrogenation of benzoic acid (Scheme 3.2). Therefore, experimental observation clearly revealed that the Ru organometallic complex catalyses H$_2$ gas generation from the formic acid through transfer hydrogenation. (Figure 3.2). These result clearly inferred that pre-synthesized Ru/C nanoparticle from organometallic-Ru precursor is the active form of catalyst for arene ring hydrogenation of benzoic acid to cyclohexanecarboxylic acid with the aid of *in situ* generated H$_2$ gas.
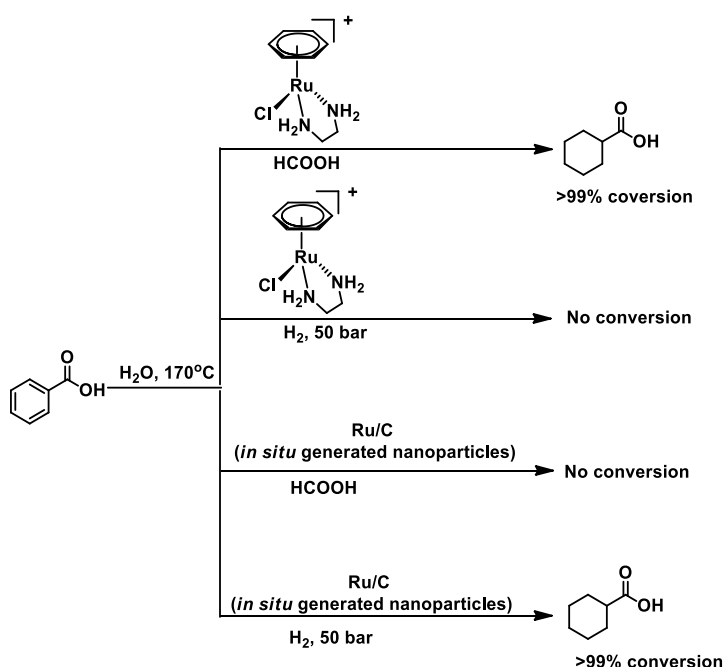
Scheme 3.2. *Catalytic hydrogenation of benzoic acid to cyclohexanecarboxylic acid conducted in the presence of various ruthenium catalysts at 170 °C for 10 h.*

Therefore, based on above findings, we anticipated that the reaction proceeds through an initial activation of formic acid to H_2 gas by the $[(\eta^6\text{-}C_6H_6)Ru(en)Cl]^+$ complex, where the presence of N-H bond is a crucial factor and is in consistence with our earlier findings, where $[(\eta^6\text{-}C_6H_6)Ru(en)Cl]^+$ complex catalyzed the hydrogenation of aldehydes with the aid of formic acid in water. The Hg(0) poisoning experiments support the homogeneous nature of the catalyst during the activation of formic acid and the formation of Ru-hydride complexes, $[(\eta^6\text{-}C_6H_6)Ru(H)(en)]^+$.[44] However, performing the catalytic reaction at high temperature may transfer this highly active *in situ* generated Ru-hydride complex into a carbon supported Ru nanoparticles (Ru/C).[51,52] Notably, we observed very low conversions for the catalytic reactions performed at lower temperature(Tables 3.3). Also, the colour of the reaction mixture remains unchanged at lower temperature suggesting that only a small portion of pre-catalyst has been converted into the Ru(0) metal nanoparticles. Notably, ^{1}H NMR and mass spectral analysis of the supernatant obtained after the reaction at 170 ºC inferred no characteristic peaks corresponding to the organometallic Ru precursor, suggesting the complete conversion of organometallic Ru precursor to Ru(0) nanoparticles (Figure 3.4). A similar metal-hydride complex were also reported during the formation of Ru(0) and Rh(0) from the respective organometallic complexes by Fink *et al.*[50-52] Formation of Ru/C nanoparticles in our reaction system is indeed in consistence with the famous Fink scheme "A→B, then A + B→2B" demonstrating the heterogeneous nucleation process.[52] Therefore, the *in situ* generated Ru/C nanoparticle catalyst facilitates the hydrogenation of benzoic acid to cyclohexanecarboxylic acid using available *in situ* generated H_2 gas (from formic acid activated by the $[(\eta^6\text{-}C_6H_6)Ru(en)Cl]^+$). Hg(0) poisoning experiments performed by conducting the catalytic experiments in the presence of Hg(0), inferred that catalytic conversion is drastically suppressed (Table 3.4). This result is consistence with earlier reports which strongly support the heterogeneous nature of the catalyst.[50-53] It is worth mentioning here, that reaction performed by using pre-synthesized Ru/C nanoparticles resulted in no conversion in the presence of formic acid (Table 3.1). These findings further suggested that the crucial activation of formic acid to generate H_2 gas, is only facilitated by the unique structural advantage with $[(\eta^6\text{-}C_6H_6)Ru(en)Cl]^+$ complex. Thus the hydrogenation of

arene using the pre-catalyst $[(\eta^6\text{-}C_6H_6)Ru(en)Cl]^+$ represents a unique combination of homogeneous (activation of formic acid by $[(\eta^6\text{-}C_6H_6)Ru(en)Cl]^+)$ and heterogeneous catalytic (hydrogenation of arenes by *in situ* generated Ru/C) cycles (Scheme 3.3).
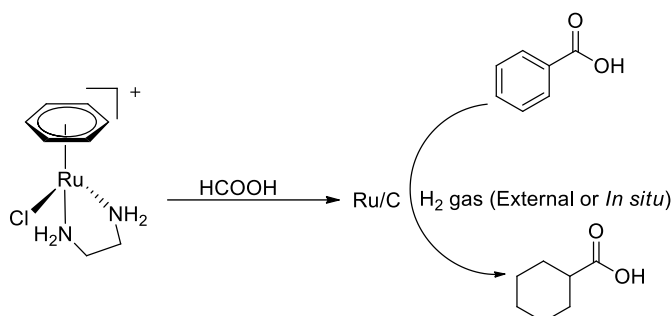
Scheme 3.3. *Schematic representation for the effect of H-source on the formation of Ru/C nanoparticle from Ru complex [(η^6-C₆H₆)Ru(en)Cl]PF₆ at 170 ℃ for 10 h.*

Table 3.4. *Mercury poison experiment of the catalytic ring hydrogenation of benzoic acid[a]*

S. N.	Catalyst	Hg(0)	Conversion
1	$[(\eta^6\text{-}C_6H_6)RuCl(en)]PF_6$ **(Control Experiment)**	--	>99%
2	$[(\eta^6\text{-}C_6H_6)RuCl(en)]PF_6$ **(Mercury Poisoning Experiment)**	Hg(0) (added in excess)	<8%

[a]Reaction conditions: Benzoic acid (1.0 mmol), HCOOH (18 equiv.), ruthenium catalyst precursor (5 mol%), H₂O (10 mL), 170 ℃, 10 h.

Notably, during the transformation of benzoic acid (**1**) to cyclohexanecarboxylic acid (**1a**), no intermediates were observed. To gain further insights into the ruthenium catalyzed hydrogenation of arenes and to understand the mode of hydrogenation reaction, catalytic hydrogenation of arenes having at least two phenyl rings, such as diphenylmethane (**2**), was investigated under the optimized reaction conditions. Analyzing the hydrogenation reaction by ¹H NMR revealed a stepwise process for the hydrogenation of phenyl rings of diphenymethane (**2**)

(Figure 3). In the initial 6 h, partially hydrogenated product (cyclohexylmethyl)benzene (**2b**) was observed with 82% selectivity, along with the completely hydrogenated product, dicyclohexylmethane (**2a**) (18% selectivity) (Figure 3.7 and Table 3.5, entry 2). Further extending the reaction to 10 h, resulted in the compete conversion of diphenylmethane (**2**) selectively to dicyclohexylmethane (**2a**) in 72% yield (Table 5, entry 2).
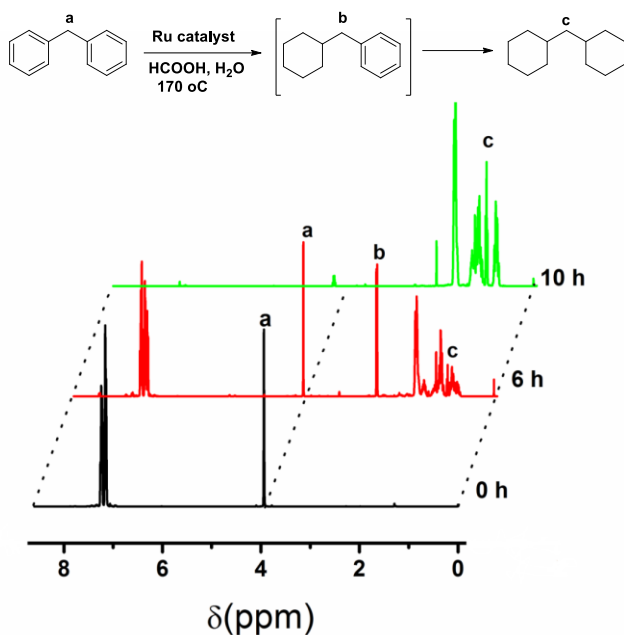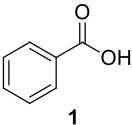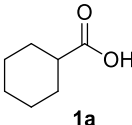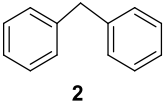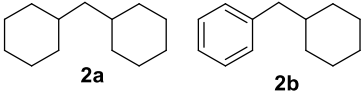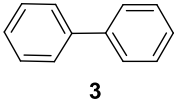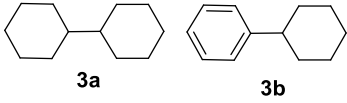
Figure 3.7. *¹H NMR monitoring for the ruthenium catalyzed hydrogenation of diphenylmethane (**2**) in water.*
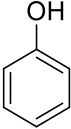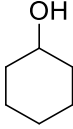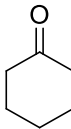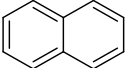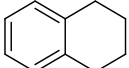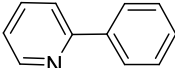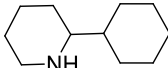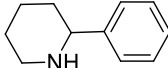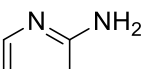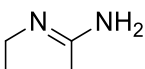
We further performed the catalytic hydrogenation reaction using a range of several other arenes and heteroarenes under the optimized reaction conditions (Table 1 summarized the results). As inferred from the results, a wide range of aromatic compounds, including those having more than one phenyl rings, biphenyl, phenylpyridine, benzophenone and naphthalene, can be transformed to corresponding hydrogenated form with good selectivity (Table 3.5, entries 1-17). Biphenyl (**3**) was hydrogenated to 1,1'-bicyclohexane (**3a**) and cyclohexylbenzene (**3b**) with 1:1 selectivity (Table 3.5, entry 3). Analogous to diphenylmethane, benzophenone (**4**) also showed the stepwise hydrogenation of two phenyl ring, where hydrogenation of ketonic group was also observed (Table 3.5, entry 4). Notably, complete hydrogenation of ketonic group of benzophenone (**2**) resulted in the formation of (cyclohexylmethyl)benzene (**2b**) as a major product, as observed with

91

the hydrogenation of diphenylmethane (**2**). Aromatic compounds having reducible substituents, such as acetophenone (**5**), cinnamaldehyde (**6**), benzonitrile (**7**), benzamide (**11**) and others were also transformed into corresponding hydrogenated products, with the hydrogenation of arene ring and the reducible functional groups (Table 3.5, entries 5-13). Benzonitrile (**7**) undergoes facile hydrogenation to form 1-cyclohexylmethylamine (**7a**) and benzylamine (**7b**) by the hydrogenation of benzene ring and nitrile group (Table 3.5, entry 7). Hydrogenation of aniline (**8**) to cyclohexylamine (**8a**) was also achieved in 58% yield (Table 3.5, entry 8). Analogous to aniline hydrogenation, hydrogenation of nitrobenzene (**9**) also led to the formation of cyclohexylamine (**8a**) in 41% yield (Table 3.5, entry 9). Hydrogenation of benzylalcohol (**12**) to 1-cyclohexylmethanol (**12a**) was also achieved with high selectivity (Table 3.5, entry 12). Hydrogenation of phenol to cyclohexanone is an industrially important challenging task due to its high demand for nylon 6 and nylon 66 production.[58] Under the reaction conditions, phenol (**13**) was reduced to form cyclohexanone (**13b**) by the hydrogenation of benzene ring of phenol (Table 3.5, entry 13).[59,60] However, the major fraction of the hydrogenated product is cyclohexanol (**13a**) formed by complete hydrogenation of phenol (Table 3.5, entry 13). Unlike biphenyl, fused ring arenes, such as naphthalene (**14**), showed the formation of only single ring hydrogenated product (**14a**) albeit with poor conversion (Table 3.5, entry 14).

Table 3.5. *Ruthenium catalyzed hydrogenation of (hetero)arenes*

Entry	Substrate	Product	Conv./Sel. (%) [yield][a]
1	**1**	**1a**	>99/>99 [61% (**1a**)]
2	**2**	**2a** **2b**	>99/>99 [72% (**2a**)] 63/18:82 (**2a/2b**)[b]
3	**3**	**3a** **3b**	89/51:49 (**3a/3b**) [40% (**3a**)]

4	**4**	**2b** **2** **4a** **4b**	>99/75:11:7:7 (**2b/2/4a/4b**)
5	**5**	**5a**	>99/>99 [62% (**5a**)]
6	**6**	**6a** **6b**	>99/75:25 (**6a/6b**)
7	**7**	**7a** **7b**	81/22:78 (**7a/7b**)
8	**8**	**8a**	>99/>99 [58% (**8a**)]
9	**9**	**8a** **8**	>99/ >99 (**8**) >99/ >99[41% (**8a**)][d]
10	**10**	**1a** **1**	81/53:47 (**1a/1**)
11	**11**	**11a** **1a**	78/67:33 (**11a/1a**) [37% (**11a**)]
12	**12**	**12a**	81/>99

13	OH 13	OH 13a O 13b	99/85:15(**13a/134b**)
14	14	14a	33/>99
15	15	NH 15a NH 15b	98/33:67 (**15a/15b**) >99/>99 [57% (**15a**)][c]
16	16	H N 16a	>99/>99[57% (**16a**)]
17	17	17a	>64.5/>99[33% (**17a**)] >99/>99[67% (**17a**)][d]

aReaction condition: arene (1.0 mmol), ruthenium catalyst (precursor complex) (5 mol%), formic acid (18 mmol), water (10 ml) at 170 °C for 10 h. b 6 h, c 20 h, d 24 h.

Interestingly with phenylpyridine (**15**), hydrogenation of pyridine ring was favoured over phenyl ring. After 10 h of the reaction, 2-cyclohexylpiperidine (**15a**) and 2-phenylpiperidine (**15b**) was observed respectively with 33% and 67% selectivities. Complete conversion of phenylpyridine selectively to 2-cyclohexylpiperidine (**15a**) in high yield (57%) was achieved in 20 h (Table 3.5, entry 15). Analogous to phenylpyridine, facile hydrogenation of pyridine to piperidine was also observed in 57% yield (Table 3.5, entry 16).[59] Notably under acetic condition, pyridine gets protonated which activates pyridine for hydrogenation.[60] Piperidine is one of the most common scaffold in natural products and several biologically important pharmaceutical and drug molecules.[60] Unlike pyridine, hydrogenation of 2-aminopyridine (**17**) resulted in the formation of 3,4,5,6-tetrahydopyridin-2-amine (**17a**) in lower yield 33% (Table 3.5, entry 17), because

17a gains resistance toward further hydrogenation under acidic condition.[61] It is important to mention that, diphenylmethane (**2**), biphenyl (**3**), acetophenone (**5**), benzylalcohol (**12**), phenol (**13**) and cinnamaldehyde (**6**), which are analogous to lignin-derived fragments, have also been successfully hydrogenated to corresponding alicyclic reaction products (Scheme 3.4).[6,7]
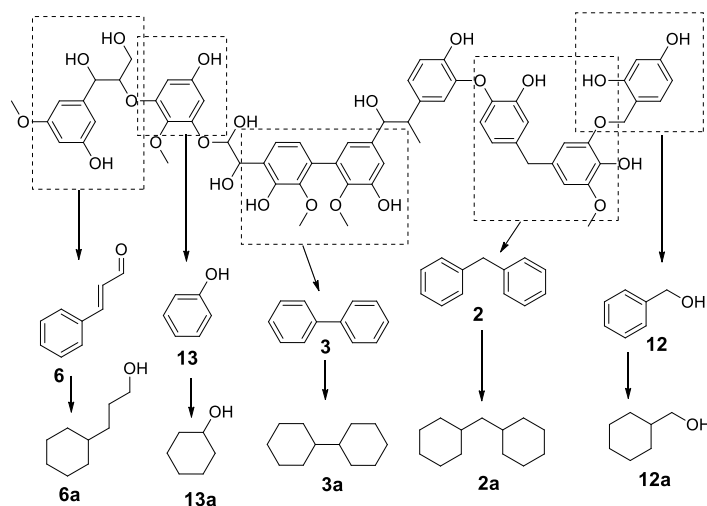
Scheme 3.4. Ruthenium catalyzed hydrogenation of several substrates analogous to lignin-derived fragments.

Further to enhance the viability of this process, gram scale reaction for the ruthenium catalyzed hydrogenation of benzoic acid (**1**) to cyclohexanecarboxylic acid (**1a**) was also conducted under the optimised reaction conditions at 170 °C for 20 h (Scheme 3.5). Results inferred a facile conversion of 1.22 g of benzoic acid (**1**) to cyclohexanecarboxylic acid (**1a**) in 60% yield (0.76 g).
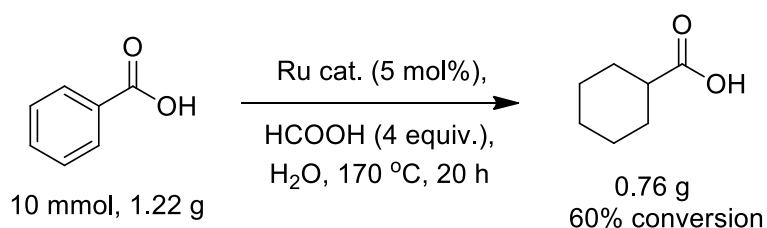
Scheme 3.5. Gram-scale reaction for the ruthenium catalyzed hydrogenation of benzoic acid

We performed recyclability of in-situ generated Ru/C catalysts in optimised reaction condition with benzoic acid to cyclohexanecarboxylic acid. After each catalytic runs, *in situ* generated Ru/C nanoparticle was separated from reaction mixture by centrifugation and reaction mixture was extracted by using a suitable organic solvent, while the separated catalyst was immediately used for the next catalytic run by adding additional specified amounts of the benzoic acid, water and external H_2 gas as H-source. Interestingly, the Ru/C catalyst was recycled for at least three catalytic cycles, without any significant loss of the catalytic activity (Figure 3.8).
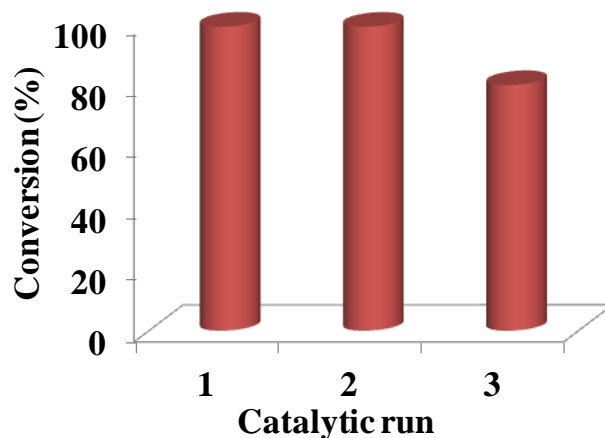
Figure 3.8. Recyclability of the Ru/C catalyst for the catalytic ring hydrogenation of benzoic acid to cyclohexanecarboxylic acid.

3.3. Conclusions

In conclusion, an efficient catalytic system was developed, where the cooperative synergy of the $[(\eta^6$-$C_6H_6)Ru(en)Cl]^+$ complex and formic acid resulted in the *in situ* generation of active ruthenium nanoparticles immobilized on carbon (Ru/C) and H_2 gas to achieved facile tandem catalytic hydrogenation of a wide range of arenes and heteroarenes in water. Catalytic activity of the reported catalytic system was attributed to the unique structural-activity relationship of the precursor complex $[(\eta^6$-$C_6H_6)Ru(en)Cl]^+$, where the presence of N-H bond plays a crucial role in the initial activation of formic acid to generate H_2 gas. Further the reaction temperature enhances the rapid reduction of the precursor complex Ru(II) complex to Ru(0). TEM observations of the presence of Ru/C nanoparticles and the Hg(0) poisoning experiments suggesting the heterogeneous nature of the catalyst. Moreover, a wide range of aromatic compounds analogous to lignin-derived fragments were also successfully hydrogenated to corresponding alicyclic products, and thus the present

catalytic system may also finds application in biomass transformation reactions. Further exploration in this direction is underway.

3.4. Experimental section

3.4.1. Materials and methods. All catalytic reactions were performed open air atmosphere, using chemicals of high purity purchased from Aldrich and Alfa Aesar. The catalytic reactions were monitored using a thin layer chromatography (TLC). ^{1}H NMR (400 MHz), and ^{13}C NMR (100 MHz) spectra were recorded at 298 K using CDCl$_3$, D$_2$O or DMSO-d_6 as the solvent on a Bruker Avance 400 spectrometer. Tetramethylsilane (TMS) was used as an external standard and the chemical shifts in ppm are reported relative to the centre of the singlet at 7.26 ppm for CDCl$_3$, 4.75 for D$_2$O and 2.49 ppm for DMSO-d_6 in ^{1}H NMR and to the centre of the triplet at 77.0 ppm for CDCl$_3$ and 39.50 ppm for DMSO-d_6 in ^{13}C NMR. ESI (positive and negative mode) and high-resolution mass spectra (HRMS) were recorded on a micro TF-Q II mass spectrometer Scanning electron microscopy (SEM) images and elemental mapping data were collected on Carl Zeiss supra 55 (operating voltage 15 kV), using amorphous carbon-coated 400 mesh copper grids for depositing sample. Transmission Electron Microscopic (TEM) imaging was carried out using PHILIPS CM 200 with operating voltages 20-200kv and resolution 2.4 Å. Elemental mapping and energy dispersive X-ray spectroscopy (EDS) point analysis were performed on FEI Tecnai G2, F30 TEM with operating voltage of 200 kV. Inductively coupled plasma atomic emission spectroscopy (ICP-AES) analysis was achieved with ARCOS, Simultaneous ICP Spectrometer of SPECTRO Analytical Instruments. Powder X-ray diffraction (XRD) measurements were performed over the dried particles using a Rigaku SmartLab, Automated Multipurpose X-ray Diffractometer at 40 kV and 30 mA using CuKα radiation (λ = 1.5418 Å).

3.4.2. General procedure for the catalytic hydrogenation of arene and hetero(arenes) over *in situ* generated ruthenium nanoparticles

(Hetero)arene (1.0 mmol) was added to the solution of ruthenium catalyst precursor ([(η^6-C$_6$H$_6$)Ru(en)Cl]PF$_6$, 0.05 mmol) in water (10 ml) followed by addition of the acid (18 mmol). The reaction mixture was heated at 170°C under Teflon coated reactor for 10 h. After the completion of the reaction crude reaction mixture was extracted with the ethyl acetate and the organic portion dried over sodium sulphate.

3.4.3. Procedure for synthesis of Ru/C nanoparticles from organometallic precursor

Formic acid (18 mmol) was added to the solution of ruthenium precursor ([(η^6-C$_6$H$_6$)Ru(en)Cl]PF$_6$, 0.05 mmol) in water (10 ml) then the reaction mixture was heated at 170°C under Teflon coated reactor for 10 h. After 10 h particle was separated by centrifugation at 8000 rpm for 15 min and wash with ethanol (2 × 10 ml). The isolated Ru/C nanoparticles were used for the catalytic reaction.

3.4.4. Procedure for Hg(0) Poisoning test

To identify the nature of catalysis (heterogeneous or homogeneous) for ring hydrogenation reaction, Hg(0) poising test was performed, where 1.0 mmol of benzoic acid (**1**) was added to a solution of ([(η^6-C$_6$H$_6$)Ru(en)Cl]PF$_6$, 0.05 mmol) in water (10 ml) then addition of the formic acid (18 mmol) and excess of Hg(0). The reaction mixture was vigorously stirred and heated at 170 °C under a Teflon coated reactor for 10 h. After the completion of the reaction crude reaction mixture was extracted with the ethyl acetate and the organic portion dried over sodium sulphate.

3.4.5. Spectral data of the products obtained from the catalytic reduction of substrates
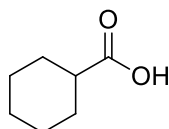
Cyclohexanecarboxylic acid: **^{1}H NMR** (400 MHz, CDCl$_3$): δ (ppm) = 11.49 (br, 1H), 2.335-2.28 (m, 1H), 1.93-1.890 (m, 2H), 1.76-1.73 (m, 2H), 1.65-1.61 (m, 1H), 1.48-1.39 (m, 2H), 1.32 1.22 (m, 3H). **^{13}C NMR** (100 MHz, CDCl$_3$): δ (ppm) = 182.85, 42.94, 28.73, 25.66, 25.30. **HRMS** (ESI) m/z calculated for Cyclohexanecarboxylic acid: 151.0837 [M+Na] $^+$, found 151.0730 [M+Na] $^+$.
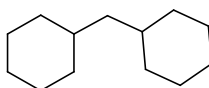
Dicyclohexylmethane: **^{1}H NMR** (400 MHz, CDCl$_3$): δ (ppm) = 1.68-1.62 (m, 10H), 1.31-1.11 (m, 8H), 1.02 (t, J = 8 Hz, 2H), 0.86-0.78 (m, 4H). **^{13}C NMR** (100 MHz, CDCl$_3$): δ (ppm) = 45.62, 34.39, 33.80, 26.84, 26.51.
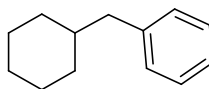
(Cyclohexylmethyl)benzene: ^{1}H NMR (400 MHz, CDCl$_3$): δ (ppm) = 7.25-7.22 (m, 1H), 7.18-7.14 (m, 2H), 7.13-7.11 (m, 2H), 2.46 (d, J = 8.00 Hz, 2H), 1.63-1.60 (m, 4H), 1.55-1.47 (m, 1H), 1.34-1.26 (m, 2H), 1.23-1.17 (m, 4H).
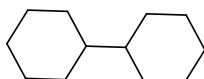
1,1'-Bi(cyclohexane): ^{1}H NMR (400 MHz, CDCl$_3$): δ (ppm) = 1.73-1.60 (m, 10H), 1.23-1.15 (m, 4H), 1.14-1.01 (m, 4H), 0.99-0.89 (m, 4H). ^{13}**C NMR** (100 MHz, CDCl$_3$): δ (ppm) = 42.51, 29.21, 25.93.
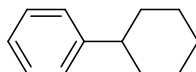
Cyclohexylbenzene: ^{1}H NMR (400 MHz, CDCl$_3$): δ (ppm) = 7.27-7.24 (m, 2H), 7.18-7.13 (m, 3H), 2.48-2.44 (m, 1H), 1.70-1.63 (m, 6H), 1.40-1.37 (m, 4H).
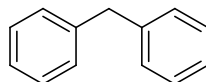
Diphenylmethane: ^{1}H NMR (400 MHz, CDCl$_3$): δ (ppm) = 7.28-7.24(m, 4H), 7.18-7.16 (m, 6H), 3.96 (s, 2H).
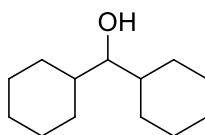
Dicyclohexylmethanol: ^{1}H NMR (400 MHz, CDCl$_3$): δ (ppm) = 2.97 (t, J = 5.60 Hz, 1H), 1.76-1.74 (m, 4H), 1.67-1.64 (m, 4H), 1.32-1.19 (m, 8H), 1.22-1.16 (m, 2H), 0.96-0.90 (m, 4H).
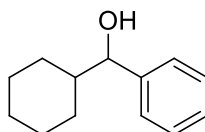
Cyclohexyl(phenyl)methanol: ^{1}**H NMR** (400 MHz, CDCl$_3$): δ (ppm) = 7.45-7.42 (m, 1H), 7.18-7.15 (m, 4H), 4.28 (d, *J* = 8.00 Hz, 1H), 2.01-1.95 (m, 1H), 1.53-1.50 (m, 4H), 1.19-1.13 (m, 4H), 0.82-0.79 (m, 2H).
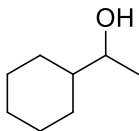
1-Cyclohexylethanol: ^{1}**H NMR** (400 MHz, CDCl$_3$): δ (ppm) = 3.57-3.51 (m, 1H), 2.35-2.28 (m, 1H), 1.85-1.64 (m, 6H), 1.14 (d, *J* = 6.40 Hz, 3H), 1.04-.93 (m, 4H).
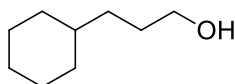
3-Cyclohexylpropan-1-ol: ^{1}**H NMR** (400 MHz, CDCl$_3$): δ (ppm) = 3.55 (t, *J* = 6.40 Hz, 2H), 1.87-1.81 (m, 1H), 1.62-1.60 (m, 4H), 1.52-1.46 (m, 4H), 1.14-1.08 (m, 4H), 0.80-0.75 (m, 4H).
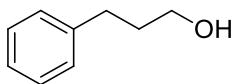
3-Phenylpropan-1-ol: ^{1}**H NMR** (400 MHz, CDCl$_3$): δ (ppm) = 7.29-7.24 (m, 3H), 7.21-7.18 (m, 2H), 3.67 (t, *J* = 6.00 Hz, 2H), 2.73-2.65 (m, 2H), 1.91-1.86 (m, 2H).
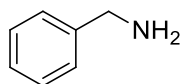
Phenylmethanamine: ^{1}**H NMR** (400 MHz, CDCl$_3$): δ (ppm) = 7.33-7.30 (m, 4H), 7.28-7.24 (m, 1H), 4.65 (s, 2H).
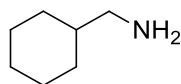
Cyclohexylmethanamine: ^{1}**H NMR** (400 MHz, CDCl$_3$): δ (ppm) = 3.39 (d, *J* = 8.00 Hz, 2H), 1.72-1.63 (m, 8H), 1.57-1.53 (m, 1H), 1.39-1.36 (m, 2H).
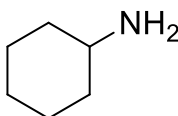
Cyclohexylamine: ^{1}H NMR (400 MHz, CDCl$_3$): δ (ppm) = 2.53-2.46 (m, 1H), 1.70-1.46 (m, 4H), 1.19-0.87 (m, 6H). **^{13}C NMR** (100 MHz, CDCl$_3$): δ (ppm) = 49.86, 36.33, 25.11, 24.55. **HRMS** (ESI) m/z calculated for Cyclohexylamine: 100.1121 [M+H]$^+$, found 100.1340 [M+H]$^+$.
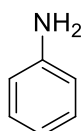
Aniline: ^{1}H NMR (400 MHz, CDCl$_3$): δ (ppm) = 7.03 (t, *J* = 8.00 Hz, 2H), 6.64 (t, *J* = 8.00 Hz, 1H), 6.55 (d, *J* = 8.00 Hz, 2H), 3.42 (s, 2H).
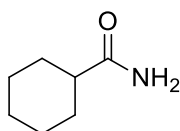
Cyclohexamide: ^{1}H NMR (400 MHz, CDCl$_3$): δ (ppm) = 2.12-2.04 (m, 1H), 1.88-1.82 (m, 2H), 1.75-1.68 (m, 2H), 1.63-1.57 (m, 1H), 1.40-1.31 (m, 2H), 1.26- 1.20 (m, 3H). **^{13}C NMR** (100 MHz, CDCl$_3$): δ (ppm) = 179.37, 44.82, 29.67, 25.73, 25.68. **HRMS** (ESI) m/z calculated for Cyclohexanoic acid: 150.0889 [M+Na]$^+$, found 150.0969 [M+Na]$^+$.
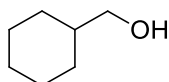
Cyclohexylmethanol: ^{1}H NMR (400 MHz, CDCl$_3$): δ (ppm) = 3.43 (d, *J* = 8.00 Hz, 2H), 1.75-1.71 (m, 4H), 1.68-1.64 (m, 2H), 1.48-1.44 (m, 1H), 1.18-1.13(m, 2H), 0.96-0.90 (m, 2H).
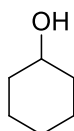
Cyclohexanol: ^{1}H NMR (400 MHz, CDCl$_3$): δ (ppm) = 3.58-3.53 (m, 1H), 1.85-1.82 (m, 2H), 1.23-1.21 (m, 2H), 1.22-1.1.20 (m, 2H), 1.17-1.67 (m, 2H), 1.16-1.10 (m, 2H). **^{13}C NMR** (100 MHz, CDCl$_3$): δ (ppm) = 70.23, 35.44, 25.40, 24.08.
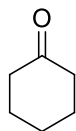
Cyclohexanone: **^{1}H NMR** (400 MHz, CDCl$_3$): δ (ppm) = 2.23 (t, *J* = 8.00 Hz, 4H), 1.84-1.81 (m, 2H), 1.51-1.48 (m, 4H). **^{13}C NMR** (100 MHz, CDCl$_3$): δ (ppm) = 212.37, 41.89, 26.94, 24.91.
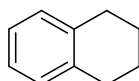
1,2,3,4-Tetrahydronaphthalene: **^{1}H NMR** (400 MHz, CDCl$_3$): δ (ppm) = 7.10-7.06 (m, 4H), 2.80-2.76 (m, 4H), 1.82-1.79 (m, 4H).
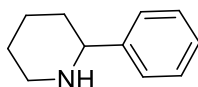
2-Phenylpiperidine: **^{1}H NMR** (400 MHz, CDCl$_3$): δ (ppm) = 7.39-7.36 (m, 2H), 7.24-7.21 (m, 1H), 7.17-7.12 (m, 2H), 3.65-3.62 (m, 1H), 2.84-2.78 (m, 1H), 2.71-2.68 (m, 1H), 1.87-1.78 (m, 3H), 1.63-1.59 (m, 1H), 1.53-1.48 (m, 2H). **^{13}C NMR** (100 MHz, CDCl$_3$): δ (ppm) = 144.09, 128.40, 128.22, 126.78, 62.05, 67.32, 34.12, 29.66, 25.18. **HRMS** (ESI) m/z calculated for 2-Phenylpiperidine: 162.1277 [M+H]$^+$, found 162.1273[M+H]$^+$.
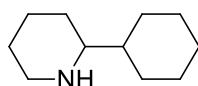
2-Cyclohexylpiperidine: **^{1}H NMR** (400 MHz, CDCl$_3$): δ (ppm) = 3.03 (d, *J* = 12.00 Hz, 1H), 2.53 (td, J_1 = 12.00 Hz, J_2 = 12.00 Hz, 1H), 2.19-2.15 (m, 1H), 1.75-1.49 (m, 10H), 1.39-1.28 (m, 2H), 1.13-1.03 (m, 3H), 0.95-0.89 (m, 2H). **^{13}C NMR** (100 MHz, CDCl$_3$): δ (ppm) = 62.02, 47.40, 43.24, 29.40, 29.28, 29.13, 26.61, 26.40, 24.98. **HRMS** (ESI) m/z calculated for 2-Cyclohexylpiperidine: 168.1747 [M+H]$^+$, found 168.1932 [M+H]$^+$.
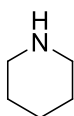
Piperidine: ^{1}**H NMR** (400 MHz, CDCl$_3$): δ (ppm) = 2.98 (t, J = 4.00 Hz, 4H), 1.74-1.72 (m, 4H), 1.57-1.55 (m, 2H). ^{13}**C NMR** (100 MHz, CDCl$_3$): δ (ppm) = 44.44, 23.03, 22.74. **HRMS** (ESI) m/z calculated for Piperidine: 86.0964 [M+H] $^+$, found 86.0989 [M+H] $^+$.
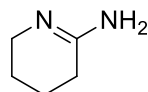
3,4,5,6-tetrahydropyridin-2-amine: ^{1}**H NMR** (400 MHz, CDCl$_3$): δ (ppm) = 3.26 (t, J = 4.80 Hz, 2H), 2.30 (t, J = 6.00 Hz 2H), 1.76-1.71(m, 4H). ^{13}**C NMR** (100 MHz, CDCl$_3$): δ (ppm) = 172.67, 41.96, 31.26, 22.03, 20.64. **MASS** (ESI) m/z calculated for 3, 4, 5, 6-tetrahydropyridin-2-amine: 121.0736 [M+Na] $^+$, found 122.0612 [M+Na] $^+$.

Note: The contents of this work have been reproduced with the permission from The Wiley online library *(ChemCatChem* 2017, *9*, 1930-1938 (DOI: 10.1002/cctc.201700056) and License Number 4234591489582.

3.5. References

1.   Thomas J. M., Johnson B. F. G., Raja R., Sankar G., Midgley P. A. (2003), High-Performance Nanocatalysts for Single-Step Hydrogenations, *Acc. Chem. Res.*, 36, 20-30 (DOI: 10.1021/ar990017q).

2.   Gual A., Godard C., Castillón S., Claver C. (2010), Soluble transition-metal nanoparticles-catalysed hydrogenation of arenes, *Dalton Trans.*, 39, 11499-11512 (DOI: 10.1039/c0dt00584c).

3.   Qi S. -C., Wei X. -Y., Zong Z. -M., Wang Y. -K. (2013), Application of supported metallic catalysts in catalytic hydrogenation of arenes, *RSC Adv.*, 3, 14219-14232 (DOI: 10.1039/c3ra40848e).

4.   Zhong J., Chen J., Chen L. (2014), Selective hydrogenation of phenol and related derivatives *Catal. Sci. Technol.*, 4, 3555-3569 (DOI: 10.1039/c4cy00583j).

5.   Gilkey M. J., Xu B. (2016), Heterogeneous Catalytic Transfer Hydrogenation as an Effective Pathway in Biomass Upgrading, *ACS Catal.*, 6, 1420-1436 (DOI: 10.1021/acscatal.5b02171).

6.   Cui X., Surkus A. -E., Junge K., Topf C., Radnik J., Kreyenschulte C., Beller

M. (2016), Highly selective hydrogenation of arenes using nanostructured ruthenium catalysts modified with a carbon–nitrogen matrix, *Nat. Commun.*, (DOI: 10.1038/ncomms11326)

7. Zhang J., Teo J., Chen X., Asakura H., Tanaka T., Teramura K., Yan N. (2014), A Series of NiM (M = Ru, Rh, and Pd) Bimetallic Catalysts for Effective Lignin Hydrogenolysis in Water, *ACS Catal.*, 4, 1574-1583 (DOI.org/10.1021/cs401199f).

8. Bi H., Tan X., Dou R., Pei Y., Qiao M., Sun B., Zong B. (2016), Ru–B nanoparticles on metal–organic frameworks as excellent catalysts for hydrogenation of benzene to cyclohexane under mild reaction conditions, *Green Chem.*, 18, 2216-2221 (DOI: 10.1039/c5gc02683k).

9. Yoon B., Pan H.-B., Wai C. M. (2009), Relative Catalytic Activities of Carbon Nanotube-Supported Metallic Nanoparticles for Room-Temperature Hydrogenation of Benzene, *J. Phys. Chem. C*, 113, 1520-1525 (DOI: 10.1021/jp809366w).

10. Morioka Y., Matsuoka A., Binder K., Knappett B. R., Wheatley A. E. H., Naka H. (2016), Selective hydrogenation of arenes to cyclohexanes in water catalyzed by chitinsupported ruthenium nanoparticles, *Catal. Sci. Technol.*, 6, 5801-5805 (DOI: 10.1039/c6cy00899b).

11. Dehm N. A., Zhang X., Buriak J. M. (2010), Screening of Bimetallic Heterogeneous Nanoparticle Catalysts for Arene Hydrogenation Activity under Ambient Conditions, *Inorg. Chem.*, 49, 2706-2714 (DOI: 10.1021/ic901928j).

12. Zhu L., Yang Z., Zheng J., Hu W., Zhang N., Li Y., Zhong C. -J., Ye H., Chen B. H. (2015), Decoration of Co/Co3O4 nanoparticles with Ru nanoclusters: a new strategy for design of highly active hydrogenation, *J. Mater. Chem. A*, 3, 11716-11719 (DOI: 10.1039/c5ta02452h).

13. Fonseca G. S., Umpierre A. P., Fichtner P. F. P., Teixeira S. R., Dupont J. (2003), The Use of Imidazolium Ionic Liquids for the Formation and Stabilization of Ir^0 and Rh^0 Nanoparticles: Efficient Catalysts for the Hydrogenation of Arenes, *Chem. Eur. J.*, 9, 3263-3269 (DOI: 10.1002/chem.200304753).

14. Léger B., Denicourt-Nowicki A., Oliver-Bourbigou H., Roucoux A. (2008), Rhodium Colloidal Suspensions Stabilised by Poly-N-donor Ligands in Non-

Aqueous Ionic Liquids: Preliminary Investigation into the Catalytic Hydrogenation of Arenes, *ChemSusChem*, 1, 984-987 (DOI: 10.1002/cssc.200800194).

15. Nowicki A., Le Boulaire V., Roucoux A. (2007), Nanoheterogeneous Catalytic Hydrogenation of Arenes: Evaluation of the Surfactant-Stabilized Aqueous Ruthenium(0) Colloidal Suspension, *Adv. Synth. Catal.*, 349, 2326-2330 (DOI: 10.1002/adsc.200700208).

16. Prechtl M. H. G., Scariot M., Scholten J. D., Machado G., Teixeira, S. R., Dupont J.(2008), Nanoscale Ru(0) Particles: Arene Hydrogenation Catalysts in Imidazolium Ionic Liquids, *Inorg. Chem.*, 47, 8995-9001 (DOI: 10.1021/ic801014f).

17. Moore B. S., Poralla K., Floss H. G. (1993), Biosynthesis of the cyclohexanecarboxylic acid starter unit of .omega.-cyclohexyl fatty acids in Alicyclobacillus acidocaldarius, *J. Am. Chem. Soc.*, 115, 5267-5274 (DOI: 10.1021/ja00065a043).

18. Gaude D., Le Goaller R., Luche J. -L., Pierre J. -L. (1984), Activation de reactions par les polyoxydes d′ethylene III: Reductions par l′eutectique sodium-potassium, *Tetrahedron Lett.*, 25, 5897-5898 (DOI: 10.1016/S0040-4039(01)81714-7).

19. Tang M., Mao S., Li M., Wei Z., Xu F., Li H., Wang Y. (2015), RuPd Alloy Nanoparticles Supported on N-Doped Carbon as an Efficient and Stable Catalyst for Benzoic Acid Hydrogenation, *ACS Catal.*, 5, 3100-3107 (DOI: 10.1021/acscatal.5b00037).

20. Anderson J. A., McKenna F. -M., Linares-Solano A., Wells R. P. K. (2007), Use of Water as a Solvent in Directing Hydrogenation Reactions of Aromatic Acids over Pd/carbon Nanofibre Catalysts, *Catal. Lett.*, 119, 16-20 (DOI: 10.1007/s10562-007-9207-5).

21. Xu X., Tang M., Li M., Li H., Wang Y. (2014), Hydrogenation of Benzoic Acid and Derivatives over Pd Nanoparticles Supported on N-Doped Carbon Derived from Glucosamine Hydrochloride, *ACS Catal.*, 4, 3132-3135 (DOI: 10.1021/cs500859n).

22. Zhang P., Wu T., Hou M., Ma J., Liu H., Jiang T., Wang W., Wu C., Han B. (2014), The Hydrogenation of Aromatic Compounds under Mild Conditions by Using a Solid Lewis Acid and Supported Palladium Catalyst,

ChemCatChem, 6, 3323-3327 (DOI: 10.1002/cctc.201402671).

23. Yu T., Wang J., Li X., Cao X., Gu H. (2013), An Improved Method for the Complete Hydrogenation of Aromatic Compounds under 1 Bar H2 with Platinum Nanowires, *ChemCatChem*, 5, 2852-2855 (DOI: 10.1002/cctc.201300394).

24. Yen C. H., Lin H. W., Tan C. -S. (2011), Hydrogenation of bisphenol A-Using a mesoporous silica based nano ruthenium catalyst Ru/MCM-41 and water as the solvent, *Catal. Today*, 174, 121-126 (DOI: 10.1016/j.cattod.2011.01.050).

25. Maegawa T., Akashi A., Yaguchi K., Iwasaki Y., Shigetsura M., Monguchi Y., Sajiki H. (2009), Efficient and Practical Arene Hydrogenation by Heterogeneous Catalysts under Mild Conditions, *Chem. Eur. J.*, 15, 6953-6963 (DOI: 10.1002/chem.200900361).

26. Gonzalez-Galvez D., Lara P., Rivada-Wheelaghan O., Conejero S., Chaudret B., Philippot K., van Leeuwen P. W. N. M. (2013), NHC-stabilized ruthenium nanoparticles as new catalysts for the hydrogenation of aromatics, *Catal. Sci. Technol.*, 3, 99-105 (DOI: 10.1039/c2cy20561k).

27. Jiang Z., Lan G., Liu X., Tang H., Li Y. (2016), Solid state synthesis of Ru–MC with highly dispersed semi-embedded ruthenium nanoparticles in a porous carbon framework for benzoic acid hydrogenation, *Catal. Sci. Technol.*, 6, 7259-7266 (DOI: 10.1039/c6cy01049k).

28. Nie R., Miao M., Du W., Shia J., Liu Y., Hou Z. (2016), Selective hydrogenation of C C bond over N-doped reduced grapheme oxides supported Pd catalyst, *Appl. Catal. B: Environ.*, 180, 607-613 (DOI: 10.1016/j.apcatb.2015.07.015).

29. Bai G. Y., Wen X., Zhao Z., Li F., Dong H. X., Qiu M. D. (2013), Chemoselective Hydrogenation of Benzoic Acid over Ni−Zr−B−PEG(800) Nanoscale Amorphous Alloy in Water, *Ind. Eng. Chem. Res.*, 52, 226-2272 (DOI: 10.1021/ie303602n).

30. Snelders D. J. M., Yan N., Gan W., Laurenczy G., Dyson P. J. (2012), Tuning the Chemoselectivity of Rh Nanoparticle Catalysts by Site- Selective Poisoning with Phosphine Ligands: The Hydrogenation of Functionalized Aromatic Compounds, *ACS Catal.*, 2, 201-207 (DOI: 10.1021/cs200575r).

31. González-Gálvez D., Nolis P., Philippot K., Chaudret B., van Leeuwen P. W. N. M. (2012), Phosphine-Stabilized Ruthenium Nanoparticles: The Effect of

the Nature of the Ligand in Catalysis, *ACS Catal.*, 2, 317-321 (DOI: 10.1021/cs200633k).

32. Ruppert A. M., Jędrzejczyk M., Sneka-Płatek O., Keller N., Dumon A. S., Michel C., Sautetc P., Gramsa J. (2016), Ru catalysts for levulinic acid hydrogenation with formic acid as a hydrogen source, *Green Chem.*, 18, 2014-2028 (DOI: 10.1039/c5gc02200b).

33. Peng G., Steib M., Gramm F., Ludwig C., Vogel F. (2014), Synthesis factors affecting the catalytic performance and stability of Ru/C catalysts for supercritical water gasification, *Catal. Sci. Technol.*, 4, 3329-3339 (DOI: 10.1039/c4cy00586d).

34. Xiao C., Goh T. -W., Qi Z., Goes S., Brashler K., Perez C., Huang W. (2016), Conversion of Levulinic Acid to γ-Valerolactone over Few-Layer Graphene-Supported Ruthenium Catalysts, *ACS Catal.*, 6, 593-599 (DOI: 10.1021/acscatal.5b02673).

35. Gallegos-Suarez E., Pérez-Cadenas M., Guerrero-Ruiz A., Rodriguez-Ramos I., Arcoya A. (2013), Effect of the functional groups of carbon on the surface and catalyticproperties of Ru/C catalysts for hydrogenolysis of glycerol, *Appl. Surf. Science*, 287, 108-116 (DOI: 10.1016/j.apsusc.2013.09.087).

36. Tomkins P., Gebauer-Henke E., Leitner W., Müller T. E. (2015), Concurrent Hydrogenation of Aromatic and Nitro Groups over Carbon-Supported Ruthenium Catalysts, *ACS Catal.*, 5, 203-209 (DOI: 10.1021/cs501122h).

37. Wei Y., Rao B., Cong X., Zeng X. (2015), Highly Selective Hydrogenation of Aromatic Ketones and Phenols Enabled by Cyclic (Amino)(alkyl)carbene Rhodium Complexes, *J. Am. Chem. Soc.*, 137, 9250-9253 (DOI: 10.1021/jacs.5b05868).

38. Kim G. -J., Kim S. -H., Chong P. -H., Kwon M. -A. (2002), N,N-Dialkylated 1,2-diamine derivatives as new efficient ligands for $RuCl_2(PPh_3)_3$ catalyzed asymmetric transfer hydrogenation of aromatic ketones, *Tetrahedron Lett.*, 43, 8059-8062 (DOI: 10.1016/S0040-4039(02)01962-7).

39. Kumar P., Gupta R. K., Pandey D. S. (2014), Half-sandwich arene ruthenium complexes: synthetic strategies and relevance in catalysis, *Chem. Soc. Rev.*, 43, 707-733 (DOI: 10.1039/c3cs60189g).

40. Warner M. C., Casey C. P., Bckvall J. -E. (2011), Shvo's Catalyst in Hydrogen Transfer Reactions, *Top. Organomet. Chem.*, 37, 85-125 (DOI:

https://doi.org/10.1007/3418_2011_7).

41. Conley B. L., Pennington-Boggio M. K., Boz E., Williams T. J. (2010), Discovery, Applications, and Catalytic Mechanisms of Shvo's Catalyst, *Chem. Rev.*, 110, 2294-2312 (DOI: 10.1021/cr9003133).

42. Karvembu R., Prabhakaran R., Natarajan K. (2005), Shvo's diruthenium complex: a robust catalyst, *Coord. Chem. Rev.*, 249, 911-918 (DOI: 10.1016/j.ccr.2004.09.025).

43. Morris R. E., Aird R. E., Murdoch P. d. S., Chen H., Cummings J., Hughes N. D., Parsons S., Parkin A., Boyd G., Jodrell D. I., Sadler P. J. (2001), Inhibition of Cancer Cell Growth by Ruthenium(II) Arene Complexes, *J. Med. Chem.*, 44, 3616-3621 (DOI: 10.1021/jm010051m).

44. Dwivedi A. D., Gupta K., Tyagi D., Rai R. K., Mobin S. M., Singh S. K. (2015), Ruthenium and Formic Acid Based Tandem Catalytic Transformation of Bioderived Furans to Levulinic Acid and Diketones in Water, *ChemCatChem*, 7, 4050-4058 (DOI : 10.1002/cctc.201501021).

45. Ma W., Chen F., Liu Y., He Y. -M., Fan Q. -H. (2016), Ruthenium-Catalyzed Enantioselective Hydrogenation of 1,8-Naphthyridine Derivatives, *Org. Lett.*, 18, 2730-2733 (DOI: 10.1021/acs.orglett.6b01186).

46. Chen F., Wang T., He Y., Ding Z., Li Z., Xu L., Fan Q.-H. (2011), Asymmetric Hydrogenation of N-Alkyl Ketimines with Phosphine-Free, Chiral, Cationic Ru-MsDPEN Catalysts, *Chem. Eur.*, *J.* 17, 1109-1113 (DOI: 10.1002/chem.201002846).

47. Kuwano R., Morioka R., Kashiwabara M., Kameyama N. (2012), Catalytic Asymmetric Hydrogenation of Naphthalenes, *Angew. Chem. Int. Ed.*, 51, 4136-4139 (DOI: 10.1002/anie.201201153).

48. Boxwell C. J., Dyson P. J., Ellis D. J., Welton T. (2002), A Highly Selective Arene Hydrogenation Catalyst that Operates in Ionic Liquid, *J. Am. Chem. Soc.*, 124, 9334-9335 (DOI: 10.1021/ja026361r).

49. Urban S., Ortega N., Glorius F. (2011), Ligand-Controlled Highly Regioselective and Asymmetric Hydrogenation of Quinoxalines Catalyzed by Ruthenium N-Heterocyclic Carbene Complexes, *Angew. Chem. Int. Ed.*, 50, 3803-3806 (DOI: 10.1002/anie.201100008).

50. Hagen C. M., Vieille-Petit L., Laurenczy G., Suss-Fink G., Finke R. G. (2005) Supramolecular Triruthenium Cluster-Based Benzene Hydrogenation

Catalysis: Fact or Fiction?, *Organometallics*, 24, 1819-1831 (DOI: 10.1021/om048976y).

51. Widegren J. A., Bennett M. A., Finke R. G. (2003), Is It Homogeneous or Heterogeneous Catalysis? Identification of Bulk Ruthenium Metal as the True Catalyst in Benzene Hydrogenations Starting with the Monometallic Precursor, Ru(II)(η^6-C$_6$Me$_6$)(OAc)$_2$, Plus Kinetic Characterization of the Heterogeneous Nucleation, Then Autocatalytic Surface-Growth Mechanism of Metal Film Formation, *J. Am. Chem. Soc.*, 125, 10301-10310 (DOI: 10.1021/ja021436c).

52. Hagen C. M., Widegren J. A., Maitlis P. M., Finke R. G. (2005), Is It Homogeneous or Heterogeneous Catalysis? Compelling Evidence for Both Types of Catalysts Derived from [Rh(η^5-C$_5$Me$_5$)Cl$_2$]$_2$ as a Function of Temperature and Hydrogen Pressure, *J. Am. Chem. Soc.*, 127, 4423-4432 (DOI: 10.1021/ja044154g).

53. Crabtree R. H. (2012), Resolving Heterogeneity Problems and Impurity Artifacts in Operationally Homogeneous Transition Metal Catalysts, *Chem. Rev.*, 112, 1536-1554 (DOI: 10.1021/cr2002905).

54. (a) Singh S. K., Zhang X. -B., Xu Q. (2009), Room-Temperature Hydrogen Generation from Hydrous Hydrazine for Chemical Hydrogen Storage, *J. Am. Chem. Soc*., 131, 9894-9895 (DOI: 10.1021/ja903869y); (b) Rai R. K., Mahata A., Mukhopadhyay S., Gupta S., Li P. -Z., Nguyen K. T., Zhao Y., Pathak B., Singh S. K. (2014), Room-Temperature Chemoselective Reduction of Nitro Groups Using Non-noble Metal Nanocatalysts in Water, *Inorg. Chem*., 53, 2904-2909 (DOI: 10.1021/ic402674z).

55. Kusada K., Kobayashi H., Yamamoto T., Matsumura S., Naoya, Sumi, Sato K., Nagaoka K., Kubota Y., Kitagawa H. (2013), Discovery of Face-Centered-Cubic Ruthenium Nanoparticles: Facile Size-Controlled Synthesis Using the Chemical Reduction Method, *J. Am. Chem. Soc*., 135, 5493-5496 (DOI: 10.1021/ja311261s).

56. Guan C., Zhang D.-D., Pan Y., Iguchi M., Ajitha M. J., Hu J., Li H., Yao C., Huang M. -H., Min S., Zheng J., Himeda Y., Kawanami H., Huang K. -W. (2017), Dehydrogenation of Formic Acid Catalyzed by a Ruthenium Complex with an N,N′-Diimine Ligand, *Inorg. Chem.*, 56, 438-445 (DOI: 10.1021/acs.inorgchem.6b02334).

57. Gupta K., Tyagi D., Dwivedi A. D., Mobin S. M., Singh S. K. (2015), Catalytic transformation of bio-derived furans to valuable ketoacids and diketones by water-soluble ruthenium catalysts, *Green Chem.*, 17, 4618-4627 (DOI: 10.1039/c5gc01376c).

58. Dodgson I., Griffin K., Barberis G., Pignataro F., Tauszik G. (1989), *Chem. Ind.*, 830-833.

59. Glorius F., Spielkamp N., Holle S., Goddard R., Lehmann C. W. (2004), Efficient Asymmetric Hydrogenation of Pyridines, *Angew. Chem. Int. Ed.*, 43, 2850-2852 (DOI: 10.1002/anie.200453942).

60. Buffat M. G. P. (2004), Synthesis of piperidines, *Tetrahedron*, 60, 1701-1729 (DOI: 10.1016/j.tet.2003.11.043).

61. Grave T. B. (1924), Attempts to prepare 1-methyl-2-methoxypiperidine. The hydrogenation of certain pyridine derivatives, *J. Am. Chem. Soc.*, 46, 1460-1470 (DOI: 10.1021/ja01671a016).

Chapter 4

Troponate-/Aminotroponate ruthenium-arene complexes: Synthesis, structure and ligand tuned mechanistic pathway for direct C-H bond arylation with arylchlorides in water

4.1 Introduction

Chemistry of ruthenium(II)-arene based complexes has been established as a promising field of organometallic chemistry because of the structural versatility and unique tunable structure-activity behaviour shown by these complexes. Therefore, these complexes are being used as important candidates as catalysts in a wide range of organic transformations[1], biological applications such as active water soluble antitumor agents [2], and so on[3]. Careful observation of the scientific progress in the field of arene-ruthenium complexes revealed that the most active class of these complexe are those containing nitrogen or oxygen donor ligands.

Roesky and Blechert et al,
2006, Hydroamination

Roesky and Blechert et al,
2007, R ≠ H
2010, R = H, Hydroamination

Asefa et al,
2011, Hydroamination

Crispini et al,
2013, Anticancer agents

Brookhart et al,
2003, Ethylene Polymerization

Roesky et al,
1998, Hydroamination

Mazzeo et al,
2005, Olefin polymerization

Yoshida et al,
2014

Steyl et al, **2007**

Visser et al,
2012

West et al,
2014

Dixneuf et al,
2013, C-H bond arylation

Singh et al,
2011

***Scheme 4.1.** Tropolone and aminotropone based metal complexes.*

Chemistry of tropolone and 2-aminotropones has been extensively explored in recent past for several applications, such as anticancer agent,[4] and active catalyst for various important reactions such as intramolecular hydroamination,[5-7] ethylene

polymerization,[8] olefin polymerization,[9] and so on[10-14] (shown in Scheme 4.1). Tropolone based complexes have several unique features such as the formation of strained five-membered chelating ring with the metal centre having enolic hydroxy group analogous to β-diketone and negative charge accumulation predominantly on nitrogen atoms of aminotropone ligands. Moreover, the planer large seven membered homoaromatic rings of tropolone or aminotropones substantially contribute in the stability of these complexes.

In recent years, remarkable progress has been accomplished in C-H bond activation using ruthenium catalysts as a direct route for C-C bond formation reactions.[15] Though several other metals such as Pd[16], Rh[17] and Ir[18] based complexes were also explored for C-H bond activation but ruthenium complexes being relatively less expensive, non-toxic, and stable in air and water, gained advantages over others. Among the most efficient ruthenium catalysts investigated so far for C-H bond activation or functionalization, ruthenium-arene complexes such as [{(η^6-arene)RuCl$_2$}$_2$] or its carboxylate complexes represent the highly active class of catalysts. [19] However, other ruthenium complexes such as those containing or involving phosphine ligands and others like RuCl$_2$(PPh$_3$)$_3$, [RuCl$_2$(cod)]$_2$, [(η^6-arene)RuCl$_2$(1,2-diphenylvinyl)phosphine)] as well as [{(η^6-arene)RuCl$_2$}$_2$] with excess of PPh$_3$ were also explored, but those are expected to follow a different reaction pathway.[20] Most of these reactions were performed in organic solvents, such as *N*-Methyl-2-pyrrolidone (NMP) or toluene, but recently huge efforts have been devoted to develop efficient catalytic systems for C-H bond activation in more environment tolerant solvents such as diethylcarbonate or water.[21]

Analogous to carboxylate ligands, ruthenium-arene complexes containing several other O,O or O,N chelating ligands for C-H bond activation were also reported in water where diarylation is favoured with O,N chelating ligands but phosphine containing complexes showed poor catalytic activity.[22] Similarly, β-ketonates based ruthenium arene complexes have also employed for C-H bond arylation in NMP, where sterically bulky diketononate favour monoarylation.[23] Unlike weakly coordinating carboxylate ligands, these strong chelating O,O or O,N ligands displayed high affinity towards metal centre, and therefore we anticipated that presumably ruthenium-arene complexes containing such strongly coordinating chelating ligands might follow a different catalytic reaction pathway or involve

different catalytically active species during C-H bond activation, in contrary to the well established carboxylate/carbonate driven cycloruthenated species, $[(\eta^6\text{-}$arene)Ru$(\kappa^2\text{-}C,N\text{-phenylpyridine})(\text{sol})]^+$ observed with ruthenium-arene complexes.

Herein, we synthesized and characterized several novel ruthenium-arene complexes, **[Ru]-9 – [Ru]-16,** containing troponate (**L1**) and substituted aminotroponate (isopropylaminotroponate (**L2**) and cyclohexylaminotroponate (**L3**)) ligands. Structures of the ligand **L3**, and two of the representative ruthenium-arene complexes $[(\eta^6\text{-}C_{10}H_{14})\text{-}Ru(\kappa^2\text{-}O,O\text{-troponate})Cl]$ (**[Ru]-13**) and $[(\eta^6\text{-}C_{10}H_{14})\text{-}Ru(\kappa^2\text{-}O,N\text{-isopropylaminotroponate})Cl]$ (**[Ru]-15**) were authenticated by single crystal X-ray diffraction studies. Further, these complexes were employed for *ortho* C-H bond arylation of 2-phenylpyridine with 4-chloroanisole in water. Effect of several carboxylate additives and structural motifs of troponate/aminotroponate ruthenium-arene complexes on catalytic activity and selectivity towards C-H bond mono *vs* diarylation were explored. Main focus of the present report is to extensively investigate, identify and characterize catalytically active species and/or reaction intermediates of the C-H bond arylation as catalyzed by newly synthesised troponate/aminotroponate ruthenium-arene complexes using mass spectral and ^{1}H NMR studies. Based on these studies, along with the support from DFT calculation, the catalytic reaction pathway was proposed.

4.2. Results and Discussion

4.2.1. Synthesis and characterization of troponate-/aminotroponate-ruthenium(II)-arene complexes. Troponate-/aminotroponate-ruthenium(II)-arene complexes were synthesised by reacting tropolone (**L1**), 2-(isopropylamino)tropone (**L2**) or 2-(cyclohexylamino)tropone (**L3**) ligands with ruthenium-arene precursors. Aminotropone based ligands **L2** and **L3** were prepared by direct nucleophilic displacement of the tosyl group of the 2-(tosyloxy)tropone by using excess of corresponding amine (isopropylamine or cyclohexylamine) applying an earlier reported method.[6] The synthesized ligands were characterized by several spectro-analytical techniques which confirmed the proposed structures (see the Experimental section). Structural characterization of the ligand **L3** was also elucidated by single-crystal X-ray diffraction of its suitable crystals obtained by slow evaporation of hexane-ethyl acetate (98:2, v/v) at room temperature. ORTEP diagram of the ligand **L3** is shown in Figure 1. Crystallographic data and bond parameters for **L3** are listed

in Tables 4.1 and 4.2. The C-O and C-N bond lengths (1.2478(18) and 1.3317(19) Å, respectively) are of intermediate value for single and double bonds which is similar to reported aminotropone ligand.[8] It indicates some degree of delocalization on the order of an amide group.
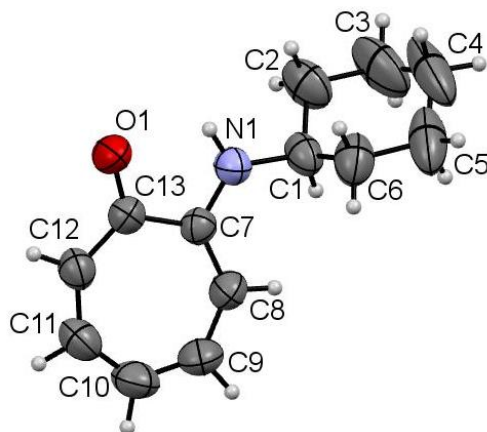
Figure 4.1. *Single crystal X-ray structure of 2-(cyclohexylamino)tropone (**L3**). Selected bond length (Å): C13-O1 = 1.2478(18), C7-N1 = 1.3317(19), C1-N1 = 1.4548(19), bond angles (°): C7-C13-O1 = 116.37(13), C13-C7-N1 = 111.27(12) and torsion angles (°): O1-C13-C7-N1 = -4.5(2), C8-C7-C13-O1 = 174.1(2), C12-C13-C7-N1 = 174.6(1).*

Table 4.1. *Crystal data and structure refinement details for Ligand **L3**.*

Crystal parameters	Ligand (L3)
empirical formula	$C_{13} H_{17} N O$
Fw	203.28
T (K)	293(2)
λ (Å)	1.54184
cryst system	Monoclinic
space group	P 21/n
cryst size, mm	0.30×0.25×0.22
a, Å	12.1210(7)
b, Å	8.5610(5)
c, Å	12.4050(8)
α, deg	90.00
β, deg	111.635(7)
γ, deg	90.00

V, Å^3	1196.56(12)
Z	4
ρ_{calcd}, g cm^{-3}	1.128
μ, mm^{-1}	0.554
$F(000)$	440
θ range, deg	6.43-73.23
completeness to θ_{max}	73.2
no. of data collected/unique data	4562 /1916
	[R(int) = 0.0254]
params/restraints	137/0
goodness of fit on F^2	1.042
Final R indices [$I > 2\sigma(I)$]	R1= 0.0607 wR2 = 0.1627
R indices (all data)	R1= 0.0517wR2 = 0.1499

Table 4.2. *Selected bond lengths and bond angles for Ligand **L3**.*

Bond lengths (Å)	
O1-C13	1.2478(18)
C13-C7	1.488(2)
C13-C12	1.414(2)
C7-C8	1.393(2)
N1-C7	1.3317(19)
N1-C1	1.4548(19)
C1-C2	1.513(3)
Bond angles (°)	
C1-N1-C7	128.62(13)
N1-C7-C13	111.27(12)
N1-C7-C8	122.60(14)
N1-C1-C2	108.38(16)
N1-C1-C6	110.53(15)
O1-C13-C7	116.37(13)
O1-C13-C12	120.07(14)

Tropolone (**L1**) or aminotropone (**L2-L3**) ligands were reacted with ruthenium-arene precursors, [{(η^6-arene)RuCl$_2$}$_2$] (η^6-arene = η^6-C$_{10}$H$_{14}$ and η^6-C$_6$H$_6$) in methanol using a base (or without base) to afford water soluble mononuclear *piano-stool* troponate-/aminotroponate ruthenium(II)-arene complexes in good yield (Scheme 4.2). The synthesized complexes have the general formula of [(η^6-arene)Ru(κ^2-L)Cl] (L = **L1**, η^6-arene = η^6-C$_{10}$H$_{14}$ (**[Ru]-13**) and η^6-C$_6$H$_6$ (**[Ru]-9**); L = **L2**, η^6-arene = η^6-C$_{10}$H$_{14}$ (**[Ru]-15**) and η^6-C$_6$H$_6$ (**[Ru]-11**); L = **L3**, η^6-arene = η^6-C$_{10}$H$_{14}$ (**[Ru]-16**) and η^6-C$_6$H$_6$ (**[Ru]-12**) and [{(η^6-arene)Ru(κ^2-L1)(PPh$_3$)]$^+$ (η^6-arene = η^6-C$_{10}$H$_{14}$ (**[Ru]-14**) and η^6-C$_6$H$_6$ (**[Ru]-10**)). The spectral analyses of the synthesized complexes corroborated well with the proposed structures (see the Experimental section).
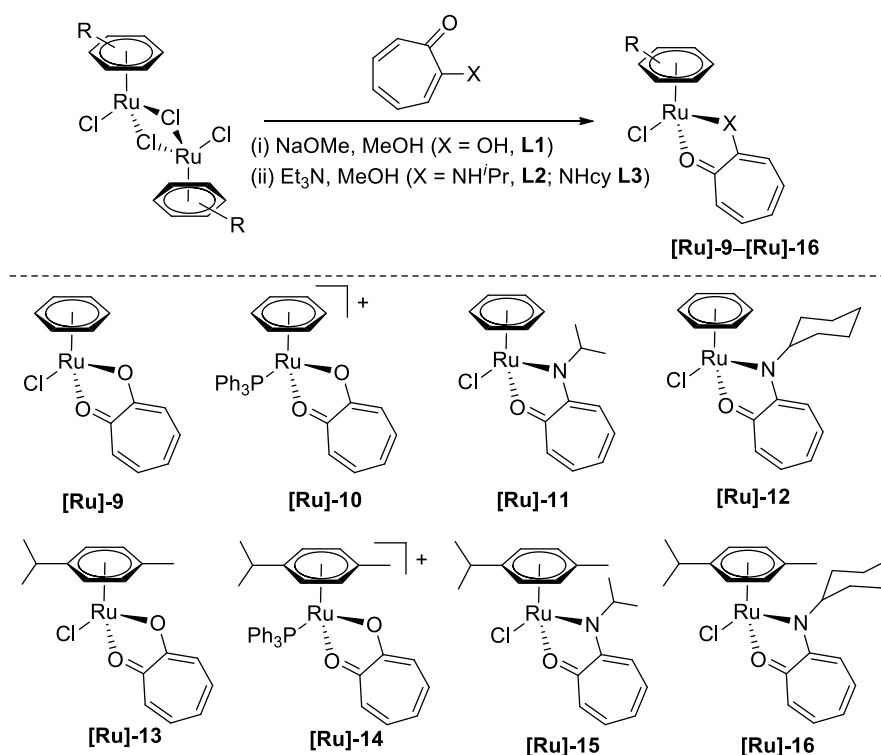
Scheme 4.2. *Synthesis of ruthenium(II)-arene complexes containing tropolone based ligands.*

In the ^{1}H NMR spectra of the mononuclear complex **[Ru]-9–[Ru]-16**, arene protons displayed downfield shift as compared to that in the respective precursor ruthenium-arene dimer. Moreover, ring carbon of the coordinated tropolone in complexes **[Ru]-9** and **[Ru]-13** also resonated in slightly deshielded region (126.34–137.80 ppm) compare to that of the free tropolone ligand. However, the carbonyl carbons, in particular, of the tropolone ligand in complexes **[Ru]-9** and

[Ru]-13 resonated in more deshielded region at 184.29-184.87 ppm compared to that for free tropolone ligand (171.84 ppm), suggesting the coordination of the ligand to the metal center. The conjugative and electron-donating abilities of the troponate/aminotroponate ligands decreases electron density at troponate/aminotroponate ring might have contributed in the observed downfield shift in the ^{1}H and ^{13}C NMR spectra.[24] In consistence with the NMR results, FT-IR spectra[25] of the complexes **[Ru]-9** and **[Ru]-13** show a typical band at 1588.21 and 1588.38 cm^{-1} respectively for the υ(C=O), while it appeared at 1609 cm^{-1} in the free tropolone ligand, suggesting the lengthening of C=O bonds upon coordination of tropolone to metal centre.[26] Cyclic voltammograms of the representative complexes **[Ru]-9** and **[Ru]-13** were obtained in CH$_2$Cl$_2$ containing 0.1 M (n-Bu$_4$N)PF$_6$ as supporting electrolyte at a sweep rate of 50 mV/s at room temperature (Figure 4.2). In the anodic window (0 to +2.0 mV) of cyclic voltammogram for complexes **[Ru]-9** and **[Ru]-13**, a well-defined quasi-reversible oxidation reduction wave was observed at 0.939 mV and 1.023 mV, respectively,[27] which may be attributed to Ru$^{II/III}$ redox couple. Analogously for the aminotroponate ruthenium-arene complex **[Ru]-14**, the Ru$^{II/III}$ redox couple appeared at 1.173 mV.
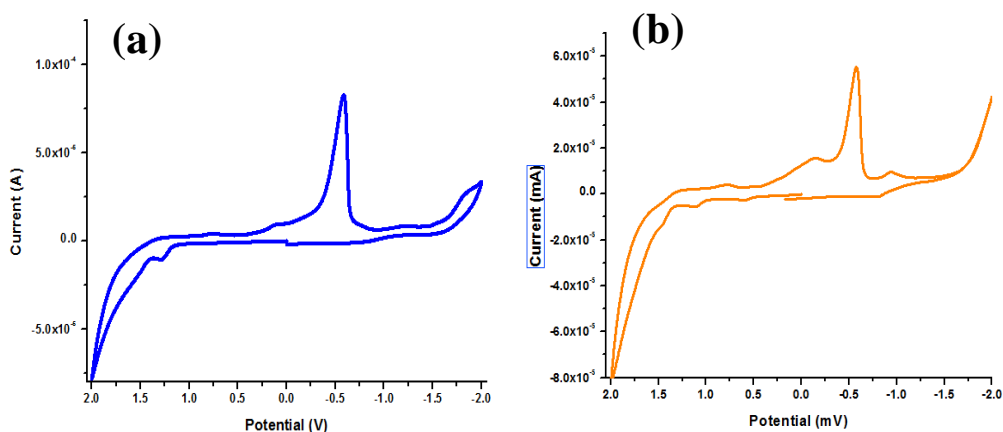
Figure 4.2. *Cyclic voltammogram of (a) [(η^6-C$_6$H$_6$)RuCl(κ^2-O,O-tropolone)]**[Ru]-9** and (b) [(η^6-C$_{10}$H$_{14}$)RuCl(κ^2-O,O-tropolone)]**[Ru]-13** in dichloromethane.*

On the other hand, tropolone based reduction waves appeared in the cathodic potential window (0 to –2.0 mV) of cyclic voltammogram of these complexes (Table 4.3). Methyl substitution at arene ligand in complex **[Ru]-13**, resulted in a shift of Ru$^{II/III}$ redox couple toward less positive side, due to the increase in electron density

on the metal centre which destabilizes the ground state energy and therefore leading to a lowering of the metal-based oxidation potentials.[28]

Table 4.3. *Cyclic voltammetric data of ruthenium complexes.*

S.No.	Complexes	Anodic pot. (E_{pa})	Cathodic pot. (E_{pc})	Oxidation half wave potential $E_{1/2}$ (mV)	ΔE (mV)
4	**[Ru]-9**	1.023	0.759	1.023	0.529
5	**[Ru]-10**	1.237	1.168	1.202	0.069
1	**[Ru]-13**	1.108	0.770	0.939	0.338
2	**[Ru]-14**	1.220	1.142	1.181	0.078
3	**[Ru]-15**	1.213	1.133	1.173	0.080

X-ray suitable crystals of complexes **[Ru]-13** and **[Ru]-15** were obtained by slow evaporation method using dichloromethane and diethyl ether as solvents and their molecular structures were confirmed by single-crystal X-ray diffraction analysis. The ORTEP view along with the selected bond parameters of the complexes **[Ru]-13** and **[Ru]-15** are shown in Figures 4.3 and 4.4, respectively. Crystallographic data and bond parameters of these complexes are listed in Table 4.4 and 4.5, respectively. Both the complexes adopted the *piano-stool* geometry, where the η^6-coordinated arene ring is present as top disc of stool and two O atoms of the ligand **L1** or N and O atoms of the ligand **L3** along with one chloride ligand are as three legs of the stool. The complex **[Ru]-13** crystallized in monoclinic crystal system with $P21/n$ space group. The arene ring (in η^6-$C_{10}H_{14}$) appears almost planar for both the complexes **[Ru]-13** and **[Ru]-15**, where the displacement of the arene ring centroid from the Ru(II) centre are 1.645 Å and 1.676 Å, respectively for complexes **[Ru]-13** and **[Ru]-15**. The Ru-C$_{centroid}$ and Ru-C bond distances are also comparable with other similar complexes.[6] The angle between the legs and the centroid of the η^6-arene ring (C_t) are in the range of 129.63°-131.17°. Both the Ru-oxygen bond distances, 2.0789 Å (Ru1-O1) and 2.079 Å (Ru1-O2) are comparable for the coordinated tropolone in complex **[Ru]-13**.[27] Moreover, the comparable bond lengths of C1-O1 (1.284 Å) and C7-O2 (1.289 Å) in complex **[Ru]-13**, suggesting a delocalization of the C=O bond of the tropolone ligand upon coordination.[26]
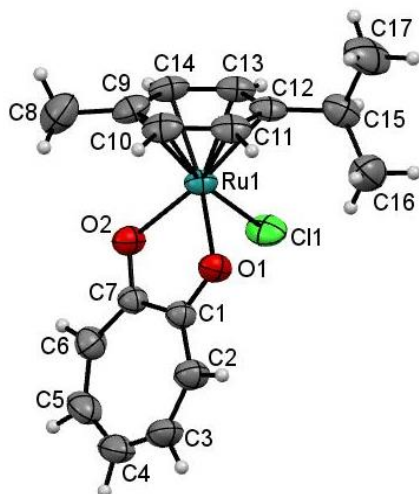
Figure 4.3. *Single crystal X-ray structure of troponate-ruthenium(II) p-cymene complex ([**Ru**]-13). Selected bond length (Å): Ru1-C$_{avg}$ = 2.167, Ru1-C$_{ct}$ = 1.645, Ru1-Cl1 = 2.4094(8), Ru1-O1 = 2.0789(18), Ru1-O2 = 2.079(2), C1-O1 = 1.284(3), C7-O2 = 1.289(3), bond angles (º): O1-Ru1-O2 = 76.63(7), O1-Ru1-Cl1 = 84.48(6), O2-Ru1-Cl1 = 84.47(6) and torsion angle (º): O1-C1-C7-O2 = -1.5(4).*
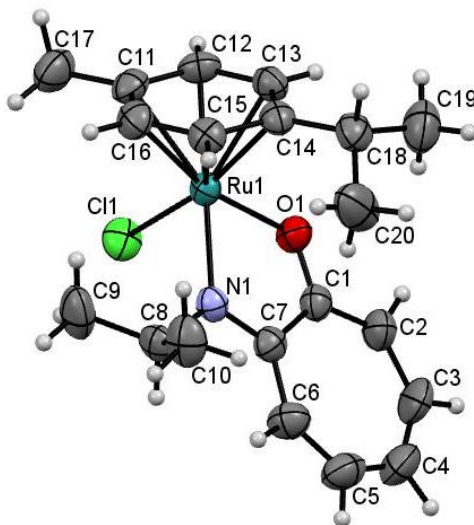
Figure 4.4. *Single crystal X-ray structure of isopropylaminotroponate-ruthenium(II) p-cymene complex ([**Ru**]-15). Selected bond length (Å): Ru1-C$_{avg}$ = 2.188, Ru1-C$_{ct}$ =1.676, Ru1-Cl1 = 2.4196(8), Ru1-O1 = 2.0463(19), Ru1-N1 = 2.115(3), C1-O1 = 1.277(4), C7-N1 = 1.319(4), bond angles (º): C1-Ru1-N1 = 84.68(7), O1-Ru1-Cl1 = 85.93(6), O1-Ru1-N1 = 75.86(9) and torsion angle (º): O1-C1-C7-N1 = 0.5(4).*

The bite angle (O1-Ru1-O2) of the tropolone ligand in complex **[Ru]-13** is 76.63°. The Cl1-Ru1-O1 and Cl1-Ru1-O2 bond angles are 84.48° and 84.47°,

respectively for complex **[Ru]-13**. The Ru1-O1 and Ru1-N1 bond lengths in complex **[Ru]-15** are 2.0463 Å and 2.115 Å, respectively. The C-O (1.277 Å) bond length appears slightly shorter in complex **[Ru]-15**, than the Ru-tropolone complex **[Ru]-13**. Moreover, the bite angle of the aminotroponate ligand in complex **[Ru]-15** is 75.86°, which deviates only slightly from the bite angle of the parent complex **[Ru]-13** with troponate ligand. Replacing one of the two oxygen atoms in ligand **L1** with nitrogen in ligand **L3**, resulted in no significant distortion in the planarity of the tropolone backbone (torsion angle). For complex **[Ru]-15**, the Cl1-Ru1-O1 and Cl1-Ru1-N1 bond angles are 85.93° and 84.68°. Bond angle between the legs and the centroid of the η^6-arene ring (C_t) is 129.63°-131.17° and 126.70°-136.67° in complex **[Ru]-13** and **[Ru]-15** respectively. The observed values are comparable to those reported for other analogous complexes.[29]

*Table 4.4. Crystal data and structure refinement details for **[Ru]-13** and **[Ru]-15**.*

Crystal parameters	Complex [Ru]-13	Complex [Ru]-15
empirical formula	$C_{17}H_{19}ClO_2Ru$	$C_{20}H_{26}ClNORu$
Fw	391.84	432.94
T (K)	293(2)	293(2)
λ (Å)	0.71073	0.71073
cryst system	Monoclinic	Monoclinic
space group	P 21/n	P 21/c
cryst size, mm(l × k × h)	0.31×0.29×0.20	0.33×0.27×0.21
a, Å	10.6918(5)	14.7074(4)
b, Å	13.3978(6)	16.6899(3)
c, Å	11.4591(5)	7.7339(2)
α, deg	90.00	90.00
β, deg	99.654(4)	102.751(2)
γ, deg	90.00	90.00
V, Å^3	1618.23(12)	1851.58(8)
Z	4	4
ρ_{calcd}, g cm^{-3}	1.608	1.553
μ, mm^{-1}	1.135	0.997
F(000)	792	888
θ range, deg	3.24-29.84	3.535-24.994

completeness to θ_{max}	83.2	99.8
no. of data collected/unique data	7476/3856 [R(int) = 0.0240]	14307/3250 [R(int)= 0.0522]
params/restraints	193/0	222/0
goodness of fit on F^2	1.043	1.100
Final R indices [$I > 2\sigma(I)$]	R1=0.0318 wR2=0.0688	R1=0.0297 wR2=0.0728
R indices (all data)	R1=0.0479 wR2=0.0786	R1=0.0350 wR2=0.0782

Table 4.5. *Selected bond lengths and bond angles for complexes **[Ru]-13** and **[Ru]-15**.*

Bond lengths (Å)	[Ru]-13	[Ru]-15
Ru1-O1	2.0789(18)	2.0463(19)
Ru1-O2	2.079(2)	-
Ru1-N1	-	2.115(3)
Ru1-C_t	1.645	1.676
Ru1-$C_{avg.}$	2.167	2.188
Ru1-Cl1	2.4094(8)	2.4196(8)
O1-C1	1.284(3)	1.277(4)
O2-C7	1.289(3)	-
N1-C7	-	1.319(4)
N1-C8	-	1.479(4)
C1-C7	1.454(4)	1.468(4)
C1-C2	1.403(4)	1.386(4)
C2-C3	1.382(4)	1.384(5)
Bond angles (°)		
O1-Ru1-O2	76.63(7)	-
O1-Ru-N1	-	75.86(9)
O1-Ru1-Cl1	84.48(6)	85.93(6)
O2-Ru1-Cl1	84.47(6)	-
N1-Ru-Cl1	-	84.68(7)
C_t-Ru1-O1	131.17	126.70
C_t-Ru1-O2	131.60	-

C$_t$-Ru-N1	-	136.67
C$_t$-Ru1-Cl1	129.63	128.18
O1-Ru-C11	91.76(9)	-
O1-Ru-C13	149.20(10)	86.99(10)
O1-Ru-C15	-	129.76(10)
O2-Ru-C11	144.18(11)	-
N1-Ru-C13	-	140.67(11)
O2-Ru-C13	133.18(9)	-
N1-Ru-C15	-	96.90(11)

4.2.2. Arene-Ru(II) catalysed C-H bond arylation in water. At an outset of our investigations for C-H bond arylation, 2-phenylpyridine (0.5 mmol) was treated with 4-chloroanisole (1.25 mmol) in water in the presence of 5 mol% troponate-Ru-*p*-cymene catalyst, **[Ru]-13**, and 3 equiv. of K$_2$CO$_3$ at 100 ºC, without using any carboxylate additive. Results inferred that **[Ru]-13** catalyst is reactive in water and facilitate C-H bond arylation even with arylchlorides with 86% conversion of 2-phenylpyridine. The monoarylated to diarylated product selectivity was found to be 61:39 (results are shown in Table 4.6). Notably, the **[Ru]-13** catalysts exhibited high conversion even in the absence of carboxylate additives. Literature reports evidenced that carboxylates have a significant role as deprotonating agent during the C-H bond activation reactions catalyzed by transition metal complexes.[30] Therefore, as an attempt to investigate the role of carboxylate additives on the C-H bond arylation (conversion and selectivities for mono- and diarylated products), **[Ru]-13** catalyst was treated with 2-phenylpyridine and 4-chloroanisole under analogous conditions as described above but with added potassium salts of carboxylates, starting from acetate to propionate, isobutyrate and pivalate. Using acetate and its methyl substituted analogues, we could able to establish a relation between the steric bulkiness of additives and the selectivity of C-H bond arylated products (mono and diarylated). As depicted in Figure 4.5, with an increase in the bulkiness of additives, the selectivity shifts towards diarylated product in the order of pivalate > isobutyrate > propionate > acetate. The selectivity for monoarylated product was 82% with acetate, which was further decreased to 38% and 28%, respectively with potassium propionate and potassium isobutyrate. This trend persists even to bulkier potassium

pivalate, where only 1% selectivity for mono arylated product (99% diarylation) was observed.
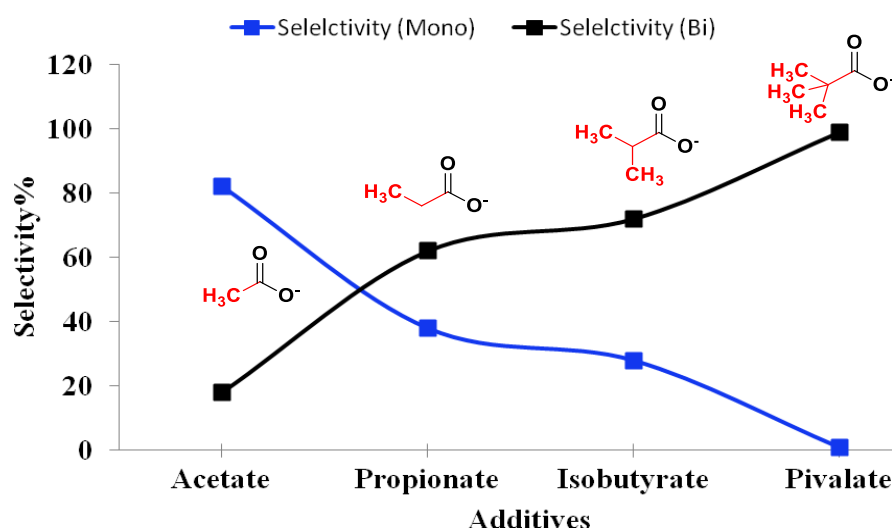
Figure 4.5. *Effect of additives on the selectivity towards mono- vs di- C-H arylated products from the reaction of 2-phenylpyridine with 4-chloroanisole catalysed by* **[Ru]-13** *catalyst.*

The observed behavior of carboxylate additives on the selectivity for C-H bond arylation is interesting and suggesting the intriguing involvement of carboxylates in C-H bond activation reaction pathway. As carboxylate can bind with metal centre (such as acetate) or remains in the solution (such as pivalate), and therefore may involve in intra/ intermolecular deprotonation of 2-phenylpyrdine.[31,32] To further investigate this phenomenon, we performed mass spectral analysis of the reaction mixture obtained after 3 h reaction of **[Ru]-13** catalyst (0.025 mmol) with carboxylate (0.05 mmol) in the presence of K_2CO_3 (1.5 mmol) at 100 ºC in water under Ar atmosphere (Figure 4.6). Mass spectral results showed that along with the peaks of the **[Ru]-13** catalyst at m/z 357.33 ([M-Cl]$^+$), acetate coordinated species $[(\eta^6\text{-arene})Ru(\kappa^2\text{-troponate})(\kappa^1\text{-acetate})] + Na^+$ at m/z 439.28 was also observed with relative abundance of 37%. In contrary to the high abundance of acetate coordinated species, abundance for analogous pivalate coordinated species, $[(\eta^6\text{-arene})Ru(\kappa^2\text{-troponate})(\kappa^1\text{-pivalate})] + CH_3CN + 2Na^+$ m/z 547.07 was observed to be very low (12%). These results are consistent with earlier reports that acidity of pivalate increases in water, which destabilises the Ru-pivalate bond and therefore resulting in the increment of free pivalate in the reaction

123

mixture.[21] Moreover, increase in the steric bulkiness of these carboxylates, from acetate to pivalate, presumably also favouring easy decoordination of bulky carboxylates. Interestingly, reaction with carboxylates does not lead the decoordination of troponate ligand in **[Ru]-13** catalyst, suggesting the stability of troponate-Ru-arene species.
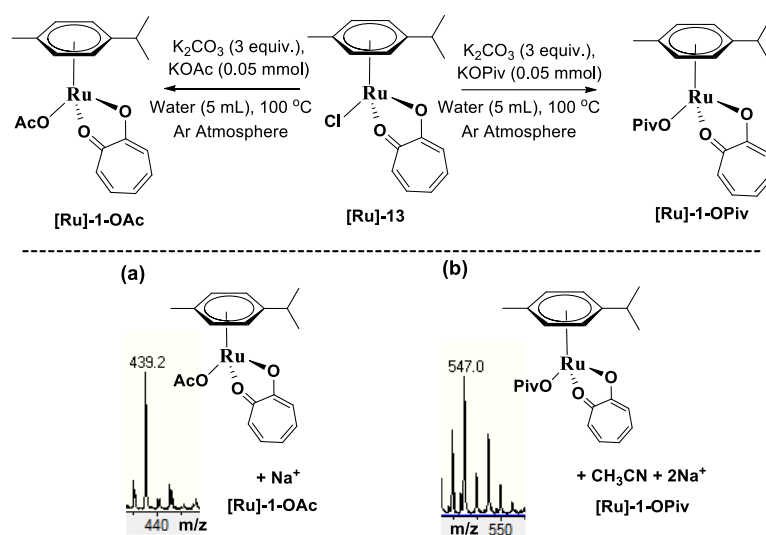
Figure 4.6. Mass spectral analysis of the reaction of [Ru]-13 catalyst with acetate and pivalate to identify (a) (η^6-arene)Ru(κ^2-troponate)(κ^1-acetate)] + Na$^+$ and (b) [(η^6-arene)Ru(κ^2-troponate)(κ^1-pivalate)] + CH$_3$CN + 2Na$^+$ species.

Further, to investigate and establish structure activity relationship, **[Ru]-9** to **[Ru]-11** and **[Ru]-13** to **[Ru]-16**, structural analogues of **[Ru]-9** catalyst were synthesized using different η^6-C$_{10}$H$_{14}$/C$_6$H$_6$ and tropolone/aminotropone liagnds, catalytic efficiency of these complexes was evaluated for the direct C-H bond arylation of 2-phenylpyridine under the optimized reaction condition (Table 4.6). Results inferred that Ru-*p*-cymene complexes, **[Ru]-13**–**[Ru]-16** (Table 4.6, entries 4–7), displayed high conversions of 2-phenylpyridine (75% to 95%), in contrarily, Ru-benzene complexes (Table 4.6, entries 5–7) exhibited relatively low conversions (48% to 90%). Moreover, Ru-*p*-cymene complexes favour biarylated products (m/d 61:39 [Ru]-13 and 73:27 **[Ru]-14**), more in comparison to Ru-benzene complexes, m/d 85:15, **[Ru]-9** and 80:20, **[Ru]-10** (Table 4.6, entries 1,2,5 and 6). In contrary to troponate-Ru-*p*-cymene complex **[Ru]-13**, a remarkable improvement in mono to diarylated product ratio was observed with aminotroponate-Ru-*p*-cymene complex,

[Ru]-15 (m/d 82:18) and **[Ru]-16** (m/d 83:17) (Figure 4.6). However, the substitution at the N-atom of the aminotroponate-Ru-arene complexes have no distinct effect on mono to diarylated ratio (m/d, *N*-isopropyl = 82:18, **[Ru]-15** and *N*-cyclohexyl = 83:17), **[Ru]-16** (Figure 4.7).

Table 4.6. *Screening of troponate-/aminotroponate-Ru-arene catalysts for C-H bond arylation reaction in water[a]*

entry	catalysts	conv. (%)	sel. % (m/d)[b]	TON
1	$[(\eta^6\text{-}C_6H_6)Ru(\kappa^2\text{-}O,O\text{-troponate})Cl]$ (**[Ru]-9**)	58	85/15	11.6
2	$[(\eta^6\text{-}C_6H_6)Ru(\kappa^2\text{-}O,O\text{-troponate})PPh_3]Cl$ (**[Ru]-10**)	90	80/20	18.0
3	$[(\eta^6\text{-}C_6H_6)Ru(\kappa^2\text{-}N,O\text{-}$ isopropylaminotroponate)Cl] (**[Ru]-11**)	48	85/15	9.6
4	$[(\eta^6\text{-}C_{10}H_{14})Ru(\kappa^2\text{-}O,O\text{-troponate})Cl]$ (**[Ru]-13**)	86	61/39	17.2
5	$[(\eta^6\text{-}C_{10}H_{14})Ru(\kappa^2\text{-}O,O\text{-troponate})PPh_3]Cl$ (**[Ru]-14**)	95	73/27	19.0
6	$[(\eta^6\text{-}C_{10}H_{14})Ru(\kappa^2\text{-}N,O\text{-}$ isopropylaminotroponate)Cl] (**[Ru]-15**)	75	82/18	15.0
7	$[(\eta^6\text{-}C_{10}H_{14})Ru(\kappa^2\text{-}N,O\text{-}$ cyclohexylaminotroponate)Cl] (**[Ru]-16**)	81	83/17	16.2

[a]Reaction conditions: 2-phenylpyridine (0.5 mmol), 4-chloroanisole (1.25 mmol), [Ru] catalyst (5 mol%), K_2CO_3 (1.5 equiv.), water (5 mL), 16 h, [b] obtained from ^{1}H NMR.
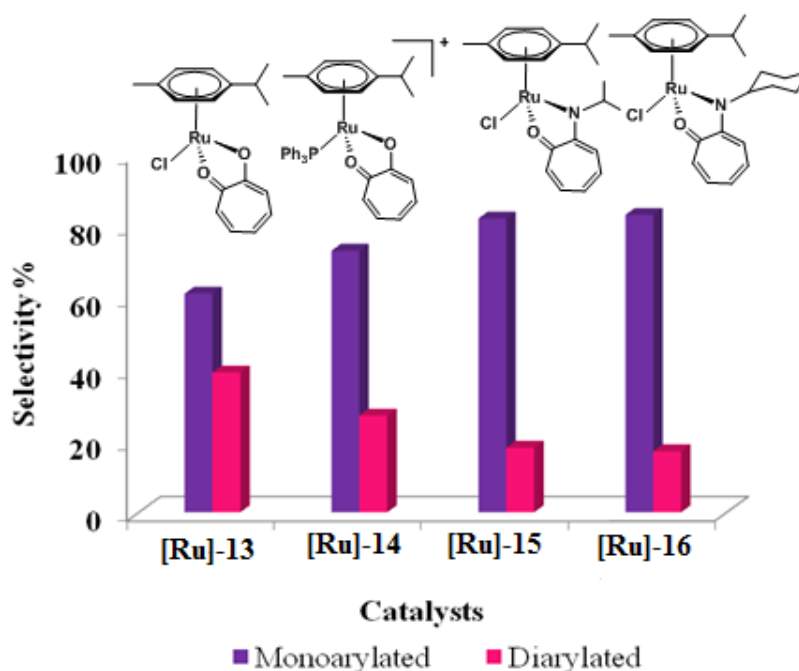
Figure 4.7. *Effect of different Ru(II) catalysts on the selectivity of mono- vs di- C-H arylated products of 2-phenylpyridine.*

Further to elucidate the reaction mechanism, extensive mass spectrometric investigations were performed for the ruthenium catalysed C-H bond activation under the optimized reaction condition. As previously reported, ruthenium complexes are found to be very efficient to form cyclometallated intermediates by C-H activation at *ortho* position of the phenyl ring.[33] Stoichiometric reactions of 2-phenylpyridine and **[Ru]-13** catalyst was performed in water in the presence of K_2CO_3 (3 equiv.) base at 100 ºC in catalyst to substrate molar ratio of 1:1. After 3 h, reaction mixture was subjected to mass spectral analysis, where several cycloruthenated 2-phenylpyridine species were identified. To our surprise, along with the well established key intermediate cyclometallated species {(η^6-arene)Ru(κ^2-*C,N*-phenylpyridine)}$^+$ **[Ru]-A** at m/z 390.01, another cyclometallated species with troponate ligand at m/z 379.13 corresponds to {(κ^2-troponate)Ru(κ^2-*C,N*-phenylpyridine)} (**[Ru]-B**) was also observed where tropolone ligand was retained instead of *p*-cymene ring.

Analogous reactions were conducted but with high substrate to catalyst (S/C) ratio (2:1) or larger (5:1), which inferred that there is more tendency of arene (η^6-$C_{10}H_{14}$) cleavage to generate the **[Ru]-B** species. Mass spectra of the reaction mixture obtained from the reaction of **[Ru]-13** catalyst with 2-phenylpyridine at

126

substrate catalyst ratio 1:1, 2:1 and 5:1 revealed that the relative percentage of the formation of **[Ru]-A** and **[Ru]-B** are 60:40, 42:58 and 16:84, respectively (Figure 4.8).
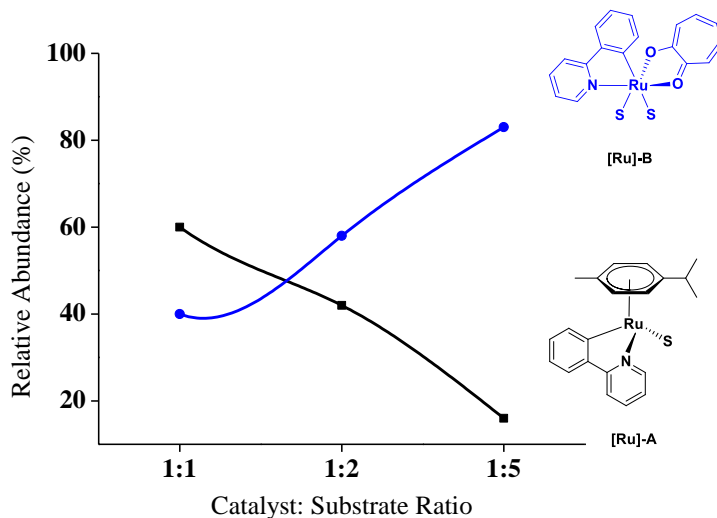
Figure 4.8. *Relative abundance of Ru (II) cyclometallated species ([Ru]-A and [Ru]-B) with different catalyst:substrate ratio with [Ru]-13 catalyst under similar reaction conditions.*

To further investigate the relevance of this newly identified troponate-Ru-cyclometallated species **[Ru]-B**, reaction mixture was analyzed by mass spectrometry with respect to reaction time. Notably, the mass spectral analysis revealed a systematic enhancement in the abundance of the **[Ru]-B** species with time, whereas that of **[Ru]-A** species decreases (Figure 4.9). To further authenticate if analogous species were also generated with the troponate/aminotroponate Ru(II) complexes, we performed the mass spectral analysis of the reaction of **[Ru]-15** catalyst with 2-phenylpyridine in substrate to catalyst ratio of 2:1 under analogous reaction conditions. Analogous to that observed with **[Ru]-1** catalyst, replacing troponate ligand with *N*-isopropyl-aminotroponate ligand in **[Ru]-3** also revealed the formation of $\{(\kappa^2\text{-aminotroponate})Ru(\kappa^2\text{-}C,N\text{-phenylpyridine})\}$ **([Ru]-B$_3$)** cyclometallated species as major component (90%) in comparison to **[Ru]-A** species (10%).
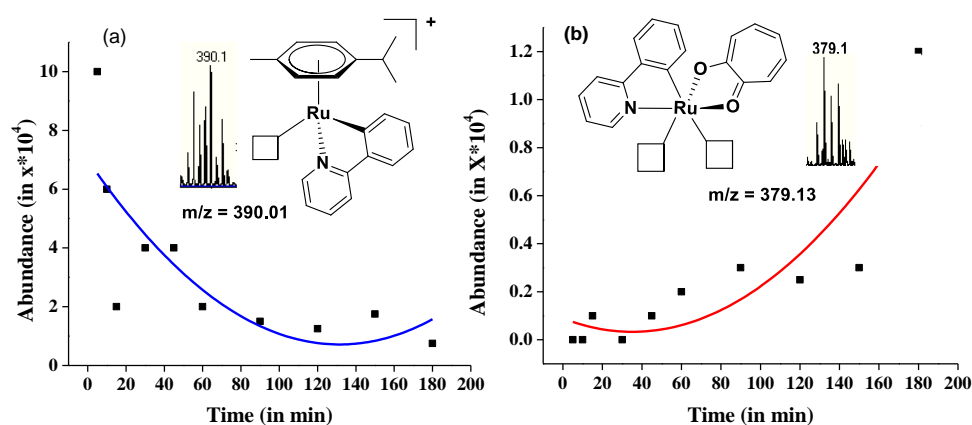
Figure 4.9. *Time dependent study for the formation of (**a**) species $[(\eta^6\text{-arene})Ru(\kappa^2\text{-}C,N\text{-phenylpyridine})(sol)]^+$, (**b**) species $[(\kappa^2\text{-troponate})Ru(\kappa^2\text{-}C,N\text{-phenylpyridine})(sol)_2]$, in substrate to catalyst ratio 2:1.*

Therefore, high catalytic efficiency and the detection of troponate-/aminotroponate Ru-cyclometallated species, **[Ru]-B₁**–**[Ru]-B₃**, also suggesting the key role of the newly identified species in C-H bond arylation reaction. Notably, reaction of **[Ru]-13** with 4-chloroanisole in S/C ratio of 5:1 in the presence of K_2CO_3 in water at 100 ℃ revealed that the **[Ru]-13** is inactive in the presence of arylchloride. Contrarily, cycloruthenation of 2-phenylpyridine occurred readily with **[Ru]-13** catalyst to generate catalytically active cycloruthenated species **[Ru]-A** and **[Ru]-B**. This further supports that initial C-H bond activation takes place by deprotonation and not by oxidative addition of C-H bond.[34] Literature also revealed that proton abstraction by a carbonate base is energetically favorable process (-13.7 kcal/mol) over hydride abstraction pathway (+28.2 kcal/mol) and during this process base to metal synergy plays a crucial role.[35] The initial carbonate induced deprotonation of the *ortho* C-H bond of the phenyl group of 2-phenylpyrdine by **[Ru]-13** (as also observed for other complexes **[Ru]-9** to **Ru]-11** and **Ru]-14** to **[Ru]-16**), led to the formation of species **[Ru]-A**, originated by the release of tropolone ligand during the deprotonation process, and **[Ru]-B**, by elimination of η^6**-**arene ring.[31] Reaction of species **[Ru]-A** with 2.5 equivalents of 4-chloroanisole in water at 100 ℃, resulted in no reaction in the absence of a base (K_2CO_3) after 8 h, whereas with 3 equivalents of K_2CO_3, both mono and diarylated products in 78:22 ratio were observed with 14% conversion. Unfortunately, all our attempts to isolate species **[Ru]-B** failed, instead we isolated a transformed spcies of

128

[Ru]-B, [Ru(trop)(Phpy)$_2$(H$_2$O)$_2$] a dinuclear species **[Ru]-B'**, in 48% yield from the reaction of complex **[Ru]-13** with 2-phenylpyridine. Presumably, reversible deprotonation-protonation equilibrium might be responsible for the formation of species **[Ru]-B'**. Interestingly, performing the same reaction in methanol formed only **[Ru]-A** species, even after prolonged reaction time, suggesting the crucial role of water in the C-H bond activation reactions. Reaction of species **[Ru]-B'** with 2.5 equivalents of 4-chloroanilsole under analogous reaction condition as used for **[Ru]-A**, also resulted in the formation of mono- and diarylated products (m/d) with % conversion, whereas reaction could not proceed in the absence of base.

We anticipated that chelation and strong conjugation effect over seven carbon atoms in the planar ring of tropolone favours the strong interaction of tropolone to ruthenium metal center. As coordination of 2-phenylpyridine earlier to the C-H deprotonation step is crucial, the relative competitive coordination strength of η^6-arene and troponate ligands drive the decoordination of either troponate ligand or η^6-arene, followed by deprotonation step to form [(η^6-arene)Ru(κ^2-C,N-phenylpyridine)(sol)]$^+$ **[Ru]-A** and [(κ^2-troponate)Ru(κ^2-phenylpyridine)(sol)$_2$] **[Ru]-B$_1$** respectively. This effect is further expected to be responsible for the formation analogous species **[Ru]-B$_3$**, also for aminotroponate complexes **[Ru]-15**, [(κ^2-isopropylaminotroponate)Ru(κ^2-phenylpyridine)(sol)$_2$]. Support for our experimental results comes from DFT calculations by comparing the relative energies for the formation of species **[Ru]-A**, [(η^6-arene)Ru(κ^2-C,N-phenylpyridine)(sol)]$^+$, and **[Ru]-B**, [(κ^2-troponate/aminotroponate)Ru(κ^2-phenylpyridine)(sol)$_2$] from complexes **[Ru]-13**, **[Ru]-14** and **[Ru]-15**. The reaction free energy profile, Figure 4.10, shows an uphill reaction pathway for the formation of both species **[Ru]-A** and **[Ru]-B** from troponate-/aminotroponate-Ru-arene complexes. Though, the formation of **[Ru]-B** is highly favoured over **[Ru]-A** for all the ruthenium complexes, **[Ru]-13** complex showed only marginally higher selectivity for species **[Ru]-B** over **[Ru]-A**, which is in close agreement with our mass spectral experimental findings. Moreover, binding energy (E$_B$) calculations (Table 4.7) also showed that p-cymene is a better leaving group than tropolone/aminotropolone, and thus the formation of species **[Ru]-B** is favoured over species **[Ru]-A**.
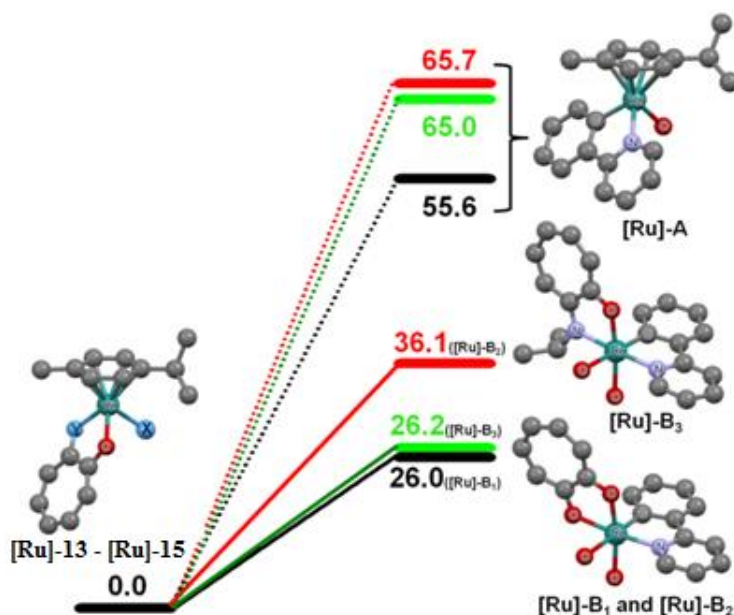
Figure 4.10. *Reaction free energy profile for the formation of cycloruthenated species,* **[Ru]-A** *and* **[Ru]-B**, *from the reaction of phenylpyridine with troponate/aminotroponate Ru-arene complexes (**[Ru]-13** – **[Ru]-15**).*
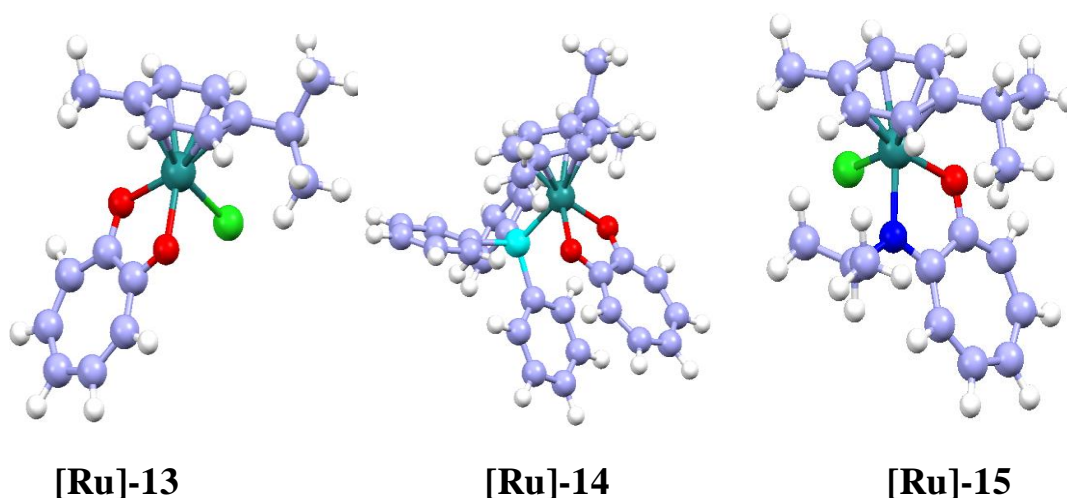
[Ru]-13   **[Ru]-14**   **[Ru]-15**

Figure 4.11: *Optimized structures of* **[Ru]-13**, **[Ru]-14**, *and* **[Ru]-15**. *Here white, skyblue, blue, red, turquoise, green and teal colour balls denote the hydrogen, carbon, nitrogen, oxygen, phosphorous, chlorine, and ruthenium atoms, respectively.*

Density functional theory (DFT) calculations were carried out using Gaussian 09 package[36] using Becke's three parameter exchange and the Lee-Yang-Parr's correlation functional (B3LYP).[37] 6-311G(d,p)[38,39] basis functions are used for non-metals (C, H, O, N, P and Cl), whereas LANL2DZ-ECP (effective core potentials)[40,41] is used for Ru. Water is used as an implicit solvent using the

polarizable continuum model (PCM) as implemented in Gaussian 09.[42-44] In all the calculations, D3 version of Grimme's dispersion corrections is included for long range interactions.[45] Harmonic vibrational frequencies are calculated to characterize the nature of the stationary points. Zero-point energy and entropy corrections (at 298.15 K) are included for the free energy calculations (Figure 4.11).

The reaction free energies (ΔG_A for **[Ru]-A** and ΔG_B **[Ru]-B**) are calculated for the formation of **[Ru]-A** and **[Ru]-B** by using the following equations:

$\Delta G_A = (G_A + G_{H3O+} + G_{Cl-} + G_{troponato/aminotroponato}) - (G_{[Ru]-cat} + 2G_{H2O} + G_{phpy})$

$\Delta G_B = (G_B + G_{H3O+} + G_{Cl-} + G_{p\text{-cymene}}) - (G_{[Ru]-cat} + 3G_{H2O} + G_{phpy})$

where G_A, G_{H3O+}, G_{Cl-}, $G_{troponato/aminotroponato}$, $G_{[Ru]-cat}$, G_{H2O}, G_{phpy}, G_B and $G_{p\text{-cymene}}$ are the total free energies (with zero point and entropy corrections) of **[Ru]-A**, H_3O^+, Cl^-, troponato/aminotroponato, [Ru]-catalysts, H_2O, 2-phenylpyridine, **[Ru]-B** and p-cymene, respectively.

We have calculated the binding energy (E_B) (Table 4.7) of the leaving groups (p-cymene and trop/aminotrop) to understand such trend. The binding energies are calculated using the following formula:

$E_B = E_{[Ru]-cat} - (E_{([Ru]-cat) - (p\text{-cymene})} + E_{(p\text{-cymene})})$

$E_B = E_{[Ru]-Cat} - (E_{([Ru]-cat) - (troponato/aminotroponato)} + E_{(troponato/aminotroponato)})$

where $E_{([Ru]-cat) - (p\text{-cymene})}$ is the single point energy of the catalyst without p-cymene ligand, $E_{(p\text{-cymene})}$ is the single point energy of the p-cymene within the geometry of catalyst, $E_{([Ru]-cat) - (troponato/aminotroponato)}$ is the single point energy of the catalyst without troponate/aminotroponate ligand, and $E_{(troponato/aminotroponato)}$ is the single point energy of the troponate/aminotroponate within the geometry of catalyst.

Table 4.7. *The binding energies (kcal/mol) calculated for p-cymene and troponato/aminotroponato ligands in ruthenium catalysts.*

	[Ru]-13	**[Ru]-14**	**[Ru]-15**
p-cymene	-43.7	-37.6	-41.2
troponato/aminotroponato	-68.8	-85.8	-87.2

Based on the mass spectral identification and well supported by DFT calculation of new cycloruthenated Ru(II) species, **[Ru]-B** formed as a major component by the release of η^6-arene group during the initial deprotonation step of 2-phenylpyrdine, along with the well established species **[Ru]-A** (minor). A reaction

pathway is proposed (Scheme 4.3) for the C-H bond arylation of 2-phenylpyridine catalyzed by troponate-/aminotroponate- ruthenium-arene complexes. Role of species **[Ru]-A** is well established in C-H bond activation reaction catalysed by Ru-arene complexes, but our experimental evidences revealed that the formation of species **[Ru]-B** is favoured over species **[Ru]-A** for the troponate/aminotroponate ruthenium arene complexes.
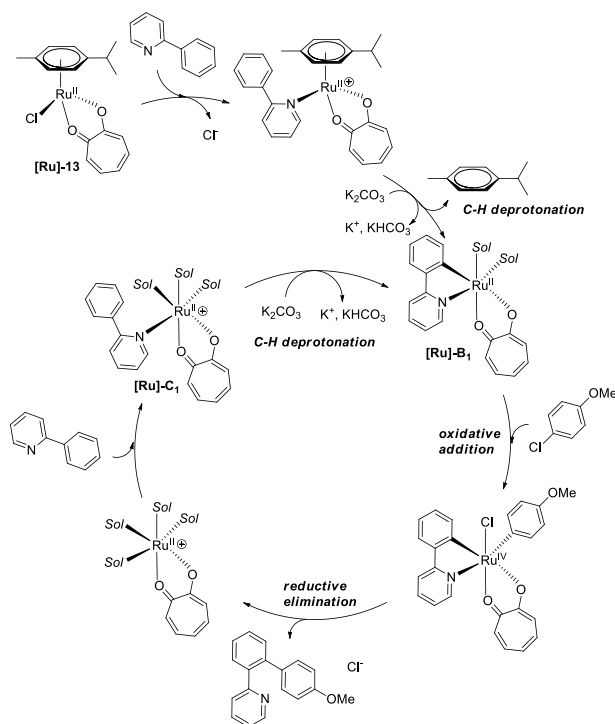
Scheme 4.3. *Proposed reaction pathway for C-H bond arylation of 2-phenylpyrdine catalysed by troponate-ruthenium(II)-arene complex* **[Ru]-13**.

Since all the troponate/aminotroponate ruthenium arene complexes displayed high catalytic activity for C-H bond arylation reaction, species **[Ru]-B** play a key role in the oxidative addition step of C-H bond activation reaction. Notably, troponate/aminotroponate ruthenium arene complexes are inactive towards direct reaction with arylchloride, whereas corresponding C-H bond activation of 2-phenylpyridine was faster. Given the experimental results for C-H bond arylation of 2-phenylpyridine by several troponate/aminotroponate-Ru-arene complexes, it has been established that (i) these complexes are highly efficient catalyst for C-H bond arylation, (ii) increase in steric bulkiness enhances the conversion as well as selectivity towards diarylated product, and (iii) replacing troponate with

aminotroponate ligands in ruthenium-arene complexes remarkably enhances the catalytic efficiency and selectivity towards diarylated product.

4.3. Conclusion

We successfully synthesised a series of half-sandwiched ruthenium(II) arene complexes with O,O and O,N donor troponate-/aminotroponate ligands, and structures of two representative complexes were established by single crystal X-ray diffraction studies. These synthesised complexes exhibited higher catalytic activity for direct *ortho* C-H bond arylation of 2-phenylpyridine with 4-chloroanisole at 100 ºC in water, without the use of any carboxylate additive, with enhanced selectivity for monoarylated product over diarylated product. In comparison to troponate-ruthenium(II) arene complex, **[Ru]-13**, the selectivity towards monoarylated products is more prominent with aminotroponate-ruthenium(II) arene complexes, **[Ru]-15** and **[Ru]-16**. Notably, these complexes are also catalytically active in the presence of carboxylate additive, where selectivity towards diarylated product is favoured over monoarylated product with the more bulky carboxylates: pivalate > isobutyrate > propionate > acetate. Extensive mass spectral studies were performed to identify active key intermediates of the catalyst and to evaluate their role in the C-H bond activation pathway. Our studies showed the formation of a new cycloruthenated species, **[Ru]-B**, by the unexpected release of arene ring from the catalyst, is favoured over the well established arene-ruthenium cycloruthenated species, **[Ru]-A.** These cycloruthenated species were readily generated by carbonate assisted deprotonation of 2-phenylpyridine by ruthenium arene complexes. In consistent with the above results, reactions free energies, calculated using DFT calculations, also favoured the formation of species **[Ru]-B** over **[Ru]-A**. In contrary to the parent ruthenium catalysts which were inactive with 4-chloroanisole, these cycloruthenated species were found to be active towards oxidative addition of 4-chloroanisole to generate C-H arylated products. Based on the experimental evidences, a reaction pathway was proposed showing the key importance of the species **[Ru]-B** in C-H bond arylation of 2-phenylpyridine. We believe, observations marked in the present study using troponate-/aminotroponate-ruthenium(II) arene complexes will contribute in enhancing the mechanistic understanding of such catalytic systems in C-H activation reactions and help in development of new and highly active catalytic system. Further investigations in this direction are underway.

4.4. Experimental section

4.4.1. Materials and Instrumentation. All reactions were performed under open atmosphere except the catalytic reactions which were performed under Ar atmosphere. Using chemicals of high purity purchased from sigma Aldrich and Alfa Aesar. Dichloro bridged arene-ruthenium(II) precursors [{(η^6-C$_6$H$_6$)RuCl$_2$}$_2$] and [{(η^6-C$_{10}$H$_{14}$)RuCl$_2$}$_2$] were synthesized according to the literature procedures.[46] ^{1}H NMR (400 MHz), ^{13}C NMR (100 MHz), and ^{31}P NMR (161.97 MHz) spectra were recorded at 298 K using CDCl$_3$ or DMSO-d_6 as the solvent on a Bruker Avance 400 spectrometer. Tetramethylsilane (TMS) was used as an external standard and the chemical shifts in ppm are reported relative to the centre of the singlet at 7.26 ppm for CDCl$_3$ and 2.49 ppm for DMSO-d_6 in ^{1}H NMR, and to the centre of the triplet at 77.0 ppm for CDCl$_3$ and 39.50 ppm for DMSO-d_6 in ^{13}C NMR. Suitable single crystals of complexes **[Ru]-13** and **[Ru]-15** along with the single crystal of ligand **L3** were subjected to single-crystal X-ray structural studies using Agilent Technologies Supernova CCD system. ESI (positive and negative mode), and high-resolution mass spectra (HRMS) were recorded on a micro TF-Q II mass spectrometer. The voltammograms were recorded on a CHI620D electrochemical analyser in dichloromethane as the solvent and 0.1 M TBAF$_6$ as the supporting electrolyte. The electrodes used were glassy carbon as a working electrode, a Pt wire as a counter electrode and the Silver as a reference electrode. Infrared spectra (4000 to 500 cm^{-1}) were recorded with a BRUKER TENSOR 27 instrument in KBr pellets.

4.4.2. Single crystal X-ray diffraction Studies. Single crystal X-ray structure studies of **[Ru]-13** and **[Ru]-15** were executed on a CCD Agilent Technologies (Oxford Diffraction) SUPER NOVA diffractometer. Using graphite-monochromated CuKα radiation (λ = 1.54184 Å) based diffraction, data were collected at 293(2) K by the standard 'phi-omega' scan techniques, and were scaled and reduced using CrysAlisPro RED software. The extracted data was evaluated using the CrysAlisPro CCD software. The structures were solved by direct methods using SHELXS-97, and refined by full matrix least-squares with SHELXL-97, refining on $F2$.[24] The positions of all the atoms were determined by direct methods. However, the X-ray data give a clear indication for Ru-coordinated p-methylaniline. All non-hydrogen atoms were refined anisotropically. The remaining hydrogen atoms were placed in geometrically constrained positions, and refined with isotropic temperature factors,

generally 1.2*Ueq* of their parent atoms. The CCDC number 1442036 contains the supplementary crystallographic data for **[Ru]-15.** This data is freely available at www.ccdc.cam.ac.uk (or can be procured from the Cambridge Crystallographic Data Centre, 12 union Road, Cambridge CB21 EZ, UK; Fax: (+44) 1223-336-033; or deposit@ccdc.cam.ac.uk).

4.4.3. General procedure for the synthesis of tropolone based ligands (L2-L3).

Ligand **L2-L3** were synthesized using a literature reported method with some modifications.[6] 2-tosyloxytropone (276 mg, 1.0 mmol), corresponding amine (1.26 mmol) and triethylamine (0.153 g, 1.51 mmol) were dissolved in ethanol (25 mL). The mixture was refluxed for 12 h and then cooled down to room temperature. All volatiles were removed under reduced pressure and the oily residue was taken up in 2N NaOH (15 mL). The aqueous phase was extracted with CH_2Cl_2 (4×10 mL). The organic phases were washed with brine (20 mL) and dried with Na_2SO_4. The crude product was purified by column chromatography using silica gel.

Synthesis of 2-(isopropylamino)cyclohepta-2,4,6-trienone (L2). Ligand L2 was prepared by following the above general procedure using 2-tosyloxytropone (0.276 g, 1.0 mmol), isopropylamine (0.074 g, 1.26 mmol) and triethylamine (0.153 g, 1.51 mmol). Yield: 0.110 g, (67.4%). ^{1}H NMR (400 MHz, $CDCl_3$): δ (ppm) = 7.18-7.04 (m, 3H), 6.56 (t, $J = 8.0$ Hz, 1H), 6.47 (d, $J = 8.0$ Hz, 1H), 3.78-3.70 (m, 1H), 1.24 (d, $J = 4.0$ Hz, 6H). ^{1}H NMR (400 MHz, DMSO-d_6): δ (ppm) = 7.29-7.23 (m, 2H), 6.93 (d, $J = 8.0$ Hz, 1H), 6.69-6.61 (m, 2H), 3.91-3.83 (m, 1H), 1.23 (d, $J = 4.0$ MHz, 6H). ^{13}C NMR (100 MHz, $CDCl_3$): δ (ppm) = 176.57, 154.67, 137.18, 136.29, 128.24, 121.83, 108.89, 43.81, 22.02. HRMS (ESI) m/z calculated for 2-(isopropylamino)cyclohepta-2,4,6-trienone: 186.0 [M+Na]$^+$, found 186.1 [M+Na]$^+$.

Synthesis of 2-(cyclohexylamino)cyclohepta-2,4,6-trienone (L3). Ligand **L3** was prepared by following the above general procedure using 2-tosyloxytropone (0.276 g, 1.0 mmol) and cyclohexylamine (0.125 g, 1.26 mmol) and triethylamine (0.153 g, 1.51 mmol). Yield: 0.140 g, (69%). ^{1}H NMR (400 MHz, $CDCl_3$): δ (ppm) = 7.17-7.05 (m, 3H), 6.60-6.50 (m, 2H), 3.46-3.41 (m, 1H), 2.02-1.96 (m, 2H), 1.77-1.74 (m, 2H) 1.62-1.59 (m, 1H), 1.37-1.30 (m, 4H), 1.27-1.21 (m, 1H). ^{1}H NMR (400 MHz, DMSO-d_6): δ (ppm) = 7.28-7.23 (m, 2H), 7.93 (d, $J = 12.0$ Hz, 1H), 7.74 (d, $J = 4.0$ Hz, 1H), 6.64 (t, $J = 4.0$ Hz, 1H), 3.60-3.54 (m, 1H), 1.92-1.89 (m, 2H), 1.70-1.67 (m, 2H) 1.60-1.57 (m, 1H), 1.43-1.29 (m, 4H), 1.23-1.18 (m, 1H). ^{13}C NMR

135

(100 MHz, CDCl$_3$): δ (ppm) = 176.49, 154.61, 137.12, 136.28, 128.03, 121.78, 108.94, 51.04, 32.07, 25.57, 24.65. HRMS (ESI) m/z calculated for 2-(cyclohexylamino)cyclohepta-2,4,6-trienone: 226.1 [M+Na]$^+$, found 226.1 [M+Na]$^+$.

4.4.4. Procedure for the synthesis of arene-ruthenium(II) complexes ([Ru]-9–[Ru]-16) containing tropolone (L1) and aminotropone (L2-L3) ligands

Synthesis of [(η^6-C$_6$H$_6$)RuCl(κ^2-O,O-tropolone)]([Ru]-9). [{(η^6-C$_6$H$_6$)RuCl$_2$}$_2$] (0.100 g, 0.20 mmol) and tropolone (**L1**) (0.050 g, 0.41 mmol) was suspended in methanol (25 mL). The suspension was refluxed for 12 h and filtered, and then precipitate was dissolved in dichloromethane followed by precipitation with excess of diethyl ether. It can be also prepared by following the procedure for the synthesis of complex **[Ru]-13.** Red microcrystalline solid was obtained. Yield: 0.110 g, (82%). FTIR (KBr, cm^{-1}): 1139, 1360 υ(C-C), 1508 υ(C=C), 1588.38 υ(C=O). ^{1}H NMR (400 MHz, CDCl$_3$): δ (ppm) = 7.23-7.21 (m, 4H), 6.84-6.80 (m, 1H), 5.69 (s, 6H). ^{13}C NMR (100 MHz, CDCl$_3$): δ (ppm) = 184.29, 137.55, 127.07, 126.41, 80.93. MS (ESI) m/z calculated for [(η^6-C$_6$H$_6$)Ru(L1)]$^+$ (L1 = tropolone), 301.0 [M − Cl]$^+$, found 301.0 [M − Cl]$^+$. Anal. Calcd: C, 46.56; H, 3.30; O, 9.55. Found: C, 46.58; H, 3.17; O, 9.52.

Synthesis of [(η^6-C$_6$H$_6$)RuPPh$_3$(κ^2-O,O-tropolone)]Cl ([Ru]-10). Complex **[Ru]-10** was prepared by following the procedure for the synthesis of complex **[Ru]-14**, using [(η^6-C$_6$H$_6$)RuCl$_2$(PPh$_3$)] (0.102 g, 0.20 mmol) and tropolone (**L1**) (0.026 g, 0.21 mmol) in methanol (25 mL). Red microcrystalline solid was obtained. Yield: 0.102 g, (85%). ^{1}H NMR (400 MHz, CDCl$_3$): δ (ppm) = 7.75-7.72 (m, 5H), 5.43-5.38 (m, 10H), 7.21-7.21 (m, 3H), 5.39 (m, 1H), 5.39 (m, 1H), 5.39 (s, 6H). MS (ESI) m/z calculated for [(η^6-C$_6$H$_6$)RuPPh$_3$(L1)]$^+$ (L1 = tropolone), 563.1 [M+], found 563.1 [M+]. Anal. Calcd: C, 62.26; H, 4.38; O, 5.35. Found: C, 62.19; H, 4.13; O, 5.61

Synthesis of [(η^6-C$_6$H$_6$)RuCl(κ^2-O,N-2-(cyclohexylamino)cyclohepta-2,4,6-trienone)] ([Ru]-11). Complex **[Ru]-11** was prepared by following the procedure for the synthesis of complex **[Ru]-15**, using [{(η^6-C$_6$H$_6$)RuCl$_2$}$_2$] (0.225 g, 0.45 mmol). Red microcrystalline solid was obtained. Yield: 0.121 g (80%). ^{1}H NMR (400 MHz, CDCl$_3$): δ (ppm) = 6.83-6.60 (m, 4H), 6.20 (t, J = 8.8 Hz, 1H), 5.61 (s, 6H), 4.41-4.35 (m, 1H), 1.38 (d, J = 6.4 Hz, 6H). MS (ESI) m/z calculated for [(η^6-

C$_6$H$_6$)Ru(L2)]$^+$ (L2 = 2-(isopropylamino)cyclohepta-2,4,6-trienone), 342.0 [M − Cl]$^+$, found 342.0 [M − Cl]$^+$. Anal. Calcd: C, 50.86; H, 5.07; O, 4.29; N, 3.71. Found: C, 50.66; H, 4.87; O, 4.50; N, 3.93.

Synthesis of [(η^6-C$_6$H$_6$)RuCl(κ^2-O,N-2-(cyclohexylamino)cyclohepta-2,4,6-trienone)] ([Ru]-12). Complex **[Ru]-12** was prepared by following the procedure for the synthesis of complex **[Ru]-11**, using 2-(cyclohexylamino)cyclohepta-2,4,6-trienone (**L3**) (0.203 g, 1.00 mmol). Red microcrystalline solid was obtained. Yield: 0.201 g, (53%). MS (ESI) m/z calculated for [(η^6-C$_6$H$_6$)Ru(L3)]$^+$ (L3 = 2-(cyclohexylamino)cyclohepta-2,4,6-trienone), 382.1 [M − Cl]$^+$, found 382.4 [M − Cl]$^+$. Anal. Calcd: C, 54.74; H, 5.32; O, 3.84; N, 3.36. Found: C, 53.13; H, 5.01; O, 2.90; N, 3.10

Synthesis of [(η^6-C$_{10}$H$_{14}$)RuCl(κ^2-O,O-tropolone)]([Ru]-13). Tropolone (**L1**) (0.050 g, 0.41 mmol) and KO^{t}Bu (0.046 g, 0.41 mmol) were suspended in methanol (25 mL). The suspension was stirred at room temperature for 3 h then added [{(η^6-C$_{10}$H$_{14}$)RuCl$_2$}$_2$] (0.122 g, 0.20 mmol) in suspension. The suspension was stirred at room temperature for 24 h. Solution was evaporated to dryness and the residue was dissolved in dichloromethane and precipitated by pouring in excess of diethyl ether. Red crystalline solid was obtained. Yield: 0.121 g (77.3%). FTIR (KBr, cm^{-1}): 1221, 1337 υ(C-C), 1508 υ(C=C), 1588.21 υ(C=O). ^{1}H NMR (400 MHz, CDCl$_3$): δ (ppm) = 7.21 (m, 4H), 6.78 (m, 1H), 5.55 (d, 2H, J = 5.2 Hz), 5.33 (d, 2H, J = 4.8 Hz), 2.89 (sept, 1H), 2.34 (s, 3H), 1.33 (d, 6H, J = 6.8 Hz). ^{13}C NMR (100 MHz, CDCl$_3$): δ (ppm) = 184.87, 137.80, 127.37, 126.34, 100.48, 96.55, 80.43, 78.89, 31.36, 22.65, 18.89. MS (ESI) m/z calculated for [(η^6-C$_{10}$H$_{14}$)Ru(L1)]$^+$ (L1 = tropolone), 357.0 [M − Cl]$^+$, found 357.1 [M − Cl]$^+$. Anal. Calcd: C, 52.04; H, 4.84; O, 8.16. Found: C, 52.08; H, 4.83; O, 8.11.

Synthesis of [(η^6-C$_{10}$H$_{14}$)RuPPh$_3$(κ^2-O,O-tropolone)]Cl ([Ru]-14). [(η^6-C$_{10}$H$_{14}$)RuCl$_2$(PPh$_3$)] (0.114 g, 0.20 mmol) and tropolone (**L1**) (0.026 g, 0.21 mmol) were dissolved in methanol (25 mL) and the solution was reflux for 12 h. Solution was evaporated to dryness and the residue was dissolved in dichloromethane and precipitated by diethyl ether. It can be also synthesized by using an alternative method, for which [(η^6-C$_{10}$H$_{14}$)RuCl(κ^2-O,O-tropolone)] (0.0.078 g, 0.20 mmol) and Triphenylphosphene (0.079 g, 0.30 mmol) were suspended in methanol (30 mL) and

then suspension was stirred for 24 h at room temperature. Red microcrystalline solid was obtained. Yield: 0.101 g, (77%). ^{1}H NMR (400 MHz, CDCl$_3$): δ (ppm) = 7.93-7.84 (m, 5H), 7.53-7.44 (m, 10H), 7.43-7.38 (m, 4H), 7.09(t, J = 8.0 Hz, 1H), 5.26 (b, 2H), 5.06 (b, 2H), 2.92-2.90 (m, 1H), 1.94 (s, 3H), 1.17 (d, J = 4.0 Hz, 6H). MS (ESI) m/z calculated for [(η^6-C$_{10}$H$_{14}$)RuPPh$_3$(L1)]$^+$ (L1 = tropolone), 619.1 [M+], found 619.1 [M+]. Anal. Calcd: C, 64.26; H, 5.24; O, 4.89. Found: C, 64.19; H, 5.28; O, 4.91.

Synthesis of [(η^6-C$_{10}$H$_{14}$)RuCl(κ^2-O,N-2-(isopropylamino)cyclohepta-2,4,6-trienone)] ([Ru]-15). 2-(isopropylamino)cyclohepta-2,4,6-trienone (**L2**) (0.163 g, 1.00 mmol) and triethylamine (0.505 g, 5.00 mmol) were suspended in methanol (30 mL) and the suspension was refluxed for 3 h. [{(η^6-C$_{10}$H$_{14}$)RuCl$_2$}$_2$] (0.275 g, 0.45 mmol) was then added to the above solution and the solution was refluxed for another 12 h. Solution was filtered and evaporated to dryness and the residue was dissolved in dichloromethane followed by the precipitation with diethyl ether. Brown crystalline solid was obtained. Yield: 0.320 g (82%). ^{1}H NMR (400 MHz, DMSO-d_6): δ (ppm) = 7.79 (d, J = 8.0 Hz, 1H), 7.40 (d, J = 8.0 Hz, 1H), 6.79 (t, J = 8.0 Hz, 1H), 6.30 (d, J = 8.0 Hz, 1H), 6.10 (t, J = 8.0 Hz, 1H), 5.80 (d, J = 4.0 Hz, 2H), 5.68 (d, J = 4 Hz, 2H), 4.27-4.20 (m, 1H), 2.86-2.78 (sept, 1H), 2.09 (s, 3H), 1.50 (d, J = 4.0 Hz, 3H), 1.40 (d, J = 4.0 Hz, 3H), 1.19 (d, J = 4.0 Hz, 6H). MS (ESI) m/z calculated for [(η^6-C$_{10}$H$_{14}$)Ru(L2)]$^+$ (L2 = 2-(isopropylamino)cyclohepta-2,4,6-trienone), 398.1 [M − Cl]$^+$, found 398.1 [M − Cl]$^+$. Anal. Calcd: C, 55.48; H, 6.05; O, 3.70; N, 3.24. Found: C, 55.76; H, 6.15; O, 4.12; N, 3.33.

Synthesis of [(η^6-C$_{10}$H$_{14}$)RuCl(κ^2-O,N-2-(cyclohexylamino)cyclohepta-2,4,6-trienone)] ([Ru]-16). Complex **[Ru]-16** was prepared by following the procedure for the synthesis of complex **[Ru]-15**, using 2-(cyclohexylamino)cyclohepta-2,4,6-trienone (**L3**) (0.203 g, 1.00 mmol). Red microcrystalline solid was obtained. Yield: 0.339 g (79%). ^{1}H NMR (400 MHz, DMSO-d_6): δ (ppm) = 6.84-6.68 (m, 3H), 6.31 (d, J = 8.0 Hz, 1H), 6.11 (t, J = 8.0 Hz, 1H), 5.80 (d, J = 6.0 Hz, 2H), 5.76 (d, J = 6.0 Hz, 2H), 3.76-3.66 (m, 1H), 2.81 (sept, 1H), 2.09 (s, 3H), 1.93-1.90 (m, 2H), 1.83-1.77 (m, 3H), 1.68-1.64 (m, 1H), 1.41-1.28 (m, 4H), 1.17 (d, J = 4.0 Hz, 6H). MS (ESI) m/z calculated for [(η^6-C$_{10}$H$_{14}$)Ru(L3)]$^+$ (L3 = 2-(cyclohexylamino)cyclohepta-2,4,6-trienone), 438.1 [M − Cl]$^+$, found 438.1 [M − Cl]$^+$. Anal. Calcd: C, 58.40; H, 6.39; O, 3.38; N, 2.96. Found: C, 57.90; H, 5.99; O, 4.01; N, 3.13

4.4.5. General procedure for catalytic C-H bond arylation of heteroarenes with aryl halides. All the reactions were carried out under Ar atmosphere. C-H bond arylation reaction of heteroarene was performed in a two necked round bottom flask. Flask was charged with ruthenium catalyst (5 mol %, 0.025 mmol) and K_2CO_3 (0.207 g, 1.50 mmol) with distilled water (5 mL). Solution was stirred for 15 minutes and then added heteroarene (0.5 mmol) and aryl halide (1.25 mmol). The reaction mixture was degassed with Ar along with the balloon at the top of the fitted condenser. The reaction was continued to stir for 16 hours at 100 ºC. After completion of reaction time, reaction mixture was cooled down to room temperature and extracted with ethyl acetate (3×10 mL) and the organic layer was dried over Na_2SO_4. Then extract was washed with the 10 mL saturated brine solution to remove moisture and the solvent volume was reduced under pressure. The conversion and selectivity of synthesized monoarylated and biarylated products were determined by ^{1}H NMR. Products were purified and collected from the crude reaction mixture using column chromatography on silica gel with ethyl acetate-*n*-hexane as eluents in 1:99 (v/v) ratio.

4.4.6. Characterization of C-H arylated products:
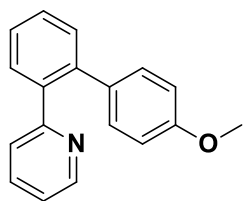
2-(4'-methoxy-[1,1'-biphenyl]-2-yl)pyridine: Yield: 0.112 g (43%). **^{1}H NMR (400 MHz, CDCl$_3$):** δ(ppm) = 8.64 (d, *J* = 4.0 Hz, 1H), 7.70-7.65 (m, 1H), 7.47-7.36 (m, 4H), 7.12-7.05 (m, 3H), 6.90 (d, *J* = 8.0 Hz, 1H), 6.79 (d, *J* = 7.5 Hz, 2H), 3.78 (s, 3H), **^{13}C NMR (100 MHz, CDCl$_3$):** δ(ppm) =159.48, 158.54, 149.42, 140.21, 139.37, 135.25, 133.73, 130.77, 130.44, 128.52, 127.29, 125.43, 121.29, 113.59, 55.19, **HRMS** (ESI) m/z: calculated 262.1 [(C$_{18}$H$_{15}$NO + H)]$^+$, Found: 262.1 [(C$_{18}$H$_{15}$NO + H)]$^+$.
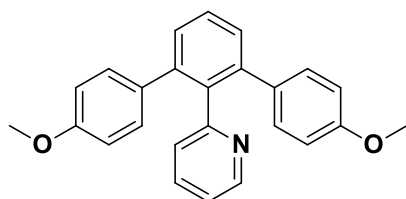
2-(4,4'-dimethoxy-[1,1',3',1''-terphenyl]-2'-yl)pyridine: **^{1}H NMR (400 MHz, CDCl$_3$):** δ(ppm) = 8.36 (d, *J* = 4.0 Hz, 1H) , 7.50-7.46 (m, 1H), 7.41-7.39 (m, 2H), 7.35-7.31 (m, 1H), 7.02 (m, 4H), 6.94-6.87 (m, 2H), 6.70-6.65 (m, 4H), 3.74 (s, 6H), **^{13}C NMR (100 MHz, CDCl$_3$):** δ(ppm) = 159.24, 158.08, 148.50, 141.43, 138.36, 135.09, 134.06, 130.68, 129.18, 128.15, 126.83, 120.86, 113.11, 55.12, **HRMS** (ESI) m/z: calculated: 368.1 [(C$_{25}$H$_{21}$NO$_2$ + H)]$^+$, Found: 368.1 [(C$_{25}$H$_{21}$NO$_2$ + H)]$^+$.

4.4.7. Mass spectrometric analysis of different intermediates for mechanistic study

Mass spectral study of the reaction of [Ru]-1 with potassium acetate (KOAc). To trap the carboxylate coordinated cyclometallated species, **[Ru]-13** (0.025 mmol, 0.0098 g) was added with potassium acetate (0.05 mmol, 0.0049 g) and 5 mL water to the two necked round bottom flask. Reaction vessel was then provided with magnetic bar and was degassed with vacuum pump followed by the gassing with Argon. Reaction mixture was stirred for 3 h at 100 ºC and after the completion of reaction time, mixture was cooled down. Crude reaction mixture was filtered through filter tip of 1000 µL and mixture was diluted with acetonitrile. ESI-MS was recorded in positive mode and analyzed further.

Mass spectral study of the reaction of [Ru]-1 with potassium pivalate (KOPiv).

To trap the carboxylate coordinated cyclometallated species, **[Ru]-13** (0.025 mmol, 0.0098 g) was added with potassium pivalate (0.05 mmol, 0.0070 g) and 5 mL water to the two necked round bottom flask. Reaction vessel was then provided with magnetic bar and was degassed with vacuum pump followed by the gassing with Argon. Reaction mixture was stirred for 3 h at 100 ºC and after the completion of reaction time, mixture was cooled down. Crude reaction mixture was filtered through filter tip of 1000 µL and mixture was diluted with acetonitrile. ESI-MS was recorded in positive mode and analyzed further.

Mass spectral study of the reaction of [Ru]-13 with 2-phenylpyridine in different catalyst to substrate ratio

[Ru]-13 was added with 2-phenylpyridine and 4-chloroanisole in C:S ratio 1:1, 1:2 and 1:5 in water (5 mL) followed by addition of potassium carbonate (3 equiv.). Reaction mixture was heated at 100 ºC for 3 h under Ar atmosphere. After completion of reaction time, crude reaction mixture was filtered through filter tip of 1000 µL and mixture was diluted with acetonitrile. ESI-MS was recorded in positive mode and analyzed further.

Time dependent mass spectral study of the reaction of [Ru]-13 with 2-phenylpyridine (S/C ratio 2:1).

To perform the time dependent study of two intermediates (**[Ru]-A** and **[Ru]-B**), a two necked round bottom flask was charged with **[Ru]-13** catalyst (0.05 mmol, 0.0196 g) and 2-phenylpyridine (0.1 mmol, 14.3 µL). Reaction was carried out in water (5 mL) at 100 ºC under Ar atmosphere for 3 h. 100 µL of aliquot was

withdrawn at 5 min, 10 min, 15 min, 30 min, 45 min, 60 min, 90 min, 120 min, 150 min and 180 min. Crude reaction mixture was filtered through filter tip of 1000 µL and further diluted with acetonitrile. ESI-MS was recorded in positive mode and analyzed further.

Abundance of [Ru]-A and [Ru]-B species with different Ru(II) catalysts ([Ru]-13 to [Ru]-16)

To strengthen the presence of species **[Ru]-A** and **[Ru]-B** with different catalysts, 0.025 mmol Ru(II) catalyst (**[Ru]-13** to **[Ru]-16**) were taken separately in a two necked round bottom flask with 3 equiv. of K_2CO_3 and 0.05 mmol 2-phenylpyridine keeping S/C ratio 2:1 in 5 mL water under argon atmosphere. Reaction was performed at 100 °C for 3 h and crude reaction mixture was filtered through filter tip of 1000 µL and further diluted with acetonitrile. ESI-MS was recorded in positive mode and analyzed further.

Preparation of intermediate species [(η^6-p-cymene)RuCl(κ^2-C,N-2-phenylpyridine)]

Reaction vessel was charged with the [{(η^6-p-cymene)RuCl$_2$}$_2$] (0.5 mmol, 0.306 g) and potassium acetate (3.0 mmol, 0.294 g) in 25 ml of methanol under Ar atmosphere. Solution was stirred for 24 h at room temperature and the product was isolated by reducing volume under vacuum. Product was precipitated with ether and washed with *n*-hexane several times to remove excess/unreacted 2-phenylpyridine. Product was air dried and analyzed by ^{1}H NMR.

^{1}H NMR (400 MHz, CDCl$_3$): δ(ppm) = 9.24 (d, J = 4.0 Hz, 1H), 8.16 (d, J = 8.0 Hz, 1H), 7.71 (d, J = 8.0 Hz, 1H), 7.68-7.64 (m, 1H), 7.62 (d, J = 8.0 Hz, 1H), 7.19-7.17 (m, 1H), 7.06-7.01 (m, 2H), 5.59-5.55 (m, 2H), 5.17 (d, J = 8.0 Hz, 1H), 4.98 (d, J = 8.0 Hz, 1H), 2.45-2.42 (m, 1H), 2.05 (s, 3H), 0.97 (d, J = 4.0 Hz, 3H), 0.85 (d, J = 8.0 Hz, 1H).
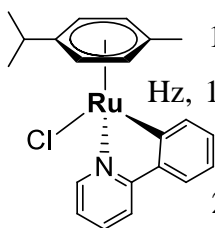
Reaction of the cycloruthenated species, [Ru]-A, with 4-chloroanisole. Cyclometallated species **[Ru]-A** was taken (0.1 mmol, 0.039 g) in a two necked round bottom flask under Ar atmosphere followed by the addition of base (K_2CO_3, 0.3 mmol, 0.0414 g) with 2.5 equivalent of 4-chloroanisole (0.25 mmol, 30 µL). 5 mL water was added and reaction mixture was stirred for 8 h at 100 ºC. Resulting reaction mixture was cooled down to room temperature and extracted with ethyl

acetate (3×10 mL) and solvent volume was reduced under pressure. Crude reaction mixture was analyzed with ^{1}H NMR.

Note: The contents of this work have been reproduced with the permission from The American Chemical Society (*Inorg. Chem.,* 2016, 55, 6739-6749 (DOI: 10.1021/acs.inorgchem.6b01028).

4.5. References

1.   (a) Ackermann L. (2015), Robust Ruthenium(II)-Catalyzed C-H Arylations: Carboxylate Assistance for the Efficient Synthesis of Angiotensin-II-Receptor Blockers, *Org. Process Res. Dev.*, 19, 260-269 (DOI: 10.1021/op500330g); (c) Mei R., Zhu C., Ackermann L. (2016), Ruthenium(II)-catalyzed C–H functionalizations on benzoic acids with aryl, alkenyl and alkynyl halides by weak-O-coordination, *Chem.Commun.*, 52, 13171-13174 (DOI: 10.1039/c6cc07773k); (c) Tyagi D., Rai, R. K., Dwivedi, A. D., Mobin S. M., Singh S. K. (2015), Phosphine-free ruthenium-arene complex for low temperature one-pot catalytic conversion of aldehydes to primary amides in water, *Inorg. Chem. Front.,* 2, 116-124 (DOI: 10.1039/c4qi00115j); (d) Gupta K., Tyagi D., Dwivedi A. D., Mobin S. M., Singh S. K. (2015), Catalytic transformation of bio-derived furans to valuable ketoacids and diketones by water-soluble ruthenium catalysts, *Green Chem.*, 17, 4618-4627 (DOI: 10.1039/c5gc01376c); (e) Dwivedi A. D., Gupta K.,Tyagi D., Rai R. K., Mobin S. M., Singh S. K. (2015), Ruthenium and Formic Acid Based Tandem Catalytic Transformation of Bioderived Furans to Levulinic Acid and Diketones in Water, *ChemCatChem*, 24, 4050-4058 (DOI: 10.1002/cctc.201501021).

2.   (a) Ang W. H., Dyson P.J. (2006), Classical and Non-Classical Ruthenium-Based Anticancer Drugs: Towards Targeted Chemotherapy, *Eur J. Inorg. Chem.*, 2006, 4008-4018 (DOI: 10.1002/ejic.200600723); (b) Fink G. S. (2010), Arene ruthenium complexes as anticancer agents, *Dalton Trans*, 39, 1637-1688 (DOI: 10.1039/b916860p); (c) Kilpin K. J., Cammack S. M., Clavel C. M., Dyson P. J. (2013), Ruthenium(II) arene PTA (RAPTA) complexes: impact of enantiomerically pure chiral ligands, *Dalton Trans*, 42,

2008-2014 (DOI: 10.1039/c2dt32333h); (d) Clavel C. M., Paunescu E., Silwinska P. N., Griffioen A. W., Scopelliti R. (2015), Modulating the Anticancer Activity of Ruthenium(II)–Arene Complexes, *J. Med. Chem.*, 58, 3356-3365 (DOI: 10.1021/jm501655t).

3. Kumar P., Gupta R. K., Pandey D. S. (2014), Half-sandwich arene ruthenium complexes: synthetic strategies and relevance in catalysis, *Chem. Soc. Rev.*, 43, 707-733 (DOI: 10.1039/c3cs60189g).

4. Mendiguchia B. S., Pucci D., Mastropietro T. F., Ghedinia M., Crispini A. (2013), Non-classical anticancer agents: on the way to water soluble zinc(II) heteroleptic complexes, *Dalton Trans.*, 42, 6768-6774 (DOI: 10.1039/c3dt50367d).

5. Meyer N., Lohnwitz K., Zulys A., Roesky P. W., Dochnahl M., Blechert S. (2006), Aminotroponate Zinc Complexes as Catalysts for the Intramolecular Hydroamination of Alkenes and Alkynes, *Organometallics*, 25, 3730-3734 (DOI: 10.1021/om060369i).

6. Dochnahl M., Lçhnwitz K., Pissarek J. W., Biyikal M., Schulz S. R., Schçn S., Meyer N., Roesky P. W., Blechert S. (2007), Intramolecular Hydroamination with Homogeneous Zinc Catalysts: Evaluation of Substituent Effects in N,N'-Disubstituted Aminotroponiminate Zinc Complexes, *Chem. Eur. J.*, 13, 6654-6666 (DOI: 10.1002/chem.200601765).

7. Duncan C., Biradar A. V., Asefa T. (2011), Aminotroponate/Aminotroponiminate Zinc Complexes Functionalized Mesoporous Silica Catalysts for Intramolecular Hydroamination of Non-Activated Alkenes with Varied Steric and Electronic Properties, *ACS Catal.*, 1, 736-750 (DOI: 10.1021/cs2000945).

8. Frederick A. H., Jason C. J., Brookhart M. (2003), Synthesis and Ethylene Polymerization Activity of a Series of 2-Anilinotropone-Based Neutral Nickel(II) Catalysts, *Organometallics*, 22, 3533-37545 (DOI: 10.1021/om030142c).

9. Mazzeo M., Lamberti M., Tuzi A., Centore R., Pellecchia C. (2005), New anilinotropone-based titanium complexes: synthesis, characterization and application as catalysts for olefin polymerization, *Dalton Trans.*, 3025-3031 (DOI:10.1039/b506079f).

10. Schutte M., Roodt A., Visser H. G. (2012), Coordinated Aqua vs Methanol

Substitution Kinetics in fac-Re(I) Tricarbonyl Tropolonato Complexes, *Inorg. Chem.*, 51, 11996-12006 (DOI: 10.1021/ic301891u).

11. Yoshida J., Kuwahara K., Yuge H. (2014), A mixed-valence dinuclear ruthenium complex composed of Ru(II)-acetylide and Ru(III)-tropolonato units: Acetylideevinylidene interconversion in solution and solid state, *J. Organomet. Chem.*, 756, 19-26 (DOI: 10.1016/j.jorganchem.2014.01.018).

12. Mori A., Mori R., Takemoto M., Yamamoto S-i., Kuribayashi D., Uno K., Kubo K., Ujiie S. (2005), Troponoid metallomesogens with 5-alkoxy, 5-alkoxycarbonyl, 5-alkanoyloxy, 5-alkyl, 5-alkoxy-2-amino, and 5-alkoxy-2-alkylamino Substituents, *J. Mater. Chem.*, 15, 3005-3014 (DOI: 10.1039/b501974e).

13. Dehnen S., Bürgstein M. R., Roesky P. W. (1998), Homoleptic yttrium and lanthanide complexes of aminotroponiminates and aminotroponates: experimental and theoretical studies, *J. Chem. Soc., Dalton Trans.*, 2425-2429 (http://dx.doi.org/10.1039/A709213J).

14. Becica J., Jackson A. B., Dougherty W. G., Kassel W. S., West N. M. (2014), Bis-tropolonate complexes of tungsten: scaffolds for selective side-on binding of nitriles, imines and ketones, *Dalton Trans.*, 43, 8738-8748 (DOI: 10.1039/c4dt00734d).

15. For selected reviews on C-H bond activation: (a) Shilov A. E., Shul'pin G. B. (1997), Activation of C-H Bonds by Metal Complexes, *Chem. Rev.*, 97, 2879-2932 (DOI: 10.1021/cr9411886); (b) Jia C., Kitamura T, Fujiwara Y. (2001), Catalytic Functionalization of Arenes and Alkanes via C-H Bond Activation *Acc. Chem. Res.*, 34, 633-639 (DOI: 10.1021/ar000209h); (c) Labinger J. A., Bercaw J. E. (2002), Understanding and exploiting C-H bond activation, *Nature* , 417, 507-514 (DOI: 10.1038/417507a); (d) Gunay A., Theopold K. H. (2010), C-H Bond Activations by Metal Oxo Compounds, *Chem. Rev.*, 110, 1060-1081 (DOI: 10.1021/cr900269x); (e) Li B., Dixneuf P. H. (2013), sp^2 C–H bond activation in water and catalytic cross-coupling reactions, *Chem. Soc. Rev.*, 42, 5744-5767 (DOI: 10.1039/c3cs60020c); (f) Zha G.-F., Qin H.-L., Knatchev E. A. B. (2016), Ruthenium-catalyzed direct arylations with aryl Chlorides. *RSC Adv.*, 6, 30875-30885 (DOI: 10.1039/c6ra02742c).

16. (a) Martinez R., Simon M.-O., Chevalier R., Pautigny C., Genet J.-P., Darses S. (2009), C-C Bond Formation via C-H Bond Activation Using an in Situ-

Generated Ruthenium Catalyst, *J. Am. Chem. Soc.*, 131, 7887-7895 (DOI: 10.1021/ja9017489); (b) Li B., Shi Z.-J. (2012), From C(sp2)-H to C(sp3)-H: systematic studies on transition metal-catalyzed oxidative C-C formation, *Chem. Soc. Rev.*, 4, 5588-5598 (DOI: 10.1039/c2cs35096c).

17.   (a) Song G., Wang F., Li X. (2012), C–C, C–O and C–N bond formation via rhodium(III)-catalyzed oxidative C-H activation, *Chem. Soc. Rev.* 41, 3651-3678 (DOI: 10.1039/c2cs15281a); (b) Ramirez T. A., Zhao B., Shi X. (2012), Recent advances in transition metal-catalyzed sp^3 C-H amination adjacent to double bonds and carbonyl groups, *Chem. Soc. Rev.*, 41, 931-942 (DOI: 10.1039/c1cs15104e); (c) Laouilat M., Patureau F.W. (2014), Oxidative C-H amination reactions, *Chem. Soc. Rev.*, 43, 901-910 (DOI: 10.1039/c3cs60318k); (d) Mindiola D. J., Waterman R., Iluc V. M., Cundari T., Hillhouse G. L. (2014), Carbon-Hydrogen Bond Activation, C-N Bond Coupling, and Cycloaddition Reactivity of a Three-Coordinate Nickel Complex Featuring a Terminal Imido Ligand, *Inorg. Chem.*, 53, 13227-13238 (DOI: 10.1021/ic5026153).

18.   (a) Matsumoto K., Sugiyama H. (2002), Organometallic-like C-H Bond Activation and C-S Bond Formation on the Disulfide Bridge in the RuSSRu Core Complexes, *Acc. Chem. Res.*, 35, 915-926 (DOI: 10.1021/ar000103m); (b) Wang H., Wang L., Shang J., Li X., Wang H., Guia J., Lei A. (2012), Fe-catalysed oxidative C-H functionalization/C-S bond formation, *Chem. Commun.*, 48, 76-78 (DOI: 10.1039/c1cc16184a); (c) Shen C., Zhang P., Sun Q., Bai S., Hor T. S. A., Liu X. (2015), Recent advances in C–S bond formation Via C-H bond functionalization and decarboxylation, *Chem. Soc. Rev.*, 44, 291-314 (DOI: 10.1039/c4cs00239c).

19.   (a) Campeau L. C., Fagnou K. (2006), Palladium-catalyzed direct arylation of simple arenes in synthesis of biaryl molecules, *Chem. Commun.*, 1253-1264 (DOI: 10.1039/b515481m); (b) Chen X., Engle K. M., Wang D. H., Yu J. Q. (2009), Palladium(II)-Catalyzed C-H Activation/C-C Cross-Coupling Reactions: Versatility and Practicality, *Angew. Chem. Int. Ed.*, 48, 5094-5115 (DOI: 10.1002/anie.200806273); (c) Lyons T. W., Sanford M. S. (2010), Palladium-Catalyzed Ligand-Directed C-H Functionalization Reactions, *Chem. Rev.*, 110, 1147-1169 (DOI: 10.1021/cr900184e); (d) Beck E. M., Gaunt M. J. (2010), Pd-Catalyzed C-H Bond Functionalization on the Indole

and Pyrrole Nucleus *Top Curr Chem.*, 292, 85-121 (https://doi.org/10.1007/128_2009_15); (e) Sun C. L., Li, B., Shi, Z. J. (2010), Pd-catalyzed oxidative coupling with organometallic reagents via C-H activation, *Chem. Commun.*, 46, 677-685 (DOI: 10.1039/b908581e).

20. (a) Oi S., Sakai K., Inoue Y. (2005), Ruthenium-Catalyzed Arylation of 2-Alkenylpyridines with Aryl Bromides: Alternative E,Z-Selectivity to Mizoroki-Heck Reaction, *Org. Lett.*, 7, 4009-4011 (DOI: 10.1021/ol051654l); (b) Yu B., Yan X., Wang S., Tang N., Xi C. (2010), A Highly Efficient Ruthenium(II) Catalyst with (1,2-Diarylvinyl)phosphine Ligands for Direct Ortho Arylation of 2-Arylpyridine with Aryl Chlorides, *Organometallics*, 29, 3222-3226 (DOI: 10.1021/om100407q); (c) Oi S., Sasomoto H., Funayama R., Inoue Y. (2008), Ortho-selective Arylation of Arylazoles with Aryl Bromides Catalyzed by Ruthenium Complexes, *Chem. Lett.*, 37, 994-995 (DOI: 10.1246/cl.2008.994).

21. Acrokiam P., Poirier V., Fischmeister C., Bruneau C., Dixneuf P. H. (2009), Diethyl carbonate as a solvent for ruthenium catalysed C-H bond functionalisation, *Green Chem.*, 11, 1871-1875 (DOI: 10.1039/b913115a).

22. Singh K. S., Dixneuf P. H. (2013), Direct C-H bond Arylation in Water Promoted by (O,O)- and (O,N)-Chelate Ruthenium(II) Catalysts, *ChemCatChem*, 5, 1313-1316 (DOI: 10.1002/cctc.201300031).

23. Sersen, S.; Kljun J. (2013), Novel Organoruthenium(II) β-Diketonates as Catalysts for Ortho Arylation via C-H Activation, *Organometallics*, 32, 609-616 (DOI: 10.1021/om3011189).

24. Steyl G. (2007), Synthesis, structure and theoretical study of two rhodium(I) complexes [Rh(TropNMe)(CO)(PPh₃)] and [Rh(Trop)(CO)(PPh₃)]. Acetone, *Polyhedron*, 26, 5324-5330 (DOI:10.1016/j.poly.2007.07.039).

25. Singh K. S., Kaminsky W. (2014), Iridium (III) and rhodium (III) triazoles by 1,3-dipolar cycloadditons to a coordinated azide in iridium (III) and rhodium (III) compounds, *J. Coord. Chem.*, 67, 3252-3269 (DOI: 10.1080/00958972.2014.960408).

26. Singh K. S., Svitlyk V., Mozharivskyj Y. (2011), Mono and dinuclear arene ruthenium(II) triazoles by 1,3-dipolar cycloadditions to a coordinated azide in ruthenium(II) compounds, *Dalton Trans.*, 40, 1020-1023 (DOI: 10.1039/c0dt00698j).

27. Singh S. K., Trivedi M., Chandra M., Sahay A. N., Pandey D. S. (2004), Luminescent Piano-Stool Complexes Incorporating 1-(4-Cyanophenyl)imidazole: Synthesis, Spectral, and Structural Studies, *Inorg. Chem.*, 43, 8600-8608 (DOI: 10.1021/ic049256m).

28. Pittracher M., Frisch U., Kopacka H., Wurst K., Müller T., Oehninger L., Ott I., Wuttke E., Scheerer S., Winter R. F., Bildstein B. (2014), π-Complexes of Tropolone and Its N-Derivatives: Ambidentate [O,O]/[N,O]/[N,N]-Cycloheptatrienyl Pentamethylcyclopentadienyl Ruthenium Sandwich Complexes, *Organometallics*, 33, 1630-1643 (DOI: 10.1021/om401200t).

29. Singh K. S., Svitlyk V., Devi P., Mozharivskyj Y. (2009), Water soluble (η^6-arene) ruthenium(II) complexes incorporating marine derived bioligand: Synthesis, spectral and structural studies, *Inorg. Chim. Acta*, 362, 5252-5258 (DOI:10.1016/j.ica.2009.09.006).

30. (a) Fabre I., Wolff N. V., Duc G. L., Flegeau E. F., Bruneau C., Dixneuf P. H., Jutand A. (2013), Autocatalytic Intermolecular versus Intramolecular Deprotonation in C-H Bond Activation of Functionalized Arenes by Ruthenium(II) or Palladium(II) Complexes, *Chem. Eur. J.*, 19, 7595-7604 (DOI: 10.1002/chem.201203813); (b) Arockiam P. B., Fischmeister C., Bruneau C., Dixneuf P. H. (2010), C-H Bond Functionalization in Water Catalyzed by Carboxylato Ruthenium(II) Systems, *Angew. Chem. Int. Ed.*, 49, 6629-6632 (DOI: 10.1002/anie.20100287); (c) Hubrich J., Himmler T., Rodefeld L., Ackermann L. (2015), Ruthenium(II)-Catalyzed C–H Arylation of Azoarenes by Carboxylate Assistance, *ACS Catal.*, 5, 4089-4093 (DOI: 10.1021/acscatal.5b00939); (d) Li J., Ackermann L. (2015), Carboxylate-assisted ruthenium(II)-catalyzed C-H activations of monodentate amides with conjugated alkenes, *Org. Chem. Front.*, 2, 1035-1039 (DOI: 10.1039/c5qo00167f).

31. Flegeau E. F., Bruneau C., Dixneuf P. H., Jutand A. (2011), Autocatalysis for C-H Bond Activation by Ruthenium(II) Complexes in Catalytic Arylation of Functional Arenes, *J. Am. Chem. Soc.*, 133, 10161-10170 (DOI: 10.1021/ja201462n).

32. Ackerman L., Vicente R., Potukuchi H. K.;, Pirovano V. (2010), Mechanistic Insight into Direct Arylations with Ruthenium(II) Carboxylate Catalysts, *Org. Lett.*, 12, 5032-5035 (DOI: 10.1021/ol102187).

33. (a) Boutadla Y., Al-Duaij O., Davies D. L., Griffith G. A., Singh K. (2009), Mechanistic Study of Acetate-Assisted C-H Activation of 2-Substituted Pyridines with $[MCl_2Cp^*]_2$ (M = Rh, Ir) and $[RuCl_2(p\text{-}cymene)]_2$, *Organometallics*, 28, 433-440 (DOI: 10.1021/om800909w); (b) Li B., Darcel C., Dixneuf P. H. (2014), Ruthenium(II)-catalysed Functionalisation of C-H Bonds via a Six-membered Cyclometallate: Monoarylation of Aryl 2-pyridyl Ketones, *ChemCatChem*, 6, 127-130 (DOI: 10.1002/cctc.201300752).

34. Ozdemir I., Demir S., Cetinkaya B., Gourlaouen C. Maseras F., Bruneau C., Dixneuf P. H. (2008), Direct Arylation of Arene C-H Bonds by Cooperative Action of NHCarbene-Ruthenium(II) Catalyst and Carbonate via Proton Abstraction Mechanism, *J. Am. Chem. Soc.*, 130, 1156-1157 (DOI: 10.1021/ja710276x).

35. Tsurugi H., Fujita S., Choi G., Yamagata T., Ito S., Miyasaka H., Mashima K. (2010), Carboxylate Ligand-Induced Intramolecular C-H Bond Activation of Iridium Complexes with N-Phenylperimidine-Based Carbene Ligands, *Organometallics*, 29, 4120-4129 (DOI: 10.1021/om100604u).

36. Frisch M. J. *et al.*, Gaussian Revision D.01, Gaussian, Inc., Wallingford CT, 2009.

37. Lee C. T., Yang W. T., Parr R. G. (1988), Development of the Colle-Salvetti correlation-energy formula into a functional of the electron density, *Phys. Rev. B*, 37, 785-789 (https://doi.org/10.1103/PhysRevB.37.785).

38. Krishnan R., Binkley J. S., Seeger R., Pople J. A. (1980), Self-consistent molecular orbital methods. XX. A basis set for correlated wave functions, *J. Chem. Phys.* 72, 650-654 (DOI: http://dx.doi.org/10.1063/1.438955).

39. McLean A. D., Chandler G. S. (1980), Contracted Gaussian basis sets for molecular calculations. I. Second row atoms, Z=11–18, *J. Chem. Phys.* 72, 5639-5648 (https://doi.org/10.1063/1.438980).

40. Hay P. J., Wadt W. R. (1985), Ab initio effective core potentials for molecular calculations. Potentials for the transition metal atoms Sc to Hg, *J. Chem. Phys.* 82, 270-283 (https://doi.org/10.1063/1.448799).

41. Hay P. J., Wadt W. R. (1985), Ab initio effective core potentials for molecular calculations. Potentials for K to Au including the outermost core orbitals, *J. Chem. Phys.*, 82, 299-310 (https://doi.org/10.1063/1.448975).

42. Cossi M., Scalmani G., Rega N., Barone V. (2002), New developments in the polarizable continuum model for quantum mechanical and classical calculations on molecules in solution, *J. Chem. Phys.*, 117, 43-54 (https://doi.org/10.1063/1.1480445).

43. Mennucci B., Tomasi J. (1997), Continuum solvation models: A new approach to the problem of solute's charge distribution and cavity boundaries, *J. Chem. Phys.*, 106, 5151-5158 (https://doi.org/10.1063/1.473558).

44. Cossi M., Barone V. Mennucci B., Tomasi J. (1998), Ab initio study of ionic solutions by a polarizable continuum dielectric model, *Chem. Phys. Lett.*, 286, 253-260 (DOI: https://doi.org/10.1016/S0009-2614(98)00106-7).

45. Grimme S., Antony J., Ehrlich S., Krieg H. (2010), A consistent and accurate ab initio parametrization of density functional dispersion correction (DFT-D) for the 94 elements H-Pu, *J. Chem. Phys.*, 132, 154104 (DOI: 10.1063/1.3382344).

46. (a) Bennett M. A., Huang T. N., Matheson T. W., Smith A. K. (1982), (η^6-Hexamethylbenzene)Ruthenium Complexes, *Inorg. Synth.*, 21, 74-78 (DOI: 10.1002/9780470132524.ch16); (b) Zelonka R. A., Baird M. C. (1972), Benzene Complexes of Ruthenium(II), *Can. J. Chem.*, 50, 3063-3072 (https://doi.org/10.1139/v72-486).

Chapter 5

Cyclopentadienyl-Ru(II)-pyridylamine complexes: Synthesis, X-ray structure and application in catalytic transformation of bio-derived furans to levulinic acid and diketones in water

5.1. Introduction

Tremendous interest towards the development of a wide range of stable cyclopentadienyl-Ru(II) ((η^5-C$_5$H$_5$)-Ru) complexes has been observed over the past five decades.[1,2] Consequently, due to the unique structural properties, stability and chemical reactivity of the (η^5-C$_5$H$_5$)-Ru(II) complexes, these complexes find application in various fields (Scheme 1), including small molecule activation, transfer hydrogenation, and in biology.[3-19] In particular context of catalysis, one of the prominent (η^5-C$_5$H$_5$)-Ru(II) based transfer hydrogenation catalyst is Shvo's catalyst, which demonstrated the involvement of both metal and the ligand to control the selectivity.[10,11] Nikonov's group also demonstrated the application of [(η^5-C$_5$H$_5$)Ru(^{i}Pr$_3$P)(NCCH$_3$)$_2$] in transfer hydrogenation of ketones, nitriles, esters and N-heterocycles.[12,13] Studies demonstrated the formation of (η^5-C$_5$H$_5$)Ru-H (ruthenium hydride) as an important intermediate species, which facilitated the transfer hydrogenation of these unsaturated groups.[14-16] Moreover, mechanistic studies by NMR also revealed the presence of a trihydride [(η^5-C$_5$H$_5$)Ru(NHC)(H)$_3$] species (NHC is a carbene ligand) as the catalyst resting stage for the transfer hydrogenation reaction.[16] Weissensteiner et al. also demonstrated the catalytic reactivity of the (η^5-C$_5$H$_5$)-Ru(II) aminophosphine (PN) complexes [(η^5-C$_5$H$_5$)Ru(κ^2-PN)CH$_3$CN]$^+$ and [(η^5-C$_5$H$_5$)Ru(κ^2-PN)Br] for the transfer hydrogenation of a wide range of ketones to secondary alcohols.[17] They proposed that the observed high catalytic activity of these (η^5-C$_5$H$_5$)-Ru(II) aminophosphine complexes was due to the reversible Ru-N bond cleavage in η^5-Cp-Ru(II) coordinated aminophosphine ligand (Scheme 1). Similarly, Pandey et al. explored (η^5-C$_5$H$_5$)-Ru(II) complexes containing pyridylphosphine ligands, such as [(η^5-C$_5$H$_5$)Ru(PyPPh$_2$)(PPh$_3$)Cl], for transfer hydrogenation of aldehydes to alcohols in the presence of HCOOH/NaOH.[18] Notably, these aminophosphine or pyridylphosphine ligands may

act as hemilabile ligands due to their reversible κ^2-κ^1-κ^2 coordination behaviour to the (η^5-C$_5$H$_5$)-Ru(II) center. These results inferred that (η^5-C$_5$H$_5$)-Ru(II) complexes represent an important class of catalyst for transfer hydrogenation reaction, but so far the application of (η^5-C$_5$H$_5$)-Ru(II) complexes in catalytic biomass transformations remains unexplored.[111]
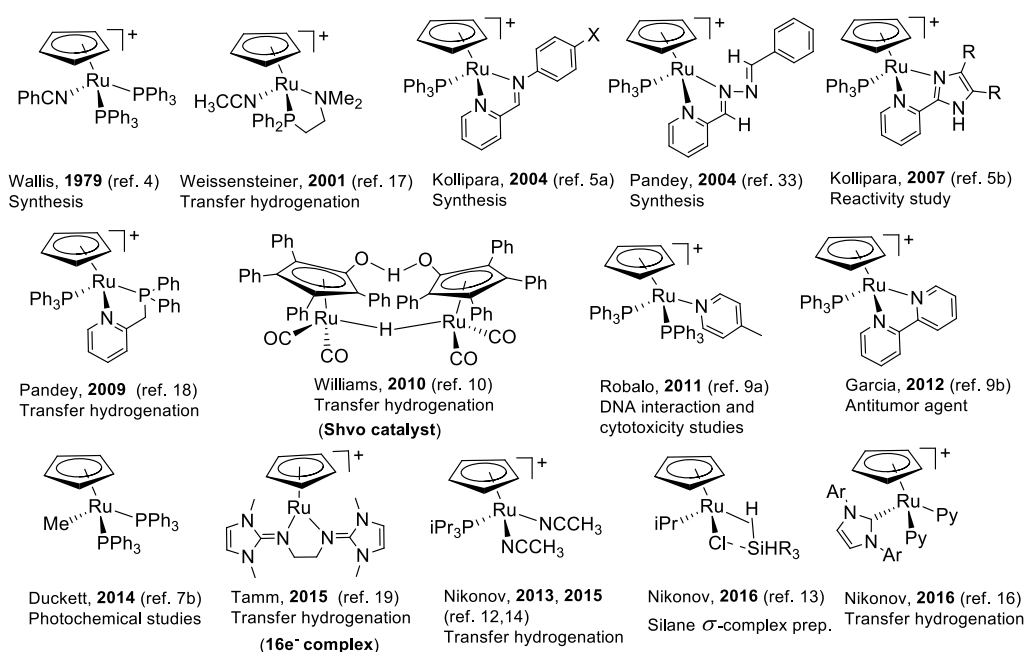
Scheme 5.1. *Literature reports on cyclopentadienyl-ruthenium based complexes.*

Catalytic transformation of biomass-derived furans and its derivatives to open ring components, such as LA and diketones, important platform precursors for the production of various fine chemicals and fuel components, have been extensively explored using various heterogeneous catalysts[19-22] These transformation were mostly carried out in the presence of catalysts based on Pt, Pd, Rh, Ru and Au metals nanoparticle or in the presence of strong acid (H$_3$PO$_4$, HCl, H$_2$SO$_4$), high temperature (120-170 °C) and high H$_2$ pressure (50-100 bar).[20-22] For instance, Montech *et al.* reported the transformation of 5-HMF to 1-HHD over Pt/C catalyst in oxalic acid at 140 °C and 30 bar H$_2$.[20] Similar 5-HMF to 1-HHD transformation was also reported over Pd/C with Amberlyst-15 under 50 bar H$_2$.[21] Analogously, transformation of furans to LA was achieved over Pd/Al$_2$O$_3$ with Amberlyst-70 at 165 °C and 70 bar H$_2$, as reported by Lie *et al.*[22] In comparison to the extensive exploration of heterogeneous catalytic system, catalyst based on transition metal based complexes

are less explored for such biomass transformations. In this direction, Zhang *et al*. reported $[(\eta^5\text{-Cp}^*)\text{Ir}(\kappa^2\text{-bpy})\text{Cl}]^+$ (where 'bpy' is bipyridine) complexes for the catalytic hydrogenolytic transformation of 5-HMF to diketones, 1-hydroxy-2,5-hexanedione (1-HHD) in water using H_2 gas (10 bar) at 120 °C.[23,24] Later, Fu *et al*. also investigated the catalytic transformation of 5-HMF to 1-HHD using formic acid/formate buffer solution at 130 °C and 30 bar H_2, over $(\eta^5\text{-Cp}^*)$-Ir complexes having hydroxyl substituted bipyridine ligands, where the hydroxyl substitutes have a promotional effect in the studied transformation.[25,26]

In recent past, we also explored several half sandwich $(\eta^6\text{-arene})\text{Ru(II)}$ complexes having nitrogen donor ligands $[(\eta^6\text{-arene})\text{Ru}(\kappa^2\text{-L})\text{Cl}]^+$ (L = ethylenediamine or 8-aminoquinoline) for the catalytic transformation of biomass-derived furans such as furfural and 5-HMF to LA and diketones (1-HHD and 3-HHD) using formic acid.[27,28] Our findings revealed that the presence of –NH groups in these complexes and presence of a labile coordinating chloro ligands facilitated an efficient transfer hydrogenation of furfural to furfuryl alcohol with the aid of formic acid. Subsequently, upon the formation of furfuryl alcohol, H^+ assisted ring opening of furfuryl alcohol led to the formation of LA and diketones. Notably, using formic acid is advantageous as it can acts as an efficient hydrogenating source as well as control the pH of the catalytic reaction and hence the selectivity of the product. Moreover, η^6-arene-ruthenium complexes usually undergo decomposition to ruthenium metal at higher temperature (>120 °C) and loss the catalytic activity.[29,30] On the other hand, the ruthenium-cyclopentadienyl based complexes displayed high stability in water, and acid at high temperature compared to η^6-arene-ruthenium complexes.[31,32] It has been hypothesized that the anionic cyclopentadienyl ligand (in ruthenium-cyclopentadienyl based complexes) bonded strongly with the Ru^{2+} centre, compared to the weakly bonded neutral η^6-arene ligand.[31,32] Moreover, it has also been suggested that due to the anionic cyclopentadienyl ligand the metal center may have higher electron density and therefore it may substantially influence the catalytic activity of the resulting $(\eta^5\text{-C}_5\text{H}_5)$-Ru(II) complexes, in comparison to the η^6-arene ligand.

Herein, we synthesized a series of half sandwich $(\eta^5\text{-C}_5\text{H}_5)$-Ru(II) complexes containing N_{amine}-substituted pyridylamine ligands, and the molecular structure of all these complexes are authenticated by X-ray crystallography. These complexes are employed for the catalytic ring opening transformation of the bio-derived furfural, 5-

HMF and other related furans to LA and diketones in water at 120 °C with the aid of formic acid. Our findings evidenced that the presence of –NH bonds, suitably balanced basicity and bulkiness at N_{amine}, and the flexible nature of the pyridylamine ligands has a remarkable effect on this catalytic transformation. Moreover, efficient direct transformation of fructose to diketone and a scaled up (gram-scale) transformation of furfural to levulinic acid are also achieved over the high performing (η^5-C$_5$H$_5$)-Ru(II)-pyridylamine catalyst.

5.2. Results and discussion

5.2.1. Synthesis and characterization of cyclopentadienyl-ruthenium(II) complexes.

Pyridylamine ligands (**L4-L9**) with N_{amine}-alkyl and benzyl substituents, 2-(aminomethyl)pyridine (**L4**), N-(pyridin-2-ylmethyl)propan-1-amine (**L5**), N-(pyridin-2-ylmethyl)propan-1-amine (**L6**), N-(pyridin-2-ylmethyl)butan-1-amine (**L7**), 3-methyl-N-(pyridin-2-ylmethyl)butan-1-amine (**L8**), N-benzyl-1-(pyridin-2-yl)methanamine (**L9**) are synthesized by direct condensation of pyridine-2-carbaldehyde with corresponding amines, and subsequent reduction of imine by NaBH$_4$ (**L5-L9**), while N-(pyridin-2-ylmethylene)propan-2-amine (**L10**) is synthesized by the condensation of pyridine-2-carbaldehyde with isopropylamine.
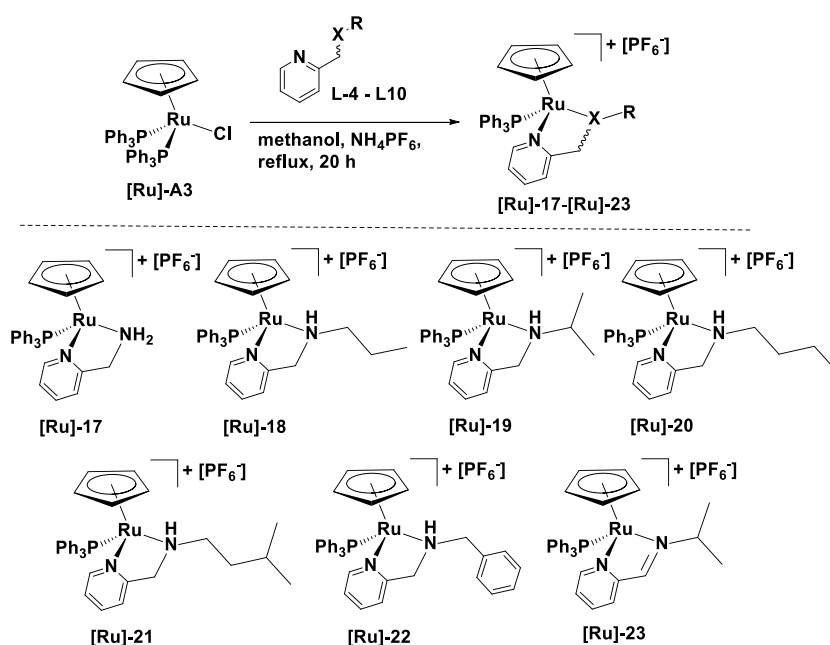
Scheme 5.2. *Synthesis of (η^5-C$_5$H$_5$)-Ru(II) complexes containing pyridylamine (**[Ru]-17** − **[Ru]-22**) and pyridylimine (**[Ru]-23**) based Ligands.*

Further, (η^5-C$_5$H$_5$)-Ru(II) precursor, [(η^5-C$_5$H$_5$)RuCl(PPh$_3$)$_2$], is treated with these N$_{amine}$-substituted pyridyamine ligands (**L4** – **L9**) in methanol under refluxed condition to afford yellow to orange coloured cationic mononuclear *piano-stool* (η^5-C$_5$H$_5$)-Ru(II) complexes **[Ru]-17** – **[Ru]-22** in good yield (Scheme 5.2). With the dissociation of a PPh$_3$ and chloro ligand, the obtained complexes **[Ru]-17** – **[Ru]-22** have a general formula of [(η^5-C$_5$H$_5$)Ru(κ^2-L)PPh$_3$]$^+$ where L = **L4**, (**[Ru]-17**), L = **L5**, (**[Ru]-18**), L = **L6**, (**[Ru]-19**), L = **L7**, (**[Ru]-20**), L = **L8**, (**[Ru]-21**), L = **L9**, (**[Ru]-22**). Analogously, N-(pyridin-2-ylmethylene)propan-2-amine (**L10**) ligand is reacted with [(η^5-C$_5$H$_5$)Ru(PPh$_3$)$_2$Cl] to afford (η^5-C$_5$H$_5$)-Ru(II)-N-isopropylpyridylimine complex, [(η^5-C$_5$H$_5$)Ru(κ^2-L10)PPh$_3$]$^+$ (**[Ru]-23**). All the complexes **[Ru]-17** – **[Ru]-23**, are highly stable in air and moisture. The spectro-analytical analyses of the synthesized complexes corroborated well with the proposed structures (see the Experimental Section).

In ^{1}H NMR of the complexes **[Ru]-17** – **[Ru]-22**, *ortho* C-H of pyridylamine resonated at 8.61-8.32 ppm compared to those of free ligand (8.50-8.29 ppm). Analogously, *ortho* C-H of complex **[Ru]-23** resonated at downfield region (9.28 ppm) as compared to free ligand **L10** (8.63 ppm). The absorbed downfield shift is consistent with the coordination of pyridylamine/pyridylimine ligands with (η^5-C$_5$H$_5$)-Ru(II) moiety.[17,18] Moreover, the observed downfield shift in the resonance of aromatic C-H proton of PPh$_3$ in the ^{1}H NMR region of 7.49-6.94 ppm along with the appearance of a sharp singlet in the ^{31}P NMR (55.33-53.17 ppm in **[Ru]-17** - **[Ru]-22** and 48.18 ppm in **[Ru]-23**) is in accordance with the coordination of PPh$_3$ to (η^5-C$_5$H$_5$)-Ru(II).[17,18,33-35] Moreover, the Ru(II) coordinated η^5-Cp proton resonated as a sharp singlet in the range of 4.80-4.30 ppm. Further the counter anion PF$_6$ resonated at ~ -144 ppm in ^{31}P NMR for these complexes.[18] ESI-MS analysis revealed the presence of mass (m/z) peaks corresponding to the expected molecular ion, {(η^5-C$_5$H$_5$)Ru(κ^2-L)PPh$_3$}$^+$ ([M]$^+$), with the characteristic ruthenium isotopic pattern. IR spectra of the complexes **[Ru]-17 - [Ru]-22** exhibited characteristic bands due to νN-H band at around 3360~3260 cm^{-1}, suggesting the presence of −N-H bonds. The νC-N band in these complexes shifted towards lower wave number and appeared around 1100-1050 cm^{-1} as compared to that for the corresponding free ligand. Analogously, the iminic νC=N band appeared at 1601 cm^{-1} for complex **[Ru]-23**, compared to that for the free imine ligand (**L10**) (νC=N 1690 cm^{-1}). Moreover,

vC=N$_{py}$ band for the complexes **[Ru]-17 - [Ru]-23** observed in the region of 1450-1430 cm^{-1} (vC=N$_{py}$ for free ligand appeared at 1591cm^{-1}). The observed shift in the position of vC=N$_{py}$, vC=N$_{imine}$, vC–N$_{amine}$ relative to the free ligands could be attributed to the involvement of these entities in the coordination of ligands to the (η^5-C$_5$H$_5$)-Ru(II). Strong bands observed in the region of 832 and 557 cm^{-1} are assigned for the counter anion PF$_6^-$. Electronic spectra of the (η^5-C$_5$H$_5$)-Ru(II)-pyridylamine complexes **[Ru]-17 - [Ru]-22** recorded in dichloromethane with concentration (4×10^{-3} mol/L), showed bands in the region of 369-363, 330-327 and 275-266 nm. The moderately intense bands in the range of 330-326 nm are assigned to MLCT transition. In addition to the band at 337 nm, complex **[Ru]-23** also showed a low intensity band at low energy region (436 nm), which can also be attributed to MLCT band. The hump in the region 349-363 nm is assigned to (η^5-C$_5$H$_5$)-Ru(II) MLCT transitions. The high intensity bands in the region of 250-270 nm are ascribed for the intra-ligand transitions (Figure 5.1). The thermogravimetric analysis of the complexes **[Ru]-17 − [Ru]-23** inferred that these complexes are stable up to ~200 $^\circ$C, with first major weight loss of 58% occurred at around 250 $^\circ$C, attributed to the loss of the PPh$_3$ and bidentate N,N-ligand (Figure 5.2).
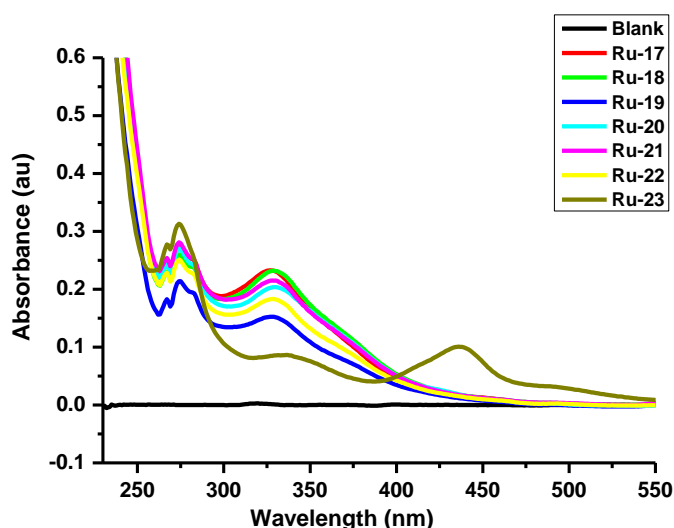
Figure 5.1. *UV-Vis. Spectral data for (η^5-C$_5$H$_5$)-Ru(II) complex **[Ru]-17 − [Ru]-23**.*
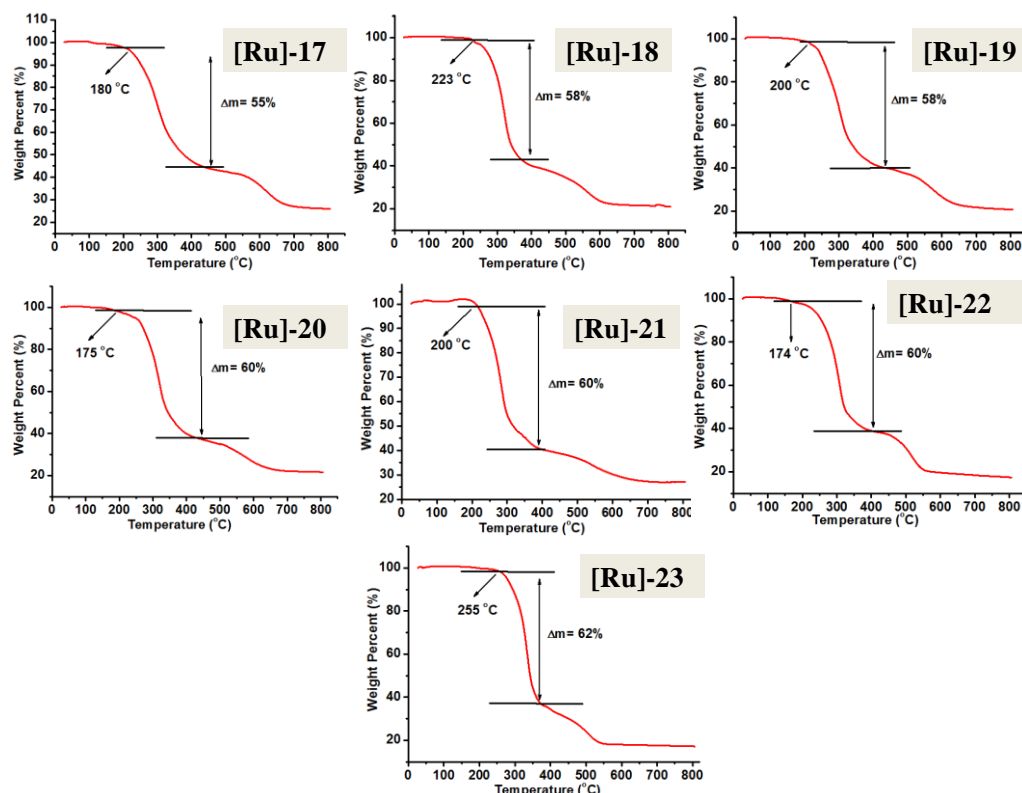
Figure 5.2. *TGA spectra of (η^5-C$_5$H$_5$)-Ru(II) complexes* ***[Ru]-17 − [Ru]-23***.

Further, molecular structures of all the complexes **[Ru]-17 − [Ru]-23** are authenticated by X-ray crystallography (Figure 5.3-5.4 and Table 5.1). The important bond parameters are shown in Table 5.2. The complexes **[Ru]-17**, **[Ru]-20**, **[Ru]-22**, **[Ru]-23** crystallised in monoclinic crystal system with *P21/n* space group (*I2/a* space group for **[Ru]-4**), while complexes **[Ru]-18** and **[Ru]-19** are in triclinic crystal system with space group *P-1*. All the complexes **[Ru]-17 − [Ru]-23** adopted a typical three legged *piano-stool* geometry around the Ru(II) center. In this *piano-stool* arrangement the κ^2 pyridylamine/pyridylimine and PPh$_3$ ligands occupied three legs of the stool and the η^5-Cp ring is placed at the apex of the stool. For η^5-Cp-Ru(II) moiety, the average Ru-C distances are in the range of 2.157~2.203 Å, whereas Ru to η^5-Cp centroid distance are in the range of 1.817~1.877 Å.[5,17,18,34,35] The Ru-P distances are observed in the range of 2.300~2.345 Å, which is in accordance to the Ru-P distances reported for other related systems.[5,17,18,34,35] The Ru-N$_{py}$ bonds (2.114-2.064 Å), as well as Ru-N$_{imine}$ bond (2.055 Å in **[Ru]-23**), are slightly shorter than the Ru-N$_{amine}$ bonds (2.198-2.144 Å).[5,17,18,33] In the complexes **[Ru]-17 − [Ru]-23**, the N$_{py}$-Ru-N$_{amine/imine}$ angles are in the range of 75.5º-77.6º,

157

suggesting the inward bending of the coordinated pyridylamine/pyridylimine groups. In contrary, $N_{py/amine/imine}$-Ru-P angle of *ca.* 94° inferred the away placement of bulky PPh_3 in the Ru(II) coordination sphere. The η^5-Cp_{ct}-Ru-P/N angle of *ca.* 125° is consistent with the *piano-stool* geometry of the η^5-Cp-Ru(II)-pyridylamine/imine complexes.
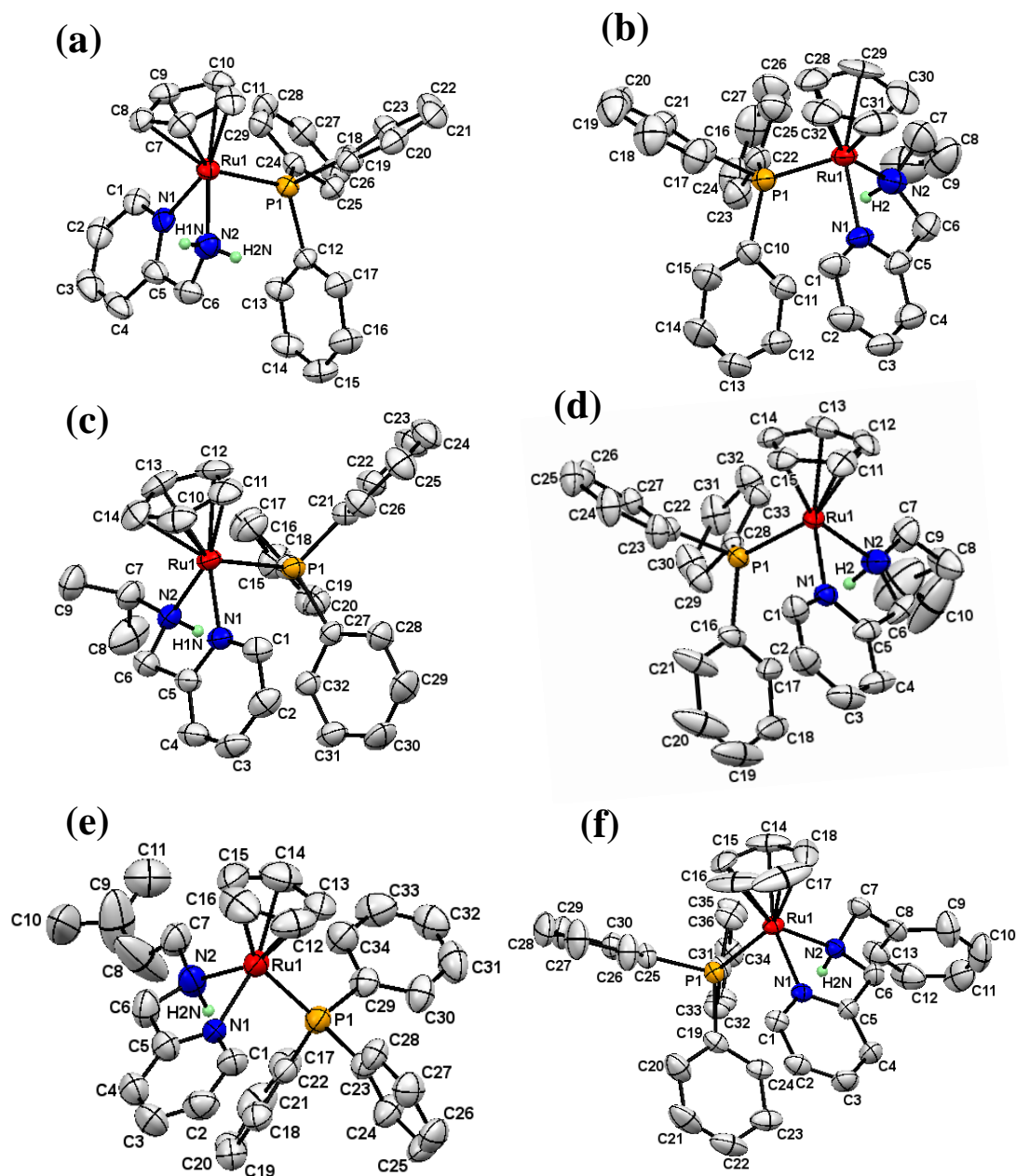
Figure 5.3. *Single crystal X-ray structure of complexes (a) **[Ru]-17**, (b) **[Ru]-18**, (c) **[Ru]-19**, (d) **[Ru]-20**, (e) **[Ru]-21** and (f) **[Ru]-22**, with 30% probability of thermal ellipsoids. Anionic counterpart (PF_6) and hydrogen atoms, except for the amine nitrogen, are omitted for the sake of clarity.*
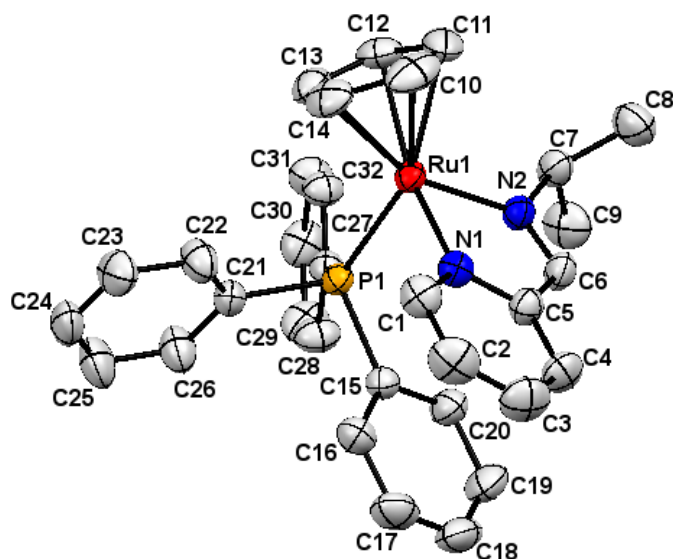
Figure 5.4. *Single crystal X-ray structure of complex **[Ru]-23** with 30% probability of thermal ellipsoids. Anionic counterpart (PF$_6$) and hydrogen atoms are omitted for the sake of clarity.*

Summation of all the angles around N_{imine} is 359.67° for the complex **[Ru]-23**, is in agreement with the planar iminic N_{imine}, which is also well supported by the lowest torsion angle (-3.0(4)°) around N_{imine}. Notably, the iminic C=N is shorter (1.282 Å) in **[Ru]-23** than the C-N_{amine} bonds (1.440 ~ 1.488 Å) in complexes **[Ru]-17 – [Ru]-22**.

Table 5.1. *Crystal data and structure refinement details for **[Ru]-17 − [Ru]-23***

Crystal parameters	[Ru]-17	[Ru]-18	[Ru]-19	[Ru]-20	[Ru]-21	[Ru]-22	[Ru]-23
empirical formula	$C_{29}H_{28}F_6N_2P_2Ru$	$C_{32}H_{34}F_6N_2P_2Ru$	$C_{32}H_{34}F_6N_2P_2Ru$	$C_{33}H_{35}F_6N_2P_2Ru$	$C_{68}H_{76}F_{12}N_4P_4Ru_2$	$C_{36}H_{34}F_6N_2P_2Ru$	$C_{32}H_{32}F_6N_2P_2Ru$
Fw	681.54	723.62	723.62	736.64	1503.34	771.66	721.60
T (K)	293(2)	293(2)	293(2)	293(2)	293(2)	293(2)	293(2)
λ (Å)	0.71073	1.54184	0.71073	1.54184	0.71073	0.71073	0.71073
crystal system	Monoclinic	Triclinic	Triclinic	Monoclinic	Triclinic	Monoclinic	Monoclinic
space group	*P 21/c*	*P -1*	*P -1*	*I 2/a*	*P -1*	*P 21/n*	*P 21/c*
crystal size, mm $(l \times k \times h)$	0.23×0.16×0.11	0.33 x 0.26 x 0.18	0.23 x 0.18 x 0.13	0.33 x 0.26 x 0.21	0.24 x 0.19 x 0.13	0.19 x 0.16 x 0.12	0.19 x 0.13 x 0.10
a, Å	8.2076(3)	9.7692(5)	9.8166(5)	21.1141(4)	13.2061(8)	11.2831(2)	9.7656(2)
b, Å	17.4015(6)	10.9629(4)	10.7718(6)	9.7185(2)	14.3801(8)	16.6360(3)	19.6486(3)
c, Å	19.0812(6)	16.8216(6)	16.7537(8)	32.6092(8)	18.3572(9)	19.5789(4)	16.4536(3)
α, deg	90	74.993(3)	75.303(4)	90	76.541(4)	90	90
β, deg	94.399(3)	84.403(4)	83.477(4)	99.930(2)	87.245(4)	104.828(2)	100.074(2)
γ, deg	90	65.684(5)	65.615(5)	90	89.641(5)	90	90
V, Å^3	2717.23(16)	1585.67(13)	1560.67(15)	6591.1(2)	3386.4(3)	3552.68(12)	3108.45(10)
Z	4	2	2	8	2	4	4
ρ_{calcd}, g cm^{-3}	1.666	1.516	1.540	1.485	1.474	1.443	1.542

μ, mm^{-1}	0.759	5.486	0.666	5.290	0.617	0.590	0.669
F(000)	1376	736	736	3000	1536	1568	1464
θ range, deg	3.020-28.822	4.714 -71.298	2.901 to 28.813	4.252-71.326	2.982 -29.123	3.101 -29.128	2.964 -28.814
Limiting indices	-11<=h<=10, -23<=k<=23, -24<=l<=25	-11<=h<=11, -13<=k<=9, -20<=l<=17	-10<=h<=13, -14<=k<=13, -22<=l<=19	-25<=h<=19, -10<=k<=11, -39<=l<=39	-17<=h<=16, -19<=k<=18, -24<=l<=23	-13<=h<=15, -20<=k<=22, -26<=l<=25	-13<=h<=12, -23<=k<=26, -20<=l<=21
completeness to θ_{max}	99.8 %	99.1 %	99.8 %	100.0 %	99.8 %	99.8 %	99.8 %
Refinement method	Full-matrix least-squares on F^2	Full-matrix least-squares on F^2	Full-matrix least-squares on F^2	Full-matrix least-squares on F^2	Full-matrix least-squares on F^2	Full-matrix least-squares on F^2	Full-matrix least-squares on F^2
no. of data collected/unique data	24100/6443 [R(int)= 0.0715]	10073/5962 [R(int) = 0.0389]	14619/7124 [R(int) = 0.0284]	22414/6348 [R(int) = 0.0463]	33624/15677 [R(int) = 0.0674]	34313/8518 [R(int) = 0.0324]	24722/7347 [R(int) = 0.0310]
params/restraints	369/0	388/0	394/1	397/0	812/0	428/0	338/0
goodness of fit on F^2	1.077	1.050	1.058	1.086	1.119	1.047	1.035
Final R indices [$I > 2\sigma(I)$]	R1= 0.0635 wR2= 0.1570	R1 = 0.0572, wR2 = 0.1607	R1 = 0.0353, wR2 = 0.0940	R1 = 0.0657, wR2 = 0.1753	R1 = 0.1126, wR2 = 0.2776	R1 = 0.0431, wR2 = 0.1086	R1 = 0.0416, wR2 = 0.1076
R indices (all data)	R1= 0.0350 wR2= 0.1647	R1 = 0.0578, wR2 = 0.1615	R1 = 0.0390, wR2 = 0.0978	R1 = 0.0679, wR2 = 0.1775	R1 = 0.1666, wR2 = 0.3436	R1 = 0.0522, wR2 = 0.1163	R1 = 0.0473, wR2 = 0.1128
Largest diff. peak and hole, eÅ^{-3}	1.910 and -1.723	0.925 and -1.440	0.600 and -0.530	2.548 and -0.616	3.731 and -2.078	0.975 and -0.694	0.847 and -0.927

Table 5.2. *Important bond lengths (Å), bond angles (º) and torsion angle (º) for complexes **[Ru]-17 − [Ru]-23***

Bond lengths (Å)	[Ru]-17	[Ru]-18	[Ru]-19	[Ru]-20	[Ru]-21	[Ru]-22	[Ru]-23
$Ru-C_t$	1.877	1.826	1.829	1.817	1.833	1.829	1.852
$Ru-C_{avg.}$	2.191	2.176	2.182	2.170	2.181	2.151	2.203
$Ru-N_{py}$	2.114(4)	2.104(3)	2.0936(19)	2.096(5)	2.064(6)	2.105(2)	2.097(2)
$Ru-N_{amine/imine}$	2.163(4)	2.175(4)	2.198(2)	2.144(5)	2.167(6)	2.185(2)	2.055(2)
$Ru-P$	2.3005(11)	2.3144(9)	2.3293(6)	2.3094(13)	2.3205(19)	2.3151(7)	2.3452(7)
$N_{amine/imine}-C_6$	1.475(6)	1.474(6)	1.485(3)	1.440(9)	1.458(11)	1.488(4)	1.282(4)
$N_{amine/imine}-C7$	-	1.481(7)	1.523(3)	1.391(9)	1.473(10)	1.504(3)	1.504(4)
Bond angles (º)							
$N_{py}-Ru-N_{amine/imine}$	77.06(16)	77.64(14)	76.60(8)	77.6(2)	75.5(2)	77.13(9)	76.29(9)
$N_{py}-Ru-P$	93.16(10)	90.15(9)	90.79(5)	91.22(12)	92.61(16)	90.81(6)	88.08(6)
$N_{amine/imine}-Ru-P$	94.46(13)	92.66(11)	90.13(6)	92.9(2)	90.8(2)	91.39(7)	90.74(7)
$N_{py}-Ru-C_t$	127.65	128.12	127.94	127.15	128.99	126.87	130.28
$N_{amine/imine}-Ru-C_t$	124.94	127.93	130.66	127.97	128.60	128.57	128.09
$P-Ru-C_t$	125.98	125.94	125.60	125.89	125.40	127.08	127.30
Torsion angle (º)							
$N_{py}-C_5-C_6-N_{amine/imine}$	23.6(6)	-25.6(6)	32.6(3)	-15.3(9)	25.92	-30.2(4)	-3.0(4)

5.2.2 Catalytic transformation of furan derivatives to levulinic acid and diketones in water. Catalytic efficacy of the synthesized η^5-Cp-Ru(II) pyridylamine complexes **[Ru]-17** – **[Ru]-22** along with η^5-Cp-Ru(II) pyridylimine complex **[Ru]-23** for the transformation of biomass-derived furans was evaluated using furfural (**1a**) as the model substrate (as shown in Table 5.3) at 120 °C in the presence of 12 equiv. of formic acid in water.

Table 5.3. *Catalytic activity of cyclopentadienyl-ruthenium(II) complexes for transformation of furfural (**1a**) to levulinic acid (**2a**)[a]*
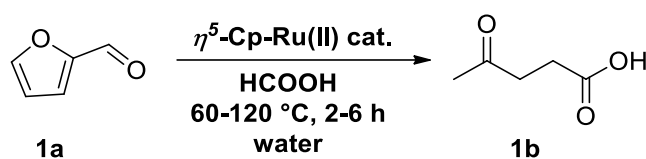
Entry	Catalyst	Temp. (°C)	Time (h)	HCOOH (mmol)	Yield (%)[b]
1	**[Ru]-17**	120	6	12	70
2	**[Ru]-18**	120	6	12	84
3[c]	**[Ru]-18**	120	2, 4	12	35, 51
4[d]	**[Ru]-18**	60, 80, 100	6	12	0, 1, 21
5[e]	**[Ru]-18**	120	6	3, 6	50, 55
3	**[Ru]-19**	120	6	12	72
4	**[Ru]-20**	120	6	12	74
5	**[Ru]-21**	120	6	12	76
6	**[Ru]-22**	120	6	12	78
7	**[Ru]-23**	120	6	12	48
8	**[Ru]-A3**	120	6	12	45

[a]Reaction conditions: Furfural (1.0 mmol), formic acid (12 equiv.), ruthenium catalyst (5 mol%), water (10 mL), [b]yield with respect to the internal standard, [c]effect of reaction time, [d]effect of reaction temperature, [e]effect of formic acid concentration.

As elaborated in table 3, complex **[Ru]-17** containing (2-pyridylmethyl)amine (**L4**) exhibited 70% yield of LA (**2a**) in 6 h (Table 5.3, entry 1). Yield of LA (**2a**) was further enhanced to 84%, when N_{amine}-*n*-propyl substituted pyridylamine (**L5**) coordinated η^5-Cp-Ru(II) complex (**[Ru]-18**) was employed (Table 5.3, entry 2). However, using η^5-Cp-Ru(II) containing various other N_{amine}-substituted pyridylamine ligands, (N_{amine}-*iso*-propyl **[Ru]-19**, N_{amine}-*n*-butyl **[Ru]-20**, N_{amine}-*iso*-pentyl **[Ru]-21** and N_{amine}-benzyl **[Ru]-22**),

yield of LA (72-78%) could not be further enhanced (Table 5.3, entries 3-6). In contrary to the high catalytic activity of η^5-Cp-Ru(II) pyridylamine complexes, **[Ru]-23** having a rigid pyridylimine ligand displayed only 48% yield of LA under analogous reaction condition (Table 5.3, entry 7). Notably, the precursor $[(\eta^5\text{-}C_5H_5)Ru(PPh_3)_2Cl]$ also exhibited poor yield of LA (Table 5.3, entry 8).). The lower catalytic activity of complex **[Ru]-17** can be attributed to the poor availability of N_{amine}, presumably due to the involvement of N_{amine} in strong interactions with solvent water molecules. Further it should be noted that with the increase in alkyl carbon chain or branching, polarizability of N_{amine} also increases.[36] However, the increase in alkyl chain may also increase the steric hindrance at the nitrogen centre (N_{amine}), which may lead to the decrease in the basicity of nitrogen.[36] Further the remarkable enhancement in the catalytic efficacy of η^5-Cp-Ru(II) pyridylamine complexes **[Ru]-17 - [Ru]-22** (70-84% yield of LA) compared to η^5-Cp-Ru(II) pyridylimine complex **[Ru]-7** (45% yield of LA), clearly evidenced the crucial importance of the flexible pyridylamine ligands over the rigid pyridylimine ligand (Figure 5.5).[17,18,37]
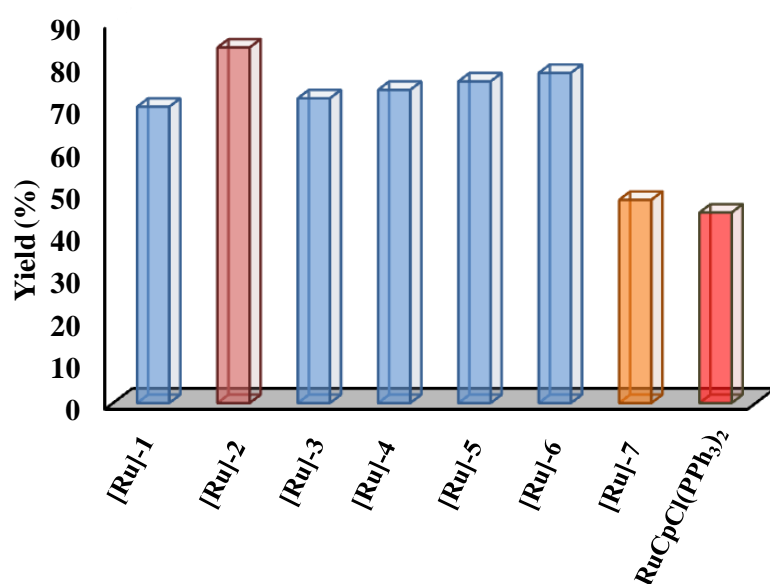
Figure 5.5. *Catalytic transformation of furfural to LA by η^5-Cp-Ru(II) complexes in water. Reaction conditions: Furfural (1.0 mmol), ruthenium catalyst (5 mol%), formic acid (12 equiv.) and water (10 mL) at 120 °C for 6 h.*

In this context, preceding studies suggested that pyridylphosphine and aminophosphine based hemilabile ligands may show flexible coordination behaviour, which consequently create a vacant coordination site at the metal centre.[17,18,37] Comparing the catalytic behaviour of various aminophosphine ligands, Weissensteiner *et*

al. demonstrated that the flexible *N,N*-dimethyl-diphenylphosphinoethylamine (PN) exhibited the highest catalytic activity for the transfer hydrogenation of ketone to secondary alcohol in compare to the rigid *N,N*-dimethyl-2-diphenylphosphinoaniline (DBD) and 2-{1-(*N,N*-dimethylamino)-ethyl}-1-diphenyl phosphinoferrocene (PPFA).[17] A similar dissociation and recoordination of amine group by the flexible pyridylamine was also observed for a Pd-pyridylamine complex catalyzed copolymerization of ethylene and norbornene.[37] Hence based on the aforementioned finding, a similar behaviour can also be expected for the pyridylamine ligands in the studies complexes **[Ru]-17 – [Ru]-22**, where pyridylamine may presumably undergoes a reversible κ^2 - κ^1 - κ^2 coordination/decoordination inter-conversion to have pyridyl group remains coordinated with the ruthenium and the amine branch is pendent.[37] This will create a new vacant site for the coordination of formate and subsequently form Ru-H species to further facilitate the transfer hydrogenation of furfural to furfuryl alcohol. Further, the furfuryl alcohol undergoes an acid assisted ring opening to LA (Scheme 5.3).
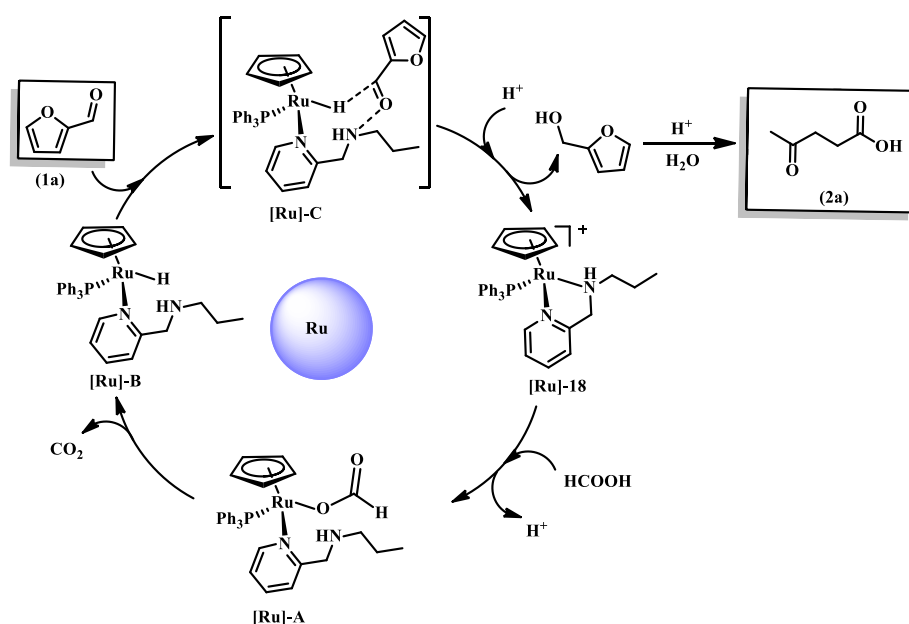
Scheme 5.3. *Plausible catalytic pathway for the **[Ru]-18** catalyzed transformation of furfural to levulinic acid.*

Further, the steric crowding at the N_{amine} centre of the complexes **[Ru]-18 – [Ru]-21** was estimated by comparing the $N \cdots C_n$ and $N\text{-}H \cdots C_n$ distances (where C_n is the farthest carbon of the alkyl chain and 'n' ($n \geq 2$) represents the position of carbon from the N_{amine}) obtained from their single crystal X-ray structures (Table 5.4). Results inferred that the

methyl groups of *iso*-propyl chain are placed very close to the N_{amine} ($N\cdots C_2$ 2.499 Å) in **[Ru]-19** compared to that in **[Ru]-18** ($N\cdots C_2$ 2.529 Å and $N\cdots C_3$ 3.251 Å), suggesting more crowding at N_{amine} in the complex **[Ru]-19**. Further, it was observed that $N\cdots C_2$ distance in complex **[Ru]-18** is comparable and even more than the other complexes **[Ru]-20** and **[Ru]-21**, having bulky long carbon chains at N_{amine}, suggesting the least steric crowding at N_{amine} in complex **[Ru]-18**. Moreover, the $N\text{-}H\cdots C_n$ distances are also in good agreement with the observed trend in $N\cdots C_n$ distances (Table 5.4). Interesting to note that the $N\cdots C_3$ (3.251 Å) and $N\text{-}H\cdots C_3$ (2.873 Å) distances in complex **[Ru]-18** are quite longer than those in the complex **[Ru]-20**, clearly showing the relatively less steric crowding at N_{amine} of complex **[Ru]-18**.

Table 5.4. Comparison of $N_{amine}\text{-}H\cdots C$ and $N\cdots C$ distances in complexes [Ru]-18 – [Ru]-22

NH⋯C distances (Å)			
	C2	**C3**	**C4**
[Ru]-18	2.608	2.873	
[Ru]-19	2.468		
[Ru]-20	2.696	2.808	4.076
[Ru]-21	2.736	2.821	4.644
N⋯C distances			
[Ru]-18	2.529	3.251	
[Ru]-19	2.499		
[Ru]-20	2.551	3.201	4.427
[Ru]-21	2.561	3.161	4.480
NH⋯$C_t^{(Ph)}$ and N⋯$C_t^{(Ph)}$ distance in [Ru]-22			
NH⋯$C_t^{(Ph)}$	3.592		
N⋯$C_t^{(Ph)}$	3.719		

Moreover, we also observed that the long *iso*-pentyl substituent at N_{amine} of complex **[Ru]-21** can fold back and hence, may cause steric crowding at N_{amine} (Figure 5.6). Therefore, the basicity and the steric crowding at N_{amine} is also expected to play a crucial role in tuning the catalytic activity of the studied η^5-Cp-Ru(II) complexes for the transformation of furfural (**1a**) to LA (**2a**).[36]

Bond length of -N....C			
	C2	C3	C4
Ru1	2.481	3.845	4.681
Ru2	2.561	3.161	3.722
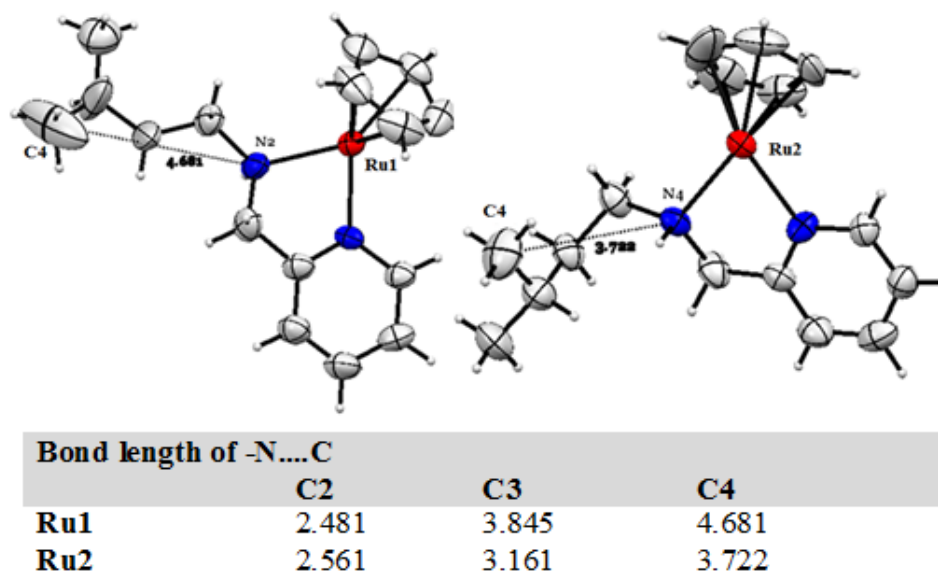
Figure 5.6. *Bending behaviour of iso-pentyl group of **L8** in **[Ru]-21** complex.*

Now, the high performing **[Ru]-18** catalysts was used for further optimization of the catalytic reaction condition for the transformation of furfural (**1a**) to LA (**2a**). Performing the reaction at a lower temperature (60–100 °C) resulted in a sharp decrease in the yield of LA (**2a**) (Figure 5.7a).

(a)

(b)
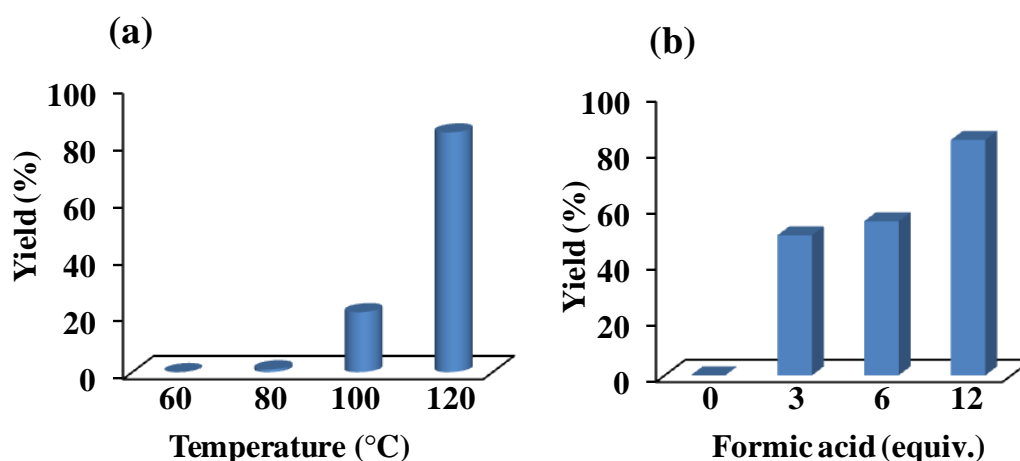
Figure 5.7. *(a) Effect of reaction temperature, (b) Effect of formic acid concentration on the catalytic transformation of furfural to levulinic acid over **[Ru]-18** catalyst.*

Moreover, decreasing the amount of formic acid to 3 or 6 equiv. was also found to have a detrimental effect on the yield of LA (**2a**) (Figure 5.7b). It should be noted that either in the presence of catalyst alone (without formic acid) or catalyst with H_2 gas or without catalyst only with formic acid (12 equiv.), the reaction could not proceed,

suggesting the presence of formic acid and the catalyst together is essential to achieve an efficient transformation of furfural (**1a**) to LA (**2a**). Time-dependent reaction progress monitored in 2, 4 and 6 h displayed a gradual increase in the yield of LA (**2a**) from 35% (2 h) to 84% (6 h) (Table 5.3 Entry 5.3). Therefore, efficiency of complex **[Ru]-18** was also further investigated for the catalytic transformation of other furan derivatives, 5-HMF (**1b**) and 5-MF (**1c**) under the optimized reaction conditions (catalyst 5 mol%, formic acid 12 equiv., at 120 $^\circ$C, 6 h in water). Unlike furfural (**1a**), only 66% conversion of 5-HMF (**1b**) was achieved in 6 h, while increasing the reaction time to 12 h, 96% conversion of 5-HMF (**1b**) to open ring products, 1-HHD (**2b**) with 69% selectivity (yield 42%) along with LA (**2a**) and 3-HHD (**2c**) (Scheme 5.4b). Formation of 1-HHD (**2b**) as the major open-ring product from 5-HMF (**1b**) was also reported earlier with other catalytic systems such as Pd/C, Cp*Ir or η^6-arene-Ru(II) complex.[21,23,27,28] Interestingly, reaction with 5-MF (**1c**) resulted in the formation of 3-HHD (**2c**, sel. 84%) and 2,5-HD (**2d**, sel. 16%) (Scheme 5.4c). Formation of 3-HHD (**2c**) as a major product over 2,5-HD (**2d**) was presumably due to the higher preference toward hydration over hydrogenation of the intermediate hex-3-ene-2,5-diene (HED).

Encouraged by the above results, catalytic transformation of fructose over **[Ru]-18** catalyst at 120 $^\circ$C with 12 equiv. of formic acid was also performed, which led to the formation of 1-HHD (**2b**), LA (**2a**), 2,5-HD (**2d**) and 5-HMF (**1b**) in 65%, 13%, 13% and 9% selectivity, respectively in 6 h (Scheme 5.4d). Formation of 5-HMF (**2a**) and 1-HHD (**2b**) products from fructose is consistent with the previous reports, suggesting that this transformation proceeded through the formation of platform dehydrogenated precursor 5-HMF (**1b**), which subsequently transformed to 1-HHD (**2b**).[38]
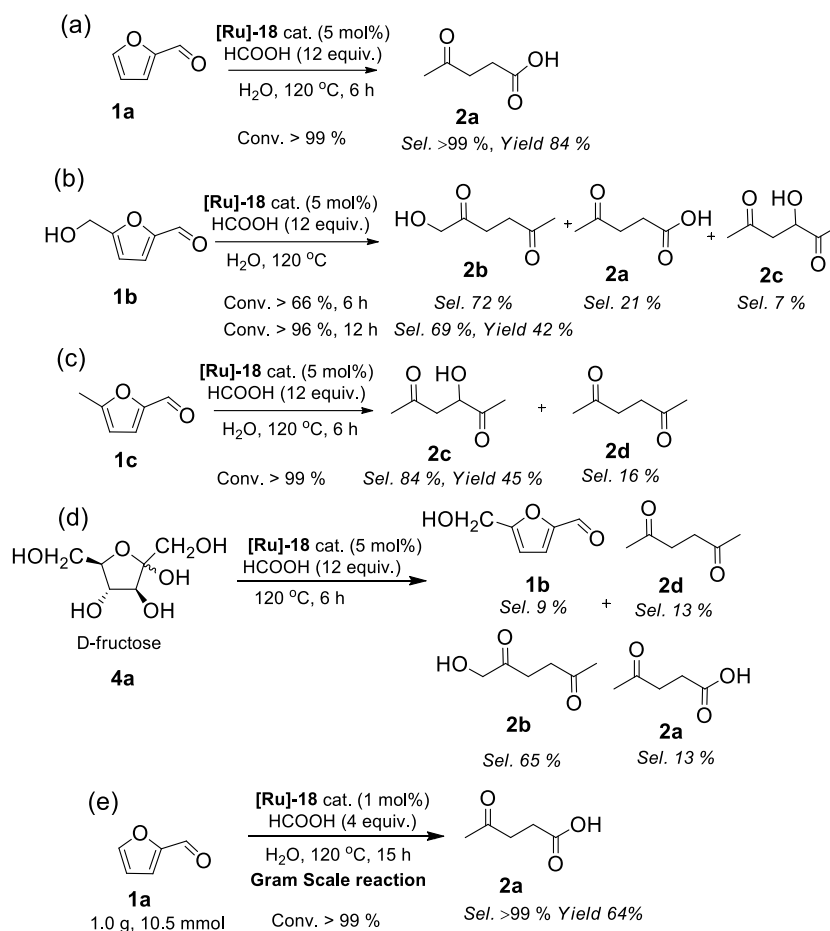
Scheme 5.4. *Catalytic transformation of different bio-derived furans over* ***[Ru]-18*** *catalyst.* [a]*determined by* [1]*H NMR with respect to the internal standard (p-anisaldehyde),* [b]*determined by column chromatography (ethylacetate/hexane 2/98 – 10/90 v/v).*

Notably, the recovered catalyst **[Ru]-18** (5 mol%) showed high stability, and could be recycled for four consecutive catalytic runs for the transformation of furfural (**1a**) to LA (**2a**), where 60% yield of LA (**2a**) was achieved even after the 4th catalytic run (TON for 1st catalytic run 16.8 and TTN 58.4) (Figure 5.8). Experiments performed in the presence of Hg metal showed no significant change in catalytic activity of **[Ru]-18** for furfural (**1a**) to LA (**2a**) transformation, suggesting that the active catalytic species is of homogeneous in nature.[39] To further explore the practical applicability of this catalytic methodology, a gram scale experiment was also carried out for the catalytic transformation of furfural over **[Ru]-18** catalyst (1 mol%), and we achieved 64% yield of LA (**2a**) (TON 64.0) (Scheme 5.4e).
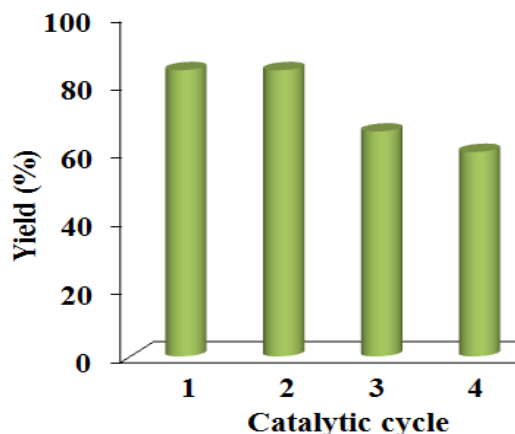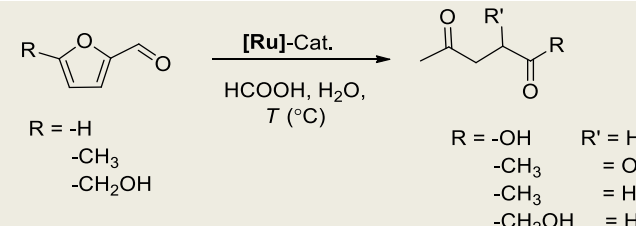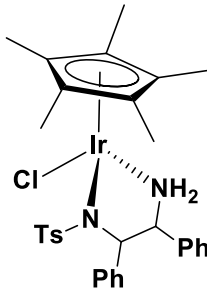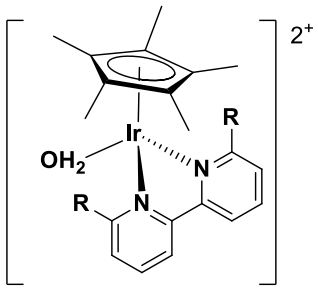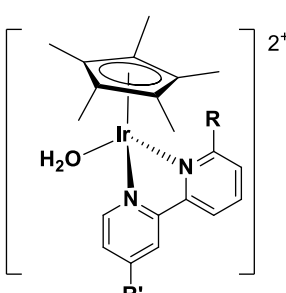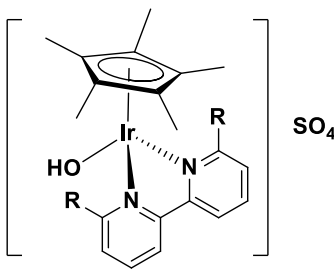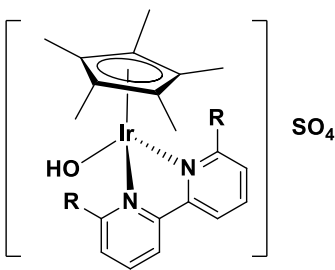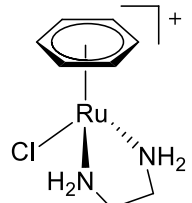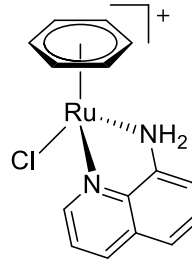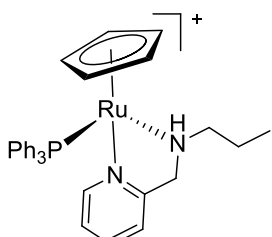
Figure 5.8. Recyclability of [Ru]-18 catalyst for the catalytic transformation of furfural (1a) to LA (2a) in the presence of formic acid (12 equiv.) in water at 120 °C for 6 h.

Therefore, the above findings clearly evidenced the high stability of the **[Ru]-18** catalyst at high temperature (>120 °C) in water and in the presence of acid (formic acid). Moreover, as inferred from the Hg poisoning experiments, no decomposition of **[Ru]-18** catalysts to Ru nanoparticles was observed under the catalytic reaction conditions (>120 °C in water). The observed high stability of **[Ru]-18** catalysts can be attributed to the strong coordination of η^5-Cp to the Ru-center, while η^6-arene-Ru(II) complexes decompose to Ru nanoparticle at higher temperature.[29,30] Moreover, the high aqueous and thermal stability of the studied η^5-Cp-Ru(II)-pyridylamine complexes is also reflected in its two fold higher catalytic activity (84% yield of LA, 6 h, 120 °C, 12 mmol HCOOH) over the analogous η^6-arene-Ru(II) (42% yield of LA, 8 h, 100 °C, 12 mmol HCOOH).[27] Notably, previously explored catalyst based on η^5-Cp*-Ir complex or other metal nanoparticle catalysts (Pd/Al$_2$O$_3$ or Au/Nb$_2$O$_5$) required high H$_2$ gas pressure (5~80 bar) and higher temperature (120~170 °C) for analogous catalytic transformations (Table 5.5).[19-26] Therefore, the studied η^5-Cp-Ru(II)-pyridylamine complexes represent a class of highly active catalyst with high thermal and aqueous stability, showing catalytic activity higher or as par with previously reported catalytic system.

Table 5.5. *Comparative table of previous literature work and this work*

S/N	Catalyst	Temp. (°C)	Yield (%)		H-source	Ref.
1		150	71 (Fructose to BHMF(2,5-bis(hydroxymethyl)) furan)		HCOOH	Ref. 38e
		40	94 (HMF to BHMF)			
2		120	84.1 (1-HHD)		H₂ gas (5 bar)	Ref. 23
3		120	>99 (conversion)		H₂ gas (10 bar)	Ref. 24
4		130	98 (1-HHD)		H₂ gas (10 bar)	Ref. 25

5		130	41 (LA)	H₂ gas (30 bar)	Ref. 26
6		80	42 (LA)	HCOOH	Ref. 27
7		80	47 (LA)	HCOOH	Ref. 28
9	Pd/C and Amberlyst-15	80	65 (1-HHD)	H₂ gas (50 bar)	Ref. 21
10	Amberlyst 70 (acid catalyst) Pd/C (hydrogenation catalyst)	170	11 (LA) 55 (polymerization product) 50 (LA)	H₂ gas (70 bar)	Ref. 22a
11	Pd/Al₂O₃	165	3.4 (LA) 21.6 (Methyl levulinate (MLE))	H₂ gas (70 bar)	Ref. 22b
13		**120**	**84 (LA)**	**HCOOH**	*This work*

5.3. Conclusions

In summary, we synthesized and characterised (by ^{1}H, ^{13}C, ^{31}P, NMR, and mass) a series of cationic η^5-Cp-Ru(II)-pyridylamine (**[Ru]-17** − **[Ru]-22**) and η^5-Cp-Ru-pyridylimine (**[Ru]-23**) complexes and authentication of molecular structure of all the complexes by X-ray crystallography. The synthesized η^5-Cp-Ru-pyridylamine complexes displayed remarkably high catalytic activity for the transformation of biomass-derived furans, furfural (**1a**), 5-HMF (**1b**) and 5-MF (**1c**), to value added open ring products, LA (**2a**) and diketones (1-HHD (**2b**), 3-HHD (**2c**) and 2,5-HD (**2d**)) with high conversion (>99%) and selectivity at 120 $^\circ$C in the presence of formic acid. Experimental findings demonstrated that the η^5-Cp-Ru-pyridylamine complexes exhibited higher catalytic performance over analogous η^5-Cp-Ru-pyridylimine complex, which can be attributed to the hemilabile nature of the pyridylamine ligands and the basicity and bulkiness at N$_{amine}$. Moreover, the studied catalytic system was also applied for the transformation of fructose and the gram-scale transformation of furfural to open ring product for practical application. Therefore, high catalytic activity along with the aqueous and thermal stability demonstrated by the studied η^5-Cp-Ru(II) complexes may also find application in various other high temperature catalytic reactions.

5.4. Experimental section

5.4.1. Materials and methods. All reactions were performed under open atmosphere using chemicals of high purity purchased from sigma Aldrich, TCI chemicals and Alfa Aesar. Cyclopentadienyl-ruthenium precursors [(η^5-C$_5$H$_5$)RuCl(PPh$_3$)$_2$] were synthesized according to the literature procedures.[40,41] ^{1}H NMR (400 MHz), ^{13}C NMR (100 MHz) and ^{31}P NMR (161.97 MHz) spectra were recorded at 298 K using DMSO-d_6 or CDCl$_3$ as the solvent on a Bruker Avance 400 spectrometer. Tetramethylsilane (TMS) was used as an external standard and the chemical shifts in ppm are reported relative to the centre of the singlet at 7.26 ppm for CDCl$_3$ and 2.49 ppm for DMSO-d_6 in ^{1}H NMR, and to the centre of the triplet at 77.0 ppm for CDCl$_3$ and 39.50 ppm for DMSO-d_6 in ^{13}C NMR. Suitable single crystals of complexes **[Ru]-17** − **[Ru]-23** were subjected to single-crystal X-ray structural studies using Agilent Technologies Supernova CCD system. ESI (positive mode), and high-resolution mass spectra (HRMS) were recorded on a micro TF-Q II mass spectrometer. Infrared spectra (4000 to 500 cm^{-1}) were recorded with a FTIR STD10 Perkin Elmer. UV–vis spectra were performed on Carry-60 UV-Visible Spectrophotometer using dichloromethane as solvent with a concentration of 4×10^{-3} mol/L

at room temperature using 10 mm quartz cuvette. Thermal gravimetric analyses (TGA) were performed on the Mettler Toledo thermal analysis system.

5.4.2. Single-crystal X-ray diffraction studies. Single-crystal X-ray structural studies of the (η^5-C$_5$H$_5$)-Ru(II) complexes **[Ru]-17 – Ru]-23** were performed on a CCD Agilent Technologies (Oxford Diffraction) SUPER NOVA diffractometer. Data were collected at 150(2) K using graphite-monochromated Cu Kα radiation ($\lambda\alpha$ = 1.5418 Å) for **[Ru]-18** and **[Ru]-20** whereas Mo Kα radiation ($\lambda\alpha$ = 0.71073 Å) for **[Ru]-17**, **[Ru]-19**, **[Ru]-21**, **[Ru]-22** and **[Ru]-23**. The strategy for the data collection was evaluated using the CrysAlisPro CCD software. The data were collected using the standard 'phi-omega' scans techniques, and were scaled and reduced using CrysAlisPro RED software. The structures were solved by direct methods using SHELXS-97, and refined using full matrix least-squares with SHELXL-97, refining on F2.[42] The positions of all the atoms were obtained by direct methods. All non-hydrogen atoms were refined anisotropically. The remaining hydrogen atoms were placed in geometrically constrained positions, and refined with isotropic temperature factors, generally 1.2 Ueq of their parent atoms. The crystal and refinement data are summarized in Table 5.1. Selected bond lengths and bond angles are summarized in Tables 5.2. CCDC deposition numbers of the complexes **[Ru]-17**, **[Ru]-18**, **[Ru]-19**, **[Ru]-20**, **[Ru]-21**, **[Ru]-22** and **[Ru]-23** are 1564514, 1556948, 1564515, 1556949, 1564516, 1564517 and 1564518, respectively.

5.4.3. General procedure for the synthesis of cyclopentadienyl-ruthenium(II) complexes ([Ru]-17−[Ru]-23). Complexes ([Ru]-17 – [Ru]-23) was synthesized by treating N-substituted pyridylamine (**L4-L9**) and pyridylimine (**L10**) ligands with cyclopentadienyl-ruthenium precursor, [(η^5-C$_5$H$_5$)RuCl(PPh$_3$)$_2$] in methanol (25 mL) under refluxing condition for 20 h. Later, volume was reduced to 10 mL, and then added NH$_4$PF$_6$ (0.489 g, 3.0 mmol). The solution was stirred at room temperature for 12 h to precipitate out the desired complexes, which was washed with diethylether (3×10 mL) and dried in air.

Synthesis of [(η^5-C$_5$H$_5$)RuPPh$_3$(κ^2-(*N,N*)-2-(aminomethyl)pyridine]PF$_6$ ([Ru]-17). Complex **[Ru]-17** was synthesized following the above general procedure, by using 2-(aminomethyl)pyridine (**L4**) (1.180 g, 1.1 mmol) and [(η^5-C$_5$H$_5$)Ru(PPh$_3$)$_2$Cl] (0.363 g, 0.5 mmol). Pale yellow solid, yield: 0.210 g (61%). FTIR (v, cm^{-1}): 3357, 3313 v(N-H stretching), 1606 v(N-H bending), 1090 v(C-N), 832 v(PF$_6$ stretching), 556 v(PF$_6$

bending). ^{1}H NMR (400 MHz, DMSO-d_6): δ (ppm) = 8.61 (d, 1H, J = 5.20 Hz), 7.56 (t, 1H, J_1 = 7.80 Hz, J_2 = 7.52 Hz), 7.39 (t, 6H, J_1 = 9.28 Hz, J_2 = 6.24 Hz), 7.32 (t, 6H, J_1 = 8.80 Hz, J_2 = 6.28 Hz), 7.28 (d, 1H, J = 8.28 Hz), 7.12 (t, 6H, J_1 = 9.28 Hz, J_2 = 8.04 Hz), 6.79 (t, 1H, J_1 = 6.52 Hz, J_2 = 6.28 Hz), 4.36 (s, 5H), 4.03-3.99 (m, 1H). ^{13}C NMR (100 MHz, DMSO-d_6): δ (ppm) = 162.28, 155.77, 136.18, 134.35, 133.97, 132.97, 132.86, 129.64, 128.32, 128.23, 123.02, 120.32, 75.09, 53.54. ^{31}P NMR (161.97 MHz, DMSO-d_6): δ (ppm) = 55.33 (s, PPh$_3$), -144.19 (sep, PF$_6$). MS (ESI) m/z calculated for [(η^5-C$_5$H$_5$)Ru(κ^2-L4)PPh$_3$]$^+$ (L4 = 2-(aminomethyl) pyridine), 537.1 [M]$^+$, found 537.1 [M]$^+$. UV-Vis.{dichloromethane, λ_{max}, nm (ε, M^{-1}cm^{-1})}: 365 (3.7×10^3), 327 (6.8×10^3), 274 (8.0×10^3), 267 (7.1×10^3). CCDC deposition number of the complex **[Ru]-17** is 1564514.

Synthesis of [(η^5-C$_5$H$_5$)RuPPh$_3$(κ^2-(*N,N*)-N-(pyridin-2-ylmethyl)propan-1-amine]PF$_6$ ([Ru]-18). Complex **[Ru]-18** was synthesized following the above general procedure, by using N-(pyridin-2-ylmethyl)propan-1-amine (**L5**) (0.165 g, 1.1 mmol) and [(η^5-C$_5$H$_5$)Ru(PPh$_3$)$_2$Cl] (0.363 g, 0.5 mmol). Pale yellow solid, yield: 0.225 g (62%). FTIR (v, cm^{-1}): 3277 v(N-H stretching), 1605 v(N-H bending), 1091 v(C-N), 833 v(PF$_6$ stretching), 557 v(PF$_6$ bending). ^{1}H NMR (400 MHz, DMSO-d_6): δ (ppm) = 8.39 (d, 1H, J = 5.24 Hz), 7.70 (t, 1H, J_1 = 7.76 Hz, J_2 = 7.52 Hz), 7.46 (t, 3H, J_1 = 6.28 Hz, J_2 = 8.28 Hz), 7.42 (d, 1H, J = 7.76 Hz), 7.39 (t, 6H, J = 7.56 Hz, J_2 = 7.00 Hz), 7.00 (t, 6H, J_1 = 9.28 Hz, J_2 = 8.28 Hz), 6.90 (t, 1H, J_1 = 6.52 Hz, J_2 = 6.52 Hz), 4.51 (s, 5H), 4.39 (dd, 1H, J_1 = 15.56 Hz, J_2 = 15.56 Hz), 4.09-4.02 (m, 1H), 3.29-3.25 (m, 1H), 3.19-3.14 (m, 1H), 2.90-2.88 (m, 1H), 1.40-1.36 (m, 1H), 1.18-1.15 (m, 1H), 0.54 (t, 3H, J_1 = 7.28 Hz, J_2 = 7.52 Hz). ^{13}C NMR (100 MHz, DMSO-d_6): δ (ppm) = 161.23, 155.37, 136.74, 132.99, 132.77, 132.65, 132.61, 130.07, 128.76, 128.67, 123.55, 120.92, 75.68, 61.13, 60.71, 21.49, 10.29. ^{31}P NMR (161.97 MHz, DMSO-d_6): δ (ppm) = 54.98 (s, PPh$_3$), -144.19 (sep, PF$_6$). MS (ESI) m/z calculated for [(η^5-C$_5$H$_5$)Ru(κ^2-L5)PPh$_3$]$^+$ (L5 = N-(pyridin-2-ylmethyl)propan-1-amine), 579.1 [M]$^+$, found 579.1 [M]$^+$. UV-Vis.{dichloromethane, λ_{max}, nm (ε, M^{-1}cm^{-1})}: 369 (3.7×10^3), 329 (6.7×10^3), 274 (7.5×10^3), 266 (6.6×10^3). CCDC deposition number of the complex **[Ru]-18** is 1556948.

Synthesis of [(η^5-C$_5$H$_5$)RuPPh$_3$(κ^2-(*N,N*)-N-(pyridin-2-ylmethyl)propan-2-amine]PF$_6$ ([Ru]-19). Complex **[Ru]-19** was synthesized following the above general procedure, by using N-(pyridin-2-ylmethyl)propan-2-amine (**L6**) (0.165 g, 1.1 mmol) and [(η^5-C$_5$H$_5$)Ru(PPh$_3$)$_2$Cl] (0.363 g, 0.5 mmol). Pale yellow solid, yield: 0.240 g (66%). FTIR (v, cm^{-1}): 3274 v(N-H stretching), 1604 v(N-H bending), 1093 v(C-N), 828 v(PF$_6$ stretching),

556 v(PF$_6$ bending). ^{1}H NMR (400 MHz, DMSO-d_6): δ (ppm) = 8.16 (d, 1H, J = 5.24 Hz), 7.76 (t, 1H, J_1 = 7.60 Hz, J_2 = 7.76 Hz), 7.50 (t, 3H, J_1 = 7.56 Hz, J_2 = 7.00 Hz), 7.48 (d, 1H, J = 7.75 Hz), 7.44 (t, 6H, J_1 = 6.28 Hz, J_2 = 8.52 Hz), 7.00 (t, 6H, J_1 = 8.80 Hz, J_2 = 8.28 Hz), 6.94 (t, 1H, J_1 = 6.28 Hz, J_2 = 7.04 Hz), 4.64 (s, 5H), 4.14-4.11 (m, 1H), 3.26-3.21 (m, 1H), 1.94-1.88 (m, 1H), 0.93 (dd, 6H, J_1 = 6.04 Hz, J_2 = 6.52 Hz). ^{13}C NMR (100 MHz, DMSO-d_6): δ (ppm) = 161.55, 154.93, 137.10, 132.82, 132.73, 132.63, 132.44, 130.27, 128.99, 128.90, 123.42, 121.08, 75.33, 58.35, 56.63, 24.72, 20.48. ^{31}P NMR (161.97 MHz, DMSO-d_6): δ (ppm) = 54.44 (s, PPh$_3$), -144.17 (sep, PF$_6$). MS (ESI) m/z calculated for [(η^5-C$_5$H$_5$)Ru(κ^2-L6)PPh$_3$]$^+$ (L6 = N-(pyridin-2-ylmethyl)propan-2-amine), 579.2 [M]$^+$, 579.2 found [M]$^+$. UV-Vis.{dichloromethane, λ_{max}, nm (ε, M^{-1}cm^{-1})}: 369 (3.7×10^3), 329 (6.9×10^3), 275 (7.7×10^3), 266 (6.7×10^3). CCDC deposition number of the complex [Ru]-19 is 1564515.

Synthesis of [(η^5-C$_5$H$_5$)RuPPh$_3$(κ^2-(*N,N*)-N-(pyridin-2-ylmethyl)butan-1-amine]PF$_6$ ([Ru]-20). Complex **[Ru]-20** was synthesized following the above general procedure, by using N-(pyridin-2-ylmethyl)butan-1-amine (**L7**) (0.180 g, 1.1 mmol) and [(η^5-C$_5$H$_5$)Ru(PPh$_3$)$_2$Cl] (0.363 g, 0.5 mmol). Pale yellow solid, yield: 0.250 g (67%). FTIR (v, cm^{-1}): 3127 v(N-H stretching), 1601 v(N-H bending), 1092 v(C-N), 830 v(PF$_6$ stretching), 557 v(PF$_6$ bending). ^{1}H NMR (400 MHz, DMSO-d_6): δ (ppm) = 8.38 (d, 1H, J = 5.28 Hz), 7.70 (t, 1H, J_1 = 7.52 Hz, J_2 = 7.52 Hz), 7.45 (t, 3H, J_1 = 6.00 Hz, J_2 = 6.80 Hz), 7.39 (t, 6H, J_1 = 6.52 Hz, J_2 = 8.04 Hz), 7.19 (t, 1H, J_1 = 9.04 Hz, J_2 = 7.28 Hz), 7.00 (t, 6H, J_1 = 9.28 Hz, J_2 = 8.28 Hz), 6.89 (t, 1H, J_1 = 6.52 Hz, J_2 = 6.52 Hz), 4.51 (s, 5H), 4.42-4.37 (m, 1H), 4.11-4.03 (m, 1H), 3.24-3.22 (m, 1H), 2.91-2.85 (m, 1H), 1.36-1.31 (m, 1H), 1.18-1.10 (m, 1H), 0.96-0.91 (m, 1H), 0.77 (t, 3H, J_1 = 7.04 Hz, J_2 = 7.24 Hz). ^{13}C NMR (100 MHz, DMSO-d_6): δ (ppm) = 161.23, 155.36, 136.75, 133.02, 132.77, 132.65, 130.06, 128.75, 128.65, 123.55, 120.92, 75.70, 60.88, 59.17, 30.53, 18.78, 13.66. ^{31}P NMR (161.97 MHz, DMSO-d_6): δ (ppm) = 54.89 (s, PPh$_3$), -144.18 (sep, PF$_6$). MS (ESI) m/z calculated for [(η^5-C$_5$H$_5$)Ru(κ^2-L7)PPh$_3$]$^+$ (L7 = N-(pyridin-2-ylmethyl)butan-1-amine), 593.2 [M]$^+$, found 593.2 [M]$^+$. UV-Vis.{dichloromethane, λ_{max}, nm (ε, M^{-1}cm^{-1})}: 369 (3.5×10^3), 330 (5.9×10^3), 274 (7.9×10^3), 266 (7.0×10^3). CCDC deposition number of the complex [Ru]-20 is 1556949.

Synthesis of [(η^5-C$_5$H$_5$)RuPPh$_3$(κ^2-(*N,N*)-3-methyl-N-(pyridin-2-ylmethyl)butan-1-amine]PF$_6$ ([Ru]-21). Complex **[Ru]-21** was synthesized following the above general procedure, by using 3-methyl-N-(pyridin-2-ylmethyl)butan-1-amine (**L8**) (0.195 g, 1.1

mmol) and [(η^5-C$_5$H$_5$)Ru(PPh$_3$)$_2$Cl] (0.363 g, 0.5 mmol). Pale yellow solid, yield: 0.255 g (68%). FTIR (v, cm^{-1}): 3306 v(N-H stretching), 1608 v(N-H bending), 1089 v(C-N), 829 v(PF$_6$ stretching), 556 v(PF$_6$ bending). ^{1}H NMR (400 MHz, DMSO-d_6): δ (ppm) = 8.37 (d, 1H, J = 5.16 Hz), 7.69 (t, 1H, J_1 = 7.76 Hz, J_2 = 9.04 Hz), 7.46 (t, 3H, J_1 = 7.52 Hz, J_2 = 5.76 Hz), 7.38 (t, 6H, J_1 = 6.28 Hz, J_2 = 7.04 Hz), 7.19 (t, 1H, J_1 = 9.04 Hz, J_2 = 8.04 Hz), 7.01 (t, 6H, J_1 = 9.00 Hz, J_2 = 8.28 Hz), 6.88 (t, 1H, J_1 = 6.28 Hz, J_2 = 6.52 Hz), 4.52 (s, 5H), 4.41 (dd, 1H, J_1 = 7.76 Hz, J_2 = 4.52 Hz), 4.11-4.04 (m, 1H), 3.24-3.21 (m, 1H), 1.28-1.19 (m, 2H), 1.11-0.98 (m, 1H), 0.80 (d, 3H, J = 6.28 Hz), 0.76 (d, 3H, J = 6.28 Hz). ^{13}C NMR (100 MHz, DMSO-d_6): δ (ppm) = 161.23, 155.44, 136.74, 133.10, 132.78, 132.72, 132.67, 130.03, 128.72, 128.62, 123.54, 120.88, 75.71, 61.17, 57.79, 37.73, 25.04, 22.56, 22.33. ^{31}P NMR (161.97 MHz, DMSO-d_6): δ (ppm) = 54.73 (s, PPh$_3$), -144.18 (sep, PF$_6$). MS (ESI) m/z calculated for [(η^5-C$_5$H$_5$)Ru(κ^2-L8)PPh$_3$]$^+$ (L8 = 3-methyl-N-(pyridin-2-ylmethyl)butan-1-amine), 607.2 [M]$^+$, found 607.2 [M]$^+$. UV-Vis.{dichloromethane, λ_{max}, nm (ε, M^{-1}cm^{-1})}: 363 (3.7×10^3), 329 (6.1×10^3), 274 (8.2×10^3), 267 (7.4×10^3). CCDC deposition number of the complex **[Ru]-21** is 1564516.

Synthesis of [(η^5-C$_5$H$_5$)RuPPh$_3$(κ^2-(N,N)-N-benzyl-1-(pyridin-2-yl)methanamine]PF$_6$ ([Ru]-22). Complex **[Ru]-22** was synthesized following the above general procedure, by using N-benzyl-1-(pyridin-2-yl)methanamine (**L9**) (0.217 g, 1.1 mmol) and [(η^5-C$_5$H$_5$)Ru(PPh$_3$)$_2$Cl] (0.363 g, 0.5 mmol). Pale yellow solid, yield: 0.251 g (65%). FTIR (v, cm^{-1}): 3254 v(N-H stretching), 1605 v(N-H bending), 1090 v(C-N), 836 v(PF$_6$ stretching), 557 v(PF$_6$ bending). ^{1}H NMR (400 MHz, DMSO-d_6): δ (ppm) = 8.36 (d, 1H, J = 5.28 Hz), 7.68 (t, 1H, J_1 = 9.28 Hz, J_2 = 7.76 Hz), 7.49 (t, 3H, J_1 = 7.52 Hz, J_2 = 7.00 Hz), 7.41 (t, 6H, J_1 = 6.24 Hz, J_2 = 8.56 Hz), 7.34-7.26 (m, 5H), 7.18-7.12 (m, 1H), 6.94 (t, 6H, J_1 = 9.32 Hz, J_2 = 8.00 Hz), 6.79 (d, 1H, J = 6.28 Hz), 4.61 (s, 5H), 4.50-4.46 (m, 1H), 4.39-4.33 (m, 1H), 4.27-4.20 (m, 1H), 3.95 (dd, 1H, J_1 = 4.52 Hz, J_2 = 4.52 Hz). ^{13}C NMR (100 MHz, DMSO-d_6): δ (ppm) = 161.04, 155.48, 137.10, 136.69, 133.49, 133.38, 132.03, 132.98, 132.92, 132.60, 130.40, 129.15, 129.05, 128.90, 128.81, 128.41, 123.86, 121.37, 75.95, 62.87, 60.96. ^{31}P NMR (161.97 MHz, DMSO-d_6): δ (ppm) = 55.317 (s, PPh$_3$), -144.18 (sep, PF$_6$). MS (ESI) m/z calculated for [(η^5-C$_5$H$_5$)Ru(κ^2-L9)PPh$_3$]$^+$ (L9 = N-benzyl-1-(pyridin-2-yl)methanamine), 627.2 [M]$^+$, found 626.8 [M]$^+$. UV-Vis.{dichloromethane, λ_{max}, nm (ε, M^{-1}cm^{-1})}: 366 (2.9×10^3), 328 (5.3×10^3), 373 (7.2×10^3), 266 (6.6×10^3). CCDC deposition number of the complex **[Ru]-22** is 1564517.

Synthesis of [(η^5-C$_5$H$_5$)RuPPh$_3$(κ^2-(*N*,*N*)-N-(pyridin-2-ylmethylene)propan-2-amine]PF$_6$ ([Ru]-23). Complex **[Ru]-23** was synthesized following the above general procedure, by using N-(pyridin-2-ylmethylene)propan-2-amine (**L10**) (0.162 g, 1.1 mmol) and [(η^5-C$_5$H$_5$)Ru(PPh$_3$)$_2$Cl] (0.363 g, 0.5 mmol). Brown solid, yield: 0.255 g (70%). FTIR (v, cm^{-1}): 1092 v(C-N), 830 v(PF$_6$ stretching), 557 v(PF$_6$ bending). ^{1}H NMR (400 MHz, DMSO-d_6): δ (ppm) = 9.28 (d, 1H, J = 5.52 Hz), 8.63 (d, 1H, J = 5.03 Hz), 7.70 (t, 1H, J_1 = 7.80 Hz, J_2 = 7.52 Hz), 7.62 (d, 6H, J = 7.76 Hz), 7.43 (t, 3H, J_1 = 7.52 Hz, J_2 = 6.76 Hz), 7.36 (t, 6H, J_1 = 6.80 Hz, J_2 = 7.00 Hz), 7.19 (t, 1H, J_1 = 7.00 Hz, J_2 = 6.00 Hz), 7.02 (t, 6H, J_1 = 9.28 Hz, J_2 = 8.56 Hz), 4.84 (s, 5H), 4.66-4.59 (m, 1H), 1.42 (d, 3H, J = 6.56 Hz), 0.80 (d, 3H, J = 6.52 Hz). ^{13}C NMR (100 MHz, DMSO-d_6): δ (ppm) = 160.69, 156.05, 155.68, 135.36, 132.71, 132.60, 131.36, 130.95, 130.13, 128.57, 128.47, 127.56, 124.45, 78.94, 66.29, 25.00, 21.63. ^{31}P NMR (161.97 MHz, DMSO-d_6): δ (ppm) = 48.18 (s, PPh$_3$), -144.18 (sep, PF$_6$). MS (ESI) m/z calculated for [(η^5-C$_5$H$_5$)Ru(κ^2-L10)PPh$_3$]$^+$ (L10 = N-(pyridin-2-ylmethylene)propan-2-amine), 577.1 [M]$^+$, found 577.1 [M]$^+$. UV-Vis.{dichloromethane, λ_{max}, nm (ε, M^{-1}cm^{-1})}: 436/2.9×10^3, 337/2.5×10^3, 273/9.1×10^3, 267/8.0×10^3. CCDC deposition number of the complex **[Ru]-23** is 1564518.

5.4.4. General procedure for η^5-Cp-Ru(II) catalysed transformation of furfural (1a) and its derivatives to levulinic acid (1b) and diketones in water.

All the reactions were carried out in Teflon coated autoclave. To an aqueous suspension (10 mL) of (η^5-C$_5$H$_5$)-Ru(II) catalyst (5 mol%), 1.0 mmol of furan (or its derivatives or fructose) and formic acid (as specified) were added and the reaction mixture was heated at 120 ºC for the specified duration. After completion of the reaction, reaction mixture was cooled to room temperature, and dried under reduced pressure. Selectivity of the products was determined by ^{1}H NMR. Yield for LA (**2a**) from furfural (**1a**) was determined by isolating the purified product through column chromatography (ethylacetate/hexane 2/98 – 10/90 v/v) and by ^{1}H NMR in CDCl$_3$ with reference to *p*-anisaldehyde added as an internal standard (Figure 5.9). Yields of the diketone products, 1-HHD (**2b**, from 5-HMF, **1b**) and 3-HHD (**2c**, from 5-MF, **1c**) were determined by isolating the purified products by column chromatography (ethylacetate/hexane 2/98 – 10/90 v/v).
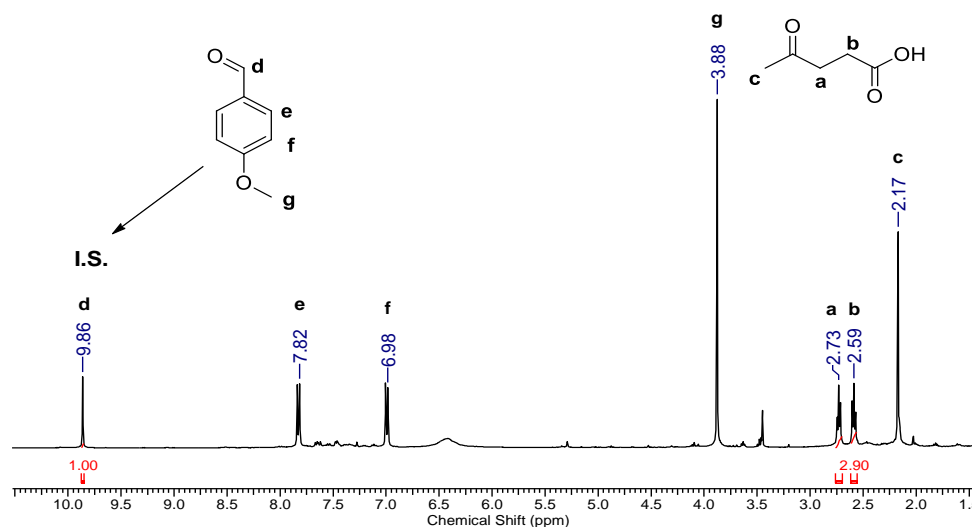
Figure 5.9. *¹H NMR spectra of catalytic reaction of **[Ru]-19** with p-anisaldehyde as internal standard.*

Note: The contents of this work have been reproduced with the permission from The American Chemical Society (*Inorg. Chem.*, 2018, 57, 4777-4787 (DOI: DOI: 10.1021/acs.inorgchem.8b00536).

5.5. References

1. Ganter C. (2003), Chiral organometallic half-sandwich complexes with defined metal configuration, *Chem. Soc. Rev.*, 32, 130-138 (DOI: 10.1039/b205996g).

2. (a) Kumar P., Gupta R. K., Pandey D. S. (2014), Half-sandwich arene ruthenium complexes: synthetic strategies and relevance in catalysis, *Chem. Soc. Rev.*, 43, 707-733 (DOI: 10.1039/c3cs60189g); (b) Dodo, N.; Matsushima, Y.; Uno, M.; Onitsuka, K.; Takahashi, S. (2000), Synthesis of ruthenium complexes with planar-chiral cyclopentadienyl-pyridine or -phosphine bidentate ligands, *J. Chem. Soc., Dalton Trans.*, 35-41 (DOI: 10.1039/A907145H); (c) Albers, M. O.; Robinson, D. J.; Singleton, E. (1986), The chemistry of cyclopentadienyl-ruthenium and -osmium complex II. Novel mononuclear cyclopentadienyl ruthenium complexes containing aromatic amine ligands. A facile synthetic route, *J. Organomet. Chem.*, 311, 207-215 (DOI: 0022-328X/86); (d) de Klerk-Engels, B.; Delis, J. G. P.; Vrieze, K. (1994), Synthesis of Cyclopentadienyl-(1,4-diisopropyl-l,3-

diazabutadie)(L))ruthenium trifluoromethanesulfonate (L = Alkene, Alkyne, CO, Pyridine, PPh$_3$). X-ray Structure of [(η^5-C$_5$H$_5$)Ru(^{i}Pr-DAB)(η^2-propen)[CF$_3$SO$_3$]$^+$, *Organometallics*, 13, 3269-3278 (DOI: 0276-7333/94/2313-3269); (e) Flsh, R. H.; Klm, H. -S.; Fong, R. H. (1989), Bonding Studies of Nltrogen Heterocyclic Ligands to (η^5-Cyclopentadienyl)ruthenium Cation: A Novel Nitrogen to T Rearrangement, *Organometallics*, 8, 1375-1377 (DOI: 0276-7333/89/2308-1375); (f) Fish, R. H.; Kim, H. -S.; Fong, R. H. (1991), Bonding Mode of Nitrogen Heterocyclic Ligands to (η^5-Cyclopentadienyl)ruthenium Cation and Reactivity Studies of the Nitrogen and π-Bonded Complexes: Mechanistic Aspects of a Nitrogen to π-Rearrangement, *Organometallics*, 10, 110-777 (DOI: 0216-1333/91/2310-0770); (g) Mbaye, M. D.; Demerseman, B.; Renaud, J. -L.; Toupet, L.; Bruneau, C. (2003), [Cp*(η^2-bipy)(MeCN)Ru^{II}][PF$_6$] Catalysts for Regioselective Allylic Substitution and Characterization of Dicationic [Cp*(η^2-bipy)- (η^3-allyl)Ru^{IV}][PF$_6$]$_2$ Intermediates, *Angew. Chem. Int. Ed.*, 42, 5066-5068 (DOI: 10.1002/anie.200352257).

3.   (a) Bauer, E. B. (2012), Chiral-at-metal complexes and their catalytic applications in organic synthesis, *Chem. Soc. Rev.*, 41, 3153-3167 (DOI: 10.1039/c2cs15234g); (b) Hintermann, L.; Xiao, L.; Labonne, A.; Englert, U. (2009), [CpRu(η^6-naphthalene)]PF$_6$ as Precursor in Complex Synthesis and Catalysis with the Cyclopentadienyl-Ruthenium(II) Cation, *Organometallics*, 28, 5739-5748 (DOI: 10.1021/om900333t); (c) Becker, E.; Stingl, V.; Mereiter, K.; Kirchner, K. (2006), Formation of a Half-Sandwich Triscarbene Ruthenium Complex: Oxidative Coupling of 2,7-Nonadiyne Mediated by [RuCp(IPr^i)(CH$_3$CN)$_2$]$^+$ (IPri) 1,3-bis(2,6-diisopropylphenyl)imidazol-2-ylidene), *Organometallics*, 25, 4166-4169 (DOI: 10.1021/om060345b); (d) Baratta, W.; Herrmann, W. A.; Kratzer, R. M.; Rigo, P. (2000), Half-Sandwich Ruthenium(II) Catalysts for C-C Coupling Reactions between Alkenes and Diazo Compounds, *Organometallics*, 19, 3664-3669 (DOI: 10.1021/om0003537); (e) Baratta, W.; Zotto, A. D.; Rigo, P. (1999), Half-Sandwich Ruthenium(II) Complexes as Catalysts for Stereoselective Carbene-Carbene Coupling Reactions, *Organometallics*, 18, 5091-5096 (DOI: 10.1021/om990582x).

4.   Ashby G. S., Bruce M. I., Tomkins I. B., Wallis R. C. (1979), Cyclopentadienyl-Ruthenium and Osmium Chemistry. VII* Complexes Containing Nitriles, Tertiary

Phosphines or Phosphites Formed by Addition or Displacement Reactions, *Aust. J. Chem.*, 32, 1003-1016 (DOI: 10.1071/CH9791003).

5. (a) Govindaswamy P., Mozharivskyj Y. A., Kollipara M. R. (2004), Synthesis and characterization of cyclopentadienylruthenium(II) complexes containing N,N'-donor Schiff base ligands: crystal and molecular structure of [(η^5-C$_5$H$_5$)Ru(C$_5$H$_4$N-2-CH=N–C$_6$H$_4$–*p*-OCH$_3$)(PPh$_3$)]PF$_6$, *Polyhedron*, 23, 1567-1572 (DOI:10.1016/j.poly.2004.03.007); (b) Pachhunga K., Therrien B., Kreisel K. A., Yap G. P. A., Kollipara M. R. (2007), Reactivity studies of cyclopentadienyl ruthenium(II), osmium(II) and pentamethylcyclopentadienyl iridium(III) complexes towards 2-(2'-pyridyl)imidazole derivatives, *Polyhedron*, 26, 3638-3644 (DOI: 10.1016/j.poly.2007.03.055).

6. (a) Trost B. M., Frederiksen M. U., Rudd M. T. (2005), Ruthenium-Catalyzed Reactions-A Treasure Trove of Atom-Economic Transformations, *Angew. Chem. Int. Ed.*, 44, 6630-6666 (DOI: 10.1002/anie.200500136); (b) Osakada K. (2011), 1,4-Hydrosilylation of Pyridine by Ruthenium Catalyst: A New Reaction and Mechanism, *Angew. Chem. Int. Ed.*, 50, 3845-3846 (DOI: 10.1002/anie.201008199).

7. (a) Mai V. H., Kuzmina L. G., Churakov A. V., Korobkov I., Howardd J. A. K., Nikonov G. I.(2016) NHC carbene supported half-sandwich hydridosilyl complexes of ruthenium: the impact of supporting ligands on Si···H interligand interactions, *Dalton Trans.*, 45, 208-215 (DOI: 10.1039/c5dt04067a); (b) Clark J. L., Duckett S. B. (2014), Photochemical studies of (η^5-C$_5$H$_5$)Ru(PPh$_3$)$_2$Cl and (η^5-C$_5$H$_5$)Ru(PPh$_3$)$_2$Me: formation of Si-H and C-H bond activation products, *Dalton Trans.*, 43, 1162-1171 (DOI: 10.1039/c3dt52069b).

8. Glöge T., Jess K., Bannenberg T., Jones P. G. (2015), Langenscheidt-Dabringhausen, N.; Salzer, A.; Tamm, M. 16-Electron pentadienyl- and cyclopentadienylruthenium half-sandwich complexes with bis(imidazol-2-imine) ligands and their use in catalytic transfer hydrogenation, *Dalton Trans.*, 44, 11717-11724 (DOI: 10.1039/c5dt01080b).

9. (a) Moreno, V.; Font-Bardia, M.; Calvet, T.; Lorenzo, J.; Avilés, F. X.; Garcia, M. H.; T. S.; Morais, Valente, A.; Robalo, M. P. (2011), DNA interaction and cytotoxicity studies of new ruthenium(II) cyclopentadienyl derivative complexes containing heteroaromatic ligands, *J. Inorg. Biochem.* 105, 241-249 (DOI: 10.1016/j.jinorgbio.2010.10.009); (b) Tomaz A. I., Jakusch T., Morais T. S.,

Marques F., de Almeida R. F. M., Mendes F., Enyedy É. A., Santos I., Pessoa J. C., Kiss T., Garcia M. H. (2012), [Ru^{II}(η^5-C$_5$H$_5$)(bipy)(PPh$_3$)]$^+$, a promising large spectrum antitumor agent: Cytotoxic activity and interaction with human serum albumin, *J. Inorg. Biochem.*, 117, 261-269 (DOI:10.1016/j.jinorgbio.2012.06.016).

10. Blum Y., Shvo Y. (1984), Catalytically Reactive Ruthenium Intermediates in the Homogeneous Oxidation of Alcohols to Esters, *Isr. J. Chem.*, 24, 144-148 (DOI: 10.1002/ijch.198400024); (b) Conley, B. L.; Pennington-Boggio, M. K.; Boz, E.; Williams, T. J. (2010), Discovery, Applications, and Catalytic Mechanisms of Shvo's Catalyst, *Chem. Rev.*, 110, 2294-2312 (DOI: 10.1021/cr9003133).

11. Fábos V., Mika L. T., Horváth I. T. (2014), Selective Conversion of Levulinic and Formic Acids to γ-Valerolactone with the Shvo Catalyst, *Organometallics*, 33, 181-187 (DOI: 10.1021/om400938h).

12. Lee S. -H., Gutsulyak D. V., Nikonov G. I. (2013), Chemo- and Regioselective Catalytic Reduction of N-Heterocycles by Silane, *Organometallics*, 32, 4457-4464 (DOI: 10.1021/om400269q).

13. Mai V. H., Korobkov I., Nikonov G. I. (2016), Half-Sandwich Silane σ-Complexes of Ruthenium Supported by NHC Carbene, *Organometallics*, 35, 936-942 (DOI: 10.1021/acs.organomet.5b00958).

14. Lee S.-H., Nikonov G. I. (2015), Transfer Hydrogenation of Ketones, Nitriles, and Esters Catalyzed by a Half-Sandwich Complex of Ruthenium, *ChemCatChem*, 7, 107-113 (DOI: 10.1002/cctc.201402780).

15. Mai V. H., Lee S. -H., Nikonov G. I. (2017), Transfer Hydrogenation of Unsaturated Substrates by Half-sandwich Ruthenium Catalysts using Ammonium Formate as Reducing Reagent, *Chemistry Select*, 2, 7751-7757 (DOI: 10.1002/slct.201701423).

16. Mai V. H., Nikonov G. I. (2016), Transfer Hydrogenation of Nitriles, Olefins, and N-Heterocycles Catalyzed by an N-Heterocyclic Carbene-Supported Half-Sandwich Complex of Ruthenium, *Organometallics*, 35, 943-949 (DOI: 10.1021/acs.organomet.5b00967).

17. Standfest-Hauser C., Slugovc C., Mereiter K., Schmid R., Kirchner K., Xiao L., Weissensteiner W. (2001), Hydrogen-transfer catalyzed by half-sandwich Ru(II) aminophosphine complexes, *J. Chem. Soc., Dalton Trans.*, 2989-2995 (DOI: 10.1039/b104128m).

18.   Kumar P., Singh A. K., Sharma S., Pandey D. S. (2009), Structures, preparation and catalytic activity of ruthenium cyclopentadienyl complexes based on pyridyl-phosphine ligand, *J. Organomet. Chem.*, 694, 3643-3652 (DOI: 10.1016/j.jorganchem.2009.07.01).

19.   Review on biomass transformations: (a) Corma A., Iborra S., Velty A. (2007), Chemical Routes for the Transformation of Biomass into Chemicals, *Chem. Rev.*, 107, 2411-2502 (DOI: 10.1021/cr050989d); (b) Morone A., Apte M., Pandey R. A. (2015), Levulinic acid production from renewable waste resources: Bottlenecks, potential remedies, advancements and applications, *Renew. Susta. Energ. Rev.*, *51*, 548-565 (DOI: http://dx.doi.org/10.1016/j.rser.2015.06.032); (c) Serrano-Ruiz J. C., Luque R., Sepulveda-Escribano A. (2011), Transformations of biomass-derived platform molecules: from high added-value chemicals to fuels *via* aqueous-phase processing, *Chem. Soc. Rev.*, *40*, 5266-5281 (DOI: 10.1039/c1cs15131b); (d) Sankar M., Dimitratos N., Miedziak P. J., Wells P. P., Kiely C. J., Hutchings G. J. (2012), Designing bimetallic catalysts for a green and sustainable future, *Chem. Soc. Rev.*, 41, 8099-8139 (DOI: 10.1039/c2cs35296f); (e) Climent M. J., Corma A., Iborra S. (2014), Conversion of biomass platform molecules into fuel additives and liquid hydrocarbon fuels, *Green Chem.*, 16, 516-547 (DOI: 10.1039/c3gc41492b); (f) Gupta, K.; Rai, R. K.; Singh, S. K. (2018), Metal catalysts for Efficient Transformation of Biomass-derived HMF and Furfural to Value Added Chemicals: Recent Progress, *ChemCatChem* (DOI: 10.1002/cctc.201701754).

20.   Schiavo, V.; Descotes, G.; Montech, J. (1991), Catalytic-hydrogenation of 5-hydroxymethyl furfural in aqueous medium, *Bull. Soc. Chim. Fr.*, 128, 704-711.

21.   Liu F., Audemar M., Vigier K. D. O., Clacens J. -M., De Campo F., Jérôme F. (2014), Combination of Pd/C and Amberlyst-15 in a single reactor for the acid/hydrogenating catalytic conversion of carbohydrates to 5-hydroxy-2,5-hexanedione, *Green Chem.*, 16, 4110-4114 (DOI: 10.1039/c4gc01158a).

22.   (a) Hu X., Westerhof R. J. M., Wu L., Dong D., Li C.-Z. (2015), Upgrading biomass-derived furans via acid-catalysis/hydrogenation: the remarkable difference between water and methanol as the solvent, *Green Chem.*, *17*, 219-224 (DOI: 10.1039/c4gc01826e); (b) Hu X., Song Y., Wu L., Gholizadeh M., Li C.-Z. (2013), One-Pot Synthesis of Levulinic Acid/Ester from C5 Carbohydrates in a Methanol Medium. *ACS Sustana. Chem. Eng.*, 1, 1593-1599 (DOI: 10.1021/sc400229w).

23. Xu Z., Yan P., Xu W., Liu X., Xia Z., Chung B., Jia S., Zhang Z. C. (2015), Hydrogenation/Hydrolytic Ring Opening of 5-HMF by Cp*-Iridium(III)Half-Sandwich Complexes for Bioketones Synthesis, *ACS Catal*., 5, 788-792 (DOI: 10.1021/cs501874v).

24. Xu Z., Yan P., Li H., Liu K., Liu X., Jia S., Zhang Z. C. (2016), Active Cp*Iridium(III) Complex with ortho-Hydroxyl Group Functionalized Bipyridine Ligand Containing an Electron-Donating Group for the Production of Diketone from 5-HMF, *ACS Catal*., 6, 3784-3788 (DOI: 10.1021/acscatal.6b00826).

25. Wu W. -P., Xu Y. -J., Zhu R., Cui M. -S., Li X. -L., Deng J., Fu Y. (2016), Selective Conversion of 5-Hydroxymethylfuraldehyde Using Cp*Ir Catalysts in Aqueous Formate Buffer Solution, *ChemSusChem*, 9, 1209-1215 (DOI: 10.1002/cssc.201501625).

26. Xu Y.-J., Shi J., Wu W.-P., Zhu R.; Li X.-L., Deng J., Fu Y. (2017), Effect of Cp*Iridium(III) Complex and acid co-catalyst on conversion of furfural compounds to cyclopentanones or straight chain ketones, *Apply. Catal. A: General*, (Doi:10.1016/j.apcata.2017.07.004).

27. Dwivedi A. D., Gupta K., Tyagi D., Rai R. K., Mobin S. M., Singh S. K. (2015), Ruthenium and Formic Acid Based Tandem Catalytic Transformation of Bioderived Furans to Levulinic Acid and Diketones in Water, *ChemCatChem*, 7, 4050-4058 (DOI : 10.1002/cctc.201501021).

28. Gupta K., Tyagi D., Dwivedi A. D., Mobin S. M., Singh S. K. (2015), Catalytic transformation of bio-derived furans to valuable ketoacids and diketones by water-soluble ruthenium catalysts, *Green Chem*., 17, 4618-4627 (DOI: 10.1039/c5gc01376c).

29. Dwivedi, A. D.; Rai, R. K.; Gupta, K.; Singh, S. K. (2017), Catalytic Hydrogenation of Arenes in Water Over In Situ Generated Ruthenium Nanoparticles Immobilized on Carbon, *ChemCatChem*, 9, 1930-1938 (DOI : 10.1002/cctc.201700056).

30 Dykemana, R. R.; Luska, K. L.; Thibault, M. E.; Jones, M. D.; Schlaf, M.; Khanfar, M.; Taylor, N. J.; Britten, J. F.; Harrington, L. (2007), Catalytic deoxygenation of terminal-diols under acidic aqueous conditions by the ruthenium complexes [(η^6-arene)Ru(X)(N∩N)](OTf)n, X=H$_2$O, H, η^6-arene = p-Me-^{i}Pr-C$_6$H$_4$, C$_6$Me$_6$, N∩N= bipy, phen, 6,6'-diamino-bipy, 2,9-diamino-phen, n=1, 2) Influence

of the *ortho*-amine substituent on catalytic activity, *J. Mol. Catal. A: Chem.*, 277, 233-251 (DOI: 10.1016/j.molcata.2007.08.008).

31. Thibault, M. E.; DiMondo, D. V.; Jennings, M.; Abdelnur, P. V.; Eberlin, M. N.; Schlaf, M. (2011), Cyclopentadienyl and pentamethylcyclopentadienyl ruthenium complexes as catalysts for the total deoxygenation of 1,2-hexanediol and glycerol, *Green Chem.*, 13, 357-366 (DOI: 10.1039/c0gc00255k).

32. DiMondo, D.; Thibault, M. E.; Britten, J.; Schlaf, M. (2013), Comparison of the Catalytic Activity of $[(\eta^5\text{-}C_5H_5)Ru(2,2'\text{-}$ bipyridine)(L)]OTf versus $[(\eta^5\text{-}C_5H_5)Ru(6,6'\text{-diamino-}2,2'\text{-bipyridine})(L)]OTf$ (L = labile ligand) in the Hydrogenation of Cyclohexanone. Evidence for the Presence of a Metal-Ligand Bifunctional Mechanism under Acidic Conditions, *Organometallics*, 32, 6541-6554 (DOI: dx.doi.org/10.1021/om400871v).

33. Singh S. K., Chandra M., Pandey D. S., Puerta M. C., Valerga P. (2004), Helices of ruthenium complexes involving pyridyl-azine ligands: synthesis, spectral and structural aspects, *J. Organomet. Chem.*, 689, 3612-3620 (DOI: 10.1016/j.jorganchem.2004.08.026).

34. Bruce M. I., Wong F.S., Skelton B. W., White A. H. (1981), Cyclopentadienyl-ruthenium and -osmium chemistry. Part 11. Reactions and structures of $[RuCl(PPh_3)_2(\eta^5\text{-}C_5H_5)]$ and its trimethyl-phosphine analogue, *J. Chem. Soc., Dalton Trans.*, 1398-1405 (DOI: 10.1039/DT9810001398).

35. Becker E., Slugovc C., Ruba E., Standfest-Hauser C., Mereiter K., Schmidt R., Kirschner K. (2002), Synthesis, characterization, and reactivity of half-sandwich Ru(II) complexes containing phosphine, arsine, stibine, and bismutine ligands. *J. Organometal. Chem.*, *649*, 55-63 (DOI: 10.1016/S0022-328X(01)01487-5).

36. (a) Chakraborty A. K., Bischoff K. B., Astarita G., Damewood J. R. (1988), Molecular orbital approach to substituent effects in amine-CO_2 interactions, *J. Am. Chem. Soc.*, 110, 6947-6954 (DOI: 10.1021/ja00229a003); (b) Graton J., Berthelot M., Laurence C. (2001), Hydrogen-bond basicity pK_{HB} scale of secondary amine, *J. Chem. Soc. Perkin Trans.*, 2, 2130-2135 (DOI: 10.1039/b105082f).

37. Lin Y.-C., Yu K.-H. Huang, S. -L., Liu Y.-H., Wang Y., Liu S.-T., Chen J.-T. (2009), Alternating ethylene-norbornene copolymerization catalyzed by cationic organopalladium complexes bearing hemilabile bidentate ligands of a-amino-pyridines, *Dalton Trans.*, 9058-9067 (DOI: 10.1039/b912068h).

38.   (a) Tajvidi K. Hausoul P. J. C., Palkovits R. (2014), Hydrogenolysis of Cellulose over Cu-Based Catalysts-Analysis of the Reaction Network, *ChemSusChem*, 7, 1311-1317 (DOI: 10.1002/cssc.201300978); (b) Yepez A., Garcia A., Climent M. S., Romero A. A., Luque R. (2014), Catalytic conversion of starch into valuable furan derivatives using supported metal nanoparticles on mesoporous aluminosilicate materials, *Catal. Sci. Technol.*, 4, 428-434 (DOI: 10.1039/c3cy00762f); (c) Alamillo R., Crisci A. J., Gallo J. M. R., Scott S. L., Dumesic J. A. (2013), A Tailored Microenvironment for Catalytic Biomass Conversion in Inorganic-Organic Nanoreactors, *Angew. Chem., Int. Ed.*, 52, 10349-10351 (DOI: 10.1002/anie.201304693); (d) Zhang J., Weitz E. (2012), An in Situ NMR Study of the Mechanism for the Catalytic Conversion of Fructose to 5-Hydroxymethylfurfural and then to Levulinic Acid Using ^{13}C Labeled D-Fructose, *ACS Catal.*, 2, 1211-1218 (DOI: 10.1021/cs300045r); (e) Thananatthanachon T., Rauchfuss T. B. (2010), Efficient Route to Hydroxymethylfurans from Sugars via Transfer Hydrogenation, *ChemSusChem*, 3, 1139-1141 (DOI: 10.1002/cssc.201000209); (f) Nikolla E., Roman-Leshkov Y., Moliner M., Davis M. E. (2011), "One-Pot" Synthesis of 5-(Hydroxymethyl)furfural from Carbohydrates using Tin-Beta Zeolite, *ACSCatal.*, 1, 408-410 (DOI: 10.1021/cs2000544).

39.   Crabtree, R. H. (2015), Deactivation in Homogeneous Transition Metal Catalysis: Causes, Avoidance, and Cure, *Chem. Rev.*, 115, 127-150 (DOI: dx.doi.org/10.1021/cr5004375).

40.   Bruce, M. I.; Windsor, N. J. (1977), Cyclopentadienyl-ruthenium and -osmium chemistry. IV. Convenient high-yield synthesis of some cyclopentadienyl ruthenium or osmium tertiary phosphine halide complexes, *Aust. J. Chem.*, 30, 1601-1604 (DOI: 10.1071/CH9771601).

41.   Gorbachuka, E. V.; Badeevaa, E. K.; Zinnatullina, R. G.; Pavlova, P. O.; Dobrynina, A. B.; Gubaidullina, A. T.; Ziganshin, M. A.; Gerasimov, A. V.; Sinyashina, O. G.; Yakhvarov, D. G. (2016), Polymorphism and thermodynamic properties of chloro(cyclopentadienyl)bis(triphenylphosphine)ruthenium(II) complex, *J. Organomet. Chem.*, 805, 49-53 (DOI: 10.1016/j.jorganchem.2016.01.008).

42.   Sheldrick, G. M. (2008), A short history of SHELX, *Acta Crystallogr., Sect. A*, 64, 112-122 (DOI: 10.1107/S0108767307043930).

Chapter 6

Conclusions and future scope

6.1. Conclusions

In summary, present thesis focused to design, synthesis and structural characterization of half sandwich Ru(II) complexes with environmentally favourable nitrogen and oxygene donor ligands and also try to explore their catalytic activity in the feild of various organic transformations. For better understanding towards plausible catalytic pathway various instrumental techniques (Mass, NMR, UV-vis. etc.) were employed for mechanistic studies of presented catalytic reactions.

In **Chapter 1**, containing introduction and background of transition metal based half sandwich complecxes and their catalytic activity for various important organic transformation reactions and their mechanistic aspects have been discussed.

In **chapter 2**, discussed synthesis, characterization and catalytic activity of a series of highly active water-soluble homogenous catalysts based on arene-ruthenium(II) complexes containing simple and readily available ethylenediamine (or its derivatives) ligands, were successfully employed for the catalytic transformation of bioderived furans into open-ring value-added ketoacid and diketones in the presence of formic acid in water. The N-H bonds present in the synthesized half sandwich arene-ruthenium(II) complexes were exhibits their significant role on the catalytic transformation, where the most active catalyst has the highest number of N-H bonds. Moreover, direct catalytic transformation of fructose to 1-hydroxyhexane-2,5-dione (1-HHD) and levulinic acid (LA) was also achieved with limited conversion. Mechanistic studies involving ^{1}H NMR spectroscopy and experiments with variable formic acid concentrations revealed a tandem mode of catalytic transformation of furfural to LA via the hydrogenated intermediate, furfuryl alcohol. Furthermore, high aqueous solubility and stability of the ruthenium catalyst offers the potential for easy recovery and reusability in at least five consecutive catalytic runs without any significant loss of the catalytic activity. Through our study, we have demonstrated a significant cooperative effect between the ruthenium catalyst and formic acid to achieve high catalytic activity for the transformation of bio-derived furans.

Chapter 3 an efficient catalytic system was developed in which the cooperative synergy of $[(\eta^6\text{-}C_6H_6)\text{-}Ru(ethylenediamine)Cl]^+$ and formic acid resulted in the *in situ* generation of active Ru nanoparticles immobilised on carbon (Ru/C) and H_2 gas to

achieve the facile tandem catalytic hydrogenation of a wide range of arenes and heteroarenes in water. Selective ring hydrogenations of nitrogen continuing heteroarenes are very difficult and it is important for natural product (alkaloids) synthesis. The catalytic activity of the reported catalytic system was attributed to the unique structure-activity relationship of the precursor complex $[(\eta^6\text{-}C_6H_6)Ru(ethylenediamine)Cl]^+$, in which the N-H bond plays a crucial role in the initial activation of formic acid to generate H_2 gas. Furthermore, a high reaction temperature enhances the rapid reduction of Ru^{II} in the precursor complex to Ru^0. TEM observations of the Ru/C nanoparticles and the Hg^0 poisoning experiments suggest the heterogeneous nature of the catalyst. Moreover, a wide range of aromatic compounds analogous to lignin fragments were hydrogenated successfully to the corresponding alicyclic products, thus the present catalytic system may find application in biomass transformations.

In **chapter 4**, synthesized a series of highly stable and water soluble half-sandwich arene-ruthenium(II) complexes with O/O and O/N donor troponate/aminotroponate ligands, and structures of two representative complexes were authenticated by single-crystal X-ray diffraction studies. These synthesized complexes exhibited higher catalytic activity for direct ortho C-H bond arylation of 2-phenylpyridine with 4-chloroanisole at 100 °C in water, without the use of any carboxylate additive, with enhanced selectivity for monoarylated product over diarylated product. In comparison to arene-ruthenium(II)-troponate complex **[Ru]-13**, the selectivity toward monoarylated products is more prominent with arene-ruthenium(II)-aminotroponate complexes **[Ru]-15** and **[Ru]-16**. Notably, these complexes are also catalytically active in the presence of carboxylate additive, where selectivity toward diarylated product is favored over monoarylated product with the more bulky carboxylates: pivalate > isobutyrate > propionate > acetate. Extensive mass-spectral studies were performed to identify active key intermediates of the catalyst and to evaluate their role in the C-H bond activation pathway. Our studies showed the formation of a new cycloruthenated species, **[Ru]-B**, by the release of arene ring from the catalyst, is favored over the well-established arene-ruthenium cycloruthenated species **[Ru]-A**. It is worth mentioning here that arene-free ruthenium species, for instance, $RuCl_3(H_2O)_n$, were also reported to be active for catalytic C-H arylation reactions. Consistent with the above results, reaction free energies, calculated by using DFT calculations, also favored the formation of species **[Ru]-B** over **[Ru]-A**. On the basis of the experimental evidence, a reaction pathway was proposed showing the key importance of the species **[Ru]-B** in C-H bond arylation of 2-phenylpyridine. We

believe observations marked in the present study using troponate/aminotroponate arene-ruthenium(II) complexes will contribute in enhancing the mechanistic understanding of such catalytic systems in C-H activation reactions and help in development of new and highly active catalytic system.

In **chapter 5**, synthesized a series of highly stable cationic η^5-Cp-Ru(II)-pyridylamine (**[Ru]-17** − **[Ru]-22**) and η^5-Cp-Ru-pyridylimine (**[Ru]-23**) complexes and characterized byvarious spectroscopic technique likes ^{1}H, ^{13}C, ^{31}P NMR and mass spectrometry. Molecular structures of all the complexes are authentication by single crystal X-ray difraction. Synthesized complexes are shown higher stability in water and acid even at high temperature and pressure. The synthesized η^5-Cp-Ru-pyridylamine complexes displayed higher catalytic activity for the transformation of biomass-derived furans, (furfural, 5-HMF and 5-MF) to value added open ring products, LA and diketones (1-HHD, 3-HHD and 2,5-HD) with high conversion (>99%) and selectivity at 120 °C in the presence of formic acid. Experimental findings confirmed that the η^5-Cp-Ru-pyridylamine complexes exhibited higher catalytic activity over analogous η^5-Cp-Ru-pyridylimine complex, which can be attributed to the hemilabile nature of the pyridylamine ligands. Higher catalytic activity of these complexes is due to combined effect of flexibility, basicity and bulkiness at N$_{amine}$. Moreover, the studied catalytic system was also applied for the transformation of fructose and the gram-scale transformation of furfural to open ring product for practical application. Therefore, high catalytic activity along with the aqueous and thermal stability demonstrated by the studied (η^5-C$_5$H$_5$)-Ru(II) complexes may also find application in various other high temperature catalytic reactions.

Thus, present thesis work concluded that design and synthesis of various half sandwich ruthenium(II) complexes based on N/N, N/O and O/O donor ligands are indeed important to achieve highly efficient catalytic systems. In addition, incorporation of easily available, environmentally benign bidentate nitrogen donor ethylenediamine based ligands in (η^6-arene)-Ru(II) complexes which enhance their stability in water and air and make them a suitable candidates for various catalytic reactions. It is efficiently suitable for transfer hydrogenation reaction in which –NH bond plays an important role in reduction step in this reaction. Moreover, use of seven membered ring containing bidentate tropolone/aminotropolone ligands provide stability to complexes due to the delocalization of −C=O bond, as well as offers the opportunity to study a ligands tuned

catalytic reaction. Various instrumental techniques and theoretical calculation further enhances the mechanistic understanding for the catalytic reactions. Synthesis of η^5-Cp-Ru(II)-pyridylamine/imine complexes which shows higher thermal stability, provide efficient catalytic system for various organic transformations due to of hemilabile nature of pyridylamine ligands. The enhanced catalytic activity of these complexes basically is the result of combined effect of basicity, flexibility and bulkyness at N_{amine}. These types of catalysts are suitable for organic transformations even at higher reaction temperature. These strategies were successfully employed for the development of new catalysts for catalytic ring opening of bioderived furans to various open ring products, selective ring hydrogenation of (hetero)arene and C-H bond activation/arylation of 2-phenylpyridine with arylhalide in water. Further efforts were made to study mechanistic investigations for gain better understanding toward catalytic reaction pathway for the catalytic reactions, which were supported by various control experiments, mass and NMR spectral experiments to trap and identify the crucial organometallic intermediates species.

6.2. Future scope

Design and synthesis of a series of new sustainable catalytic system based on nitrogen and oxygen donor ligands is highly desired. Interestingly, ligands having -NH moiety shows wide scope in field of catalysis like one used in asymmetric hydrogenations catalysts is Noyori's catalysts which have systematically studied the role of –NH bond present in catalyst for various catalytic transformations. In spite of the advantageous role of $–NH_2$ donor ligands its exploration in field of biomass transformation is limited. There is a wide scope of studies using such type of complexes in the field of biomass which is very demamding and less explored yet. Moreover, structure-activity relationship plays an important role in their catalytic activity and involvement of the concept for activation of substrates by cooperative effect as well as metal-coordinated intermediated, may favor to achieve for the such challenging tasks like selective ring hydrogenation of (hetero)arene, small molecules activation, C-H bond functionalization and generation of H_2 gas from formic acid. However, mechanistic understanding of catalytic reactions may help to improve drawbacks of a particular reaction. Identification and isolation of active intermediate catalytic species also plays a crucial role to control the conversion and selectivity of catalytic reactions by performing controlled experiments. Experimental techniques such as NMR, mass, IR and UV-vis spectroscopy, and single crystal X-ray diffraction studies may also help in isolation and identification of active organometallic

intermediate species, which helps to improve the catalytic system for efficient catalytic activity.

Appendix A

Title: Ruthenium and Formic Acid Based Tandem Catalytic Transformation of Bioderived Furans to Levulinic Acid and Diketones in Water

Author: Ambikesh D. Dwivedi,Kavita Gupta,Deepika Tyagi,Rohit K. Rai,Shaikh M. Mobin,Sanjay K. Singh

Publication: ChemCatChem

Publisher: John Wiley and Sons

Date: Nov 23, 2015

Copyright © 2015, John Wiley and Sons

Logged in as:
Ambikesh Dwivedi
Account #:
3001221096

LOGOUT

Order Completed

Thank you for your order.

This Agreement between Mr. Ambikesh Dwivedi ("You") and John Wiley and Sons ("John Wiley and Sons") consists of your license details and the terms and conditions provided by John Wiley and Sons and Copyright Clearance Center.

Your confirmation email will contain your order number for future reference.

printable details

License Number	4385750152073
License date	Jul 11, 2018
Licensed Content Publisher	John Wiley and Sons
Licensed Content Publication	ChemCatChem
Licensed Content Title	Ruthenium and Formic Acid Based Tandem Catalytic Transformation of Bioderived Furans to Levulinic Acid and Diketones in Water
Licensed Content Author	Ambikesh D. Dwivedi,Kavita Gupta,Deepika Tyagi,Rohit K. Rai,Shaikh M. Mobin,Sanjay K. Singh
Licensed Content Date	Nov 23, 2015
Licensed Content Pages	9
Type of use	Dissertation/Thesis
Requestor type	Author of this Wiley article
Format	Print and electronic
Portion	Full article
Will you be translating?	No
Title of your thesis / dissertation	Synthesis, Characterization and Catalytic applications of Half sandwich Ruthenium(II) Complexes based on N/N, N/O and O/O Donor Ligands
Expected completion date	Mar 2018
Expected size (number of pages)	56
Requestor Location	Mr. Ambikesh Dwivedi Discipline of Chemistry Indian Institute of Technology Indore Indore, 453552 India Attn: Mr. Ambikesh Dwivedi
Publisher Tax ID	EU826007151

Copyright Clearance Center   **RightsLink®**

Home   Account Info   Help

CHEMCATCHEM

Title:	Catalytic Hydrogenation of Arenes in Water Over In Situ Generated Ruthenium Nanoparticles Immobilized on Carbon
Author:	Ambikesh Dhar Dwivedi,Rohit Kumar Rai,Kavita Gupta,Sanjay Kumar Singh
Publication:	ChemCatChem
Publisher:	John Wiley and Sons
Date:	May 26, 2017
	Copyright © 2017, John Wiley and Sons

Order Completed

Thank you for your order.

This Agreement between Mr. Ambikesh Dwivedi ("You") and John Wiley and Sons ("John Wiley and Sons") consists of your license details and the terms and conditions provided by John Wiley and Sons and Copyright Clearance Center.

Your confirmation email will contain your order number for future reference.

printable details

|	
License Number	4385740623772
License date	Jul 11, 2018
Licensed Content Publisher	John Wiley and Sons
Licensed Content Publication	ChemCatChem
Licensed Content Title	Catalytic Hydrogenation of Arenes in Water Over In Situ Generated Ruthenium Nanoparticles Immobilized on Carbon
Licensed Content Author	Ambikesh Dhar Dwivedi,Rohit Kumar Rai,Kavita Gupta,Sanjay Kumar Singh
Licensed Content Date	May 26, 2017
Licensed Content Pages	9
Type of use	Dissertation/Thesis
Requestor type	Author of this Wiley article
Format	Print and electronic
Portion	Full article
Will you be translating?	No
Title of your thesis / dissertation	Synthesis, Characterization and Catalytic applications of Half sandwich Ruthenium(II) Complexes based on N/N, N/O and O/O Donor Ligands
Expected completion date	Mar 2018
Expected size (number of pages)	56
Requestor Location	Mr. Ambikesh Dwivedi Discipline of Chemistry Indian Institute of Technology Indore Indore, 453552 India Attn: Mr. Ambikesh Dwivedi
Publisher Tax ID	EU826007151
Total	0.00 USD

Home   Account Info   Help

Title: Troponate/Aminotroponate Ruthenium–Arene Complexes: Synthesis, Structure, and Ligand-Tuned Mechanistic Pathway for Direct C–H Bond Arylation with Aryl Chlorides in Water

Author: Ambikesh D. Dwivedi, Chinky Binnani, Deepika Tyagi, et al

Publication: Inorganic Chemistry

Publisher: American Chemical Society

Date: Jul 1, 2016

Copyright © 2016, American Chemical Society

Logged in as:
Ambikesh Dwivedi
Account #:
3001221096

LOGOUT

PERMISSION/LICENSE IS GRANTED FOR YOUR ORDER AT NO CHARGE

This type of permission/license, instead of the standard Terms & Conditions, is sent to you because no fee is being charged for your order. Please note the following:

BACK   CLOSE WINDOW

Copyright Clearance Center
RightsLink®

Home | Account Info | Help

ACS Publications
Most Trusted. Most Cited. Most Read.

Title: Cyclopentadienyl–Ru(II)–Pyridylamine Complexes: Synthesis, X-ray Structure, and Application in Catalytic Transformation of Bio-Derived Furans to Levulinic Acid and Diketones in Water

Author: Ambikesh D. Dwivedi, Vinod K. Sahu, Shaikh M. Mobin, et al

Publication: Inorganic Chemistry

Publisher: American Chemical Society

Date: Apr 1, 2018

Copyright © 2018, American Chemical Society

Logged in as:
Ambikesh Dwivedi
Account #:
3001221096

LOGOUT

PERMISSION/LICENSE IS GRANTED FOR YOUR ORDER AT NO CHARGE

This type of permission/license, instead of the standard Terms & Conditions, is sent to you because no fee is being charged for your order. Please note the following:

BACK | CLOSE WINDOW